UNIVERSIDADE D
COIMBRA

Cátia Moreira de Sousa

Elucidation of the structure-activity relationship of *p*-menthane derivatives:

from a screening assay of anti-inflammatory properties to a lead compound and its mechanism of action

Tese no âmbito do Doutoramento em Ciências Farmacêuticas, na especialidade de Farmacologia e Farmacoterapia orientada pela Professora Doutora Alexandrina Maria Ferreira Santos Pinto Mendes e pelo Professor Doutor Alcino Jorge Lopes Leitão e apresentada à Faculdade de Farmácia da Universidade de Coimbra.

Dezembro de 2020

Faculdade de Farmácia da Universidade de Coimbra

ELUCIDATION OF THE STRUCTURE-ACTIVITY RELATIONSHIP OF *p*-MENTHANE DERIVATIVES: From a screening assay of anti-inflammatory properties to a lead compound and its mechanism of action

Cátia Moreira de Sousa

Tese no âmbito do Doutoramento em Ciências Farmacêuticas, na especialidade de Farmacologia e Farmacoterapia orientada pela Professora Doutora Alexandrina Maria Ferreira Santos Pinto Mendes e pelo Professor Doutor Alcino Jorge Lopes Leitão apresentada à Faculdade de Farmácia.

Dezembro de 2020

UNIVERSIDADE D
COIMBRA

Este trabalho foi realizado na Faculdade de Farmácia da Universidade de Coimbra e no Centro de Neurociências e Biologia Celular da Universidade de Coimbra, ao abrigo da bolsa de Doutoramento SFRH/BD/79600/2011 concedida pela Fundação para a Ciência e a Tecnologia.

Orientação: Professora Doutora Alexandrina Maria Santos Ferreira Pinto Mendes e Professor Doutor Alcino Jorge Lopes Leitão

“É nas derrotas que se preparam as vitórias”

Autor Desconhecido

À minha Mãe

Ao meu Pai

Ao meu Tio

Às minhas primas, Mariana e Marta

Agradecimentos

Realizar um doutoramento não significa solidão, isolamento e/ou alheamento do mundo real. Significa um caminho de partilha, opiniões, entreajuda e, acima de tudo, descoberta. Descoberta essa que é feita conjuntamente com pessoas, que, de uma forma ou de outra, ajudaram a que este processo tivesse um FIM. Queria, desde já, agradecer a todos aqueles que, ao longo destes anos, contribuíram para este FIM. Contudo, algumas pessoas e/ou grupos merecem um particular OBRIGADO!

À Professora Doutora Alexandrina Ferreira Mendes, queria agradecer a oportunidade de a ter como minha orientadora. Foi, é e sempre será o exemplo de ética, profissionalismo e exigência que pretendo seguir na minha vida. Partilhar e questionar conhecimento com a Professora foi uma experiência que não tem valor. Houve momentos menos bons, sim! Mas, sempre houve a humildade de reconhece-los e avançar. Nesse avançar, fizemos e partilhamos momentos, que irei levar comigo para toda a vida. Muitas vezes, mais que uma orientadora, uma amiga, uma segunda mãe. O meu sincero obrigado!

Ao Professor Doutor Alcino Jorge, queria agradecer por ter acreditado sempre em mim e por ter realizado este caminho comigo.

Ao Professor Doutor Carlos Cavaleiro, o meu muito obrigado pela partilha, ajuda e pela palavra de incentivo sempre presente.

Ao Bruno Neves, o meu muito obrigado por sempre me incentivar a seguir em frente, por ter partilhado a sua experiência e, claro, por ter ajudado na realização deste trabalho. E, acima de tudo, pela amizade!

À Professora Doutora Cláudia Cavadas, queria agradecer por me ter acolhido amavelmente no seu grupo e por sempre transmitir que: “O homem sonha, a obra nasce “. Gostaria, ainda, de agradecer o facto de sempre incentivar a valorização das pessoas e o pensar “fora da caixa”.

À Professora Doutora Teresa Cruz, o meu muito obrigado pela amizade, pelas palavras generosas e pelas gargalhadas partilhadas. Fizeram dias cinzentos parecer cor-de-rosa.

À Ana Teresa Rufino, queria agradecer o ensinar a estar num laboratório. Para além disso, a paciência e a amizade que sempre demonstrou.

À Maria Madalena Ribeiro, o obrigado por termos partilhado este caminho e o fazer sentir-me menos só quando tudo parecia não fazer sentido. Obrigado por me teres deixado entrar no teu mundo e, assim, poder dizer que: “Quem tem uma Madalena, tem tudo!”

À Mónica Zuzarte (“microscopista de serviço”), o meu obrigado por sempre me fazeres sair da minha zona de conforto e por me fazeres acreditar que tudo é possível. O meu obrigado por estares sempre comigo nos bons e nos maus momentos e, principalmente, nestes últimos sempre dizeres que:” Não era para ser”. E claro, o meu obrigado por seres a minha *Best Friend Forever*. Nesta sequência, deixo um obrigado ao grupo Ubiquitin-dependent Proteolysis and Intercellular Communication pela estima e partilha ao longo destes anos.

Ao grupo da Professora Doutora Alexandrina Ferreira Mendes (Ana Rufino, Maria Madalena Ribeiro, João Ferreira, Inês Ferreira, Soraia Silva, Caren Rodrigues e Ana Capitão), o meu muito obrigado pelo companheirismo. À Ana Capitão, o meu sincero obrigado pela sua contribuição na formatação deste documento, que foi fundamental do início ao fim!

Ao grupo da Professora Doutora Teresa Cruz (Vera Francisco, Joana Liberal, Ana Silva, João Demétrio Martins, Isabel Ferreira, Ana Catarina Pereira, Gonçalo Brites, João Calmeiro, Myléne Carrascal e Fábio Sousa), o meu obrigado por tornarem a vida no laboratório divertida e cheia de amizade! À Joana Liberal, o meu sincero obrigado pelas risadas partilhadas e amizade. Ao João Calmeiro e Gonçalo Brites, o meu especial obrigado por serem os fervorosos incentivadores da escrita deste documento e como diz o Gonçalo: “E cara alegre!”. Obrigado pela amizade!

Ao grupo Neuroendocrinology & Aging, o meu sincero obrigado pelo apoio, partilha e motivação.

Ao grupo da Professora Doutora Celeste Lopes, em particular, à Joana Balça Silva pelas manhãs partilhadas na sala de cultura, pelos cafés e almoços animados e, acima de tudo, pela amizade e companheirismo.

Ao Laboratório de Química Farmacêutica, em especial à D. Graça, ao Professor Doutor Jorge Salvador e respectivo grupo, à Professora Doutora Luísa Sá e Melo e à Professora Doutora Maria Manuel Cruz Silva, o meu agradecimento pelo apoio e incentivo.

À D. Gina, Vera, Daniela, D. Fernanda, D. Natividade e D. Céu, o meu sincero obrigado por terem permitido a execução laboratorial deste trabalho em condições exemplares. Queria deixar um agradecimento especial à D. Céu pela amizade e apoio sempre demonstrados.

À equipa da ProtexAging, o meu agradecimento por me ter ensinado a valorizar os meus resultados.

Aos alunos das disciplinas de Bioquímica I/Bioquímica e Bioquímica II/Metabolismo do ano lectivo 2019/2020, o meu obrigado por me ouvirem a transmitir aquilo que aprendi ao longo destes anos e por me mostrarem quão feliz sou a ensinar. Queria agradecer ainda o facto de terem trazido luz à parte da final deste doutoramento, nomeadamente à redacção deste documento.

Ao Dr. Fernando Pocinho e ao Professor Doutor Pio Abreu, o meu sincero obrigado por me ensinarem a transformar as minhas fraquezas em pontos fortes e, assim, suavizar a realização deste doutoramento.

À Tertúlia do Ananás (Ana Raquel, Ana Rita, Marisa, Joana, Inês Luzio, Maria Inês, Inês Pereira, Madalena e Teresa), o meu obrigado por me proporcionarem momentos de descontracção durante estes anos.

Ao Gonçalo, João, Maria Inês e Maria de La Salete, o meu muito obrigado por estarem sempre presentes, embora que nem sempre fisicamente. Obrigado pelo apoio nos momentos mais difíceis, pela partilha das alegrias e, acima de tudo, por sempre acreditarem que eu sou capaz! Sem vocês, este caminho teria sido muito mais tortuoso.

À minha família (Mãe, Pai, Tio e primas Marta e Mariana), o meu sincero obrigado por sempre terem sido o meu suporte e a minha razão de viver. Um agradecimento especial à minha Mãe por ter sido sempre o meu porto seguro e a minha principal apoiante nesta aventura!

A todos, o meu sincero e sentido

Bem-Hajam!

Abbreviations

ADAMTS5	A Desintegrin and Metalloproteinase with TromboSpondin Motif 5
AGE	Advanced Glycation End products
AnKR	Ankyrin Repeats
AP-1	Activating Protein-1
Arg	Arginine
ATF	Activating Transcription Factor
ATP	Adenosine triphosphate
BAFF-R	B cell Activating Factor Receptor
Bay	Bay 11-7082
Bcl-2	B cell lymphoma 2
Brd4	Bromodomain 4 protein
BSA	Bovine Serum Albumin
C/EBPβ	Transcription factor CCAAT/ Enhancer Binding Protein beta
cAMP	Cyclic adenosine monophosphate
CBP	CREB-Binding Protein
CC1/2	Coiled-Coil domain 1/2
CCL2/MCP-1	C-C motif Chemokine Ligand 2 or Monocyte chemoattractant protein-1
CDK9/P-TEFb	Cyclin Dependent Kinase 9 and Positive Transcription Elongation Factor b
cDNA	Complementary DNA
CHUC	University and Hospital Centre of Coimbra
CI	Confidence Interval
CLRs	C-type Lectin Receptors
Col I	Collagen I
COMMD1	COMM Domain-containing protein-1
COX	Cyclooxygenase
Ctrl	Control
CUL2	Cullin-2
CXCL	C-X-C Motif Chemokine Ligand
DAMPs	Damage-Associated Molecular Patterns
DAPI	4´,6'-diamidino-2-phenylindole
DD	Death Domain
DMSO	Dimethyl sulfoxide
DNA	Deoxyribonucleic acid
DUBs	Deubiquitinases
E1	Ubiquitin-activating enzyme
E2	Ubiquitin-conjugating enzyme
E3	Ubiquitin ligase
ECM	Extracellular matrix
EGTA	Ethylene glycol-bis(2-aminoethylether)-N,N,N´,N´´- tetraacetic acid
Elk-1	ETS domain-containing protein-1
EMT or EndMT	Epithelial- or endothelial-mesenchymal transition
ER	Endoplasmic reticulum
ERK1/2	Extracellular signal-Regulated Kinase1/2

FBS	Foetal bovine serum
FBXL11	F-Box and Leucine-rich repeat protein 11
GC-MS	Gas chromatography-Mass spectrometry
GLP	G9a-Like Protein
GM-CSF	Granulocyte Macrophage Colony-Stimulating Factor
GRO	Growth Regulated Oncogene
GRR	Glycine-Rich Region
GSK-3β	Glycogen Synthase Kinase-3β
HATs	Histone AcetyltTransferases
HDACs	Histone DeAcetylases
HLH	Helix-Loop-Helix domain
HMGB1	High-Mobility Group Box 1 protein
IC_{50}	Half-maximal inhibitory concentration
IGF	Insulin-like Growth Factor
IKB-α	Nuclear Factor kappa B Inhibitor-α
IKK	IκB Kinase
IL	Interleukin
IL-1R	Interleukin-1 receptor
iNOS/NOS2	Inducible NO synthase/ NO synthase 2
IRAKs	IL-1 Receptor Associated Kinases
IRE-1	Inositol-Requiring Enzyme 1
JNK	Jun N-terminal Kinase
K^+	Potassium ion
LIM	Abnormal cell Lineage 11-Islet 1-Mechanosensory abnormal 3
LMP2	Large Multifunctional Peptidase 2 or Proteasome 20S subunit beta
LOX-1	Lectin-like Ox-LDL receptor 1
LPS	Lipopolysaccharide
LTβR	LymphoToxin β Receptor
Lys	Lysine
LZ	Leucine Zipper
MAMPs	Microorganism-Associated Molecular Patterns
MAP2K	MAPK kinase
MAP3K	MAPK kinase kinase
MAPKs	Mitogen-Activated Protein Kinases
MMPs	Matrix MetalloProteinases
MSK-1	Mitogen- and Stress- Activated Kinase-1
NAD^+	Nicotinamide Adenine Dinucleotide oxidized form
NADH	Nicotinamide Adenine Dinucleotide reduced form
NADPH	Nicotinamide Adenine Dinucleotide Phosphate reduced form
NBD	NEMO-Binding Domain
NEMO	NF-κB Essential Modulator
NES	Nuclear export sequences
NETs	Neutrophil Extracellular Traps
NF-κB	Nuclear Factor kappa-light-chain-enhancer of activated B cells
NIK	NF-κB-Inducing Kinase
NLRP3	NOD-Like Receptor Protein 3
NLRs	NOD-Like Receptors

NLS	Nuclear localization sequence
NO	Nitric oxide
NSD1	Nuclear receptor-binding Set Domain-containing protein 1
OA	Osteoarthritis
ox-LDL	Oxidized Low-Density Protein
P	Phosphate
PAMPs	Pathogen-Associated Molecular Patterns
PBS	Phosphate buffered saline
PCAF	P300/CBP-Associated Factor
PDLIM2	PDZ LIM Domain 2
PDZ	Postsynaptic density 65-Discs large-Zonula occludens 1
PERK	Double-stranded RNA-activated Protein kinase R-like ER Kinase
PEST	Region rich in the amino acids proline (P), glutamic acid (E), serine (S) and threonine (T)
Pim-1	Serine/threonine-protein kinase Pim-1
PKA	Protein Kinase A
PKAc	PKA catalytic subunit
PP1	Protein Phosphatase 1
PP2A	Protein Phosphatase 2A
PRMT5	Protein arginine MethylTransferase 5
PRR	Pattern-Recognition Receptors
PSMD11	26S proteasome subunit, non-ATPase 11
PTM	Posttranslational modifications
PVDF	Polyvinylidene difluoride
qRT-PCR	Reverse Transcription-quantitative polymerase chain reaction
Res	Resveratrol
RHD	Rel Homology Domain
RIG-RLR	Retinoic acid-Inducible Gene I-Like Receptors
RIPs	Receptor-Interacting Proteins
RNS	Reactive nitrogen species
ROS	Reactive oxygen species
RSK1	Ribosomal Subunit Kinase-1
SAR	Structure-Activity Relationship
SASP	Senescence-Associated Secretory Phenotype
SDS	Sodium dodecyl sulphate
SDS-PAGE	Sodium dodecyl sulfate polyacrylamide gel electrophoresis
SEM	Standard error of the mean
Ser	Serine
Set9	Histone-lysine N-methyltransferase set9
SetD6	N-lysine methyltransferase SetD6
SIRTs	Sirtuins
SMS	Senescence-messaging secretome
SOX9	SRY-box transcription factor 9
SPMs	Specialised Pro-resolving Mediators
TAD	Transactivation domain
TAK1	TGF-β-Activated Kinase-1
TBK1	TANK-Bnding Kinase 1

TGF-β	Transforming Growth Factor-β
TIMPs	Tissue Inhibitors of MetalloProteinases
TLP-2	Tumor progression Locus 2
TLR4	Toll-Like Receptor-4
TNFR	Tumor Necrosis Factor Receptor
TNF-α	Tumor Necrosis Factor-α
TRAFs	Tumor necrosis factor Receptor-Associated Factors
Ub	Ubiquitin
UPR	Unfolded Protein Response
UPS	Ubiquitin-Proteasome System
USP7	Ubiquitin Specific Protease 7
VEGF	Vascular Endothelial Growth Factor
WHO	World Health Organization
WIP1	Wild type p53 Induced Phosphatase 1
XBP1	X-box-Binding Protein 1
Z	Zinc finger domain

Resumo

A inflamação crónica constitui um dos mecanismos responsáveis por doenças crónicas associadas ao envelhecimento. O Factor Nuclear–kapaB (NF-κB) e as *cinases de proteínas activadas por mitogénios* (MAPK) são importantes mediadores da inflamação e dos seus efeitos nocivos. Assim, encontrar novas moléculas capazes de interferir com estes mediadores é uma importante estratégia para interromper a progressão daquelas doenças.

Os produtos naturais representam uma fonte de novas moléculas com actividades biológicas, em particular actividade anti-inflamatória. Estudos etnofarmacológicos descreveram a actividade anti-inflamatória de espécies de menta, nomeadamente as dos seus óleos essenciais. Os monoterpenos são os compostos mais abundantes nesses óleos essenciais, em particular aqueles com a estrutura básica do *p*-mentano e pertencentes à via biossintética do limoneno. No entanto, existem discrepâncias significativas entre diferentes estudos pelo que o primeiro objectivo deste estudo foi realizar um ensaio de *screening* de um grupo de 21 monoterpenos com a estrutura básica do *p*-mentano. Como ensaio de *screening* primário, avaliou-se a capacidade dos compostos teste para inibir a produção de óxido nítrico (NO) induzida por lipopolissacarídeo bacteriano (LPS) em macrófagos murinos. Os resultados indicam que:

- Nove moléculas inibiram significativamente a produção de NO.
- O IC_{50} de oito moléculas estabeleceu a ordem de potências: (S)-(+)-carvona (**4**) > (R)-(-)-carvona (**5**) >> (+)-dihidrocarveol (**8**) > (S)-8-hidroxicarvotanacetona (**20**) > (R)-8-hidroxicarvotanacetona (**21**) > (+)-dihidrocarvona (**7**) > (-)-carveol (**6**) > (-)-dihidrocarveol (**9**).
- Os estudos de relação estrutura-actividade demonstraram que a conjugação da dupla ligação α,β em C1 com o grupo carbonilo em C6 é o maior determinante da potência, enquanto a presença de um grupo isopropenilo em C4 e a configuração S do centro quiral em C4 são relativamente menos importantes.

A actividade anti-inflamatória dos compostos mais potentes, (S)-(+)-carvona e (R)-(-)-carvona, foi confirmada pela inibição da expressão de outros mediadores pro-inflamatórios, nomeadamente sintase indutível do NO (NOS2) e interleucina-1β (IL-1β), no mesmo modelo. Avaliou-se, então, a actividade anti-inflamatória do composto mais potente num modelo celular de osteoartrite que consiste em condrócitos humanos tratados com IL-1β, no

qual se confirmou a capacidade da (S)-(+)-carvona para diminuir a expressão da IL-1β e da NOS2 e a produção de NO.

Tendo em conta o papel do NF-κB e das MAPKs na inflamação, o efeito da (S)-(+)-carvona nessas vias foi avaliado em macrófagos tratados com LPS. Os resultados demonstraram que a (S)-(+)-carvona diminui a activação da *Cinase do terminal amínico da proteína c-Jun* (JNK), em particular da JNK1, não tendo qualquer efeito nos restantes elementos da família das MAPKs, nem no bloqueio da activação do NF-κB e sua translocação nuclear. No entanto, a (S)-(+)-carvona inibiu a actividade transcripcional do NF-κB, diminuindo a expressão de IκB-α, o inibidor natural e alvo do NF-κB. A (S)-(+)-carvona também diminuiu a acetilação do NF-κB/p65 na lisina (Lys) 310 que é fundamental para a sua completa actividade transcripcional. Uma vez que a Sirtuína 1 (SIRT1) desacetila directamente o NF-κB/p65 na Lys310, formulámos a hipótese da (S)-(+)-carvona poder reduzir a acetilação do NF-κB/p65 por actuar na actividade e/ou expressão da SIRT1. Ensaios *in chemico* e em células confirmaram que a (S)-(+)-carvona activa directamente a SIRT1, diminuindo os níveis de NF-κB/p65 acetilado na Lys310, sem interferir com a expressão desta. Para além disso, a (S)-(+)-carvona reduziu igualmente os níveis de NF-κB/p65 acetilado e aumentou os níveis basais de *SRY-Box Transcription Factor 9*, outro alvo da SIRT1, em condrócitos humanos.

A (R)-(-)-carvona diminuiu a fosforilação da JNK1, sem afectar os restantes elementos da família das MAPKs, nem a activação da via canónica do NF-κB e sua translocação nuclear, a acetilação do NF-κB/p65 na Lys310 e a actividade e expressão da SIRT1.

Em suma, este estudo identificou os requisitos químicos importantes para a actividade anti-inflamatória dos monoterpenos derivados do *p*-mentano e identificou o primeiro monoterpeno, a (S)-(+)-carvona, como activador directo da SIRT1. Identificou, igualmente, a (R)-(-)-carvona como inibidor da JNK1 com potencial para interferir com a actividade transcripcional do NF-κB.

Os enantiómeros da carvona modulam mecanismos distintos e relevantes na promoção e manutenção de respostas inflamatórias crónicas de baixo grau. Estudos *in vitro* e *in vivo* são necessários para confirmar o potencial terapêutico destes compostos. A combinação desses resultados com os apresentados nesta dissertação serão essenciais para guiar o processo de *drug design* e desenvolvimento de estratégias terapêuticas bem sucedidas para travar a

inflamação crónica de baixo grau que conduz ao declínio funcional característico do envelhecimento e das doenças associadas.

Palavras-chave: envelhecimento; inflamação; NF-κB; MAPKs; SIRT1; monoterpenos; derivados do *p*-mentano; relação estrutura-actividade; (S)-(+)-carvona; (R)-(-)-carvona.

Abstract

Inflammation, in particular chronic low-grade inflammation, is strongly associated with the mechanisms behind chronic age-related diseases. Nuclear Factor kappa-light-chain-enhancer of activated B cells (NF-κB) and Mitogen-Activated Protein Kinase (MAPK) are important players in mediating inflammation and its deleterious effects. Thus, finding new molecules capable of interfering with those players may have potential to halt the progression of chronic age-related diseases.

Natural products have traditionally been a source of new molecules with biological activities, in particular anti-inflammatory properties. Ethnopharmacological studies reported the anti-inflammatory activity of mint species, specifically those related to their essential oils. Among their composition, monoterpenes are the most abundant class, in particular those having the *p*-menthane backbone and belonging to the limonene synthase pathway. Nevertheless, there is significant heterogeneity about the reported anti-inflammatory activities due to different experimental conditions. Thus, the first aim of this study was to perform a standardised screening assay of a selected group of 21 monoterpenes, derived from *p*-menthane. For that, their ability to inhibit the production of nitric oxide (NO) induced by bacterial lipopolysaccharides (LPS) in murine macrophages was evaluated as a primary screening assay. The results obtained show that:

- Nine molecules significantly inhibited LPS-induced NO production.
- IC_{50} was determined for eight molecules and the rank of potency was established: (S)-(+)-carvone (**4**) > (R)-(-)-carvone (**5**) >> (+)-dihydrocarveol (**8**) > (S)-8-hidroxycarvotanacetone (**20**) > (R)-8-hidroxycarvotanacetone (**21**) > (+)-dihydrocarvone (**7**) > (-)-carveol (**6**) > (-)-dihydrocarveol (**9**).
- Structure-activity relationship analyses demonstrate that conjugation of an α,β double bond at C1 with a carbonyl group at C6 is the major determinant of potency, while the presence of an isopropenyl group at C4 and the S configuration of the chiral center at C4 are decreasingly important.

Then, the anti-inflammatory activity of the two most potent compounds, (S)-(+)-carvone and (R)-(-)-carvone, was confirmed by their ability to inhibit the expression of other pro-inflammatory mediators, namely inducible nitric oxide synthase (NOS2) and interleukin-1β (IL-1β), in the same model. Since (S)-(+)-carvone was the most potent compound, its ability to interfere with inflammatory pathways in human chondrocytes treated with IL-1β, a cell

model of osteoarthritis, was explored. As in murine macrophages, (S)-(+)-carvone decreased the expression of IL-1 β and NOS2, as well as NO production induced by IL-1β.

Considering the role of NF-κB and MAPKs in inflammation, the effect of (S)-(+)-carvone on those signaling pathways was evaluated in LPS-treated macrophages. The results obtained demonstrate that (S)-(+)-carvone decreased c-Jun N terminal Kinase (JNK), in particular JNK1 phosphorylation, but had no effect on the other MAPK family members and also did not block NF-κB activation and nuclear translocation. Nonetheless, (S)-(+)-carvone inhibited NF-κB transcriptional activity, evidenced by the decreased expression of IκB-α, the natural inhibitor and target of NF-κB. (S)-(+)-carvone also decreased NF-κB/p65 acetylation at Lys310 which is essential for full transcriptional activity. Since Sirtuin 1 (SIRT1) directly deacetylates NF-κB/p65 at Lys310, we hypothesized that (S)-(+)-carvone reduces NF-κB/p65 acetylation by acting on SIRT1 activity and/or expression. *In chemico* and in cell assays confirmed that (S)-(+)-carvone directly activates SIRT1 and decreases the levels of acetylated NF-κB/p65 at Lys310 without interfering with SIRT1 expression. Moreover, (S)-(+)-carvone also decreased acetylated levels of NF-κB/p65 and increased the basal levels of SRY-Box Transcription Factor 9, another target of SIRT1, in human chondrocytes.

On the other hand, (R)-(-)-carvone decreased JNK1 phosphorylation, but did not affect any of the other MAPKs, nor the canonical NF-κB activation pathway, its nuclear translocation, acetylation of NF-κB/p65 at Lys310 or SIRT1 activity and expression.

To conclude, this study identified the chemical features important for the anti-inflammatory activity of *p*-menthane-derived monoterpenes. Moreover, it pointed out the first monoterpene, (S)-(+)-carvone, as a direct activator of SIRT1. It also identified (R)-(-)-carvone as an inhibitor of JNK1 with impact on NF-κB transcriptional activity. The carvone enantiomers have the potential to tackle distinct mechanisms relevant in promoting and maintaining chronic low-grade inflammatory responses. Further studies, *in vitro* and *in vivo*, are required to fully ascertain their therapeutic potential. Combining those results with the ones presented here will be essential to inform drug design and development to successfully halt the chronic low-grade inflammation that drives age-related functional decline and associated diseases.

Keywords: aging; inflammation; NF-κB; MAPKs; SIRT1; monoterpenes; *p*-menthane derivatives; Structure-Activity Relationship; (S)-(+)-carvone; (R)-(-)-carvone.

Index

Figures and Tables Index

Chapter 1: Introduction

1.1 Chronic diseases, aging and inflammation

Chronic diseases represent a group of illnesses and conditions that "tend to be of long duration and are the result of a combination of genetic, physiological, environmental and behavioural factors" (WHO 2018). Bernell and Howard (2016) drew attention to the fact that there is no uniformity about chronic disease definition and the diseases belonging to this category. Moreover, these authors claimed that a broader and actual definition should be assumed in order to be more inclusive and conscious (Bernell and Howard 2016). For instance, with treatment advances, human immunodeficiency virus infection is now considered a chronic disease despite being an infectious disease (Deeks, Lewin et al. 2013). Besides the controversy about the definition, it is well accepted that people of all age groups, regions and countries are affected by chronic diseases (WHO 2018). However, these diseases, especially the non-communicable, are often associated with older age groups (WHO 2018). According to the Word Health Organization (WHO), cardiovascular diseases, cancers, chronic respiratory diseases,diabetes, musculoskeletal diseases and mental disorders are the main types of chronic non-communicable diseases.

Aging is the most important risk factor driving chronic diseases (Kennedy, Berger et al. 2014, Seals, Justice et al. 2016). It is important to emphasize that aging itself is not a disease, but a progressive loss of physiological integrity and impaired function that increases vulnerability to pathology or age-associated diseases, such as chronic diseases (Hayflick 2007, Lopez-Otin, Blasco et al. 2013, Seals, Justice et al. 2016). Aging *per se* does not cause these diseases, but makes them manifest clinically (Fulop, Witkowski et al. 2018), since the mechanisms driving aging and those driving age-associated diseases largely overlap (Sierra 2016). One of these processses is inflammation (Freund, Orjalo et al. 2010).

Besides its association with age-related diseases, such as neurodegenerative diseases, metabolic disorders, cardiovascular diseases, musculoskeletal disorders and cancer (Freund, Orjalo et al. 2010, Fulop, Witkowski et al. 2018), inflammation has also been considered one of "the hallmarks of aging" (Lopez-Otin, Blasco et al. 2013), and, more recently, a "pillar of aging" (Sierra 2016, Franceschi, Garagnani et al. 2018), representing a processs that drives chronic diseases and contributes to the acceleration of aging (Franceschi, Garagnani et al. 2018) (Fig.1).

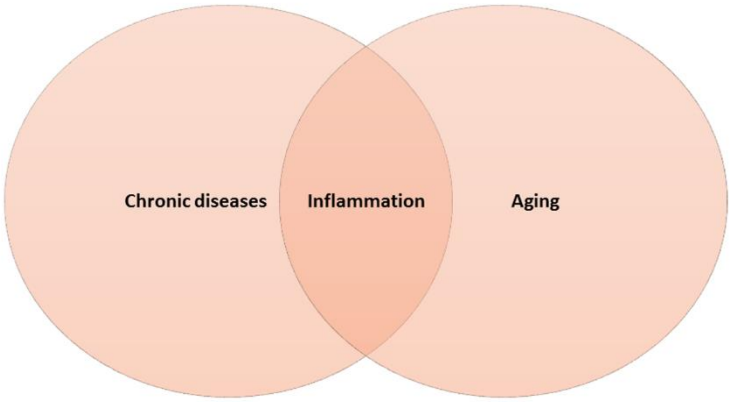

Figure 1. **Interconnection between chronic diseases, aging and inflammation.**

1.2 Inflammation: from a protective and homeostatic mechanism to a fuel for age-associated diseases

1.2.1 Inflammation – understanding the concept

"The classical definition of inflammation comprising its cardinal signs - *rubor* (redness), *calor* (warmth), *dolor* (pain) and *tumor* (swelling) - as described by Celsus and *function laesa* (loss of function) added by Galen, has persisted in modern times" (Netea, Balkwill et al. 2017). Functionally, inflammation has been traditionally considered a defense response of the organism triggered by infection or tissue injury in order to eliminate the initial aggressors (Netea, Balkwill et al. 2017). Nevertheless, some authors claim that the concept of inflammation should be updated namely to include any type of endogenous stress as a potential initiator of inflammation (Weissmann 2010, Chovatiya and Medzhitov 2014, Antonelli and Kushner 2017). According to this concept, Antonelli and Kushner (2017) define inflammation as "an innate immune response to harmful stimuli such as pathogens, injury and metabolic stress that aims to restore homeostasis". This new definition repurposes inflammation as a mechanism that maintains and defends homeostasis, regardless of whether the insult is exogenous, as in the case of infections, or endogenous, as occurs, for instance, in metabolic disorders (Medzhitov 2008, Chovatiya and Medzhitov 2014, Antonelli and Kushner 2017).

1.2.2 The inflammatory pathway

The inflammatory pathway is an orchestrated mechanism which includes the following components: inducers, sensors, mediators and effectors (Medzhitov 2008) (Fig. 2). Inducers, which are the signals that initiate the inflammatory response, activate specialized sensors. Then, this activation prompts the production of a specific range of mediators, responsible for modifying the functional states of tissues and organs, which are the effectors of inflammation, in order to allow them to adjust to the conditions indicated by a specific inducer (Fig.2). These components form a complex regulatory network and each of them determines the type of inflammatory response (Medzhitov 2008).

Figure 2. The inflammatory pathway. Reproduced with permission from Medzhitov, 2008.

1.2.2.1 Inducers

Inducers of inflammation can be exogenous or endogenous (Fig.3).

Exogenous inducers can be categorized into microbial and non-microbial (Fig.3) (Medzhitov 2008). Microorganism-Associated Molecular Patterns (MAMPs), Pathogen-Associated Molecular Patterns (PAMPs) and virulence factors are classes of microbial inducers. MAMPs and PAMPs are a set of conserved molecular patterns that elicit an immune response to commensal and pathogenic microorganisms, respectively (Stuart, Paquette et al. 2013). For instance, lipopolysaccharide (LPS) is a component of the cell wall of Gram-negative bacteria and its lipid portion, namely lipid A, is responsible for the pathogenicity associated to infection with this class of bacteria (Akira, Uematsu et al. 2006). The last class of microbial inducers (virulence factors) refers to the content secreted by pathogens, namely toxins and bacterial effectors, like proteolytic enzymes, which are required for their establishment within the host (Medzhitov 2008, Stuart, Paquette et al. 2013). On the other hand, non-microbial exogenous inducers comprise allergens, irritants, foreign bodies (e.g. silica and asbestos) and toxic compounds (Medzhitov 2008).

Endogenous inducers of inflammation are named Damage-Associated Molecular Patterns (DAMPs, Fig.3) which are a heterogenous group of endogenous molecules released from the intracellular or the extracellular space by stressed, damaged or malfunctioning tissues

(Medzhitov 2008, Schaefer 2014). DAMPs are molecules such as Adenosine Triphosphate (ATP), potassium (K^+) ions, uric acid, monosodium urate, Advanced Glycation End products (AGE), alarmins, like High-Mobility Group Box 1 protein (HMGB1) and several members of the S100 calcium-binding protein family, and breakdown products of the extracellular matrix (Medzhitov 2008, Schaefer 2014, Yang, Han et al. 2017).

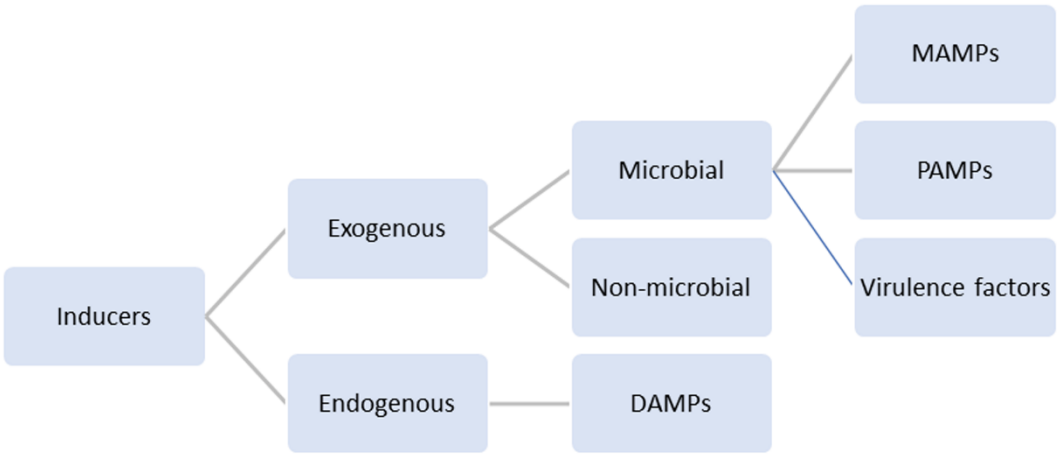

Figure 3. Inducers of inflammation: a schematic representation. Adapted from Medzhitov, 2008.

1.2.2.2 Sensors

Pattern-Recognition Receptors (PRRs) are responsible for sensing the presence of inducers of inflammation, in particular PAMPs and DAMPs (Pandey, Kawai et al. 2014). Depending on their structural similarities, PRRs are grouped in different classes which include Toll-Like Receptors (TLRs), NOD-Like Receptors (NLRs), C-type Lectin Receptors (CLRs), Retinoic acid-Inducible Gene (RIG) I-Like Receptors (RLRs) and cytosolic DNA sensors (Pandey, Kawai et al. 2014). For example, TLR4 was identified as the receptor for LPS (Poltorak, He et al. 1998). NLRP3, which belongs to the NLR family of receptors, was identified as a sensor component of the multiprotein enzymatic complex, termed inflammasome, and is activated by specific bacterial infections and treatments that deplete intracellular K^+ (Mariathasan, Weiss et al. 2006). Moreover, NLPR3 inflammasome is responsible for the activation of pro-inflammatory cytokines interleukin-1β (IL-1β) and interleukin-18 (IL-18) (Patel, Carroll et al. 2017). PRRs are expressed in myeloid cells such as monocytes, macrophages, neutrophils and dendritic cells as well as in various nonprofessional immune cells, namely fibroblasts, epithelial cells (Netea, Balkwill et al.

2017) and cells of mesenchymal origin [e.g. bone (Kikuchi, Matsuguchi et al. 2001), muscle (Schreiner, Voss et al. 2006) and cartilage (Sillat, Barreto et al. 2013) cells and adipocytes (Poulain-Godefroy, Le Bacquer et al. 2010)]. Activation of these receptors by the inducers of inflammation leads to the production of numerous inflammatory mediators.

1.2.2.3 Mediators

Mediators of inflammation (Table 1) can be derived from plasma proteins or secreted by cells such as specialized leukocytes (e.g. tissue-resident macrophages and mast cells) and tissue-specific cells. According to their biochemical properties, inflammatory mediators can be grouped into the following classes (Medzhitov 2008, Zlotnik and Yoshie 2012):

Table 1: Types of inflammatory mediators.

Inflammatory mediators	Examples
Vasoactive amines	Histamine; Serotonin.
Vasoactive peptides	Substance P; Fibrinopeptide A; Fibrinopeptide B.
Complement fragments	C3a; C4a; C5a.
Lipid mediators	Eicosanoids (e.g. prostaglandins, thromboxanes, leukotrienes and lipoxins); Platelet-Activating Factors.
Cytokines	Tumour-Necrosis Factor-α (TNF- α); Interleukin-1; Interleukin-6 (IL-6).
Chemokines	Interleukin-8 (IL-8/CXCL8); Monocyte chemoattractant protein-1 (MCP-1/CCL2).
Proteolytic Enzymes	Elastin; Cathepsins; Matrix metalloproteinases.

It should be emphasized that many mediators not only exert direct effects on target tissues or cells, but also induce the production of additional mediators (Medzhitov 2008).

1.2.2.4 Effectors

The effectors of the inflammatory pathway are the tissues and cells which are affected by mediators of inflammation. The ultimate goal of those mediators is to control tissue and cell homeostasis, promoting their adaptation to noxious conditions (Medzhitov 2008).

1.2.3 From acute to chronic inflammation

Acute inflammation has been best described for microbial infection, in particular for bacterial infections. Tissue-resident macrophages and mast cells are responsible for the initial recognition of an infection and for the production of a range of inflammatory mediators – chemokines, cytokines, vasoactive amines, eicosanoids and products of proteolytic cascades (Medzhitov 2008). These mediators elicit an inflammatory exudate locally, which is composed by plasma proteins and leukocytes (e. g. neutrophils), as the main and immediate effect (Kolaczkowska and Kubes 2013). The selective extravasation of leukocytes is promoted by activation of the endothelium of the blood vessels. This mechanism is based on the expression of cell-adhesion molecules, also known as selectins, in endothelial cells which allows the binding of integrins and chemokine receptors of leukocytes and, consequently, promote their diapedesis (Kolaczkowska and Kubes 2013, Rea, Gibson et al. 2018). In the afflicted tissue site, leukocytes, in particular neutrophils, become activated either by contact with pathogens or through the action of cytokines secreted by tissue-resident cells (Medzhitov 2008). In turn, activated neutrophils can phagocytose the invading agents or promote their extracellular lysis. Upon phagocytosis, neutrophils kill the engulfed microorganisms by using NADPH oxygenase-derived reactive oxygen species (ROS) or antibacterial proteins, namely cathepsins and lysozyme, that are released in granules into the phagosome. These antibacterial proteins can also be released into the extracellular space to act on extracellular pathogens (Kolaczkowska and Kubes 2013). Moreover, Neutrophil Extracellular Traps (NETs), which are composed of histone proteins and enzymes, are released by highly activated neutrophils to eliminate extracellular microorganisms. NETs prevent the spreading of microorganisms by immobilizing them and facilitating their phagocytosis (Kolaczkowska and Kubes 2013). However, not only the invading agent is affected, but also host tissues can be damaged by these effectors, including ROS and reactive nitrogen species (RNS) that leak out of the activated neutrophils.

An effective acute inflammatory response culminates in the elimination of the invading agent and, finally, in its resolution (Medzhitov 2008). The resolution of inflammation is an active process mainly mediated by tissue-resident and recruited macrophages (Headland and Norling 2015). Transition of inflammation to resolution is orchestrated by lipid mediators whose switch from pro-inflammatory to anti-inflammatory is a key step (Rea, Gibson et al. 2018). The anti-inflammatory lipid mediators are called Specialised Pro-resolving Mediators

(SPMs) and include lipoxins, resolvins, protectins and maresins (Serhan 2017). Activation of resolution comprises the limitation or cessation of neutrophil recruitment and induction of activated neutrophil apoptosis (Basil and Levy 2016). The removal of these apoptotic cells by macrophages, termed efferocytosis, requires a switch in their phenotype, from pro- to anti-inflammatory, which is a prerequisite for their egress via the lymphatic vessels (Basil and Levy 2016). Additional production of SPMs, stimulated by efferocytosis, promotes restoration of vascular integrity, repair of injured tissues, remission of fever and relief of inflammatory pain (Headland and Norling 2015, Basil and Levy 2016). The main outcome of resolution of acute inflammation is the return to homeostasis (Headland and Norling 2015). It is noteworthy that besides SPMs, other mediators take part in the resolution process such as annexin A1, interleukin-10, Transforming Growth Factor-β (TGF-β) and carbon monoxide (Basil and Levy 2016).

If the inflammatory trigger is not eliminated by the acute inflammatory response or persists for any other reason or the resolution phase is not appropriately induced, a chronic inflammatory process will take place (Feehan and Gilroy 2019). This response is localized at the initial afflicted site and is frequently associated to a different type of local tissue remodeling (Medzhitov 2010). For instance, tuberculosis is a classical example of persistent infection by *Mycobacterium tuberculosis* (Nathan and Ding 2010). Due to its evasion strategies, this pathogen instigates chronic inflammation in the lung (Barth, Remick et al. 2013).

As mentioned above, the inflammatory process has been well described for bacterial infections. Moreover, non-microbial exogenous inducers and DAMPs can also trigger an inflammatory response (Medzhitov 2008). However, inflammation which occurs in the absence of any microorganism has been termed *sterile inflammation* (Rock, Latz et al. 2010). Sterile inflammation has the same downstream vascular and cellular manifestations as inflammation induced by PAMPs (Rock, Latz et al. 2010, Gong, Liu et al. 2020). On the other hand, the initial events that elicit and control the inflammatory response can be very different (Rock, Latz et al. 2010, Gong, Liu et al. 2020).

1.2.4 From *para-inflammation* to chronic low-grade inflammation in chronic age-associated diseases

In basal conditions, tissues are maintained in the homeostatic state with the aid of tissue-resident macrophages when it is required. Nevertheless, in noxious conditions, tissues undergo stress and can malfunction. In case of considerable changes, adaption to these conditions requires the help of tissue-resident macrophages or the recruitment of macrophages and may require small-scale delivery of additional leukocytes and plasma proteins. This response has characteristics that are intermediate between basal and inflammatory states and was termed *para-inflammation* by Medzhitov in 2008, in his essay published in Nature.

Para-inflammation is not a classic form of inflammation triggered by exogenous tissue injury or infection, but it is switched on by tissue malfunction in order to promote its adaptation to a harmful environment and to maintain its adequate functionality. This state is characterized by a low-grade/sub-clinical immune reaction (Medzhitov 2008). Nevertheless, if the tissue malfunction is present for a sustained period, *para-inflammation* progresses into a chronic low-grade inflammation (pathophysiological para-inflammation) (Nita, Grzybowski et al. 2014, Robinson, Lepus et al. 2016).

Chronic human diseases, including obesity, type 2 diabetes mellitus, atherosclerosis, neurodegenerative diseases and cancer, are characterized by the presence of chronic low-grade inflammation (Medzhitov 2010). In these diseases, there appears to be a vicious cycle connecting inflammation and the underlying pathological process (Medzhitov 2010, Robinson, Lepus et al. 2016). For example, obesity can lead to inflammation whereas chronic inflammation can promote obesity-associated diabetes in part by inducing insulin resistance (Hotamisligil 2006, Mraz and Haluzik 2014).

1.2.5 Pathological alterations associated with inflammation

1.2.5.1 Oxidative stress

Oxidative stress was classically defined as “an imbalance between prooxidant stress and oxidant defense” (Biswas 2016). A prooxidant is “any substance that can generate reactive species or induce oxidative stress” (Biswas 2016). On the other hand, an antioxidant is defined as “any substance capable of delaying or preventing oxidation of a certain substrate when present in low concentrations” (Biswas 2016). Nevertheless, recent evidence points out that the disruption of redox signaling is more important for inducing oxidative stress than the imbalance of prooxidants and oxidants or the consequences of their disproportion such as tissue damage (Biswas 2016). Thus, an update on oxidative stress definition has been proposed: “an imbalance between oxidants and antioxidants in favor of the oxidants, leading to a disruption of redox signaling and control and/or molecular damage”(Jones 2006).

Generation of oxidative stress can lead to oxidative damage to biomolecules, disruption of signal transduction, mutation and cell death (Biswas 2016).

During the inflammatory response, the activated phagocytic cells such as neutrophils and macrophages produce an extensive quantity of reactive species in order to eliminate the invading agents (Fialkow, Wang et al. 2007). Reactive species include ROS (e.g. superoxide and hydrogen peroxide), RNS [e.g. nitric oxide (NO) and peroxynitrite] and reactive chlorine species (e.g. hypochlorous acid) (Biswas 2016). Nevertheless, under pathological inflammatory conditions, an exaggerated generation of reactive species occurs and, consequently, those species “diffuse out of the phagocytic cells and can induce a localized oxidative stress and tissue injury” (Biswas 2016). Moreover, non-professional phagocytic cells such as pancreatic cancer cells (Wu, Lu et al. 2013), non-small cell lung cancer cells (Li, Lan et al. 2015) and chondrocytes (Mendes, Caramona et al. 2003) can also produce reactive species when stimulated with pro-inflammatory cytokines.

On the other way around, oxidative stress can induce inflammation (Biswas 2016). By activating the NLPR3 inflammasome or the transcription factor, Nuclear Factor kappa-light-chain-enhancer of activated B Cells (NF-κB), oxidative stress triggers the inflammatory pathway (Biswas 2016). For instance, oxidized mitochondrial DNA has been shown to activate the NLPR3 inflammasome and, consequently, the secretion of IL-1β during apoptosis (Shimada, Crother et al. 2012). Binding of oxidized Low-Density Protein (ox-LDL) to its receptor, Lectin-like Ox-LDL receptor-1 (LOX-1), may lead to NF-κB activation

and production of intracellular ROS in bovine aortic endothelial cells (Cominacini, Pasini et al. 2000).

Inflammation and oxidative stress are interdependent pathological processes that are involved in many chronic diseases. If inflammation appears first, oxidative stress will eventually develop and accentuate the inflammatory process or *vice-versa* (Biswas 2016). The interdependence of inflammation and oxidative stress is a vicious cycle that promotes the perpetuation of mechanism-driven chronic age-associated diseases.

1.2.5.2 Tissue remodeling

Repair of damaged tissues is a vital process that will end up restoring homeostasis (Kulkarni, Lichtnekert et al. 2016). The purpose of tissue remodeling is to orderly replace the damage or dead cells after injury (Wynn 2007). This process usually proceeds an inflammatory process (Kulkarni, Lichtnekert et al. 2016) and typically involves two distinct phases: a regenerative phase which is based on the replacement of injured cells by cells of the same type; and a phase named fibroplasia or fibrosis where normal parenchymal tissue is replaced by connective tissue (Wynn 2007). Nevertheless, in case of chronic inflammation, fibrosis goes out of control (Wynn 2007). Pathological fibrosis is characterized by an excessive deposition of extracellular matrix (ECM), mainly composed of Collagen I (Col I) (Suzuki, Hayashi et al. 2008). Main producers of ECM are myofibroblasts which directly derive from tissue-resident fibroblasts and have the ability to produce enormous amounts of Col I (Ueha, Shand et al. 2012, Suthahar, Meijers et al. 2017). Other sources of myofibroblasts have been suggested, such as bone marrow-derived fibrocytes and hepatic stellate cells (Ueha, Shand et al. 2012). Moreover, epithelial cells are described to trans-differentiate into myofibroblasts induced by chronic inflammation (Ueha, Shand et al. 2012). This process is known as epithelial- or endothelial-mesenchymal transition (EMT or EndMT) and is characterized by the loss of the original phenotypic features and functions of epithelial cells such as cell-cell adhesion and cell polarity, while acquiring migratory and invasive properties, as well as mesenchymal markers (Kryczka and Boncela 2017). Inflammatory cells of the immune system have also been implicated in fibrosis (Kulkarni, Lichtnekert et al. 2016). In particular, macrophages play an important role in maintaining ECM composition (Kulkarni, Lichtnekert et al. 2016). In most tissues, these immune cells are the main source of Matrix MetalloProteinases (MMPs) and Tissue

Inhibitors of MetalloProteinases (TIMPs) (Kulkarni, Lichtnekert et al. 2016). The balance between these two groups of enzymes determines ECM remodeling and, thus, its composition (Kulkarni, Lichtnekert et al. 2016).

Inflammatory mediators, including cytokines and chemokines released by activated tissue cells and infiltrating leukocytes, are potent inducers of tissue damage and fibroproliferative changes (Ueha, Shand et al. 2012, Kulkarni, Lichtnekert et al. 2016). Special emphasis is given to TGF-β (Gyorfi, Matei et al. 2018). TGF-β plays a central role in fibrosis since it induces fibroblast activation and differentiation into myofibroblasts (Kulkarni, Lichtnekert et al. 2016). Additionally, this growth factor also induces the expression of genes for ECM components such as *Col 1* (Kulkarni, Lichtnekert et al. 2016).

As a consequence, fibrosis severely impairs tissue architecture and function, eventually leading to organ damage and, consequently, failure (Suthahar, Meijers et al. 2017). For instance, synovial fibrosis, which is detected in later stages of osteoarthritis (OA), has been described as contributing to joint pain and stiffness, the main OA symptoms (Remst, Blaney Davidson et al. 2015).

1.2.5.3 Mitochondrial dysfunction

Mitochondria are organelles that play a vital role in homeostasis maintenance (Cherry and Piantadosi 2015). Impairment of mitochondria activity has been associated with inflammation (Lopez-Armada, Riveiro-Naveira et al. 2013, Cherry and Piantadosi 2015, van Horssen, van Schaik et al. 2017). Inflammatory mediators, such as IL-1β, TNF-α and NO, have been reported as leading to mitochondrial dysfunction in different types of cells, including cardiomyocytes (Zell, Geck et al. 1997), hepatocytes (Samavati, Lee et al. 2008), astrocytes (Motori, Puyal et al. 2013), adipocytes (Chen, Zhao et al. 2010, Hahn, Kuzmicic et al. 2014), chondrocytes (Maneiro, Lopez-Armada et al. 2005, Lopez-Armada, Carames et al. 2006) and synovial cells (Cillero-Pastor, Martin et al. 2011). For instance, TNF-α and IL-1β induced inhibition of complex I of mitochondrial respiratory chain, ATP production and mitochondrial membrane potential in human chondrocytes (Lopez-Armada, Carames et al. 2006).

On the other hand, mitochondrial dysfunction can also trigger inflammation via ROS generation or the release of mitochondrial intracellular content such as mitochondrial DNA and ATP. (Lopez-Armada, Riveiro-Naveira et al. 2013, van Horssen, van Schaik et al. 2017).

The interrelationship between mitochondrial dysfunction and inflammation promotes a vicious inflammatory cycle that contributes to perpetuation of disease-driven mechanisms and failure to re-establish homeostasis (van Horssen, van Schaik et al. 2017).

1.2.5.4 Proteostasis abnormalities

Protein homeostasis or proteostasis regulates protein course from biogenesis to conformation folding, subcellular trafficking and degradation within the cells (Klaips, Jayaraj et al. 2018). By controlling protein fate, "proteostasis maintains the health of cells during development, aging and resistance to environmental stressors, as well as prevents disease elicited by excessive protein misfolding, aggregation or degradation" (Liu-Bryan and Terkeltaub 2015). This quality control process includes the Unfolded Protein Response (UPR), autophagy and the Ubiquitin-Proteasome System (UPS) (Liu-Bryan and Terkeltaub 2015).

The endoplasmic reticulum (ER) is a membrane-bound organelle which consists of interconnected highly branched tubules, vesicles and cisternae (Voeltz, Rolls et al. 2002). The main functions of the ER are translocation and integration of proteins, assistance in their folding and transport, lipid biosynthesis and maintenance of calcium homeostasis (Chaudhari, Talwar et al. 2014). Moreover, the ER is a site for post-translational modifications of proteins (Chaudhari, Talwar et al. 2014). However, the ER function is determined by cell type, cell function and cell needs (Chaudhari, Talwar et al. 2014).

Folding and modifications of proteins in the ER occur under the vigilance of ER resident molecular chaperones and folding enzymes (Chaudhari, Talwar et al. 2014). When unassembled, misfolded or unfolded proteins occur, the ER has the ability to remove them from its lumen to the cytosol for subsequent degradation by the UPS (Grootjans, Kaser et al. 2016). Nevertheless, when ER homeostasis is disturbed by several endogenous and exogenous stressors such as oxidative stress, abnormal calcium content, hypoxia, hyperlipidemia and viral infections, this organelle can become stressed or even dysfunctional (Chaudhari, Talwar et al. 2014, So 2018). In order to respond to those stressors, the ER triggers a protective mechanism termed UPR which aims to restore ER homeostasis (Chaudhari, Talwar et al. 2014, So 2018). The UPR is activated by the coordinated action of three ER transmembrane sensors: Inositol-Requiring Enzyme 1 (IRE1), double-stranded

RNA-activated Protein kinase R (PKR)-like ER Kinase (PERK) and Activating Transcription Factor 6 (ATF6) (Martins, Alves et al. 2016). Activation of the UPR promotes the expression of genes related to protein folding and degradation machinery induced by transcription factors such as ATF6, X-box-Binding Protein 1 (XBP1) and Activating Transcription Factor 4 (ATF4) (Chaudhari, Talwar et al. 2014). However, in case of severe and prolonged stress signals, the ER can elicit cell death pathways (Chaudhari, Talwar et al. 2014).

When triggered, the UPR promotes inflammation by activating NF-κB, the master transcriptional regulator of pro-inflammatory pathways (Grootjans, Kaser et al. 2016). For instance, treatment of rat chondrocytes with thapsigargin, a classic ER stress inducer, leads to NF-κB activation, and consequently, to pro-inflammatory cytokine expression, namely TNF-α and IL-6 (Chen, Xie et al. 2018). However, the other way around is also possible (Hasnain, Lourie et al. 2012). Not as extensively studied as the ER stress as an inflammation trigger, inflammatory mediators have also been described as being capable of inducing UPR activation (Hasnain, Lourie et al. 2012, Grootjans, Kaser et al. 2016). In insulin-secreting INS1E cells, IL-1β increases ER stress in a NO dependent manner (Kacheva, Lenzen et al. 2011).

Autophagy is a physiological cellular mechanism whereby cytoplasmic material is delivered to the lysosome for degradation (Galluzzi, Baehrecke et al. 2017). Different routes of autophagy have been described, namely macroautophagy, microauthophagy and chaperone-mediated autophagy (Galluzzi, Baehrecke et al. 2017). Macroauthophagy is the most well characterized and involves the sequestration of cytoplasmic material, including soluble macromolecules and organelles, into a double or a multi-membrane-bound structure, named autophagosome, which will fuse with the lysosome, promoting degradation and recycling of its content (Galluzzi, Baehrecke et al. 2017). This section will focus only on macroautophagy, henceforth referred to simply as autophagy.

Under normal conditions, constitutive autophagy occurs as a housekeeping mechanism (Netea-Maier, Plantinga et al. 2016). However, autophagy can be activated during starvation and stress conditions such as hypoxia, increased ROS production, DNA damage, protein aggregates, damaged organelles or intracellular pathogens, in order to restore homeostasis (Qian, Fang et al. 2017).

Despite maintaining cell homeostasis, autophagy has been considered an important player in host defense (Cadwell 2016, Netea-Maier, Plantinga et al. 2016). By direct elimination of invading pathogens, control of adaptative immunity, induction of immune memory and modulation of inflammation, autophagy improves the defense mechanisms (Netea-Maier, Plantinga et al. 2016). As the inflammatory response is triggered, autophagy is also induced by activation of PRRs (Netea-Maier, Plantinga et al. 2016). For instance, it was reported that LPS, through activation of TLR4, leads to autophagy activation in primary human macrophages and in the murine macrophage cell line, RAW 264.7 (Xu, Jagannath et al. 2007). Besides PRRs, autophagy can also be induced by pro-inflammatory cytokines such as TNF-α and IL-1β (Netea-Maier, Plantinga et al. 2016). Thus, autophagy activation by sensors and mediators of the inflammatory pathway constitutes an important mechanism to contend the harmful stimuli responsible for homeostasis disequilibrium (Netea-Maier, Plantinga et al. 2016).

In case of abnormal inflammation, autophagy is also triggered to protect cells from this exacerbated response and, consequently, restore homeostasis (Lapaquette, Guzzo et al. 2015, Netea-Maier, Plantinga et al. 2016). For instance, by regulating the inflammasome and secretion of IL-1β, autophagy may temper inflammation (Lapaquette, Guzzo et al. 2015, Netea-Maier, Plantinga et al. 2016). It was reported that autophagy controls the production of IL-1β by targeting its precursor for lysosomal degradation and by regulating NLRP3 inflammasome activation in antigen-presenting cells (Harris, Hartman et al. 2011). Autophagy mediated NLRP3 inflammasome inhibition by improving mitochondria quality control (Nakahira, Haspel et al. 2011, Zhou, Yazdi et al. 2011) and by removing mitochondrial ROS (Nakahira, Haspel et al. 2011, Zhou, Yazdi et al. 2011) and cytosolic translocation of mitochondrial DNA (Nakahira, Haspel et al. 2011). Moreover, it was demonstrated that inflammasome activation induces autophagy in order to limit its activity by physical engulfment (Shi, Shenderov et al. 2012). Although these autophagy effects on inflammasome activation and IL-1β production represent the most studied aspect of the interaction between inflammation and autophagy, there are other mechanisms possibly involved (Lapaquette, Guzzo et al. 2015, Netea-Maier, Plantinga et al. 2016, Qian, Fang et al. 2017).

According to the literature, it is well-established that autophagy declines with age (Lopez-Otin, Blasco et al. 2013, Leidal, Levine et al. 2018), allowing the exacerbation of the

inflammatory process. Thus, impairment of autophagy "predisposes individuals to age-associated diseases" (Leidal, Levine et al. 2018), especially those associated with chronic low-grade inflammation (Medzhitov 2008). For example, impaired autophagy in neurons contributes to the accumulation of damaged organelles and toxic protein aggregates which are associated with neurodegenerative diseases (Leidal, Levine et al. 2018). In Parkinson´s Disease, perturbations of autophagy lead to accumulation of α-synuclein (Leidal, Levine et al. 2018) which will elicit microglia activation and, consequently, a neuroinflammatory process (Zhang, Xia et al. 2018). Another age-associated disease where autophagy is compromised is OA (Carames, Taniguchi et al. 2010). Using an *in vivo* model of OA, treatment with an autophagy inducer, rapamycin, led to a reduction in the severity of the disease, accompanied by an increase in cell number and decreased expression of IL-1β and the aggrecan-degrading enzyme, ADAMTS5 (Caramés, Hasegawa et al. 2012).

The UPS is the primary source of protein degradation (Labbadia and Morimoto 2015) and accounts for approximately 80-90% of cell protein breakdown (Serrano, Chen et al. 2018). In the UPS, proteins are initially targeted for degradation by the ubiquitination apparatus (Labbadia and Morimoto 2015). Then, the ubiquitinated substrates are recognized, unfolded and proteolyzed by the proteasome (Thibaudeau and Smith 2019). The proteasome is located in the cytosol and requires ATP to exert its function (Thibaudeau and Smith 2019). The assembly of several subunits forms the proteasome, usually, referred to as the 26S proteasome (Thibaudeau and Smith 2019). This molecular machine is composed by a core catalytic particle, named 20S proteasome, and by a regulatory part, termed 19S proteasome, which limits one or both ends of the core (Thibaudeau and Smith 2019). Proteasome activity is modulated by different regulators and conditions (Thibaudeau and Smith 2019). Besides the maintenance of proteostasis, the proteasome is involved in many other physiologic processes such as cell cycle regulation, neuronal function, ER-associated protein degradation and NF-κB activation (Thibaudeau and Smith 2019). The proteasome mediates the degradation of regulatory elements required for activation of NF-κB via the canonical and noncanonical pathways (Thibaudeau and Smith 2019). The relevance of this proteasome function is well illustrated by studies in a rat model of OA where the use of a proteasome inhibitor, MG-132, effectively alleviated cartilage degradation and synovial inflammation by decreasing the expression of NF-κB/p65 and its endogenous inhibitor, IκB-α, MMP-9

and cyclooxygenase (COX)-2, as well as the protein levels of TNF-α and IL-1β in the synovial fluid, probably by blocking the IL-β/IKKβ/NF-κB signaling pathway (Ye, Qing et al. 2017). On the other hand, it was also suggested that there is a proteasome impairment in human knee OA since the 26S proteasome subunit, non-ATPase 11 (PSMD11), was found to be decreased in OA chondrocytes and its overexpression resulted in increased proteasome function and levels of SRY-box transcription factor 9 (SOX9)-induced aggrecan and collagen 2 mRNA expression, as well as in the inhibition of the extracellular levels of NO and MMP-13 induced by IL-1β (Serrano, Chen et al. 2018).

1.2.5.5 Cellular senescence

Cellular senescence is a state of permanent cell cycle arrest occurring when telomere length decreases below a critical size, in response to different damaging stimuli, such as oxidative stress and DNA damage (Hernandez-Segura, Nehme et al. 2018, Calcinotto, Kohli et al. 2019). This is an important barrier mechanism to tumorigenesis by limiting the growth of potentially oncogenic cells (Calcinotto, Kohli et al. 2019). Moreover, cellular senescence plays a key role in some physiological processes such as embryogenesis, tissue remodeling and tissue repair (Calcinotto, Kohli et al. 2019).

The senescent phenotype is characterized by chronic activation of the DNA damage response, upregulation of cyclin-dependent kinase inhibitors (e.g. $p16^{INK4a}$, $p15^{INK4b}$ and $p21^{CIP}$), apoptosis resistance, altered metabolic rates, ER stress and increasing secretion of proinflammatory and tissue-remodeling factors, known as the Senescence-Associated Secretory Phenotype (SASP) or senescence-messaging secretome (SMS) (Hernandez-Segura, Nehme et al. 2018). The SASP is quite important to ensure the efficient growth arrest by autocrine signaling, in particular immediately after senescence induction, to signal senescent cells for clearance by the immune system and, consequently, for tissue repair and remodeling (Freund, Orjalo et al. 2010, Soto-Gamez and Demaria 2017). Moreover, the SASP is highly heterogenous (Hernandez-Segura, Nehme et al. 2018) and can include a wide range of cytokines (e.g. IL-6 and IL-1), chemokines (e.g. IL-8, Monocyte chemotactic Protein-2 and-3), proteases (e.g. MMP-1, MMP-3), growth factors [e.g. Granulocyte Macrophage Colony-Stimulating Factor (GM-CSF), Growth Regulated Oncogene (GRO) α, Insulin-like Growth Factor (IGF)-binding proteins and Vascular Endothelial Growth Factor (VEGF)] (Freund, Orjalo et al. 2010) and non-macromolecular elements (e.g. NO and ROS)

(Calcinotto, Kohli et al. 2019). Although various signaling pathways are involved in the regulation of SASP components, most of them converge at NF-κB activation (Freund, Orjalo et al. 2010, Calcinotto, Kohli et al. 2019). Moreover, activation of the transcription factor CCAAT/Enhancer Binding Protein beta (C/EBPβ) also plays an important role in the expression of SASP components (Freund, Orjalo et al. 2010, Calcinotto, Kohli et al. 2019).

Morphologically, senescent cells show structural aberrations, from enlarged and more flattened shape, changed composition of the plasma membrane by an upregulation of caveolin-1, increased lysosomal content which is directly correlated with higher senescence-associated beta-galactosidase activity at pH 6.0, accumulation of mitochondria and nuclear changes, such as loss of Lamin B1 and formation of senescence-associated heterochromatin *foci* (Hernandez-Segura, Nehme et al. 2018).

Excessive and anomalous accumulation of senescent cells in tissues has a negative impact on homeostasis mainly via SASP (Soto-Gamez and Demaria 2017). This phenomenon can be detrimental to regenerative capacities and generate a disruptive proinflammatory environment that is favorable for the onset and progression of a variety of age-related diseases (Soto-Gamez and Demaria 2017, Hernandez-Segura, Nehme et al. 2018). The accumulation of these cells can occur with age and at sites of age-related diseases such as atherosclerosis and OA (Calcinotto, Kohli et al. 2019). In particular, OA hallmarks include inflammation and tissue degradation which can be mediated by SASP components (Jeon, David et al. 2018). For instance, senescent chondrocytes were identified in human cartilage tissues and their localization was predominantly near osteoarthritic lesions (Price, Waters et al. 2002). Moreover, accumulation of these cells was associated with aging (Martin, Brown et al. 2004) and their selective elimination was shown to ameliorate injury- and age-induced OA (Jeon, Kim et al. 2017). The senescent chondrocyte SASP can promote and/or exacerbate the inflammatory process and the imbalance between synthesis and degradation of the ECM by having IL-1β, IL-6, IL-8, MMP-1 and MMP-13 in its secretory phenotype (Jeon, David et al. 2018). Another study showed that extracellular vesicles produced by senescent chondrocytes isolated from human arthritic cartilage can propagate senescence to non-senescent chondrocytes and inhibit their ability to synthesize ECM components (Jeon, Wilson et al. 2019). Taken together, these studies clearly establish a significant pathophysiologic role for senescent cells in OA and most likely in many other age-related diseases.

1.2.5.6 Cell death

Cell death is characterized by an irreversible degeneration of vital cellular functions which culminate in the loss of cellular integrity (Galluzzi, Vitale et al. 2018). Particularly in host defense, cell death is a mechanism that aims to restore homeostasis (Yang, Jiang et al. 2015). For instance, activation of PRRs, such as TLRs and NLRs, by pathogens and their components, can induce apoptosis, a programmed type of cell death. (Yang, Jiang et al. 2015, Amarante-Mendes, Adjemian et al. 2018). During the resolution of inflammation, previously activated neutrophils undergo apoptosis (Basil and Levy 2016).

The release of inflammatory mediators, such as NO (Blanco, Ochs et al. 1995, Snyder, Shroff et al. 2009), IL-1β and TNF-α (Lopez-Armada, Carames et al. 2006), can induce cell death in various cell types. Moreover, neutrophils, which are recruited during the inflammatory process, have the propensity to release destructive enzymes into the extracellular space (Martin 2016). This can lead to undesirable collateral tissue damage that can further end up in cell death and exacerbation of the inflammatory process (Martin 2016).

Apart from being a consequence of inflammation, cell death can also be its cause (Amarante-Mendes, Adjemian et al. 2018). There are some types of cell death, such as necrosis, necroptosis and pyroptosis, which are characterized by the release of intracellular materials that act as DAMPs (Yang, Jiang et al. 2015, Amarante-Mendes, Adjemian et al. 2018).

To sum up, inflammation can be the cause and/ or consequence of other pathological alterations, giving emphasis to the fact that inflammation is a “common soil” for all the mentioned alterations (Fig.4).

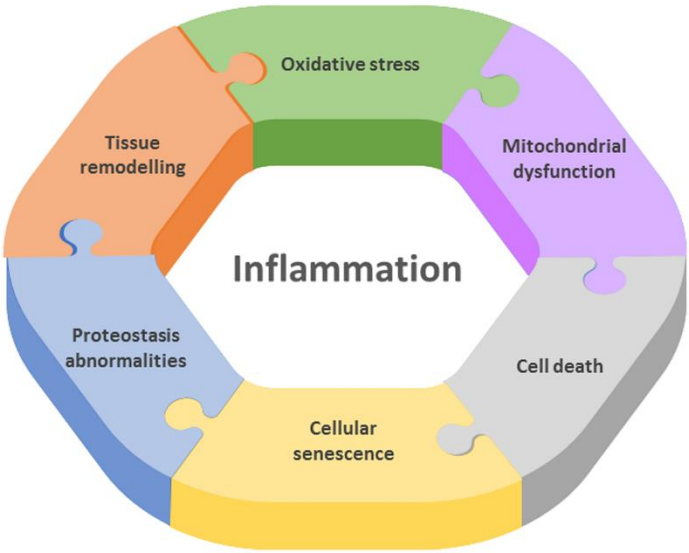

Figure 4. Pathological alterations associated with inflammation.

1.2.6 NF-κB – the master regulator of inflammation

NF-κB was first identified in 1986 as transcription factor with specific binding affinity for the decameric DNA sequence 5´-GGACTTTCC-3´ located within the enhancer region of the immunoglobulin kappa (κ) light chain gene in mature B and plasma cells (Sen and Baltimore 1986). Due to this, this transcription factor was named according to the cell type in which it was identified and the gene that was affected (Zhang, Lenardo et al. 2017). Although it was identified in B-lymphoid cells, NF-κB is ubiquitously present in most cell types (Sen and Baltimore 1986, Zhang, Yousefzadeh et al. 2019) and its transcriptional activity is inducible by a wide range of endogenous and exogenous stimuli (Lee and Burckart 1998, Pahl 1999, Tilstra, Clauson et al. 2011) with the exception of B cells, certain T cell lines, monocytes and neurons which present constitutive NF-κB activity (Schmitz and Baeuerle 1995). NF-κB regulates the expression a large number of genes that encode for cytokines (e.g. IL-1β and IL-6), chemokines (e.g. IL-8), cell adhesion molecules (e.g. vascular cell adhesion molecule-1 and intracellular adhesion molecule-1), acute phase proteins (e.g. C-reactive protein), immunoreceptors (e.g. immunoglobulin κ light chain), proteins involved in antigen presentation (e.g. proteasome subunit LMP2), stress response genes [e.g. inducible NO synthase (iNOS or NOS2) and COX2], cell surface receptors (e.g. receptor for advanced glycation end products), apoptosis regulators (e.g. Bcl-2 and other inhibitors of apoptosis), growth factors (e.g. GM-CSF and VEGF), early response genes (e.g. p62), transcription factors (e.g. proto-oncogene c-myc and tumor suppression p53), enzymes (e.g. Collagenase I and Gelatinase B) and many other genes (Pahl 1999, Kumar, Takada et al. 2004, Tilstra, Clauson et al. 2011). Normal activation of NF-κB is vital for many physiological functions such as innate and adaptative immunity, stress responses, metabolism, proliferation, apoptosis and differentiation (Kumar, Takada et al. 2004, Mauro, Leow et al. 2011, Zhang, Yousefzadeh et al. 2019). Nevertheless, persistent and chronic activation of NF-κB is associated with various pathological conditions (Kumar, Takada et al. 2004), namely cardiovascular diseases (Fiordelisi, Iaccarino et al. 2019), cancer (Xia, Tan et al. 2018), OA (Choi, Jo et al. 2019), neurodegenerative diseases (Sivandzade, Prasad et al. 2019), chronic obstructive airway disease (Schuliga 2015) and diabetes (Suryavanshi and Kulkarni 2017). Apart from its role in human disease, NF-κB has been described as a driver of the aging process (Salminen and Kaarniranta 2009, Lopez-Otin, Blasco et al. 2013,

Osorio, Soria-Valles et al. 2016), being an important player in the pathogenesis of age-associated diseases.

1.2.6.1 The NF-κB family: molecular constituents, structure and interactions

The NF-κB or Rel family of transcription factors is comprised of five members: p50, p52, p65/RelA, c-Rel and RelB which are encoded by NFKB1, NFKB2, RELA, REL and RELB, respectively (Hayden and Ghosh 2008, Zhang, Lenardo et al. 2017). These constituents share a highly conserved 300 amino acid long N-terminal Rel Homology Domain (RHD) responsible for DNA-binding to the NF-κB consensus sequence (5′-GGGRNWYYCC-3′ where R = adenine or guanine; N = any nucleotide; W = adenine or thymine; Y = cytosine or thymine), homo- and hetero- dimerization and inhibitory protein binding (Fig.5) (Hayden and Ghosh 2008, Zhang, Lenardo et al. 2017). Another region, the nuclear localization sequence (NLS), is located after the RHD and is essential for nuclear import (Zhang, Lenardo et al. 2017). However, the members of the NF-κB family differ in the presence of a transactivation domain (TAD) in the C-terminus (Fig.5) (Zhang, Lenardo et al. 2017). p50 and p52 do not contain a TAD, whereas p65/RelA, RelB and c-Rel do have one or more of such domains (Zhang, Lenardo et al. 2017). Another aspect that differentiates p50 and p52 from the other members of the NF-κB family is the fact that the former arise from partial proteolysis of the precursor proteins, p105 (NFKB1) and p100 (NFKB2), respectively, that cleaves off a C-terminal region containing Ankyrin Repeats (AnkR) and a Death Domain (DD)" (Fig.5) (Zhang, Lenardo et al. 2017). Moreover, the C-terminal region of these precursors also contains a Glycine-Rich Region (GRR), which remains after proteolytic processing to yield the mature p50 and p52 proteins (Fig.5) (Hayden and Ghosh 2008, Mulero, Huxford et al. 2019).

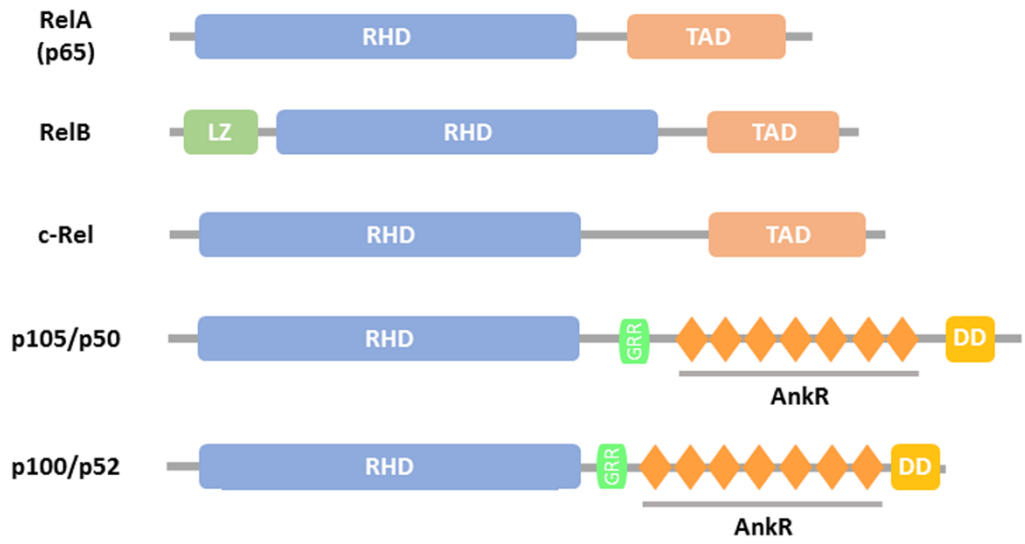

Figure 5. The NF-κB protein family. Domains that characterize the NF-κB protein family are indicated. AnkR, Ankyrin Repeats; DD, Death Domain; GRR, Glycine-Rich Region; LZ, Leucine Zipper; RHD, Rel Homology Domain; TAD, Transcription Domain.

Rel/NF-κB transcription factors bind to 10 base pair DNA sites as dimers (homo or heterodimers) since the monomers are unstable (Mitchell, Vargas et al. 2016, Zhang, Yousefzadeh et al. 2019). Among the 15 possible dimers (Fig.6), only 12 have sufficiently high affinity to stably bind the DNA κB element, whereas those containing RelB bound to any other Rel family member (RelB:RelB, RelB:RelA and RelB:RelC) form low-affinity dimers that are unable to bind DNA (Mitchell, Vargas et al. 2016). Of the 12 DNA binding dimers (Fig.6), only those that contain at least one Rel family member, namely RelA, RelB and c-Rel, can function as transcription activators since only these proteins contain the required TAD (Mitchell, Vargas et al. 2016). The remaining three dimers, including p50:p50, p52:p52 and p50:p52, function essentially as transcriptional repressors because they can bind DNA, but lack the TAD. Nonetheless, these dimers can contribute to activate transcription when they associate with co-activators (Mitchell, Vargas et al. 2016).

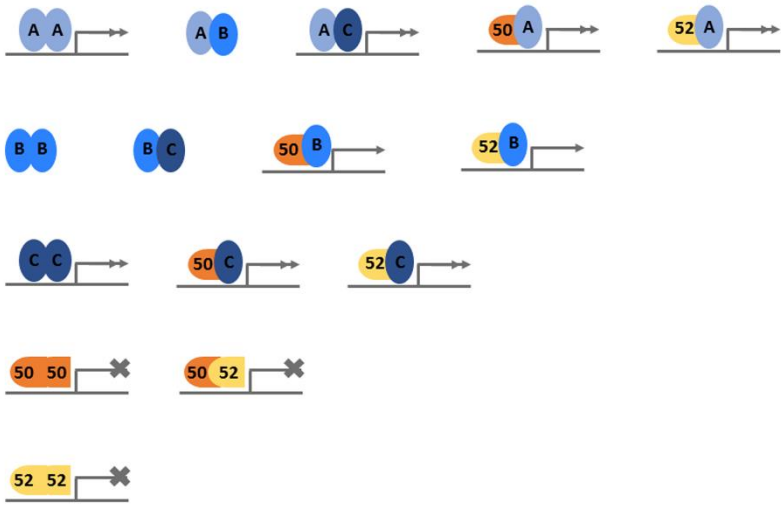

Figure 6. The NF-κB dimers. Combinatorial composition of potential NF-κB dimers, indicating their capacity to bind DNA (indicated by horizontal grey line) and to activate transcriptions (indicated by grey arrows). A – RelA/p65; B – RelB; C – c-Rel; 50 – p50; 52 – p52. Reproduced with permission from Mitchel, Vargas et al 2006.

It has been reported that the different NF-κB family members have distinct dimerization affinities (Mitchell, Vargas et al. 2016). Tsui and co-workers reported affinities of the RelA:p50, p50:p50 and RelA:RelA dimers to be in the range of 1-5 nM, 20-50 nM and 0.8-1.5 μM, respectively (Tsui, Kearns et al. 2015). Moreover, dimerization stability is another crucial parameter (Mulero, Huxford et al. 2019) also correlated with affinity. Thus, the predicted rank of dimerization stability is: RelA:p50 > p50:p50 > RelA:RelA (Mulero, Huxford et al. 2019). The most thermodynamically stable, RelA:p50, is the most ubiquitous NF-κB dimer (Mulero, Huxford et al. 2019). Taken together, the generation of NF-κB dimers is a highly dynamic mechanism that can also depend on the cell type and the trigger stimuli (Mitchell, Vargas et al. 2016, Mulero, Huxford et al. 2019).

As mentioned before, NF-κB dimers bind to a specific double-stranded κB DNA element placed within the promoters or enhancers of numerous target genes (Mulero, Huxford et al. 2019). These κB sites are "pseudosymmetric containing two nearly identical half sites" (Mulero, Huxford et al. 2019). Each component of the NF-κB dimer binds to a half site through the RHD located in the N-terminus (Mulero, Huxford et al. 2019).

1.2.6.2 The IκB family: molecular constituents, structure and interactions

Inhibitors of κB activity, also known as IκB, are important players in the NF-κB signaling pathway (Hayden and Ghosh 2008, Mulero, Huxford et al. 2019). Proteins of this family act as inhibitors of NF-κB through non-covalent binding which interferes with its nucleocytoplasmic dynamics and, consequently, blocks its DNA binding (Mulero, Huxford et al. 2019). All IκB proteins are characterized by the presence of multiple ankyrin repeats, which are 33 amino acid ankyrin-like protein-protein association domains (Mulero, Huxford et al. 2019) and are functionally classified into three distinct groups: classical IκB, precursor IκB and nuclear or “atypical“ IκB (Mulero, Huxford et al. 2019) (Fig.7).

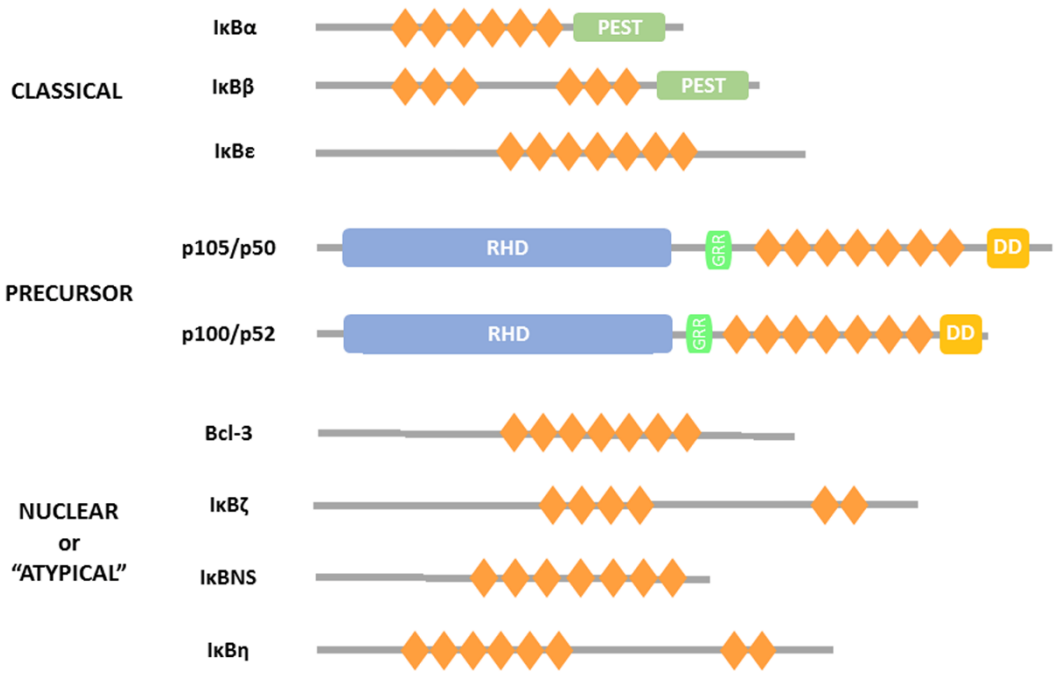

Figure 7. Members of the IκB family. Domains that characterize the IκB family are shown as well as its division into three groups according to functionality. AnkR, Ankyrin Repeats; DD, Death Domain; GRR, Glycine-Rich Region; PEST, region rich in the amino acids proline (P), glutamic acid (E), serine (S) and threonine (T); RHD, Rel Homology Domain.

The classical or canonical IκB proteins include IκB-α, IκB-β and IκB-ε, which are encoded by the *nfκbia*, *nfκbib* and *nfκbie* genes, respectively (Hayden and Ghosh 2008). In addition to ankyrin repeat domains, each IκB protein contains a signal-responsive domain that contains phosphorylation and ubiquitination sites in the N-terminus (O'Dea and Hoffmann 2009, Mulero, Huxford et al. 2019). In the C-terminus, IκB-α and IκB-β have a flexible region "rich in the amino acids proline, glutamic acid, serine and threonine that is called a PEST domain" (Hayden and Ghosh 2008, Mulero, Huxford et al. 2019) (Fig.7). This PEST domain is commonly found in proteins which have a rapid proteolytic turnover in cells (Mulero, Huxford et al. 2019). IκB-α is the prototypical and most extensively studied member of this family (Hayden and Ghosh 2008, Mulero, Huxford et al. 2019). Due to its folding, IκB-α is thermodynamically instable, being rapidly degraded in cells by a mechanism dependent on its own PEST domain and the 20S proteasome (Mulero, Huxford et al. 2019). However, the stability of IκB-α significantly increases when bound to NF-κB dimers and its degradation becomes dependent on signaling events (Mulero, Huxford et al.

2019). Among the NF-κB dimers, RelA/p65:p50 is the main target of IκB-α (Hayden and Ghosh 2008). In resting cells, this NF-κB dimer is sequestered in the cytoplasm by IκB-α (Hayden and Ghosh 2008). By analyzing the crystal structure of the complex IκB-α:RelA/p65:p50, it was demonstrated that the "IκB-α protein masks only the NLS of RelA/p65 whereas that of p50 remains exposed" (Hayden and Ghosh 2008, Mulero, Huxford et al. 2019). The exposed NLS of p50 joins to nuclear export sequences (NES) of IκB-α and Rel A, being responsible for the constant transport of the complex IκB-α:RelA/p65:p50 between the cytoplasm and the nucleus (Hayden and Ghosh 2008). The NLS of RelA/p65 is masked by the combination of PEST domain residues and the sixth ankyrin repeats of IκB-α which "creates a vast acidic surface that appears to electrostatically attract the N-terminus of Rel A" to a considerably different position from that found when it is bound to DNA (Mulero, Huxford et al. 2019). When the signaling pathway is triggered, IκB-α undergoes posttranslational modifications (PTM) that lead to its degradation and consequent release and nuclear translocation of NF-κB dimers (Mitchell, Vargas et al. 2016). In addition to retaining NF-κB dimers, in particular RelA:p50, in the cytoplasm, IκBα is also capable of stripping NF-κB off DNA (Mitchell, Vargas et al. 2016, Mulero, Huxford et al. 2019). This mechanism of "molecular stripping" is based on the fact that the PEST sequence of IκB-α which is negatively charged, interacts with the positive charged residues of the DNA-binding pocket of NF-κB leading to an electrostatically repulsion of NF-κB from DNA (Mulero, Huxford et al. 2019). Moreover, this mechanism is also described as a negative feedback loop since NF-κB is the transcription factor responsible for IκB-α expression (Mitchell, Vargas et al. 2016). It is important to emphasize that IκB-α degradation and resynthesis are rapid processes (Mitchell, Vargas et al. 2016). For instance, after 30 minutes of exposure to LPS, IκB-α was completely degraded and its re-synthesis was detected upon 1 hour of LPS treatment in the Raw 264.7 cell line (Campa, Iglesias et al. 2005).

Like IκB-α, IκB-ε expression is upregulated by NF-κB and, consequently, exerts a negative feedback loop (Hayden and Ghosh 2008). However, its degradation and resynthesis are delayed compared to IκB-α, by almost 45 minutes (O'Dea and Hoffmann 2009). This antiphase negative feedback loop was suggested to dampen IκB-α-mediated oscillations (Mitchell, Vargas et al. 2016). On the other hand, IκB-ε does not possess a PEST domain and is mainly expressed in hematopoietic cells (Hayden and Ghosh 2008) (Fig.7).

IκB-β is another member of this group. Similar to IκB-ε, it has a slower degradation and re-synthesis cycle (Hayden and Ghosh 2008). Nevertheless, its expression is not dependent on NF-κB transcriptional activity and, consequently, it cannot exert a feedback loop (Mitchell, Vargas et al. 2016). Moreover, IκB-β is not able to strip NF-κB off DNA (Mitchell, Vargas et al. 2016). However, a hypophosphorylated form of IκB-β is capable of associating with NF-κB dimers bound to DNA in order to prolong the transcriptional activity in certain cell types, after stimulation (Hayden and Ghosh 2008, Scheibel, Klein et al. 2010).

The precursor IκB proteins comprise p100 and p105 (Mulero, Huxford et al. 2019). Despite being the immature precursors of NF-κB subunits, unprocessed p100 and p105 act as inhibitors of NF-κB and are referred to as IκB-δ and IκB-γ, respectively (Mulero, Huxford et al. 2019). By forming multimeric high molecular weight complexes, p100 and p105 bind all NF-κB subunits, excluding p50 and RELB, respectively, and, consequently, act as IκB-like molecules (Mitchell, Vargas et al. 2016, Mulero, Huxford et al. 2019). These multi-protein inhibitory complexes have been referred to as "kappaBsomes"(Mulero, Huxford et al. 2019).

The nuclear or "atypical" IκB proteins include Bcl-3, IκB-ζ, IκB-NS and IκB-η (Mulero, Huxford et al. 2019). Since these proteins contain ankyrin repeats and bind with specificity to NF-κB, they are classified as IκB proteins (Mulero, Huxford et al. 2019). Nevertheless, nuclear IκB proteins function to modulate the transcriptional activity of NF-κB in the nucleus, unlike classical IκB proteins which function as inhibitors of NF-κB activation in the cytoplasm (Mitchell and Carmody 2018).

1.2.6.3 IκB kinase complex

The IκB Kinase (IKK) complex catalyzes the key event in the activation of the NF-κB signaling pathway which is the PTM of IκB proteins that leads to the release of NF-κB dimers (Mitchell and Carmody 2018, Mulero, Huxford et al. 2019).

The IKK complex is composed of three subunits (Hayden and Ghosh 2008, Mulero, Huxford et al. 2019). Two of these polypeptides, IKKα (also known as IKK1) and IKKβ (also known as IKK2), are the catalytic kinase subunits, while the third polypeptide, NF-κB Essential Modulator (NEMO) or IKKγ, is the regulatory subunit (Hayden and Ghosh 2008,

Mulero, Huxford et al. 2019). IKKα and IKKβ "share nearly 50% sequence identity" and contain serine/ threonine kinase domains at their N-terminus, dimerization domains which include leucine zippers and helix-loop-helix motifs and a C-terminal NEMO-Binding Domain (NBD) (Karin 1999, Mulero, Huxford et al. 2019) (Fig.8). Despite sharing a similar domain organization, IKKα, but not IKKβ, contains a putative NLS (Mulero, Huxford et al. 2019). Regarding NEMO, it lacks a kinase domain and its structure is dominated by alpha-helical elements, including two coiled-coil domains, a leucine zipper and a C-terminal zinc-finger region (Hinz and Scheidereit 2014, Mulero, Huxford et al. 2019) (Fig.8).

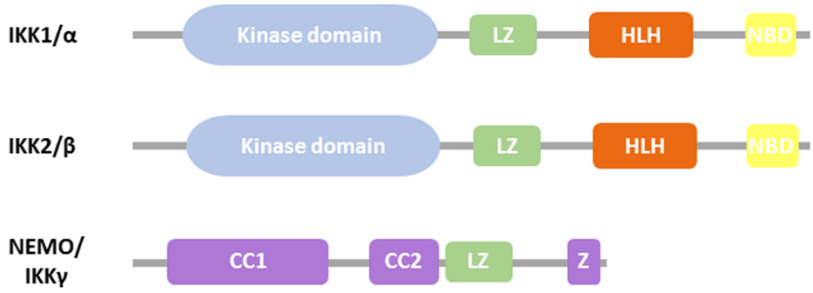

Figure 8. Members of the IKK family. Domains that characterize the IKK family. CC1/2, Coiled-Coil domain 1/2; HLH, Helix-Loop-Helix domain; LZ, Leucine Zipper domain; NBD, NEMO-Binding Domain; Z, zinc finger domain.

The two catalytic subunits of IKK (IKKα and IKKβ) dimerize through the leucine zipper domain, which is also a requirement for the kinase activity (Karin 1999, Hayden and Ghosh 2008). Heterodimers of IKKα and IKKβ are preferentially formed *in vivo* and *in vitro* studies demonstrated that heterodimers have higher catalytic efficiency than homodimers (Huynh, Boddupalli et al. 2000). Although both catalytic IKK subunits have a NBD in the C-terminus, NEMO interacts preferentially with IKKβ for which it has considerably higher affinity than for IKKα (Huynh, Boddupalli et al. 2000, Hayden and Ghosh 2008). In the resting state, IKKα and IKKβ heterodimers are held inactive through their interaction with NEMO (Hayden and Ghosh 2008). Upon stimulation, a conformational change of NEMO is induced, allowing transautophosphorylation or IKK kinase phosphorylation of the IKK T loop serine residues (Hayden and Ghosh 2008). Then, active IKK phosphorylates its substrates that will end up in the activation of NF-κB transcriptional activity (Hayden and Ghosh 2008, Osorio, Soria-Valles et al. 2016).

1.2.6.4 NF-κB signaling pathway

NF-κB transcriptional activity is activated by two different routes (Mulero, Huxford et al. 2019). These two are referred to as the classical or canonical and the alternative or noncanonical NF-κB signaling pathways (Hayden and Ghosh 2004, Mulero, Huxford et al. 2019). A key step in both these signaling pathways is the PTM of IκB proteins by the IKK complex (Mitchell and Carmody 2018). Therefore, activation of the IKK complex is essential in both the classical and the alternative NF-κB signaling pathways (Mitchell and Carmody 2018). Nevertheless, only the classical NF-κB signaling pathway is NEMO-dependent (Hayden and Ghosh 2008, Mitchell, Vargas et al. 2016).

Classical NF-κB signaling pathway

The classical NF-κB signaling pathway can be initiated by physiological stimuli through cytokines receptors (e.g. IL-1 receptor and TNF receptor), PRRs (e.g. TLRs), antigen receptors (e.g. T-cell receptor and B-cell receptor) and growth receptors (Zhang, Yousefzadeh et al. 2019). The binding of specific ligands (e.g. LPS and IL-1β) to those receptors relays the signal transduction into the cytoplasm by recruiting different adaptor proteins (Wong and Tergaonkar 2009, Zhang, Yousefzadeh et al. 2019). Then, subsequent signaling cascades converge on the IKK complex (Wong and Tergaonkar 2009, Zhang, Yousefzadeh et al. 2019). Here, NEMO can interact with upstream proteins of the signaling cascades [e.g. Tumor necrosis factor Receptor-Associated Factors (TRAFs) and Receptor-Interacting Proteins (RIPs) or IL-1 Receptor Associated Kinases (IRAKs)] which can induce a conformational change that allows transautophosphorylation or phosphorylation of the IKK T loop serine residues by upstream kinases [e.g. TGF-β-Activated Kinase-1(TAK1)] (Hayden and Ghosh 2008, Zhang, Yousefzadeh et al. 2019). The activated IKK complex, in particular IKKβ, phosphorylates IκB-α on serine (Ser) 32 and 36 residues (Zhang, Yousefzadeh et al. 2019). This PTM targets IκB-α for polyubiquitination by the $SCF^{\beta\text{-}TRCP}$ ubiquitin ligase at lysine (Lys) 21 and Lys22 (Mitchell and Carmody 2018). Subsequently, this leads to IκB-α degradation by the 26S proteasome (Mitchell and Carmody 2018). Upon IκB-α degradation, NF-κB dimers, in particular RelA/p65:p50, are free to translocate into the nucleus where they can bind to specific DNA sequences, the κB sites present within promoter or enhancer regions of distinct target genes, and elevate their levels of transcription (Mitchell and Carmody 2018, Mulero, Huxford et al. 2019) (Fig.9).

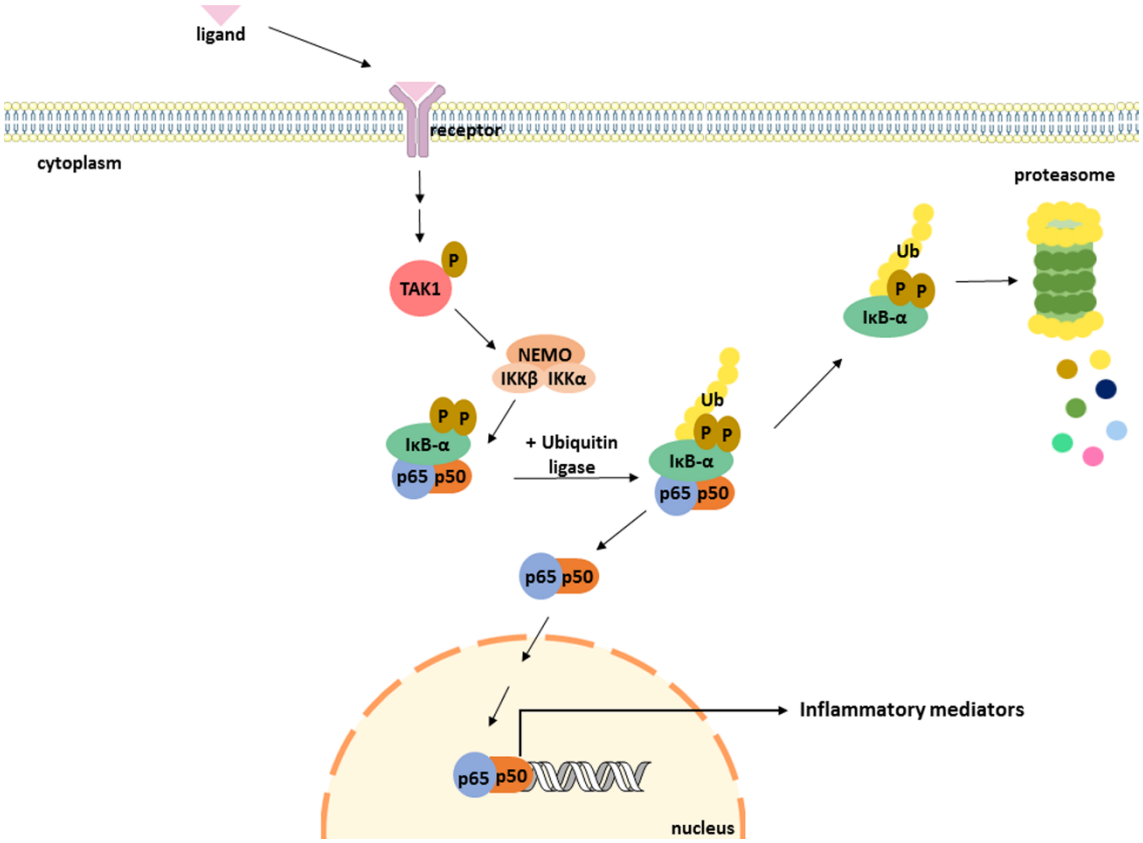

Figure 9. Classical NF-κB signaling pathway. Upon ligand binding to its specific receptor, adaptor proteins are activated and lead to TAK1 phosphorylation which triggers activation of the IKK complex. Then, the IKK complex, particularly IKKβ, phosphorylates IκB-α. This phosphorylation signals IκB-α for ubiquitination and, subsequently, proteasome degradation. After IκB-α degradation, freed NF-κB dimers (p65:p50) translocate to the nucleus where they bind to the κB sites, present within promoter regions of pro-inflammatory target genes, inducing their transcription. IκB-α, Inhibitor of κB activity; IKKα/β, IκB Kinase α/β; NEMO, NF-κB Essential Modulator; p65, RelA/p65; P, phosphate; Ub, Ubiquitin.

Alternative NF-κB signaling pathway

The alternative NF-κB signaling pathway is activated by non-inflammatory and developmental signals through specific receptors such as the LymphoToxin β Receptor (LTβR), B cell Activating Factor Receptor (BAFF-R) or CD40 (Mulero, Huxford et al. 2019). This pathway does not require IKKβ, but relies on NF-κB-Inducing Kinase (NIK) and IKKα homodimers (Mulero, Huxford et al. 2019, Zhang, Yousefzadeh et al. 2019). NIK is a serine/threonine kinase which is continuously ubiquitinated by E3 ligases and degraded in the proteasome in resting cells (Osorio, Soria-Valles et al. 2016, Zhang, Yousefzadeh et

al. 2019). Upon pathway activation, NIK degradation is prevented and, consequently accumulates in cells (Osorio, Soria-Valles et al. 2016). This NIK accumulation leads to phosphorylation of IKKα (Zhang, Yousefzadeh et al. 2019). Then, activated IKKα phosphorylates the precursor IκB protein, p100, which is in a complex with RelB (Sun 2017, Mulero, Huxford et al. 2019). Phosphorylation signals p100 as a substrate for ubiquitination via recruitment of the $SCF^{\beta\text{-}TRCP}$ ubiquitin ligase (Mulero, Huxford et al. 2019). This later PTM of p100 leads to a partial degradation by the 26S proteasome, generating the mature p52 monomer (Mulero, Huxford et al. 2019). Then, the p52 subunit is able to dimerize to form a transcriptionally active RelB:p52 and other NF-κB dimers (Mulero, Huxford et al. 2019). RelB:p52 heterodimers translocate to the nucleus, bind to specific DNA sequences, the κB sites (Mulero, Huxford et al. 2019). Activation of this NF-κB signaling pathway is associated to the regulation of important biological functions, such as adaptative immunity, lymphoid organogenesis, B-cell survival and maturation and dendritic cell activation (Sun 2011, Cildir, Low et al. 2016) (Fig.10).

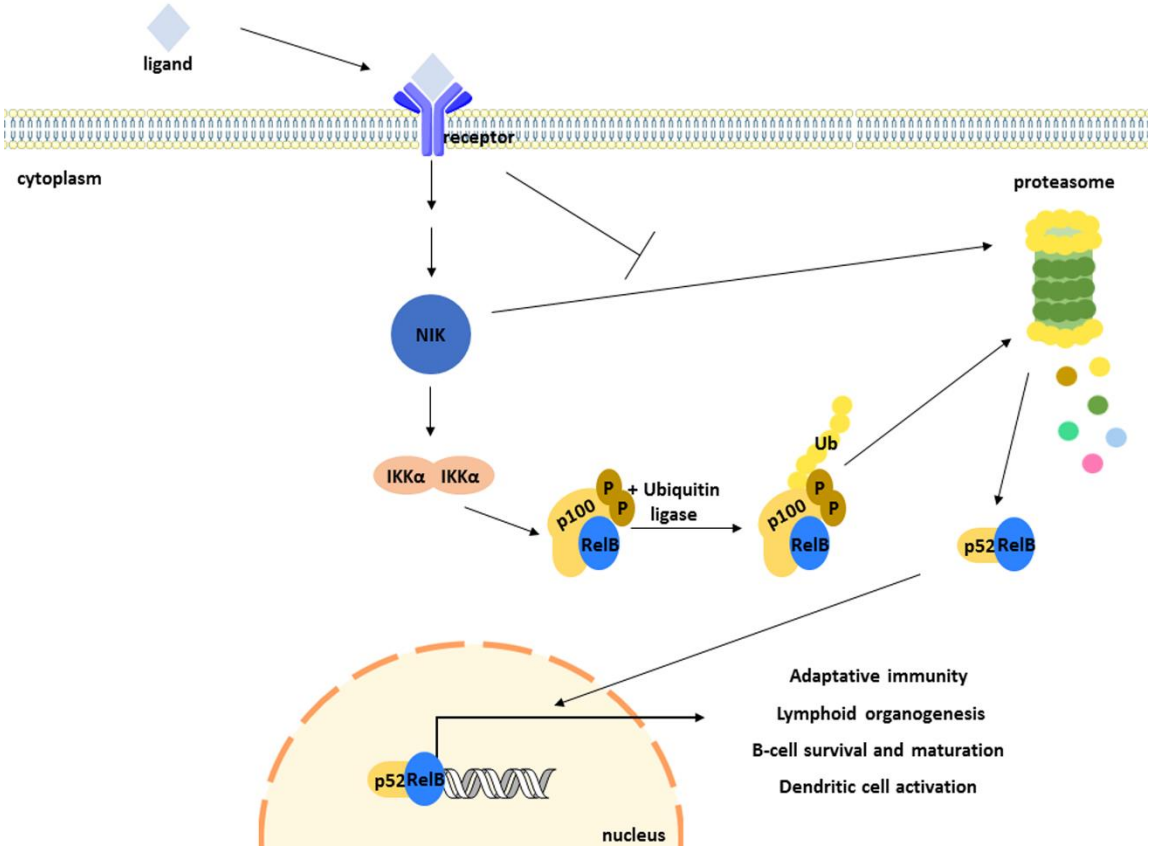

Figure 10. Alternative NF-κB signaling pathway. Upon ligand binding to its specific receptor, constitutive proteasome degradation of NIK is blocked, leading to its accumulation in the cytoplasm. Accumulation of NIK enables it to phosphorylate IKKα which becomes active and phosphorylates p100, that was acting as IκB in a complex with RelB. Phosphorylation of p100 triggers its ubiquitination and partial proteolysis in the proteasome. This partial degradation yields p52 which, dimerized with RelB, undergoes nuclear translocation, binds to specific DNA sequences, the κB sites present within promoter regions of distinct target genes, and induces their expression. IKKα, IκB Kinase α; NIK, NF-κB-Inducing Kinase; P, phosphate; Ub, Ubiquitin.

In comparison to the classical pathway, the alternative NF-κB signaling pathway is slower and its kinetics is dependent on the synthesis of new proteins (Mitchell and Carmody 2018). Despite acting independently, it was demonstrated that activation of the classical pathway regulates key components of the alternative signaling pathway (Basak, Shih et al. 2008).

Besides the classical and the alternative pathways, additional pathways of NF-κB activation exist and are termed *atypical pathways* (Zhang, Yousefzadeh et al. 2019). Physical, genotoxic, oxidative or organelle stresses, such as ultraviolet radiation, ionizing radiation, oxidative stress, hypoxia, dysfunctional mitochondria or ER stress, can lead to NF-κB activation via IKK-dependent and independent mechanisms (Perkins and Gilmore

2006, Zhang, Yousefzadeh et al. 2019) . However, these mechanisms are quite distinct from those found within the classical and the alternative NF-κB signaling pathways (Perkins and Gilmore 2006, Zhang, Yousefzadeh et al. 2019). For instance, hydrogen peroxide triggered NF-κB activation in a T lymphocytic cell line by inducing IκB-α phosphorylation at the tyrosine 42 residue and Ser/threonine residues of the PEST domain. IκB-α degradation involves calpain proteases and the proteasome. These findings pointed out new NF-κB activation mechanisms unrelated to those triggered by pro-inflammatory cytokines and mitogens (Schoonbroodt, Ferreira et al. 2000).

1.2.6.5 Regulation of NF-κB transcriptional activity

NF-κB is responsible for the expression of a variety of genes which could cause harmful consequences in case of dysregulation of this transcription factor (Mitchell and Carmody 2018). Therefore, there is the need for a tight control of NF-κB activity (Mitchell and Carmody 2018). As mentioned before, one of the mechanisms that limits NF-κB activity is through a negative feedback loop requiring NF-κB-induced IκB-α expression (Castro-Caldas, Mendes et al. 2003). Thus, newly synthesized IκB-α enters the nucleus, strips NF-κB off DNA and relocates it to the cytoplasm, thereby terminating NF-κB-directed transcription (Mitchell, Vargas et al. 2016, Mitchell and Carmody 2018). Nevertheless, this termination mechanism is not sufficient for the optimal control of NF-κB activity. Over the past 20 years, many studies have identified additional mechanisms regulating NF-κB transcriptional activity, in particular those involving PTM of NF-κB subunits, such as phosphorylation, acetylation, methylation, glycosylation, nitrosylation and ubiquitination, which add another important layer of complexity to the transcriptional regulation of NF-κB (Huang, Yang et al. 2010, Mitchell and Carmody 2018) (Fig.11).

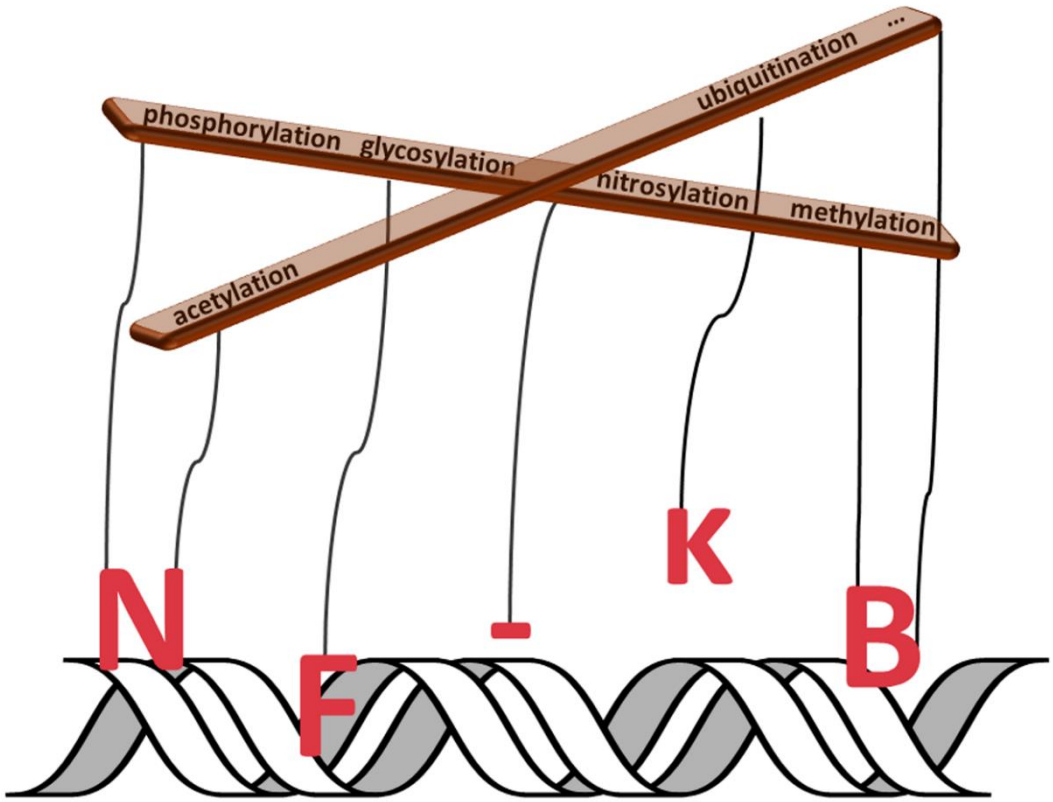

Figure 11. Posttranslational modifications of NF-κB as another layer of regulation. Phosphorylation, acetylation, methylation, ubiquitination, glycosylation and nitrosylation are examples of NF-κB modifications relevant for its transcriptional activity.

Among the NF-κB subunits, p65/RelA has been the most extensively studied in this context (Huang, Yang et al. 2010, Christian, Smith et al. 2016, Collins, Mitxitorena et al. 2016). The following section summarizes the PTM that affect the transcriptional activity of p65/RelA.

Phosphorylation and dephosphorylation

Phosphorylation of RelA/p65 can occur both in the cytoplasm and in the nucleus in response to a variety of stimuli (Huang, Yang et al. 2010). Most phosphorylation sites of the RelA/p65 subunit, namely Ser and tyrosine residues, are within the N-terminal RHD and the C-terminal TAD (Christian, Smith et al. 2016, Mitchell and Carmody 2018). Depending on the sites of phosphorylation, the target genes and the stimuli, phosphorylation results in either increased or decreased levels of transcription (Huang, Yang et al. 2010). Of the

identified phosphorylation sites of RelA/p65, phosphorylation of Ser276, Ser536 and Ser468 are the best characterized regarding their impact on NF-κB transcriptional activity (Christian, Smith et al. 2016, Mitchell and Carmody 2018). Ser276 of RelA/p65 is the target of different kinases such as Protein Kinase A (PKA), Mitogen- and Stress- Activated Kinase-1 (MSK1) and Pim-1 (Huang, Yang et al. 2010, Christian, Smith et al. 2016). Phosphorylation of Ser276 was first identified to be mediated by the catalytic subunit of PKA (PKAc) in the pre-B cell line 70Z/3 in response to LPS and in a cAMP-independent manner (Zhong, SuYang et al. 1997). Interestingly, Zhong and co-workers (1997) demonstrated that in resting cells, PKAc is associated to the IκB-α:NF-κB complex, thus being in an inactive state. However, cell treatment with inducers of NF-κB activity result in degradation of IκB-α which causes activation of PKAc and subsequent phosphorylation of Ser276 of the RelA/p65 subunit (Zhong, SuYang et al. 1997). Phosphorylation on this residue is required for efficient transcriptional activation of NF-κB by promoting a conformational change that allows its association with the cellular co-activator CREB-Binding Protein (CBP)/p300 (Zhong, SuYang et al. 1997, Zhong, Voll et al. 1998). Contrary to phosphorylation by PKAc which occurs in the cytoplasm, MSK1 phosphorylates RelA/p65 on Ser276 in the nucleus in TNF-treated L929sA mouse fibroblasts (Vermeulen, De Wilde et al. 2003). Similarly, phosphorylation of Ser276 by MSK1 facilitates the recruitment of CBP/p300 to the promoters of NF-κB target genes, such as IL-6, increasing their transcription (Vermeulen, De Wilde et al. 2003, Reber, Vermeulen et al. 2009).

Ser536 of RelA/p65 is also phosphorylated under various conditions, by multiple kinases, including IKKs (e.g. IKKα, β and ε), Ribosomal Subunit Kinase-1 (RSK1) and TANK-Binding Kinase 1 (TBK1), culminating in different outputs (Huang, Yang et al. 2010, Christian, Smith et al. 2016). Phosphorylation of the Ser536 residue of RelA/p65 was first reported in response to TNF-α treatment in HeLa cells (Sakurai, Chiba et al. 1999). It was described that this phosphorylation is mediated by IKKs prior to nuclear translocation (Sakurai, Chiba et al. 1999). Likewise, Yang and co-workers (2003) demonstrated that LPS induces phosphorylation on Ser536 of RelA/p65 in monocytes/macrophages. In this study, the involvement of IKKβ was clearly demonstrated (Yang, Tang et al. 2003). Besides, phosphorylation of this residue increases the RelA/p65 transcriptional activity by enhancing the interaction of this subunit with other proteins, namely p300 (Yang, Tang et al. 2003,

Chen, Williams et al. 2005). Thus, phosphorylation of Ser536 is considered an active mark for classical NF-κB pathway activation (Huang, Yang et al. 2010).

Ser468 is one of the residues whose phosphorylation negatively modulates NF-κB transcriptional activity (Huang, Yang et al. 2010, Christian, Smith et al. 2016). Three kinases have been described as phosphorylating this residue such as Glycogen Synthase Kinase-3β (GSK-3β), IKKβ and IKKε (Christian, Smith et al. 2016). Ser468 is constitutively phosphorylated by GSK-3β in unstimulated cells, blocking NF-κB transcriptional activity. In parallel, Protein Phosphatase 1 (PP1) is activated which leads to dephosphorylation of both Ser468 of RelA/p65 and Ser9 of GSK-3β. Thus, relative activity of GSK-3β and PP1 determines the phosphorylation level of Ser468 of RelA/p65 in unstimulated cells (Buss, Dorrie et al. 2004). This Ser residue is also phosphorylated by IKKβ in response to TNF-α and IL-1β treatment in distinct cell lines and primary cultures despite not being essential for NF-κB activation and its nuclear translocation (Schwabe and Sakurai 2005). Interestingly, Mao and co-workers (2009) found that phosphorylation of Ser468 mediated by IKK promotes p65/RelA ubiquitination and, consequently, its proteasomal degradation. Thus, phosphorylation on this residue by IKK sets in motion a process that ends up inhibiting NF-κB transcriptional activity (Mao, Gluck et al. 2009). Nonetheless, phosphorylation on Ser468 by IKKε in response to T cell co-stimulation, which implies pre-activation with phorbol-12-myristate-13-acetate and ionomycin, enhances the transcriptional activity of NF-κB (Mattioli, Geng et al. 2006). To sum up, the different outcomes of phosphorylation on Ser468 suggest that this PTM regulates NF-κB transcriptional activity in a context-dependent manner (Huang, Yang et al. 2010).

Dephosphorylation has been associated to termination of NF-κB activity (Huang, Yang et al. 2010, Chen, Li et al. 2016, Gu, Lei et al. 2017). Dephosphorylation of Ser536 reduces RelA/p65´s interaction with p300 and hence, NF-κB transcriptional activity (Chen, Williams et al. 2005, Huang, Yang et al. 2010). Protein Phosphatase 2A (PP2A) is one of the enzymes responsible for directly dephosphorylating RelA/p65 subunit at the Ser536 residue (Yang, Fan et al. 2001, Li, Wang et al. 2006, Tsuchiya, Osaki et al. 2017). Moreover, Wild type p53 Induced Phosphatase 1 (WIP1) was also described as a direct phosphatase of RelA/p65 subunit at Ser536 (Chew, Biswas et al. 2009). Although PP2A and WIP1 act on the same Ser residue of the p65/RelA subunit, these phosphatases do not cooperate and have non-redundant roles *in vivo* (Chew, Biswas et al. 2009).

Acetylation and deacetylation

Acetylation is another important PTM of RelA/p65 which regulates NF-κB transcriptional activity (Huang, Yang et al. 2010). This PTM consists in addition of an acetyl group to Lys residues of the substrate proteins, mediated by Histone AcetylTransferases (HATs) (Park, Jo et al. 2015). Contrary to phosphorylation, acetylation typically occurs in the nucleus where most of the HATs catalyzing this modification reside (Huang, Yang et al. 2010). Coactivators p300/CBP and p300/CBP-Associated Factor (PCAF) are the HATs that have been implicated as effectors of RelA/p65 acetylation, both *in vitro* and *in vivo* (Chen, Fischle et al. 2001, Kiernan, Bres et al. 2003). Acetylation of RelA/p65 has been described in seven Lys residues namely 122,123, 218, 221, 310, 314 and 315 (Chen, Mu et al. 2002, Kiernan, Bres et al. 2003, Buerki, Rothgiesser et al. 2008).

Lys310 of RelA/p65 is one of the first acetylation sites that has been reported (Chen, Mu et al. 2002). Acetylation of this residue is mediated by p300/CBP (Chen, Mu et al. 2002) and although it does not interfere with DNA binding nor impairs the assembly of RelA/p65 with IκB-α, it is required for full transactivation function of this NF-κB subunit (Chen, Mu et al. 2002). Abolishing Lys310 acetylation by mutation to arginine significantly inhibited the transactivation activity of NF-κB and the expression of pro-inflammatory cytokines (Chen, Mu et al. 2002). Thus, Chen and co-workers (2002) proposed that Lys310 acetylation might form a platform for the binding of a bromodomain-containing protein that is required for full RelA/p65 transcriptional activity. In line with this proposal, Huang and colleagues (2009) demonstrated that acetylated RelA/p65 contributes to the transcriptional activation of NF-κB and, consequently, to the expression of pro-inflammatory genes by specific recruitment of the transcriptional activator, Bromodomain 4 protein (Brd4), via an interaction between the acetylated Lys310 and the bromodomain of Bdr4. Then, Brd4 recruits the association of Cyclin Dependent Kinase 9 and Positive Transcription Elongation Factor b (CDK9/P-TEFb) which phosphorylates the C-terminal domain of RNA polymerase II to stimulate the transcription of a subset of NF-κB genes, namely cytokines and chemokines, which are P-TEFb-dependent (Amir-Zilberstein, Ainbinder et al. 2007, Huang, Yang et al. 2009).

Unlike Lys310, acetylation of Lys221 by p300/CBP was reported to enhance the binding affinity of RelA/p65 and, consequently, that of the NF-κB complex, for DNA-κB sites (Chen, Mu et al. 2002). This effect might be caused by a conformational change within the protein (Chen, Mu et al. 2002). Moreover, acetylation of Lys221, alone or in combination

with Lys218, interferes with RelA/p65 assembly with IκB-α (Chen, Mu et al. 2002). Lys221 directly interacts with methionine 279 located within the six ankyrin repeats of IκB-α (Chen, Mu et al. 2002). Consequently, acetylation of Lys221 impairs that interaction, inhibiting IκB-α binding (Chen, Mu et al. 2002). Furthermore, phosphorylation of the PEST sequence of IκB-α is required for inhibition of DNA binding and might interact with Lys218 of RelA/p65 (Chen, Mu et al. 2002). However, acetylation of Lys218 may interfere with this interaction, contributing to inhibition of IκB-α binding (Chen, Mu et al. 2002)

On the opposite, upon immune stimulation of cells and activation of NF-κB transcriptional activity, acetylation of Lys122 and 123 of RelA/p65 by p300 and PCAF, lowers its affinity for DNA-κB sites (Kiernan, Bres et al. 2003). This facilitates removal of NF-κB from enhancer elements by newly synthesized IκB-α and, consequently, export of NF-κB:IκB-α from the nucleus to the cytoplasm (Kiernan, Bres et al. 2003). Thus, acetylation of Lys122 and 123 of RelA/p65 is vital for turning off NF-κB-mediated gene expression (Kiernan, Bres et al. 2003).

Lys314 and 315 in RelA/p65 are also acetylated by p300 (Buerki, Rothgiesser et al. 2008). Acetylation of these residues does not affect shuttling, DNA binding nor induction of anti-apoptotic genes by TNF-α (Buerki, Rothgiesser et al. 2008). Nevertheless, acetylation of RelA/p65 at Lys314 and 315 is reported to possibly modulate the expression of only a subset of genes, namely increasing *Ccl-20*, *Ifi-44* and *Gbp-2* expressions and decreasing *Ccl-7* (Buerki, Rothgiesser et al. 2008). Moreover, mutation of Lys314 and 315, but not Lys310, increases *Mmp10* and *Mmp13* expressions suggesting that acetylation at Lys314 and possibly Lys315 might be related with repression of gene expression (Rothgiesser, Fey et al. 2010).

Interestingly, of all the acetylation sites reported for RelA/p65, only Lys310 was confirmed by a study carried out by Buerki and co-workers (2008). Differences in the experimental approach used could be the explanation for the discrepancy (Kiernan, Bres et al. 2003, Buerki, Rothgiesser et al. 2008). Moreover, none of these studies excluded the possibility of the existence of other acetylation sites in RelA/p65 besides those already identified (Chen, Mu et al. 2002, Buerki, Rothgiesser et al. 2008).

Similar to phosphorylation, acetylation is also a reversible event (Huang, Yang et al. 2010). The removal of the acetyl group from lysine residues is mediated by Histone DeAcetylases (HDACs). Thus, the effect of HATs is opposed in the cells by HDACs.

Several HDACs have been reported to deacetylate RelA/p65 and, consequently, regulate NF-κB functions (Huang, Yang et al. 2010). An early study on HDAC-NF-κB interaction demonstrated that HDAC3 directly deacetylates RelA/p65 which leads to termination of the NF-κB transcriptional response (Chen, Fischle et al. 2001). Deacetylation of RelA/p65 by HDAC3 functions as an intranuclear molecular switch promoting IκB-α binding and IκBα-dependent nuclear export of the NF-κB complex (Chen, Fischle et al. 2001). Chen and co-workers (2002) demonstrated that deacetylation of RelA/p65 promoted by HDAC3 is likely to occur at Lys 221, alone or in combination with Lys 218. Moreover, HDAC3 has also been reported to deacetylate Lys122 and Lys123 of RelA/p65 (Kiernan, Bres et al. 2003). As mentioned before, acetylation of these two Lys residues by p300 and PCAF is required for removal of the DNA-bound NF-kB complex to the cytoplasm by binding to newly synthesized IκB-α. Then, the relocated cytoplasmic NF-κB:IκB-α complex can serve additional rounds of activation following deacetylation of those Lys residues by HDAC3 (Kiernan, Bres et al. 2003). In agreement with this mechanism, another study demonstrated that HDAC3 mediates deacetylation of RelA/p65 at Lys 122, 123, 314 and 315 and, consequently, promotes IL-1-induced inflammatory gene expression (Ziesche, Kettner-Buhrow et al. 2013).

Other members of this class of HDACs have been reported to modulate the acetylation status of different Lys residues of RelA/p65 (McIntyre, Daniels et al. 2019). HDAC1, enhanced by Breast Cancer Metastasis Suppressor binds to RelA/p65 and deacetylates Lys310, thus suppressing NF-κB transcriptional activity and promoting apoptosis (Liu, Smith et al. 2006). Moreover, HDAC1 and HDAC2 were described as also capable of deacetylating RelA/p65 at Lys314 and Lys315 residues (Ziesche, Kettner-Buhrow et al. 2013). Nevertheless, the interaction of these two HDACs and RelA/p65 is controversial due to discrepant results from different studies (Ashburner, Westerheide et al. 2001, Chen, Fischle et al. 2001, Kiernan, Bres et al. 2003, Liu, Smith et al. 2006, Ziesche, Kettner-Buhrow et al. 2013). HDAC6, a member of another class of HDACs (McIntyre, Daniels et al. 2019), was also reported to bind and deacetylate RelA/p65, decreasing its DNA-binding activity to the *MMP2* promoter and downregulating MMP-2 expression in non-small cell lung cancer cells, thus inhibiting their invasiveness. It was postulated that deacetylation of p65/RelA by HDAC6 may occur at Lys218, Lys221 and Lys310 residues leading to

inactivation of the NF-κB transcriptional activity. However, further studies are required to clarify which Lys residues are involved (Yang, Liu et al. 2015).

Other classes of the HDAC family have also been reported to deacetylate p65/RelA subunit, among which Sirtuins (SIRTs) are especially relevant. SIRTs, homologs of the yeast SIR2 family, belong to the atypical class III HDACs and unlike the others HDACs mentioned, require Nicotinamide Adenine Dinucleotide oxidized form (NAD^+) as a cofactor, rather than zinc (Wang, He et al. 2019). Several members of the SIRT family have been shown to modulate NF-κB transcriptional activity. Among those, SIRT1 was shown to inhibit NF-κB transcriptional activity by directly deacetylating the RelA/p65 protein at Lys310, sensitizing cells to TNF-α-induced apoptosis (Yeung, Hoberg et al. 2004). Many other studies corroborate the role of SIRT1 in antagonizing NF-κB activity which is now well established (Hwang, Yao et al. 2013, Kauppinen, Suuronen et al. 2013, Mendes, Lelis et al. 2017). For instance, it was demonstrated that overexpression of SIRT1 or addition of a SIRT1 activator decreases amyloid-β peptide-induced acetylation of RelA/p65 at Lys310 in microglia, thus reducing the expression of NF-κB-dependent genes and having neuroprotective effects (Chen, Zhou et al. 2005). Moreover, inhibition of SIRT1 expression and activity by LPS and two major alcohol metabolites was associated with a marked increase in the acetylation of RelA/p65, NF-κB transcriptional activity and release of TNF-α in RKC1 and Raw 264.7 cell lines (Shen, Ajmo et al. 2009).

Besides SIRT1, SIRT2 was also described as a deacetylase of RelA/p65 at Lys310 *in vitro* and when overexpressed in cells after TNF-α stimulation (Rothgiesser, Erener et al. 2010). Rothgiesser and colleagues (2010) postulated that in unstimulated cells, SIRT2 exists in a complex with RelA/p65. Following TNF-α stimulation, RelA/p65 translocates to the nucleus, whereas SIRT2 remains in the cytoplasm. In the nucleus, p300 binds to RelA/p65 and acetylates it at Lys310, Lys314 and Lys315 to fine-tune gene transcription. Once the NF-κB response is finished, RelA/p65 returns to the cytoplasm, where SIRT2 deacetylates RelA/p65 at Lys310, thus resetting the whole NF-κB response (Rothgiesser, Erener et al. 2010). Moreover, it was also demonstrated that, in microglia, SIRT2 deacetylates Lys310 on RelA/p65, affecting pro-inflammatory gene expression, by interfering with NF-κB full transcriptional activity (Pais, Szego et al. 2013). Deacetylation of RelA/p65 at Lys310 by SIRT2 was also reported in a collagen-induced arthritis model, resulting in reduced expression of NF-κB-dependent genes since acetylation at this Lys residue is essential for

its full transcriptional activity (Lin, Sun et al. 2013). Nevertheless, other groups reported contradictory findings towards the anti-inflammatory effect of SIRT2 (Lee, Jung et al. 2014, Chen, Wu et al. 2015, Wang, Zhang et al. 2016). Further studies are needed to clarify the role of SIRT2 on inflammation, in particular in modulating the NF-κB pathway (Wang, Yang et al. 2019).

Methylation

In addition to phosphorylation and acetylation, methylation has been emerging as another important PTM for the regulation of NF-κB function (Lu and Stark 2015, Wei, Prabhu et al. 2018). This PTM is characterized by the addition of a methyl group to non-histone proteins, namely NF-κB, in particular to Lys and arginine (Arg) residues of RelA/p65 subunit (Lu and Stark 2015, Wei, Prabhu et al. 2018). This reaction is catalyzed by different histone methyltransferases (Lu and Stark 2015, Wei, Prabhu et al. 2018). One of these enzymes is a histone lysine methyltransferase, named Set9 (Ea and Baltimore 2009, Yang, Huang et al. 2009). Yang and colleagues (2009) showed that methylation of RelA/p65 at Lys314 and Lys315 by Set9 negatively regulates the transcriptional activity of NF-κB by inducing the proteasome-mediated degradation of promoter-associated RelA/p65. This PTM is required for the effective degradation of RelA/p65 in part by recruiting an unknown E_3 ligase responsible for ubiquitination (Yang, Huang et al. 2009). On the other hand, Ea and co-workers (2009) demonstrated that RelA/p65 is monomethylated at Lys37 by Set9 in response to TNF-α and IL-1β stimulation. Methylation at this Lys residue of RelA/p65 is required for the induction of a subset of genes regulated by NF-κB (Ea and Baltimore 2009). This nuclear modification of RelA/p65 affects the stability of DNA-RelA/p65 complexes to the promoter (Ea and Baltimore 2009). Differences in the results between these two studies may be due to different methodological approaches (Ea and Baltimore 2009). However, methylation at Lys37 of RelA/p65 is likely to occur before Lys314 and Lys315 modification (Ea and Baltimore 2009). Lys37 methylation is required for the gene activation whereas Lys314 and Lys315 methylations are essential for the termination of NF-κB transcriptional activity (Ea and Baltimore 2009). Another member of Set family, SetD6, was reported to monomethylate RelA/p65 at Lys310 (Levy, Kuo et al. 2011). This methylation attenuates NF-κB transcriptional activity by forming a docking site to protein Lys methyltransferase G9a-Like Protein (GLP) via its AnkR on RelA/p65 gene promoter. Thus, GLP promotes methylation

of histone H3 at Lys9 which represses the expression of inducible inflammatory genes, creating a silent chromatin state. Levy and colleagues (2011) found that SetD6-mediated methylation at Lys310 of RelA/p65 occurs in the absence of stimulation, being a physiological repressor of the population of RelA/p65 which resides in the nucleus (Levy, Kuo et al. 2011). It was also demonstrated that RelA/p65 subunit is methylated at Lys218 and Lys221 residues by Nuclear receptor-binding Set Domain-contain protein 1 (NSD1) in response to a trigger such as TNF-α or IL-1β treatment or when NF-κB is constitutively activated. Methylation of RelA/p65 by NSD1 enhances NF-κB transcriptional activity (Lu, Jackson et al. 2010). Lu and co-workers (2010) also reported that RelA/p65 is demethylated at Lys218 and Lys221 residues by F-Box and Leucine-rich repeat protein 11 (FBXL11), leading to inhibition of NF-κB transcriptional activity. However, it was also shown that *FBXL11* gene is induced upon NF-κB activation (Lu, Jackson et al. 2010). Therefore, FBXL11 expression is NF-κB-dependent and, like IκB-α, is a negative regulator of NF-κB (Lu, Jackson et al. 2010).

Apart from Lys modifications, methylation of RelA/p65 at Arg residues has also been reported (Lu and Stark 2015, Wei, Prabhu et al. 2018). According to Wei *et al.* (2013), RelA/p65 subunit is dimethylated at Arg30 by Protein arginine MethylTransferase 5 (PRMT5) after being freed from IκB-α. This PTM leads to an increase of NF-κB affinity for the κB elements of many genes and, consequently, enhances the expression of these genes which encode, for example, cytokines, chemokines and growth factors (Wei, Wang et al. 2013). Still about PRMT5, it was also reported that this enzyme methylates RelA/p65 at Arg30 and Arg35, enhancing CXCL10 gene expression in response to TNF-α in endothelial cells (Harris, Bandyopadhyay et al. 2014). Moreover, Harris *et al.* (2016) concluded that methylation at Arg174, Arg30 and Arg35 of RelA/p65 by PRMT5 is critical for the recruitment of this NF-κB subunit to the CXCL11 gene promoter and, consequently, its induction in response to TNF-α plus INF-γ co-stimulation (Harris, Chandrasekharan et al. 2016). Methylation at Arg174 is required for RelA/p65 recruitment to the CXCL11 gene promoter (Harris, Chandrasekharan et al. 2016). Thus, methylation at Arg residues tends to enhance the association of RelA/p65 to the gene promoter and improve gene transcription (Harris, Bandyopadhyay et al. 2014, Harris, Chandrasekharan et al. 2016).

Ubiquitination

Ubiquitination is a highly adaptable PTM characterized by the attachment of ubiquitin, a small protein with 76 aminoacids, to a protein substrate. This process is achieved by a three component enzymatic system, the UPS, consisting of an ubiquitin-activating enzyme (E_1), an ubiquitin-conjugating enzyme (E_2) and an ubiquitin ligase (E_3). Covalent attachment of ubiquitin is vital for a plethora of cellular processes, such as regulation of protein stability. Moreover, ubiquitination can serve as a molecular signal targeting the modified protein to the proteasome for degradation (Collins, Mitxitorena et al. 2016). Regarding NF-κB, ubiquitination plays an important role in its upstream activation through both the classical and alternative pathways (Mitchell and Carmody 2018) and is also required to terminate its transcriptional activity as described above. This mechanism acts in synergism with newly synthesized IκB-α to assure a timely termination of the NF-κB response in normal cells (Saccani, Marazzi et al. 2004, Collins, Mitxitorena et al. 2016).

Seven Lys residues (Lys6, Lys11, Lys27, Lys29, Lys33, Lys48 and Lys63) of ubiquitin are used during the formation of a polyubiquitin chain. Polyubiquitin chains assembled through Lys48 are the predominant form of RelA/p65 ubiquitination, targeting this subunit for proteasome degradation. However, other ubiquitin linkages have been reported (Collins, Mitxitorena et al. 2016). Furthermore, it was also described that RelA/p65 is monoubiquitinated in case of RelA/p65 hypo-phosphorylation or proteasome inhibition (Hochrainer, Racchumi et al. 2012). According to Hochrainer *et al.* (2012), monoubiquitination of RelA/p65 decreases NF-κB transcriptional activity by lowering the affinity of RelA/p65 to its co-activator CBP, despite extending its nuclear presence. Thus, this modification represents a degradation-independent mechanism for regulation of nuclear RelA/p65 activity. However, further studies are required to fully elucidate the role of this PTM (Hochrainer, Racchumi et al. 2012).

Several E_3 ligases have been reported to be involved in RelA/p65 ubiquitination, such as Suppressor of Cytokine Signaling 1 (Ryo, Suizu et al. 2003, Maine, Mao et al. 2007, Mao, Gluck et al. 2009), Postsynaptic density 65–Discs large–Zonula occludens 1(PDZ) and Abnormal cell Lineage 11–Islet 1–Mechanosensory abnormal 3 (LIM) Domain 2 (PDLIM2) (Tanaka, Grusby et al. 2007), Peroxisome Proliferator Activated Receptor-γ (Hou, Moreau et al. 2012), Inhibitor of Growth 4 (Hou, Zhang et al. 2014), Makorin Ring Finger Protein 2

(Shin, Ito et al. 2017), RNF182 (Cao, Sun et al. 2019) and Tripartite Motif Containing 7 (Jin, Lu et al. 2020).

Analogous to other PTM, ubiquitination of proteins is counteracted by deubiquitination which is based on the proteolytic removal of polyubiquitin chains from substrates. This reaction is catalyzed by deubiquitinases (DUBs) (Colleran, Collins et al. 2013). Deubiquitination of p65/RelA by Ubiquitin Specific Protease 7 (USP7), a nuclear DUB, was demonstrated following TLR and TNFR activation (Colleran, Collins et al. 2013). USP7 is recruited to NF-κB target promoters and binds to RelA/p65 where it removes polyubiquitin chains from this subunit. This PTM promotes NF-κB activity by increasing the stability and half-life of transcriptionally active RelA/p65. Therefore, USP7 is a NF-κB regulator which defines a transcription control mechanism through the active recycling of ubiquitinated RelA/p65 (Colleran, Collins et al. 2013).

Interplay between PTM

According to the literature, there are several different interactions between PTM of p65/RelA. These interactions may regulate each other and, consequently, NF-κB transcriptional activity (Huang, Yang et al. 2010). For example, it was demonstrated that prior phosphorylation of RelA/p65 at Ser276 is essential for the acetylation of this subunit at Lys310 by enhancing the binding of RelA/p65 to p300, while phosphorylation of Ser536 seems to facilitate that process without being indispensable (Chen, Williams et al. 2005). Therefore, these sequential modifications are important for the full transcriptional activity of NF-κB (Chen, Williams et al. 2005).

The interplay between acetylation and methylation is another example (Huang, Yang et al. 2010). Yang and co-workers (2010) reported that acetylation of RelA/p65 at Lys310 inhibits methylation at Lys314 and Lys315 of this subunit by Set9, and, the subsequent ubiquitination and degradation (Yang, Tajkhorshid et al. 2010). Consequently, the stability of RelA/p65 increases, leading to enhanced NF-κB transcriptional activity (Yang, Tajkhorshid et al. 2010). Acetylation at Lys310 interferes with the binding of Set9 to RelA/p65 by neutralizing the positive charge of Lys310 (Yang, Tajkhorshid et al. 2010). This positive charge is crucial for its recognition by a “exosite” which is negatively charged and located within the Set domain of Set9 (Yang, Tajkhorshid et al. 2010). Nevertheless, the interplay between acetylation and methylation of RelA/p65 is unidirectional since prior

methylation at Lys314 and Lys315 has no effect on acetylation at Lys310 (Yang, Tajkhorshid et al. 2010).

Site-specific phosphorylation of RelA/p65 may also be regulated by the ubiquitination of this subunit (Huang, Yang et al. 2010). As mentioned before, phosphorylation at Ser468 of RelA/p65 favors its ubiquitination and, consequently, proteasome degradation (Geng, Wittwer et al. 2009, Mao, Gluck et al. 2009). According to Geng *et al.* (2009), phosphorylation of RelA/p65 at Ser468 affects its conformation, promoting the relief of an intramolecular masking that allows the interaction with the E_3 ligase complex and the subsequent polyubiquitination and degradation (Geng, Wittwer et al. 2009). Other example is the phosphorylation at Ser536 of RelA/p65 by casein kinase 1 which promotes its ubiquitination by the E_3 ligases, COMM Domain-containing protein-1 (COMMD1) and Cullin-2 (CUL2), and consequent degradation and inhibition of NF-κB transcriptional activity (Wang, Hu et al. 2014).

The interplay between methylation and phosphorylation has also been described (Christian, Smith et al. 2016). As previously described, SetD6-mediated methylation at Lys310 of RelA/p65 under basal conditions acts as a repressor of its population residing in the nucleus (Levy, Kuo et al. 2011). However, TNF-induced phosphorylation at Ser311 of RelA/p65 by the atypical protein kinase C suppresses SetD6 methylation at Lys310 by disrupting the association of GLP and RelA/p65, thus promoting activation of the NF-κB target genes that were repressed (Levy, Kuo et al. 2011).

1.2.7 Mitogen-Activated Protein Kinases

Signaling through PRRs also leads to the activation of other pathways, such as Mitogen-Activated Protein Kinases (MAPKs). MAPKs are a family of Ser/threonine protein kinases which play an important role in proliferation, differentiation, apoptosis, survival, inflammation and innate immunity (Arthur and Ley 2013, Chen, Deng et al. 2018). In mammals, MAPKs subfamilies include the Extracellular signal-Regulated Kinase (ERK), p38 and Jun N-terminal Kinase (JNK). Each member of subfamilies of MAPKs "exists in several isoforms". ERK1 and 2 represent the "prototype of eight isoforms of ERK". Four isoforms of p38 have been described, namely α, β, γ and δ. JNK1, 2 and 3 are the isoforms of JNK that have been reported, being JNK 1 and 2 expressed in most tissues (Kim and Choi 2015). MAPKs subfamilies are activated in response to diverse stimuli, namely osmotic stress, mitogens, heat shock and inflammatory cytokines (Chen, Deng et al. 2018). In particular, ERKs are usually activated by mitogens and differentiation signals while JNK and p38 are triggered by inflammatory mediators and stress (Sabio and Davis 2014).

1.2.7.1 MAPK cascade and its cross-signaling with the NF-κB pathway

The MAPK signaling pathway (Fig.12) is composed of, at least, three components, namely a MAPK kinase kinase (MAP3K), a MAPK kinase (MAP2K) and a MAPK. MAP3K phosphorylates MAP2K, which, in turn, phosphorylates MAPK. Then, activated MAPKs can phosphorylate or activate other target proteins, namely transcription factors, pro- and anti-apoptotic proteins, both at the cytoplasm and the nucleus (Herlaar and Brown 1999, Kim and Choi 2015).

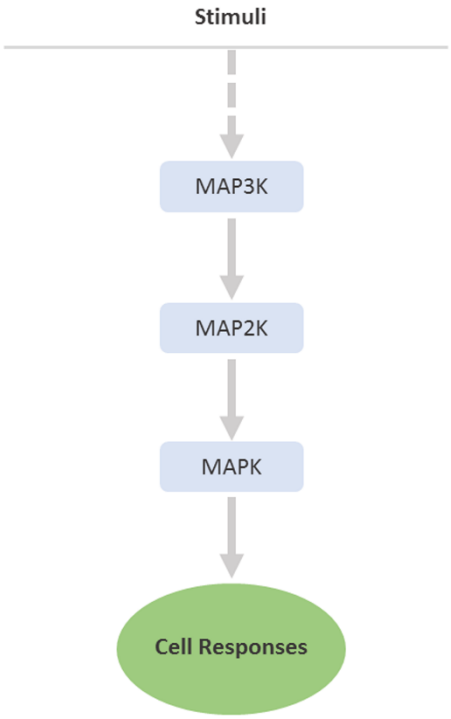

Figure 12. MAPK signaling cascade. MAP3K, MAPK kinase kinase; MAP2K, MAPK kinase; MAPK, Mitogen-Activated Protein Kinase. Reproduced with permission from Kim and Choi, 2015.

In particular, TAK1, also known as MAP3K7, is a member of MAP3K family (Sakurai 2012) and it was shown that this kinase is essential for MAPK and NF-κB activation in response to stimulation of TLRs, IL-1R and TNFR (Sato, Sanjo et al. 2005). As mentioned before, TAK1 is pointed out as the IKK kinase responsible for activating the IKK complex and, consequently, leading to NF-κB activation (Hayden and Ghosh 2008, Hinz and Scheidereit 2014). Moreover, it was demonstrated that TAK1 can directly phosphorylate MAPK kinases for both p38 and JNK activation (Wang, Deng et al. 2001, Arthur and Ley 2013). Regarding ERK activation, TAK1 is not directly involved, but it was shown that the MAP3K, Tumor progression Locus 2 (TLP-2), plays an important role in establishing the connection between these two (Arthur and Ley 2013). Studies in TLR-stimulated macrophages demonstrated that IKKβ is responsible for releasing TLP-2 from its inhibitor, p105, by triggering this to proteolysis in the proteasome (Beinke, Robinson et al. 2004) and for directly phosphorylating TLP-2 on Ser 400 residue (Roget, Ben-Addi et al. 2012). This allows TLP-2 to function as a MEK1/2 kinase which mediates the activation of ERK1/2 (Beinke, Robinson et al. 2004, Roget, Ben-Addi et al. 2012). Despite the clear participation

of TAK1 in MAPK activation, other MAP3Ks can be involved such as Apoptosis Signal-Regulating Kinase-1 (Arthur and Ley 2013).

1.2.7.2 MAPK targets: Activator Protein-1

Activating Protein-1 (AP-1) is a family of transcription factors composed of four sub-families, Jun (c-Jun, JunB and JunD), Fos (c-Fos, FosB, Fra1 and Fra2), Activating Transcription Factor (ATF; ATF2, LRF1/ATF3, BATF, JDP1 AND JDP2) and Musculoaponeurotic fibrosarcoma (Maf; c-Maf, MafB, MafA, MafG/F/K and Nrl) which are characterized by pleiotropic effects such as modulation of proliferation, apoptosis, differentiation, survival, migration and transformation (Trop-Steinberg and Azar 2017, Atsaves, Leventaki et al. 2019). AP-1 controls the constitutive and inducible transcription of several genes (Trop-Steinberg and Azar 2017) and its activity is controlled by a variety of MAPKs which are, in turn, activated by a variety of extracellular stimuli (Trop-Steinberg and Azar 2017, Atsaves, Leventaki et al. 2019).

By phosphorylating distinct substrates, MAPKs enhance AP-1 activity (Shaulian and Karin 2002, Atsaves, Leventaki et al. 2019). For instance, JNK phosphorylation of c-Jun at Ser73 and Ser63 residues located within its transactivation domain, heightens its ability to activate transcription as either a homo- or heterodimer with c-Fos (Karin 1995). Moreover, AP-1 activity is also controlled at the level of gene expression by several distinct transcription factors, like Elk-1 and MSK1, that are activated by different MAPKs and induce the expression of various members of the AP-1 family (Herlaar and Brown 1999).

The transcriptional activity of AP-1 is associated with the expression of pro-inflammatory mediators such as MMPs (Angel, Imagawa et al. 1987), COX-2 (Hannemann, Jordan et al. 2017), IL-8 (Harris, Smith et al. 2002) and IL-23 (Liu, Ouyang et al. 2009). Nevertheless, the expression of pro-inflammatory genes frequently requires not one but two or more transcription factors, namely NF-κB and AP-1 (Perkins 2007) (Fig.13).

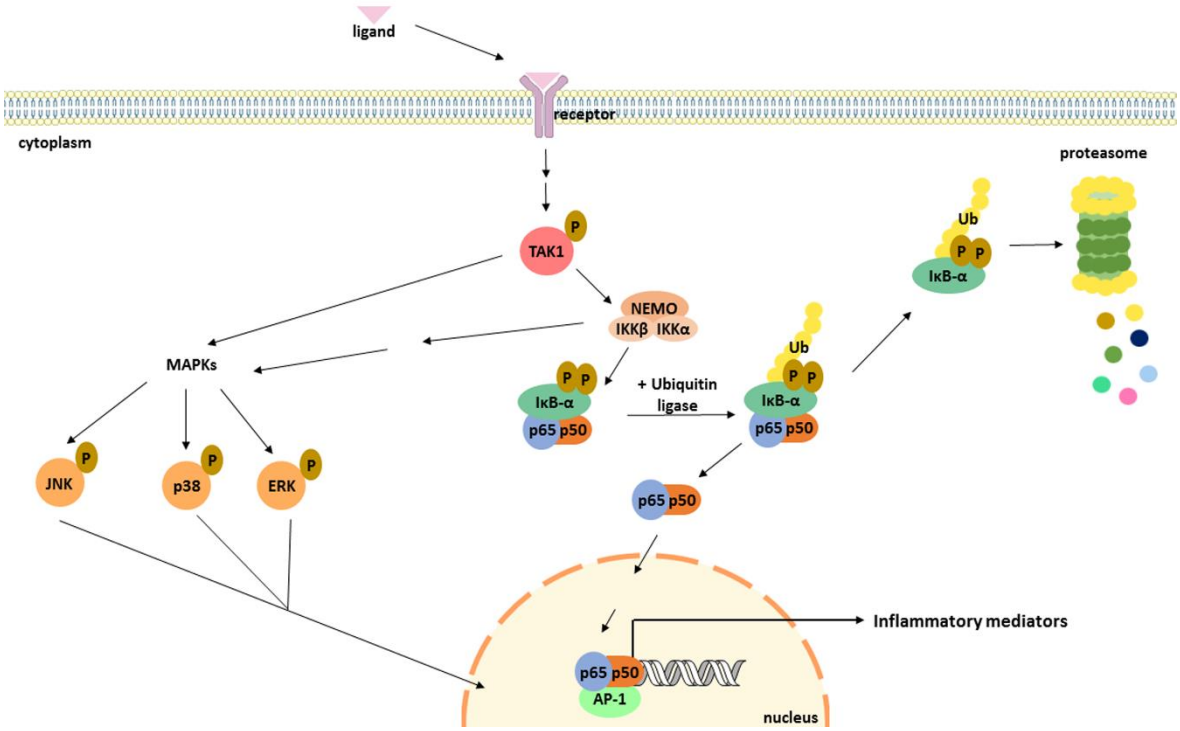

Figure 13. Cross-signaling between NF-κB and MAPK activation pathways. Upon ligand binding to its specific receptor, adaptor proteins are activated and lead to TAK1 phosphorylation which triggers activation of the IKK complex. Then, the IKK complex, particularly IKKβ, phosphorylates IκB-α. This phosphorylation signals IκB-α for ubiquitination and, subsequently, proteasome degradation. After IκB-α degradation, freed NF-κB dimers (p65:p50) translocate to the nucleus where they bind to the κB sites, present within promoter regions of pro-inflammatory target genes, inducing their transcription. In parallel, activated TAK1 also leads to MAPK activation, namely p38 and JNK, which culminates with enhancing AP-1 transcriptional activity. Moreover, IKKβ also triggers a cascade that ends up in ERK1/2 phosphorylation, which then phosphorylates components of the AP-1 complex and other transcription factors that regulate the expression of AP-1 family members, thus enhancing their transcriptional activity. AP-1, Activating Protein-1; ERK1/2, Extracellular-Regulated Kinases 1/2; IκB-α, Inhibitor of κB activity; IKKα/β, IκB Kinase α/β; JNK, Jun N-terminal Kinase; MAPKs, Mitogen-Activated Protein Kinases; NEMO, NF-κB Essential modulator; p65, RelA/p65; P, phosphate;TAK1,TGF-β-Activated Kinase; Ub, ubiquitin.

Taking into consideration the relevance of the canonical NF-κB and MAPK signaling pathways in the inflammation-driven mechanisms, interfering with these two pathways may be a therapeutic opportunity to block the progression of chronic age-related diseases and even prevent their consequences (Gaspar, Sousa et al. 2020).

1.3 Objectives and organization of the dissertation

Considering the impact and involvement of inflammation, in particular chronic low-grade inflammation, in chronic age-related diseases (Rea, Gibson et al. 2018), it is essential to find new therapeutic strategies capable of interfering with inflammation-driven mechanisms. Moreover, anti-inflammatory therapies available are not targeted to chronic low-grade inflammation (Gejjalagere Honnappa and Mazhuvancherry Kesavan 2016). Non-steroidal anti-inflammatory drugs and COX inhibitors, which act by modulating the arachidonic acid cascade, are the traditional anti-inflammatory drugs (Gejjalagere Honnappa and Mazhuvancherry Kesavan 2016). Despite their popularity, these drugs are associated with various adverse effects, especially in the course of their long-term use at high doses (Gejjalagere Honnappa and Mazhuvancherry Kesavan 2016). Therefore, there is an urgent need for new drugs capable of constraining chronic low-grade inflammation in age-related diseases. Taking this need into account, natural products emerge as potential sources of new molecules with anti-inflammatory properties (Recio, Andujar et al. 2012, Killeen, Linder et al. 2014, Azab, Nassar et al. 2016).

Mint species, in particular their essential oils, are among those with reported anti-inflammatory properties in ethnopharmacological studies. Monoterpenes are major components of those essential oils and several members of this class, namely those belonging to the limonene synthase pathway, have been shown to have anti-inflammatory properties in distinct cell and animal models of various diseases (Miguel 2010). Moreover, our previous work demonstrated that limonene has anti-inflammatory properties in human chondrocytes (Rufino, Ribeiro et al. 2015).

Nonetheless, studies regarding the anti-inflammatory activity of monoterpenes frequently report discrepant results, at least in part, related to the significant heterogeneity of their experimental design. Moreover, information regarding the structure-activity relationship (SAR) of monoterpenes is scarce, although essential for optimizing their development as drugs with therapeutic potential. In this way, the first objective of this dissertation was to perform a standardised screening assay of the anti-inflammatory properties of limonene-derived monoterpenes and establish the SAR. Once the SAR has been established, the second objective of this dissertation is to explore the mechanism of action of the most potent compounds found in the screening assay. The study of the mechanism of action of these

compounds was focused on the NF-κB pathway and the MAPK cascade, given their central role in the inflammatory process.

In the following chapters (2, 3 and 4) of this dissertation, the results addressing these objectives will be presented. Chapter 2 will focus on the first objective of this dissertation – the standardised screening assay and the SAR. Chapters 3 and 4 will show the results concerning the investigation of the mechanism of action of the most potent compounds – second objective. Finally, chapter 5 will summarise the main conclusions and point out future perspectives of the lead compounds.

Chapter 2: Standardised comparison of limonene-derived monoterpenes identifies structural determinants of anti-inflammatory activity

Cátia Sousa, Alcino Jorge Leitão, Bruno Miguel Neves, Fernando Judas, Carlos Cavaleiro, Alexandrina Ferreira Mendes

Scientific Reports, 2020, 10 (1), 7199
doi: 10.1038/s41598-020-64032-1

Note: The results presented in this chapter are formatted according to the style of the journal where the paper was published, with minor modifications.

Abstract

Mint species are widely used in traditional and conventional medicine as topical analgesics for osteoarthritic pain and for disorders of the gastrointestinal and respiratory tracts which are all associated with chronic inflammation. To identify the structural determinants of anti-inflammatory activity and potency which are required for chemical optimization towards development of new anti-inflammatory drugs, a selected group of monoterpenes especially abundant in mint species was screened by measuring bacterial lipopolysacharide (LPS)-induced nitric oxide (NO) production in murine macrophages.

Nine compounds significantly decreased LPS-induced NO production by more than 30%. IC_{50} values were calculated showing that the order of potency is: (S)-(+)-carvone > (R)-(-)-carvone > (+)-dihydrocarveol > (S)-8-hydroxycarvotanacetone > (R)-8-hydroxycarvotanacetone > (+)-dihydrocarvone > (-)-carveol > (-)-dihydrocarveol > (S)-(+)-pulegone. Considering the carbon numbering relative to the common precursor, limonene, the presence of an oxygenated group at C6 conjugated to a double bond at C1 and an isopropenyl group and S configuration at C4 are the major chemical features relevant for activity and potency. The most potent compound, (S)-(+)-carvone, significantly decreased the expression of NOS2 and IL-1β in macrophages and in a cell model of osteoarthritis using primary human chondrocytes.

(S)-(+)-carvone may be efficient in halting inflammation-related diseases, like osteoarthritis.

2.1 Introduction

Inflammation is an orchestrated physiological response elicited by exogenous inducers such as infectious agents, allergens, irritants and toxic compounds, as well as by endogenous triggers released from stressed or damaged tissues/cells (Antonelli and Kushner 2017). Although aiming at restoring homeostasis, inflammation has the potential to cause tissue damage and perpetuate itself (Kotas and Medzhitov 2015). Likewise, inflammation has been reported as an important component associated with most chronic human diseases, such as rheumatic (Rosa, Judas et al. 2008), metabolic and neurodegenerative diseases and cancer (Nathan and Ding 2010, Kotas and Medzhitov 2015). Due to the increased incidence of these diseases in relation with population aging and the lack of efficacy and adverse side effects of currently available anti-inflammatory drugs more directed to acute inflammation, new therapeutic agents are needed to contend chronic inflammation-associated diseases (Dinarello 2010, Killeen, Linder et al. 2014, Ghosh, Ali et al. 2016).

Natural products are increasingly used for their anti-inflammatory properties and as sources of new anti-inflammatory compounds (Killeen, Linder et al. 2014, Ghosh, Ali et al. 2016). Among the species most widely used, those of the family Lamiaceae, genus *Mentha* L., commonly designated as mint species, are widely used in traditional (Mimica-Dukic and Bozin 2008) and conventional medicine, especially as essential oils. These are well-known for anti-inflammatory, antimicrobial, carminative, antispasmodic and analgesic properties. Among several chemical classes identified in mint essential oils, monoterpenes belonging to the limonene synthase pathway, such as menthol, menthone, pulegone and carvone, are especially abundant (Mimica-Dukic and Bozin 2008). Some components of this group of monoterpenes have been reported to possess anti-inflammatory activity (de Cassia da Silveira e Sa, Andrade et al. 2013) that may justify, at least in part, the beneficial effects attributed to mint species by traditional and conventional medicine (Karousou, Balta et al. 2007, Fatiha Brahmi 2017). However, mint species exhibit many different chemotypes with significant diversity in qualitative and quantitative chemical composition (Fatiha Brahmi 2017, Singh and Pandey 2018) that causes substantial variability, although poorly characterized, in terms of pharmacological activity of distinct plants and their essential oils. Besides differences related to distinct chemotypes, disparities in the experimental design, namely concerning the range of concentrations tested and the cell and animal models and inflammatory stimuli used, also make comparisons or prediction of the efficacy and potency

of different plants, their essential oils and individual compounds impossible. This heterogeneity also makes it impossible to identify the structural determinants of activity, that is the structure-activity relationship (SAR) of this class of natural compounds.

The chemical optimization of an active compound requires that knowledge and is essential to improve its physicochemical properties and/or increase its potency and safety, thus yielding a suitable lead. This is especially important for monoterpenes whose volatility is a major drawback significantly limiting their use as active ingredients for the large scale production of medicines. Hence, elucidating the SAR is essential to guide the chemical modification of these compounds, namely to lower their vapour pressure at room temperature, without compromising pharmacological activity and/or increasing toxicity, and therefore to enable their progression towards new therapeutic agents (Hughes, Rees et al. 2011). Further, such knowledge is also essential to explain the different anti-inflammatory properties and potency of distinct mint chemotypes and their essential oils and can be used to predict the therapeutic potential of a given product based on its chemical composition.

Thus, the purpose of this study was to assess, under standardized conditions, the anti-inflammatory activity of a selected group of monoterpenes belonging to the limonene synthase pathway that are abundant in mint species (Fig. 1a) and to compare the potency of the active ones by determining their half-maximal inhibitory concentrations (IC_{50}). These data were then correlated with structural features to identify chemical determinants of activity and potency useful to enable chemical optimization of the active compounds.

For this, the ability of the test compounds to inhibit the production of nitric oxide (NO), a potent and destructive inflammatory mediator (Nagy, Clark et al. 2007, Chung, Lee et al. 2011, Thomas and Wink 2017), induced by bacterial lipopolysaccharide (LPS) in the mouse macrophage cell line, Raw 264.7, was used as a well-established primary screening assay for the identification of small molecules with anti-inflammatory activity (Yu, Zeng et al. 2016, Kumar and Abraham 2017). Then and to further confirm their anti-inflammatory activity, we determined the ability of the two most potent compounds to inhibit the expression of NO synthase 2 (NOS2), the enzyme that produces large amounts of NO in response to inflammatory stimuli (Forstermann and Kleinert 1995, Nagy, Clark et al. 2007), and interleukin-1β (IL-1β), two critical inflammatory mediators strongly associated with several acute and chronic human inflammatory diseases (Rosa, Judas et al. 2008, Asiimwe, Yeo et al. 2016, Thomas and Wink 2017).

Finally, the most potent compound identified in macrophages, S-(+)-carvone (**4**), was tested in primary human chondrocyte cultures treated with the pro-inflammatory and catabolic cytokine, IL-1β, as a widely used cell model of osteoarthritis (OA) (Johnson, Argyle et al. 2016). This is the most common musculoskeletal disease, causing pain and loss of mobility and quality of life to millions of people worldwide (Cross, Smith et al. 2014). While no curative therapies are yet available (Goldring and Berenbaum 2015, Martel-Pelletier, Barr et al. 2016) essential oils from *Mentha spicata,* which is especially abundant in S-(+)-carvone (**4**), are broadly used to decrease osteoarthritic pain (Mahboubi 2017). Therefore, we hypothesized that such analgesic effect can be, at least in part, secondary to the anti-inflammatory properties of that compound. To test this hypothesis and evaluate its potential as an anti-osteoarthritic drug, we determined whether S-(+)-carvone (**4**) is also effective in reducing inflammatory responses in human chondrocytes.

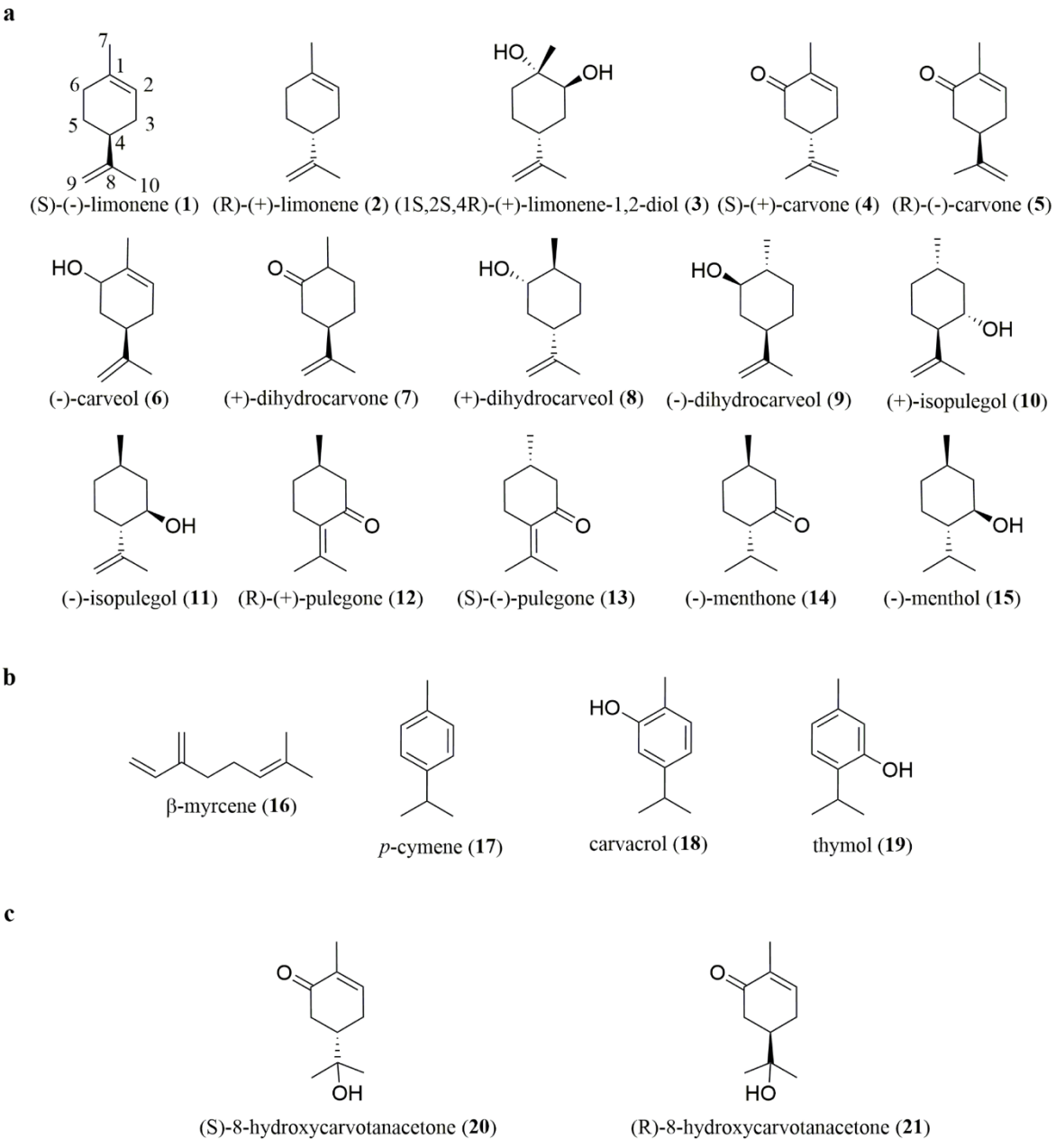

Figure 1. Structures of the monoterpenes tested. (**a**) Selected commercially available limonene-derived monoterpenes found in *Mentha* spp. (**b**) non-limonene-derived monoterpenes and (**c**) semi-synthetic limonene-derived monoterpenes were used to elucidate the role of specific chemical features. Stereochemistry of each chiral centre is indicated only where enantiomerically pure compounds were used. The numbering system employed here is based on compound **1**.

2.2 Results

2.2.1 Nine out of twenty-one test compounds inhibit LPS-induced NO production in Raw 264.7 macrophages

Commercially available compounds with substituents in specific positions of the *p*-menthane skeleton in limonene were selected for the primary screening assay (Fig.1a). We also tested four unrelated natural compounds (Fig. 1b), as well as two semi-synthetic carvone derivatives (Fig. 1c), to further elucidate the relevance to anti-inflammatory activity of specific chemical features of the limonene-derived compounds tested.

Various concentrations of the test compounds, in the absence or presence of LPS, were first evaluated for cytotoxicity using the resazurin reduction assay (O'Brien, Wilson et al. 2000) (figure S1 and figure S2). Concentrations above 400 µg/mL (approximately 2600 µM on average) were found not to be completely miscible in aqueous solution, even in the presence of 0.1% DMSO, and so this was the maximal concentration tested. Cytotoxicity was defined, according to the standard for cytotoxicity assessment, ISO 10993-5 (Standardization 2009), as the highest concentration that did not decrease cell viability by more than 30% relative to cells treated with LPS alone. Non-cytotoxic concentrations of each compound were then selected for the screening assay and subsequent studies.

To confirm the quality of the screening assay, we used Bay 11-7082, a selective IκB Kinase inhibitor that abrogates NF-κB activation (Pierce, Schoenleber et al. 1997) and the expression of its target genes, including NOS2 (Mendes Sdos, Candi et al. 2009), as a pharmacological control. Pre-treatment with 5 µM Bay 11-7082 decreased NO production to 48.1 ± 5.2% relative to cells treated with LPS alone, as expected.

At non-cytotoxic concentrations, none of the compounds tested affected basal NO production when added to macrophage cultures in the absence of LPS (data not shown) and eight (**1**, **2**, **10**, **11**, **12**, **14**, **15** and **16**) also had no effect on LPS-induced NO production (Table 1). Thirteen compounds were found to elicit a statistically significant decrease of LPS-induced NO production at the highest concentration tested, but of these, four (**3**, **17, 18** and **19**) had only a negligible effect of less than 20%. The other nine compounds (**4**, **5**, **6**, **7**, **8**, **9**, **13, 20** and **21**) elicited a robust inhibition greater than 30% (Table 1) and, therefore, were selected for further studies.

Table 1. Results of the primary screening assay relating the highest non-cytotoxic concentration tested and the % inhibition of LPS-induced NO production

Compound	**Highest non-cytotoxic concentration tested** [**µM (µg/mL)**]	**% inhibition of LPS-induced NO production** [a] **[% ± SEM]**	**Adjusted *p* value** [b]
(S)-(-)-limonene (**1**)	36.7 (5)	11.08 ± 4.65	0.1968
(R)-(+)-limonene (**2**)	367 (50)	-1.80 ± 0.55	0.4140
(1S,2S,4R)-(+)-limonene-1,2-diol (**3**)	2349 (400)	13.90 ± 2.03	< 0.0001
(S)-(+)-carvone (**4**) [c]	666 (100)	68.73 ± 1.55	< 0.0001
(R)-(-)-carvone (**5**) [c]	666 (100)	71.50 ± 1.74	< 0.0001
(-)-carveol **(6)**	2628 (400)	52.30 ± 5.54	0.0020
(+)-dihydrocarvone (**7**)	2628 (400)	73.57 ± 2.81	< 0.0001
(+)-dihydrocarveol (**8**)	1297 (200)	71.03 ± 2.28	0.0002
(-)-dihydrocarveol (**9**)	2593 (400)	62.03 ± 8.62	0.0141
(+)-isopulegol (**10**)	2593 (400)	-18.47 ± 5.65	0.0002
(-)-isopulegol (**11**)	2593 (400)	-12.63 ± 1.30	< 0.0001
(R)-(+)-pulegone (**12**)	1314 (200)	7.80 ± 2.98	0.1881
(S)-(-)-pulegone (**13**)	2628 (400)	35.60 ± 4.86	< 0.0001
(-)-menthone (**14**)	1297 (200)	-9.88 ± 2.85	0.0041
(-)-menthol (**15**)	2560 (400)	-6.90 ± 1.24	0.0071
β-myrcene (**16**)	183 (25)	16.48 ± 17.00	0.1496
p-cymene (**17**)	37 (5)	8.50 ± 5.53	0.0100
carvacrol (**18**)	33 (5)	10.78 ± 1.34	< 0.0001
thymol (**19**)	83 (12.5)	8.93 ± 1.91	0.0002
(S)-8-hydroxycarvotanacetone (**20**)	2378 (400)	78.43 ± 1.60	< 0.0001
(R)-8-hydroxycarvotanacetone (**21**)	2378 (400)	76.25 ± 1.97	< 0.0001

a NO production was assessed as the amount of nitrite (NO_2^-) accumulated in culture supernatants. % inhibition of NO production was calculated with the formula:

$$100 - \left(\frac{([NO_2^-]_{LPS} - [NO_2^-]_{test}) \text{ x } 100\ \%}{[NO_2^-]_{LPS}} \right)$$

where $[NO_2^-]_{LPS}$ is the concentration of NO_2^- in LPS-treated cells and $[NO_2^-]_{test}$ is the concentration of NO_2^- in cells treated with LPS in the presence of each test compound.

b Adjusted *p* value relative to LPS-treated cells.

c The highest non-cytotoxic concentration tested in the presence of LPS was 1331 µM (200 µg/mL). As 666 µM (100 µg/mL) decreased LPS-induced NO production to control levels, no further concentrations were tested in this primary screening assay.

Thus and to compare the active compounds in terms of potency, the respective concentration required to inhibit NO production by 50% (IC_{50}) was determined by testing further non-cytotoxic concentrations. Since the maximal inhibition achieved with the highest non-cytotoxic concentration of (S)-(-)-pulegone (**13**) tested, did not exceed 36%, the IC_{50} for this compound was not determined. Results in Table 2 show that the order of potency of the remaining 8 active compounds is (S)-(+)-carvone (**4**) > (R)-(-)-carvone (**5**) >> (+)-dihydrocarveol (**8**) > (S)-8-hydroxycarvotanacetone (**20**) > (R)-8-hydroxycarvotanacetone (**21**) > (+)-dihydrocarvone (**7**) > (-)-carveol (**6**) > (-)-dihydrocarveol (**9**).

Table 2. IC_{50} values for the eight compounds found to significantly decrease LPS-induced NO production in the Raw 264.7 cell line

Compound	**IC_{50} [µM (µg/mL)]**	**95% CI[a] [µM (µg/mL)]**
(S)-(+)-carvone (**4**)	109.7 (16.50)	100.6-119.6 (15.13-17.98)
(R)-(-)-carvone (**5**)	122.8 (18.46)	113.8-132.7 (17.08-19.95)
(-)-carveol (**6**)	1997 (304.0)	1731-2303 (263.5-350.6)
(+)-dihydrocarvone (**7**)	1472 (224.0)	1105-1961 (168.2-298.4)
(+)-dihydrocarveol (**8**)	532.2 (82.13)	444.2-637.7 (68.54-98.41)
(-)-dihydrocarveol (**9**)	2141 (330.2)	1851-2475 (285.5-381.8)
(S)-8-hydroxycarvonatacetone (**20**)	762.0 (116.3)	670.4-866.0 (101.3-133.5)
(R)-8-hydroxycarvonatacetone (**21**)	841.5 (141.6)	776.0-912.4 (130.5-153.5)

[a] Concentration range within the 95% Confidence Interval (CI) of the IC_{50} value.

2.2.2 Identification of chemical features relevant for activity by correlation with potency

Having determined the order of potency of the active compounds, we then correlated those results with structural features of all compounds tested to identify the relevant structural determinants of anti-inflammatory activity. For this, we defined a carbon numbering system applicable to all compounds tested, since their different functional groups and application of IUPAC rules would lead to different numbering of the same carbon atoms. Thus, IUPAC rules were used to define carbon numbering for limonene (Fig.1) and the resulting numbering sequence was applied to all test compounds without considering their specific substituents. Besides limonene-derived compounds, four other natural monoterpenes, β-myrcene (**16**), *p*-cymene (**17**), carvacrol (**18**) and thymol (**19**) (Fig. 1b), were tested mainly to assess the relevance of the rigidity or flexibility of the molecule for anti-inflammatory activity. Additionally, two carvone derivatives (**20** and **21**, Fig. 1c) were synthesized and tested to assess the relevance of the isopropenyl group at C4.

A functional oxygenated group, either a carbonyl or a hydroxyl group, at C6 is present in all active compounds (**4**-**9**, **20** and **21**) and absent (**1** and **2)** or present at other positions (**3**, **10**-**12**, **14** and **15**) in all inactive or only slightly active (below 20% inhibition at the maximal non-cytotoxic concentration tested) compounds with the exception of (S)-(-)-pulegone (**13**) which bears a carbonyl group at C3 and showed weak activity.

Another important feature for activity seems to be the presence of an α,β double bond at C1, since its absence is the only difference between (+)-dihydrocarvone (**7**) and the much more potent carvone enantiomers (**4** and **5**). Moreover, the conjugation of this double bond to the carbonyl group at C6 also seems relevant for activity since the two most potent compounds, (S)-(+)-carvone (**4**) and (R)-(-)-carvone (**5**), present this feature which is also present in their derivatives (**20** and **21**), but not in the other less potent compounds. Nonetheless, (R)-(+)-pulegone (**12**) and (S)-(-)-pulegone (**13**) which have no or little activity, also have an α,β double bond conjugated to a carbonyl group, but involving the carbonyl group at C3 and the double bond at C4. Thus, the localization of the conjugated double bond and carbonyl group seems especially relevant for activity. Nevertheless, while (R)-(+)-pulegone (**12**) is inactive, its S enantiomer (**13**) showed weak activity, indicating that the stereochemistry can be relevant for activity.

Then and to elucidate the relevance of the isopropenyl group at C4, present in six active compounds (**4**, **5**, **6**, **7**, **8** and **9**), but also in five inactive ones (**1**, **2**, **3**, **10** and **11**), we synthesized derivatives of the two most potent compounds, the carvone enantiomers, where that group was replaced by a 2-hydroxyisopropanyl group. The 8-hydroxycarvotanacetone enantiomers (**20** and **21**) synthesized showed significant activity, although much lower than the respective parent compounds (**4** and **5**) (Table 2), thus confirming the relevance of the isopropenyl group at C4 for anti-inflammatory activity. Nonetheless, the isopropenyl group per se is not sufficient for activity, as compounds with such group, but lacking the oxygenated group at C6 (**1**, **2**, **3**, **10** and **11**) are inactive.

The results also show that (S)-(+)-carvone (**4**) and its derivative (**20**) are slightly more potent than their respective R isomers (**5** and **21**), from which they differ only in terms of stereochemistry at the chiral C4 atom. The third most potent compound used, (+)-dihydrocarveol (**8**), is a mixture of isomers of which the most abundant, (1S,2S,5S)-dihydrocarveol, presents the S configuration at all its chiral centres, including C5 that corresponds to C4 of limonene, while its isomer, (-)-dihydrocarveol (**9**), four times less potent, is also a mixture of isomers, the most abundant of which, (1R,2R,5R)-dihydrocarveol, presents the R configuration (detailed composition and purity of each test compound in Supplementary Table S1). Moreover, (-)-carveol (**6**) and (+)-dihydrocarvone (**7**) also have additional chiral centres at C6 or C1 and the products used are mixtures of S and R isomers at those positions, but in both, the most abundant is the isomer presenting the R configuration at the carbon atom corresponding to C4 (detailed composition in Supplementary Table S1). Similarly, (R)-(+)-pulegone (**12**) is inactive, while its S enantiomer (**13**) shows weak activity. Taken together, these results suggest that the S configuration, especially at C4, is more favourable for activity.

Finally, we tested four monoterpenes (**16**-**19**) unrelated to the limonene synthase pathway (Fig. 1b), but presenting various degrees of rigidity to elucidate the relevance of this feature for activity. Neither the more rigid (**17**-**19**), nor the more flexible (**16**) of these four compounds showed any activity.

Table 3 summarizes the chemical features found relevant for anti-inflammatory activity.

Table 3. Relationship between chemical features and potency of the nine active compounds

Chemical features	**Order of potency**								
	4	**> 5**	**>> 8***	**> 20**	**> 21**	**>7***	**>6***	**>9***	**>>13**
=CO (C6)	+	+	-	+	+	+	-	-	-
-OH (C6)	-	-	+	-	-	-	+	+	-
= bond at C1	+	+	-	+	+	-	+	-	-
Michael centre	+	+	-	+	+	-	-	-	+
Michael centre sterically hindered	No	No	-	No	No	-	-	-	Yes
Isopropenyl group at C4	Yes	Yes	Yes	No	No	Yes	Yes	Yes	No
Chirality at C4	S	R	S	S	R	R	R	R	-
Chirality at C1	-	-	S	-	-	S/R	-	R	S
Chirality at C6	-	-	S	-	-	-	S/R	R	-

+/- denotes presence/absence; S/R denotes mixture of diastomers; *denotes the stereochemistry of the most abundant isomer in the compound tested. Detailed composition is provided in Supplementary Table S1.

2.2.3 The carvone enantiomers inhibit LPS-induced NOS2 and IL-1β expression in macrophages

To further confirm the anti-inflammatory properties of the two most potent compounds, the expression of NOS2 and IL-1β were evaluated at the mRNA and protein levels. Macrophage treatment with 1 μg/mL LPS significantly increased NOS2 mRNA (Fig. 2a) and protein (Fig. 2b) levels which, as expected, were decreased by Bay 11-7082. The carvone enantiomers, (**4**) or (**5**), also significantly reduced LPS-induced NOS2 mRNA (Fig. 2a) and protein levels (Fig. 2b), as well as IL-1β mRNA levels (Fig. 3a). Upon transcription, this mRNA is translated into a precursor protein (pro-IL-1β) that undergoes partial hydrolysis by a proteolytic complex, the inflammasome, being converted into the mature IL-1β protein which is then secreted (Patel, Carroll et al. 2017). In agreement with the decrease in IL-1β mRNA levels, (S)-(+)-carvone (**4**) and (R)-(-)-carvone (**5**) significantly decreased the levels of both pro-IL-1β (Fig. 3b) and mature IL-1β secreted into the cell culture medium (Fig. 3c), relative to treatment with LPS alone.

To further characterize the mechanism of action of the carvone enantiomers (**4** and **5**), we determined whether they are also effective when added to the cells after the inflammatory stimulus and the mechanism involved, that is, whether they act by modifying NOS2 protein levels and/or its enzyme activity. For this, we treated macrophages with LPS for 8 h to induce NOS2 expression and protein synthesis. Then, the cells were washed to remove LPS and new medium with the carvone enantiomers (**4** and **5**) was added to the respective wells for 18 h. The results in Figure 4a show that treatment with either compound decreased NO production by approximately 30% while NOS2 protein levels were reduced by approximately 60% (Fig. 4b). This suggests that the decrease in NO production is secondary to the decrease in NOS2 protein and not to a direct inhibition of the enzyme activity.

To determine whether this decrease was due to inhibition of NOS2 protein synthesis, still occurring after removal of LPS, or to induction of its degradation, we evaluated its protein levels 8 h after treatment with LPS. The results obtained show that NOS2 protein levels still increased after removal of LPS (Fig. 4c), indicating that NOS2 protein synthesis continues even after removal of the inducing stimulus. This indicates that the decrease in NO production observed in Figure 4a is not due to inhibition of NOS2 enzyme activity, but rather to inhibition of its synthesis.

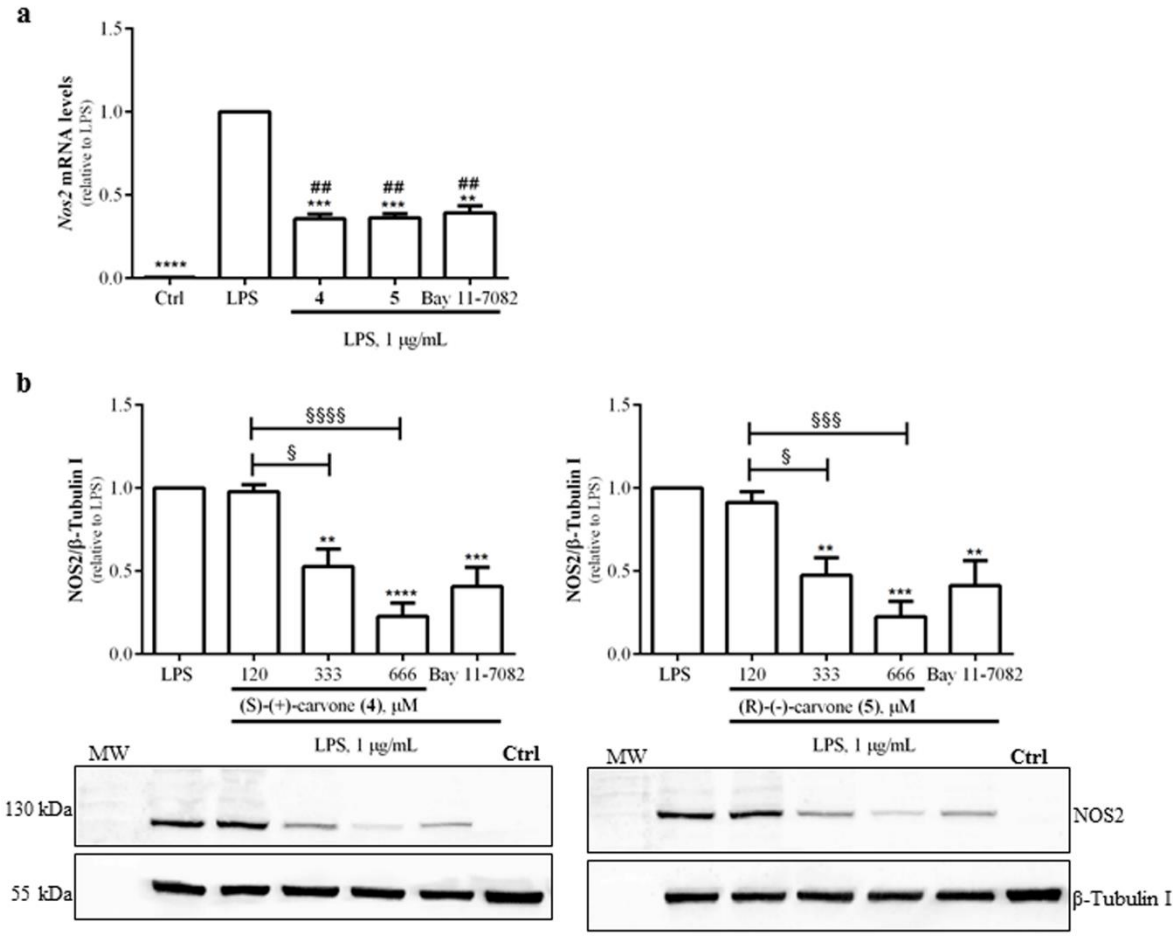

Figure 2. (S)-(+)-carvone (4) and (R)-(-)-carvone (5) decrease LPS-induced *Nos2* mRNA (a) and protein (b) levels in the Raw 264.7 cell line. Macrophage cultures were treated with 1 µg/mL LPS, for 6 h (**a**) or 18 h (**b**), following pre-treatment for 1 h with 666 µM of each test compound (**a**) or with the concentrations indicated in (**b**). As a positive control, the cells were similarly treated with the selective NF-κB inhibitor, Bay 11-7082, 5 µM. Control cells (Ctrl) were treated with the vehicle (0.1% DMSO) in the absence of LPS. Each column represents the mean ± SEM of four independent experiments. The blots shown are representative of, at least, three independent experiments and are cropped for clarity and conciseness. The corresponding full-length blots are presented in figure S3. $^{**}p<0.01$, $^{***}p<0.001$ and $^{****}p<0.0001$ relative to LPS-treated cells. $^{\#\#}p<0.01$ relative to the Ctrl. $^{\S}p<0.05$, $^{\S\S\S}p<0.001$ and $^{\S\S\S\S}p<0.0001$ between the conditions indicated. MW: molecular weight marker.

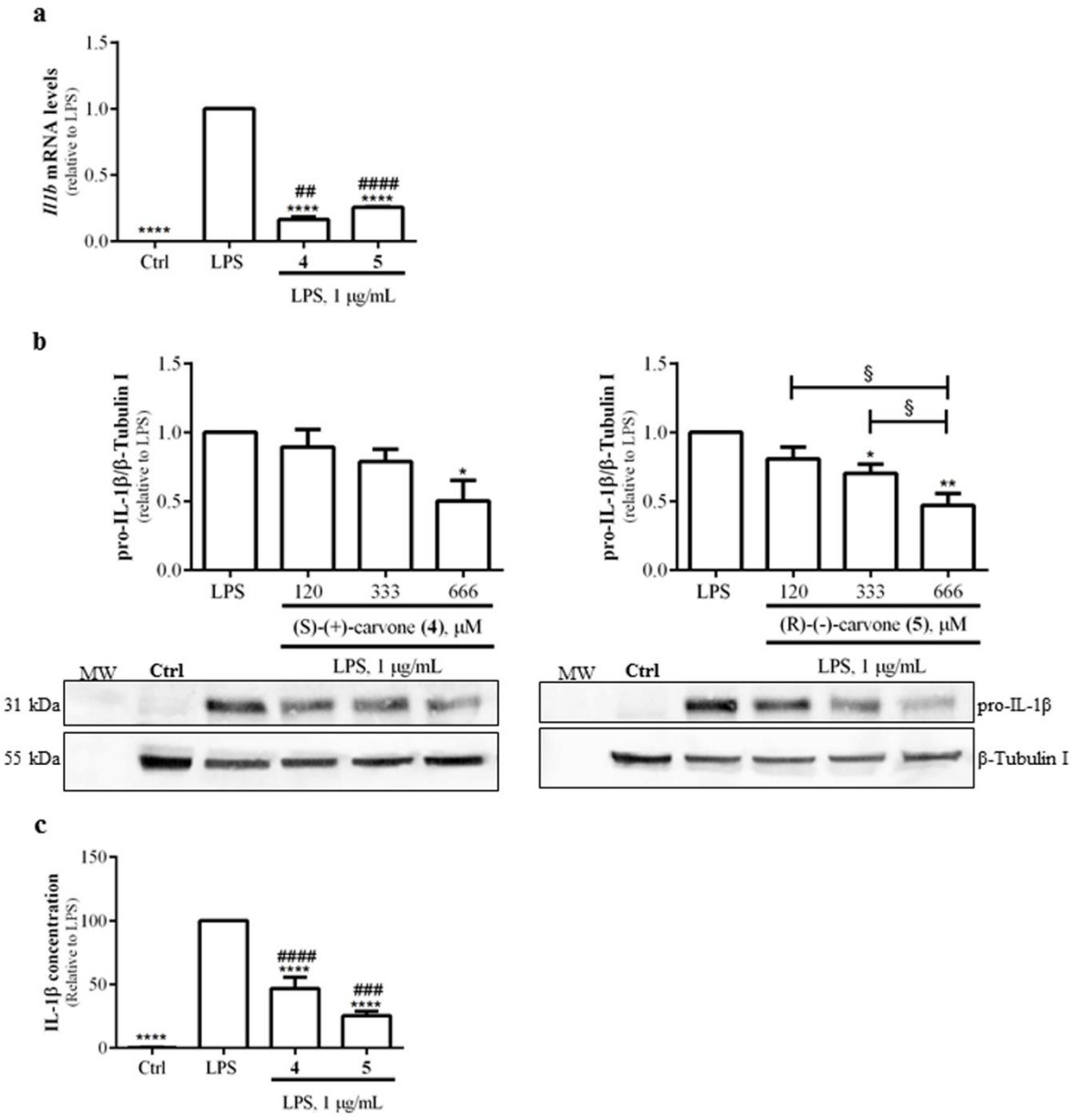

Figure 3. (S)-(+)-carvone (4) and (R)-(-)-carvone (5) decrease LPS-induced IL-1β mRNA (a) and protein (b and c) levels in the Raw 264.7 cell line. Macrophage cultures were treated with 1 µg/mL LPS, for 6 h (**a**) or 18 h (**b** and **c**), following pre-treatment for 1 h with 666 µM of each test compound (**a** and **c**) or with the concentrations indicated in (**b**). Control cells (Ctrl) were treated with vehicle (0.1% DMSO) in the absence of LPS. Each column represents the mean ± SEM of, at least, three independent experiments. The blots shown are representative of, at least, three independent experiments and are cropped for clarity and conciseness. The corresponding full-length blots are presented in figure S3. *p<0.05, **p<0.01 and ****p<0.0001 relative to LPS-treated cells. $^{\#\#}p$<0.01, $^{\#\#\#}p$<0.001 and $^{\#\#\#\#}p$<0.0001 relative to the Ctrl. $^{\S}p$<0.05 between the conditions indicated. MW: molecular weight marker.

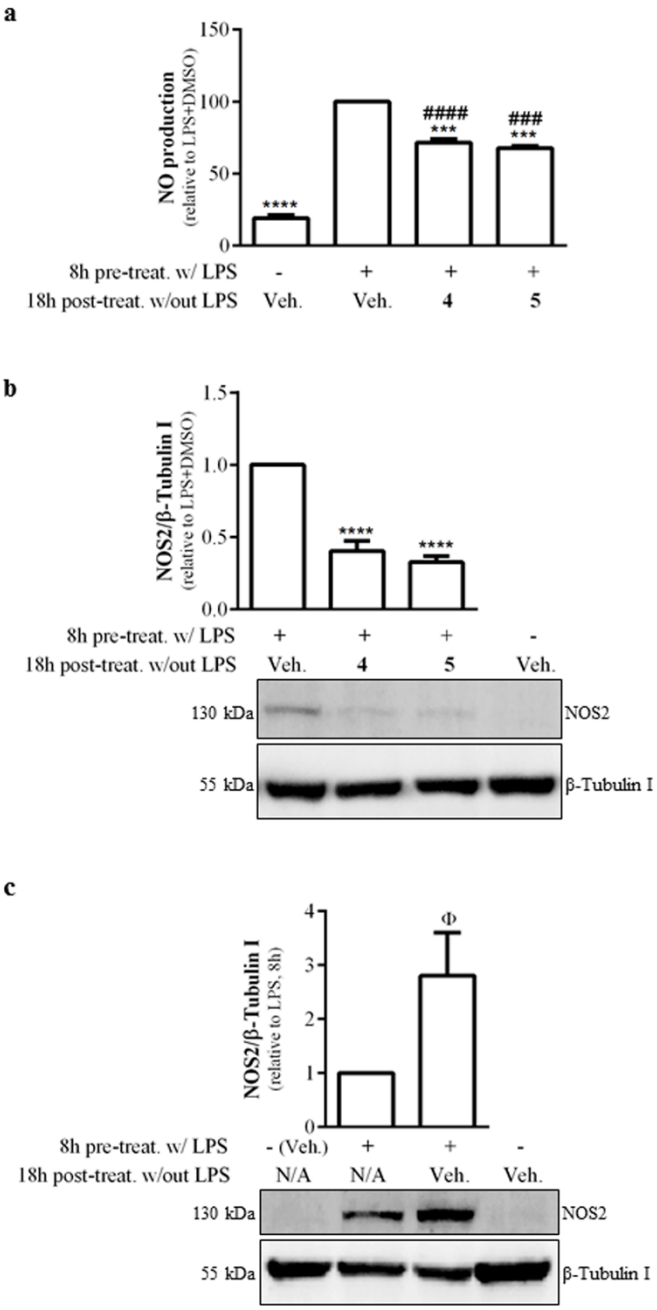

Figure 4. Effects of (S)-(+)-carvone (4) and (R)-(-)-carvone (5) on NO production and NOS2 protein levels pre-induced by treatment with LPS. In panels **a** and **b**, macrophage cultures were treated with 1 μg/mL LPS, for 8 h to induce NOS2 expression. Then, the medium was changed to remove LPS and the cells were treated for another 18 h with 666 μM of each test compound or the vehicle (0.1% DMSO). Controls were set up by leaving the cells untreated for 8h followed by addition of vehicle for 18h. In panel **c**, cells were pre-treated with LPS or left untreated for 8h and immediately processed for protein extraction or treated with or without LPS for 8 h and then further incubated with vehicle for another 18 h. Each column represents the mean ± SEM of, at least, three independent experiments. The blots shown are representative of, at least, three independent experiments and are cropped for clarity and conciseness. The corresponding full-length blots are

presented in figure S3. ***p<0.001 and ****p<0.0001 relative to LPS, 8 h + vehicle, 18 h. $^{###}p$<0.001 and $^{####}p$<0.0001 relative to untreated cells, 8 h + DMSO, 18h. $^{\Phi}p$<0.05 relative to LPS, 8h. N/A: not applicable.

2.2.4 S-(+)-carvone (4) inhibits inflammatory responses induced by IL-1β in human chondrocytes

First, the highest concentrations of (S)-(+)-carvone (**4**) not toxic to murine macrophages were tested in human chondrocytes and found not to affect cell viability relative to cells treated with IL-1β alone (Fig. 5a). At the same concentrations, (S)-(+)-carvone (**4**) significantly decreased IL-1β-induced NOS2 protein levels (Fig. 5b) and NO production (Fig. 5c) in human chondrocytes. 5 µM Bay 11-7082 significantly decreased both parameters (Figs. 5b and 5c), confirming the quality of the model system. Finally, (S)-(+)-carvone (**4**) also significantly decreased pro-IL-1β protein levels in a concentration-dependent manner (Fig. 5d).

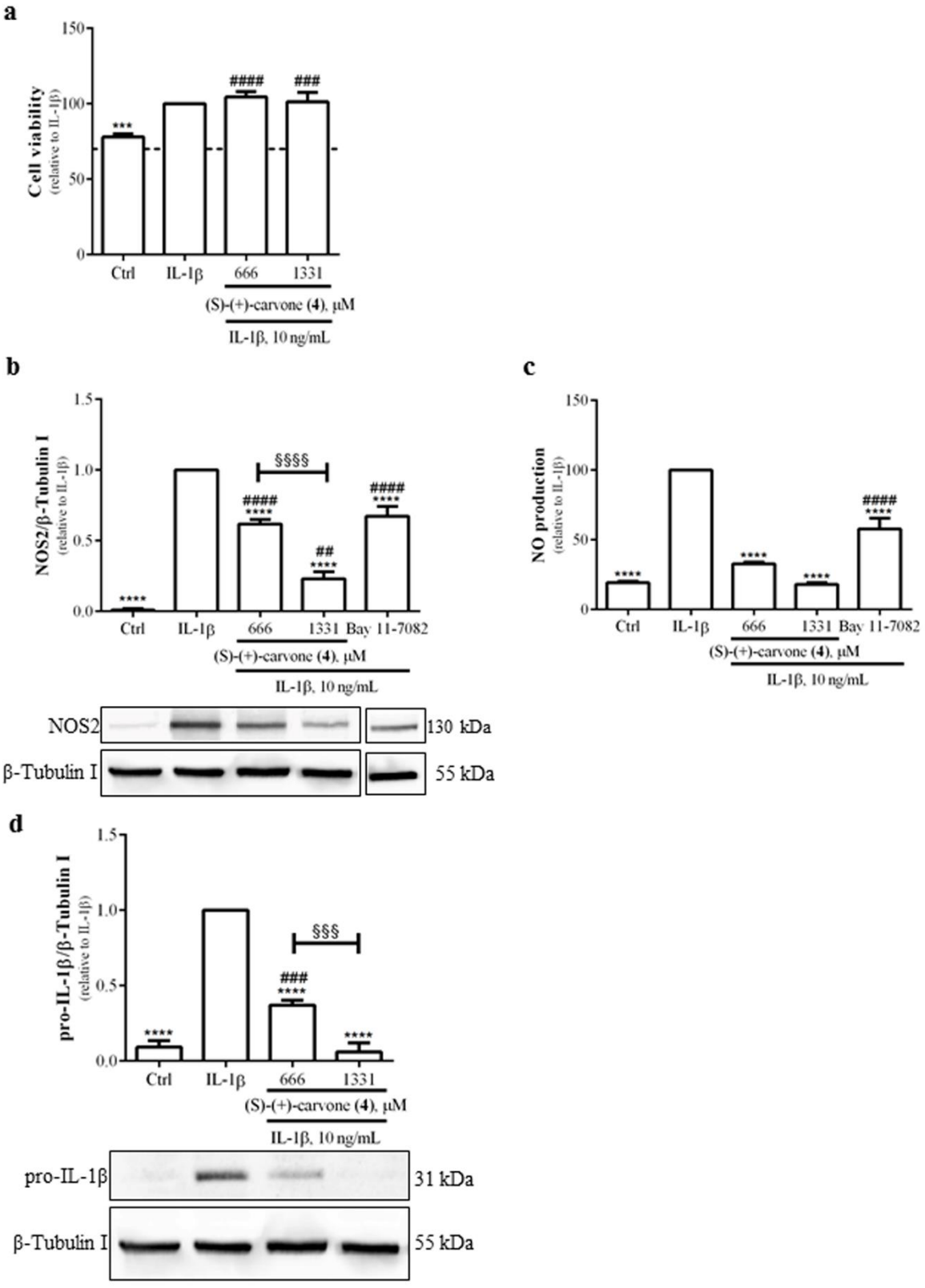

Figure 5. (S)-(+)-carvone (4) does not affect cell viability (a) and decreases IL-1β-induced NOS2 protein levels (b) and NO production (c) as well as pro-IL-1β protein levels (d) in human chondrocytes. The cells

were treated with 10 ng/mL IL-1β for 24 h (**a**, **b**, **c** and **d**), following pre-treatment for 1 h with 666 or 1331 μM of (S)-(+)-carvone (**4**). As a positive control, the cells were similarly treated with 5 μM Bay 11-7082 (**b** and **c**). Control cells (Ctrl) were treated with the vehicle (0.1% DMSO) in the absence of IL-1β. Each column represents the mean ± SEM of, at least, three independent experiments. The blots shown are representative of, at least, three independent experiments and are cropped for clarity and conciseness. The blots shown in Fig. 5b were vertically sliced before the last condition (Bay 11-7082) to exclude a condition not relevant for the present study. The corresponding full-length blots are presented in figure S3. ***p<0.001 and ****p<0.0001 relative to IL-1β-treated cells. $^{\#\#}p$<0.01, $^{\#\#\#}p$<0.001 and $^{\#\#\#\#}p$<0.0001 relative to the Ctrl. $^{\S\S\S}p$<0.001 and $^{\S\S\S\S}p$<0.0001 between the conditions indicated.

2.3 Discussion

To the best of our knowledge and among the nine active compounds, (S)-(+)-carvone (**4**), (+)-dihydrocarvone (**7**), (+)- (**8**) and (-)-dihydrocarveol (**9**), (S)-(-)-pulegone (**13**) and the carvone derivatives (**20** and **21**), were never reported to have anti-inflammatory effects, while carvone, either as the racemic mixture (Sepúlveda-Arias, Veloza et al. 2013) or the (R)-(-) enantiomer (**5**) (Abe, Maruyama et al. 2003, Marques, Figueira et al. 2019) and (-)-carveol (**6**) (Marques, Figueira et al. 2019) were recently reported to inhibit some effects correlated with inflammation.

Among the compounds that showed no activity, the lack of inhibition of LPS-induced NO production by the limonene enantiomers (**1** and **2**), (R)-(+)-pulegone (**12**), (-)-menthone (**14**), (-)-menthol (**15**), β-myrcene (**16**), *p*-cymene (**17**), carvacrol (**18**) and thymol (**19**) contrasts with other reports that suggest anti-inflammatory activity for these compounds (Yao and Chiou 1993, Yoon, Lee et al. 2010, Kim, Ko et al. 2013, Nagoor Meeran, Jagadeesh et al. 2015, Rufino, Ribeiro et al. 2015, Xue, Li et al. 2015, Li, Hua et al. 2016, Ghasemi-Pirbaluti, Motaghi et al. 2017, Choi, Kim et al. 2018). At least in part, these discrepancies can be due to the use of distinct models, namely cell lines, animal models and endpoints analysed, as well as to different concentrations tested. Significant anti-inflammatory effects were recently reported for limonene (racemic mixture, up to 200 μg/mL) and β-myrcene (up to 50 μg/mL) in human chondrocytes (Rufino, Ribeiro et al. 2015), as well as in the Raw 264.7 cell line (Yoon, Lee et al. 2010, Kim, Ko et al. 2013), but at concentrations much higher than those used in the current study. These discrepancies can be due in part to the use of distinct methods to assess cell viability, namely the lactate dehydrogenase (LDH) release assay, based on the integrity of the plasma membrane (Fotakis and Timbrell 2006), used in the studies by Kim et al. (2013) and Yoon et al. (2010), versus the resazurin or the MTT

reduction assays dependent on the integrity and activity of mitochondria (Rampersad 2012), used in our studies. Nonetheless, since cytotoxicity to human chondrocytes and murine macrophages was evaluated by similar methods, the much lower cytotoxic concentrations observed in mouse macrophages indicate that these cells are more sensitive to cytotoxicity induced by those monoterpenes, suggesting that their effects are species and/or cell type-specific, which further highlights the importance of standardised side-by-side comparisons of different compounds.

Having performed such a standardized comparison, some chemical features were identified as relevant for activity and potency (Table 3). Among those, the presence of a functional oxygenated group at C6 appears as the major determinant for activity while the conjugation of the carbonyl group at that position with the α,β double bond at C1, present in the carvone enantiomers (**4** and **5**) and their derivatives (**20** and **21**), was found to further increase potency. Such a conjugation provides a Michael acceptor site, that is, an electrophilic site due to the presence of an electron-withdrawing group in close proximity to a double bond, which is a chemical feature relevant for interaction with biomolecules, namely proteins (Talalay, De Long et al. 1988, Zheng, Kenney et al. 1992), and thus likely relevant for interaction of these molecules with their target. However, the pulegone enantiomers (**12** and **13**) which have no or little activity, also have an α,β double bond conjugated to a carbonyl group, but involving the carbonyl group at C3 and the double bond of the isopropylidene group at C4. In this case, the proximity of the methyl group at C10 to the carbonyl group at C3 can cause a sterical hindrance impairing the interaction with the molecular target (Talalay, De Long et al. 1988) and thus impeding activity.

The lower potency of the carvone derivatives (**20** and **21**) relative to the parent compounds (**4** and **5**) can only be due to the replacement of the isopropenyl at C4 by a 2-hydroxyisopropanyl group. The presence of the hydroxyl group can provide an additional hydrogen binding site, thus creating a new site for chemical interactions that may negatively impact anti-inflammatory activity. Furthermore, this hydroxyl group also increases the volume of the molecule at that region which can hinder access to the pharmacological target and thus decrease the activity of those compounds. Replacement of the isopropenyl group at C4 can also explain why these two compounds are less potent than the third most potent compound, (+)-dihydrocarveol (**8**), which despite bearing a hydroxyl group at C6, retains the isopropenyl group at C4.

Another relevant feature for activity must be chirality as, otherwise, all the enantiomer pairs tested should have similar activities which is not the case. Moreover, 3 of the active compounds (**6**-**8**) have additional chiral centres at C1 and/or C6. Interestingly, the order of potency of the nine active compounds is closely related to the S configuration of the chiral atom at C4, although other chemical features, namely the presence of a functional oxygenated group at C6, the double bond at C1 and the isopropenyl group at C4, seem more relevant (Table 3). Since the S or R configurations significantly affect the 3D conformation of a molecule, the S conformation at C4 by conferring some planarity to that region of the molecules is likely relevant for access to and interaction with the target.

Finally, we tested four monoterpenes (Fig. 1b) unrelated to the limonene synthase pathway, but presenting various degrees of rigidity to elucidate the relevance of this feature for activity. None of these four compounds showed activity, including carvacrol (**18**) even though it bears a hydroxyl group at C6. Unlike the nine active compounds, including those bearing a hydroxyl group at the same position (**6**, **8** and **9**), the cyclohexane ring in carvacrol (**18**) is aromatic suggesting that its rigidity impairs the interaction with the target, leading to almost no activity. Likewise, thymol (**19**) which differs from carvacrol only in the position of the hydroxyl group, and *p*-cymene (**17**) which has no functional groups, also showed no activity. On the other hand, β-myrcene (**16**), an aliphatic compound representing a flexible structure, also showed no activity, suggesting that too flexible (**16**) or too rigid (**17, 18** and **19**) structures are unfavourable for activity.

In summary, the results obtained indicate that higher potency is conferred by 1) the carbonyl group at C6, rather than the hydroxyl group, 2) the presence of a Michael centre resulting from the conjugation of an α,β double bond at C1 to a carbonyl group at C6, 3) an isopropenyl group at C4 or, at least, the absence of hydrogen binding sites and bulky groups at that position, and 4) the S configuration, especially at C4. These findings can be useful to predict the anti-inflammatory activity of distinct mint species and their chemotypes once their composition in limonene-derived monoterpenes is known.

As found for inhibition of NO production, the two most potent compounds found, the carvone enantiomers, also significantly decreased the mRNA and protein levels of NOS2 (Figs. 2 and 4) and IL-1β (Fig. 3), further strengthening their anti-inflammatory activity and suggesting that they act at the transcriptional or pre-transcriptional levels. Moreover, (S)-(+)-carvone (**4**) was found to have similar anti-inflammatory effects in human chondrocytes.

This indicates that (S)-(+)-carvone (**4**) is not only effective in inhibiting LPS-induced inflammatory responses in macrophages, but also efficiently inhibits the responses induced by a distinct inflammatory and catabolic stimulus in a different cell type. The anti-inflammatory effects of (S)-(+)-carvone (**4**) in human chondrocytes are especially relevant because inflammatory cytokines, like IL-1β, drive joint destruction by inducing the expression of catabolic enzymes (Liu-Bryan and Terkeltaub 2015) and also contribute to OA pain (Eitner, Hofmann et al. 2017), namely by inducing the expression of nerve growth factor by synovial macrophages (Takano, Uchida et al. 2017). Moreover, unlike other monoterpenes, e.g. limonene, (S)-(+)-carvone (**4**) is effective as an anti-inflammatory agent both in macrophages and human chondrocytes at similar concentrations. Given the relevance of both cell types and the inflammatory stimuli used to OA pathophysiology (Goldring and Berenbaum 2015, Liu-Bryan and Terkeltaub 2015), (S)-(+)-carvone (**4**) may be efficient in halting joint destruction in OA and also contribute to reduce pain. Future studies will aim at further elucidating its mechanism of action and evaluating its anti-osteoarthritic properties *in vivo*.

2.4 Methods

2.4.1 Test compounds

Test compounds **1**-**17** and **19** were from Sigma-Aldrich Co. (St Louis, MO, USA). Thymol (**18**) was from British Drug Houses. Compounds **20** and **21** were synthesized at our laboratory, as described below. Details about purity and isomer composition are provided in Supplementary Table S1.

2.4.2 Chemical synthesis of compounds 20 and 21

The synthetic procedure was adapted from Buechi and Wueest (1979).

*a) Synthesis of (S)-5-(2-hydroxypropan-2-yl)-2-methylcyclohex-2-en-1-one [(S)-8-hydroxycarvotanacetone, **20**].*

1 mL of 50% aqueous sulphuric acid was slowly added to 150 mg (1 mmol) of (S)-(+)-carvone (**4**) at 0ºC. The mixture was stirred for 24 h at 0ºC. After extraction with 2 mL of hexane-ether (3:1), the aqueous layer was extracted with diethyl ether (6 x 2 mL) for 24 h. The ether solution was washed with brine containing sodium bicarbonate, dried over anhydrous sodium sulphate and evaporated under reduced pressure. The remaining aqueous

layer was extracted with ethyl acetate (3 x 2 mL) for 12 h. The organic phases were washed with brine containing sodium bicarbonate, dried over anhydrous sodium sulphate and evaporated under reduced pressure. The combined crude extract was purified by flash chromatography (hexane: ethyl acetate 1:1) to give compound **20** (80 mg, 48% yield) as a viscous liquid. Purity (GC-MS): 99.7%. ^{1}H NMR (400 MHz, $CDCl_3$) δ: 6.77 (m, 1H), 2.64-2.42 (m, 1H), 2.28-2.21 (m, 1H), 2.28-2.21 (m, 2H), 1.78 (s, 3H), 1.24 (s, 3H), 1.23 (s, 3H). ^{13}C NMR (101 MHz, $CDCl_3$) δ: 200.35 (C=O), 145.15 (CH), 135.24 (CH), 71.64 (C-OH), 46.05 (CH), 39.61 (CH_2), 27.31 (CH_3), 27.25(CH_2), 27.02(CH_3), 15.61(CH_3). IR (ATR) cm^{-1}: 3424, 2973, 2925, 2891, 1656, 1381, 1367, 1143, 1111, 1059, 928, 903,813, 711, 678. MS m/z: 28.1, 43.0, 59.1, 95.0, 110.1, 135.1, 150.1, 168.1.

*b) Synthesis of (R)-5-(2-hydroxypropan-2-yl)-2-methylcyclohex-2-en-1-one [(R)-8-hydroxycarvotanacetone, **21**].*

Compound **21** was synthesized as described for compound **20** using as starting material (R)-(-)-carvone (**5**). The combined crude was purified by flash chromatography (hexane: ethyl acetate 1:1) to give compound **21** (78 mg, 48% yield) as a viscous liquid. Purity (GC-MS): 99.5%. ^{1}H NMR (400 MHz, $CDCl_3$) δ: 6.77 (m, 1H), 2.64-2.42 (m, 1H), 2.28-2.21 (m, 1H), 2.28-2.21 (m, 2H), 1.78 (s, 3H), 1.24 (s, 3H), 1.23 (s, 3H). ^{13}C NMR (101 MHz, $CDCl_3$) δ: 200.35 (C=O), 145.15 (CH), 135.24 (CH), 71.64 (C-OH), 46.05 (CH), 39.61 (CH_2), 27.31 (CH_3), 27.25(CH_2), 27.02(CH_3), 15.61(CH_3). IR (ATR) cm^{-1}: 3424, 2973, 2925, 2891, 1656, 1381, 1367, 1143, 1111, 1059, 928, 903,813, 711, 678. MS m/z: 28.1, 43.0, 59.1, 95.0, 110.1, 135.1, 150.1, 168.1.

2.4.3 Cell culture and treatment

a) Macrophages

The mouse macrophage cell line, Raw 264.7 (ATCC No. TIB-71), was cultured in DMEM supplemented with 10% non-heat inactivated foetal bovine serum (FBS), 100 U/mL penicillin and 100 µg/mL streptomycin. Raw 264.7 cells were plated at a density of $3x10^5$ cells/mL and left to stabilize for up to 24 h.

b) Human chondrocytes

Human knee cartilage was collected within 24 h of death from the distal femoral condyles of multi-organ donors (48-77 years old, mean=65, n=7) at the Bone and Tissue Bank of the University and Hospital Centre of Coimbra (CHUC). Only waste tissue resulting from the preparation of bone tissue for cryopreservation was used. All procedures were approved by

the Ethics Committee of CHUC (protocol approval number 8654/DC), which follows the Declaration of Helsinki and Oviedo Convention and the Portuguese legislation for organ donation.

Chondrocytes were isolated by enzymatic digestion from cartilage samples as previously described (Rosa, Judas et al. 2008). Briefly, cartilage shavings underwent sequential digestion with Pronase (Roche, Indianapolis, IN, USA) and collagenase A (Roche, Indianapolis, IN, USA). To avoid chondrocyte dedifferentiation, non-proliferating monolayer cultures were setup by plating $1x10^6$ chondrocytes/mL in HAM: F12 medium containing 3% antibiotics and 5% FBS and allowed to recover for 24 h at 37ºC in a humidified atmosphere with 5% CO_2. Prior to any treatments, chondrocytes were serum-starved overnight and thereafter maintained in culture medium without FBS.

c) Cell treatments

Test compounds and Bay 11-7082 (Calbiochem, San Diego, CA, USA), used as a pharmacological control, were dissolved in dimethyl sulfoxide (DMSO; Sigma-Aldrich Co) so that its final concentration in the culture medium did not exceed 0.1% (v/v). This vehicle was used as control. Lipopolysaccharides from Escherichia coli 026:B6 (LPS; Sigma-Aldrich Co.) were dissolved in phosphate buffered saline (PBS). Recombinant human interleukin-1β (IL-1β; Peprotech, Rocky Hill, NJ, USA) was dissolved in PBS containing 0.1% Bovine Serum Albumin. Test compounds or the vehicle were added to macrophage cell cultures or human chondrocytes 1 h before the pro-inflammatory stimulus, 1 µg/mL LPS or 10 ng/mL IL-1β respectively, and maintained for the rest of the experimental period, except for experiments in figure 4 (details in the Results section and figure legend). The concentrations of each compound and the experimental treatment periods are indicated in figure legends.

2.4.4 Selection of non-cytotoxic concentrations by the resazurin reduction assay

Resazurin is a redox dye used as an indicator of cellular metabolic activity for various applications, namely cell viability, proliferation and toxicity. The assay is based on the intracellular reduction of the non-fluorescent resazurin to resorufin (a fluorescent and pink coloured compound) by mitochondrial or microsomal enzymes that use NADH or NADPH as electron sources. Since only metabolically active cells can reduce the dye, the increase in

fluorescence or absorbance is directly proportional to the number of viable cells (O'Brien, Wilson et al. 2000, Prabst, Engelhardt et al. 2017).

To select non-cytotoxic concentrations of the test compounds, the resazurin solution was added to each well to a final concentration of 50 µM, 90 min before the end of the treatment period indicated in the figure legends. Then, absorbances at 570 nm and 620 nm (reference wavelength) were read in a Biotek Synergy HT plate reader (Biotek, Winooski, VT, USA).

2.4.5 Nitric oxide production

NO production was measured as the amount of nitrite accumulated in the culture supernatants using the Griess reaction which is based in the reaction of nitrite with sulfanilamide under acidic conditions, yielding a diazonium ion that couples to N-(1-napthtyl)ethylenediamine dihydrochloride to form a water-soluble red-violet azo dye that absorbs at 550 nm (Green, Wagner et al. 1982). Briefly, equal volumes of culture supernatants and reagents [equal volumes of 1% (w/v) sulphanilamide in 5% (v/v) phosphoric acid and 0.1% (w/v) N-(1-napthtyl)ethylenediamine dihydrochloride] were mixed and incubated for 10 min, at room temperature, in the dark. The concentration of nitrite accumulated in the culture supernatants was calculated by interpolation of the absorbance of each sample, read in Biotek Synergy HT plate reader (Biotek), in a standard curve of sodium nitrite.

2.4.6 Total RNA extraction and quantitative real-time PCR (qRT-PCR)

Total RNA extraction and qRT-PCR were performed as described before (Rosa, Goncalves et al. 2009). Briefly, total RNA was extracted using the NZYol (NZYTECH, Lisbon, Portugal) and quantified in a NanoDrop ND-1000 spectrophotometer at 260 nm. RNA purity was assessed by analysis of 260/230 and 260/280 absorption ratios. The cDNA was reverse-transcribed using NZY First Strand cDNA Synthesis Kit (NZYTECH), beginning with 2 µg of total RNA. qRT-PCR was performed, in duplicate for each sample, using NZYSpeedy qPCR Green Master Mix (2x) (NZYTECH) on CFX96 Real-Time PCR Detection System (Bio-Rad, Hercules, CA, USA).

The efficiency of the amplification reaction for each gene was calculated using a standard curve of a series of diluted cDNA samples and the specificity of the amplification products was assessed by analysing the melting curve generated in the process.

Table 4. Oligonucleotide Primer Pairs Used for qRT-PCR

Gene name	Genbank accession number	Forward sequence	Reverse sequence
Hprt-1	NM_013556	GTTGAAGATATAATTG ACACTG	GGCATATCCAACAACA AAC
Nos2	NM_010927	GCTGTTAGAGACACTTC TGAG	CACTTTGGTAGGATTTG ACTTTG
Il1b	NM_008361	ACCTGTCCTGTGTAATG AAAG	GCTTGTGCTCTGCTTGT G

Gene expression changes were analysed using the built-in CFX Manager software which enables the analysis of the results by the Pfaffl method, a variation of the ΔΔCT method corrected for gene-specific efficiencies (Pfaffl 2001). The results were normalized using *Hprt1* as housekeeping gene. This gene was experimentally determined with Genex software using NormFinder and geNorm algorithms (MultiD Analyses AB, Göteberg, Sweden) as the most stable for the treatment conditions used. Specific sets of primers for *Nos2*, *Il1b* and *Hprt1* (Table 4) were designed using Beacon Designer software version 8 (Premier Biosoft International, Palo Alto, CA, USA).

2.4.7 Western blotting

Total cell extracts were prepared and western blot was performed as described before (Sousa, Ribeiro et al. 2017). Briefly, total (25 µg for Raw 264.7 cell line and 20 µg for human chondrocytes) proteins were separated by SDS-PAGE under reducing conditions and electrotransferred onto PVDF membranes. These were probed overnight at 4 ºC or for 2 h at room temperature with rabbit polyclonal antibody against IL-1β (dilution 1:500; sc-7884, Santa Cruz Biotechnology, INC., Texas, USA) or mouse monoclonal antibody NOS2 (dilution 1:500; MAB9502, R&D Systems, Minneapolis, MN, USA) and then with anti-rabbit or anti-mouse alkaline phosphatase-conjugated secondary antibodies (dilution 1:20000; GE Healthcare, Chalfont St. Giles, UK) for 1 h at room temperature. Immune complexes were detected with Enhanced ChemiFluorescence reagent (GE Healthcare) in the imaging system Thyphoon FLA 9000 (GE Healthcare). The membranes were reprobed with a mouse monoclonal anti-β-Tubulin I antibody (Sigma-Aldrich Co.), diluted at 1:20000, as a loading control, for 1 h at room temperature. Image analysis was performed with TotalLab TL120 software (Nonlinear Dynamics Ltd).

2.4.8 Measurement of secreted IL-1β

The concentration of IL-1β in the culture supernatants was measured using the Mouse IL-1β ELISA kit (ThermoScientific, Rockford, USA), following the manufacturer's instructions.

2.4.9 Statistical Analysis

Results are presented as means ± SEM. Statistical analysis using GraphPad Prism version 6.0 (GraphPad Software, San Diego, CA, USA). Normal distribution of the data was evaluated with the D'Agostino & Pearson omnibus, the Shapiro-Wilk and the Kolmogorov-Smirnov tests. In cases where the number of samples is too small, we assumed the data follow a normal distribution, as this was verified in all cases where the sample number was larger, including analysis of the same analyte under different experimental treatments. Statistical analysis was performed by one-way ANOVA with the Dunnett post-test for comparison to a control group and the Tukey post-test for multiple comparisons, except in Fig. 4c where the unpaired t-test was used to compare a specific condition with its respective control. Results were considered statistically significant at $p < 0.05$.

Data Availability

The datasets generated and analysed during the current study are available from the corresponding author on reasonable request.

Acknowledgments

This work was funded by the European Regional Development Fund (ERDF), through the Centro 2020 Regional Operational Program and through the COMPETE 2020 - Operational Program for Competitiveness and Internationalization and Portuguese national funds via FCT – Fundação para a Ciência e a Tecnologia, under projects POCI-01-0145-FEDER-028424 (CARTILFACTORY) and UID/NEU/04539/2019 and the PhD fellowship SFRH/79600/2011 to C. Sousa.

The authors are grateful to Mónica Zuzarte for critical reading of this manuscript.

Author contributions

AFM conceived, designed and supervised the whole study. CS collaborated in the study design and performed the experimental work. BN collaborated in quantitative real-time RT-PCR analysis. AJL performed the synthesis and structural analysis of the semi-synthetic compounds and collaborated in the identification of structural features relevant for activity, as well as on the interpretation and discussion of results. CC collaborated in the selection of compounds to be tested and their analysis by GC, as well as on the interpretation and discussion of results. FJ was responsible for cartilage collection and collaborated in the discussion of the results. AFM and CS drafted the manuscript. All authors read and approved the final manuscript.

Additional Information

The authors declare no competing interests.

2.5 Supplementary material

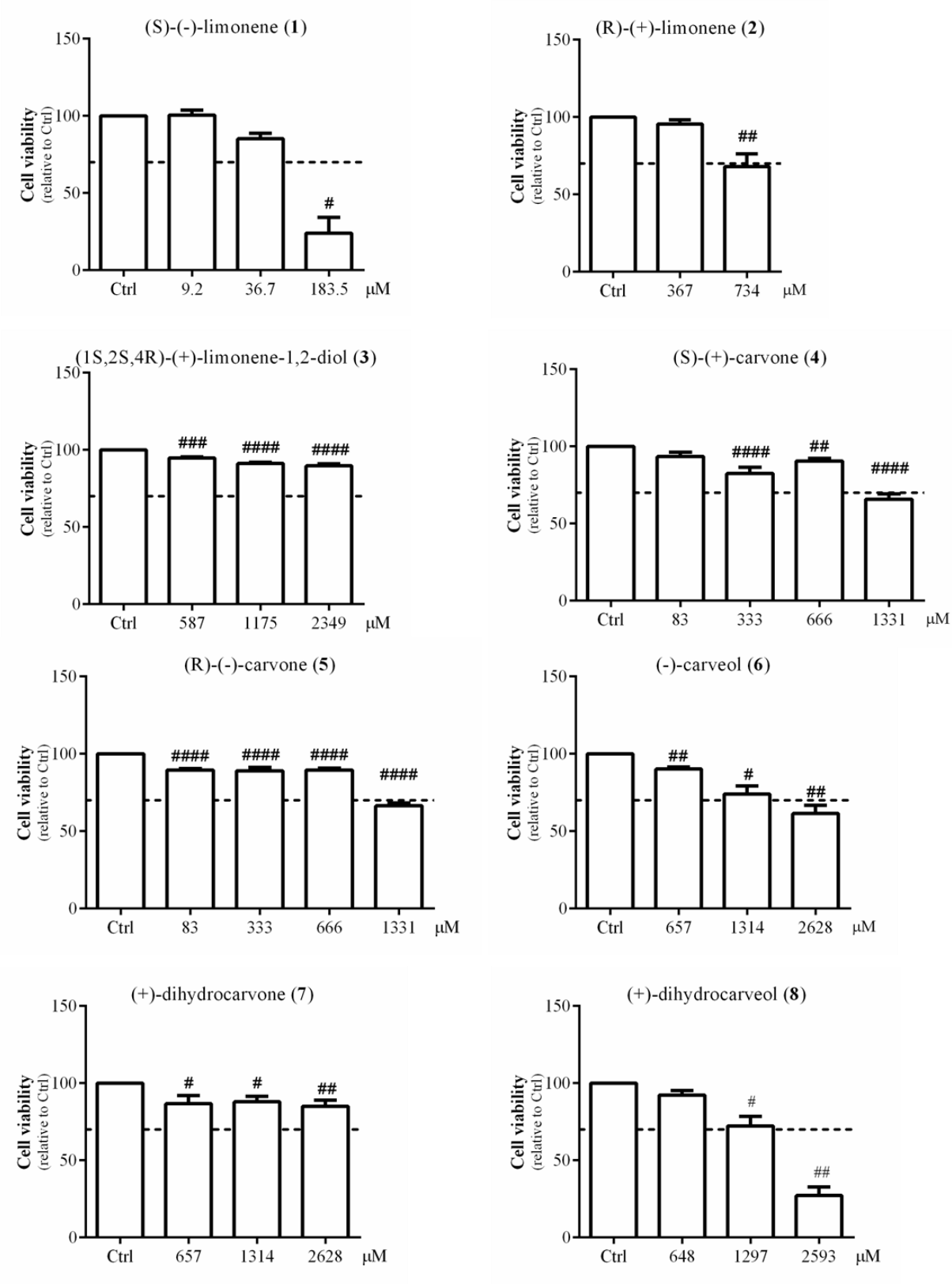

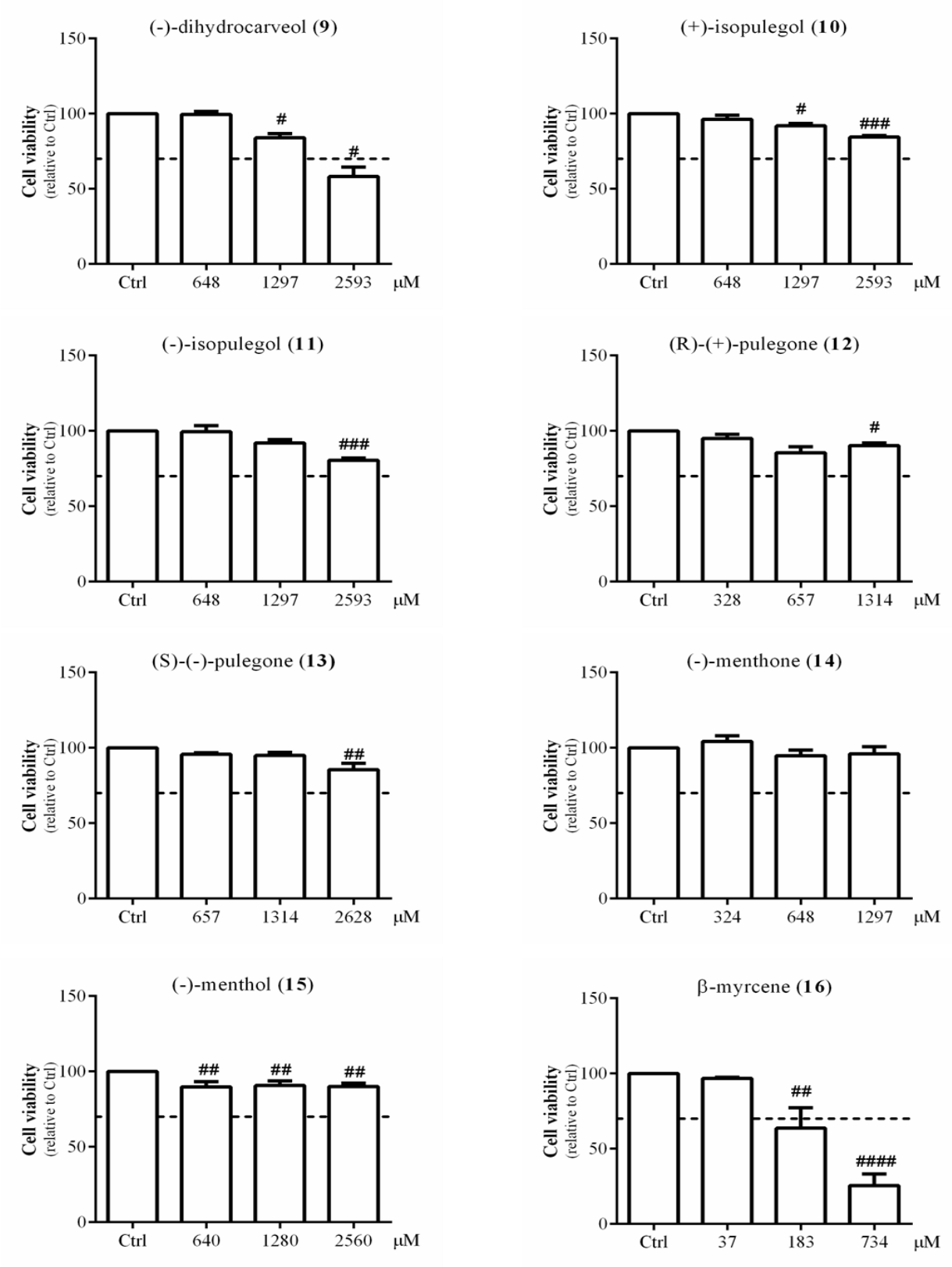
(-)-dihydrocarveol (9)
(+)-isopulegol (10)
(-)-isopulegol (11)
(R)-(+)-pulegone (12)
(S)-(-)-pulegone (13)
(-)-menthone (14)
(-)-menthol (15)
β-myrcene (16)
Cell viability
(relative to Ctrl)
150
100
50
0
Ctrl
648
1297
2593
328
657
1314
2628
324
640
1280
2560
37
183
734
μM
#
##
###
####

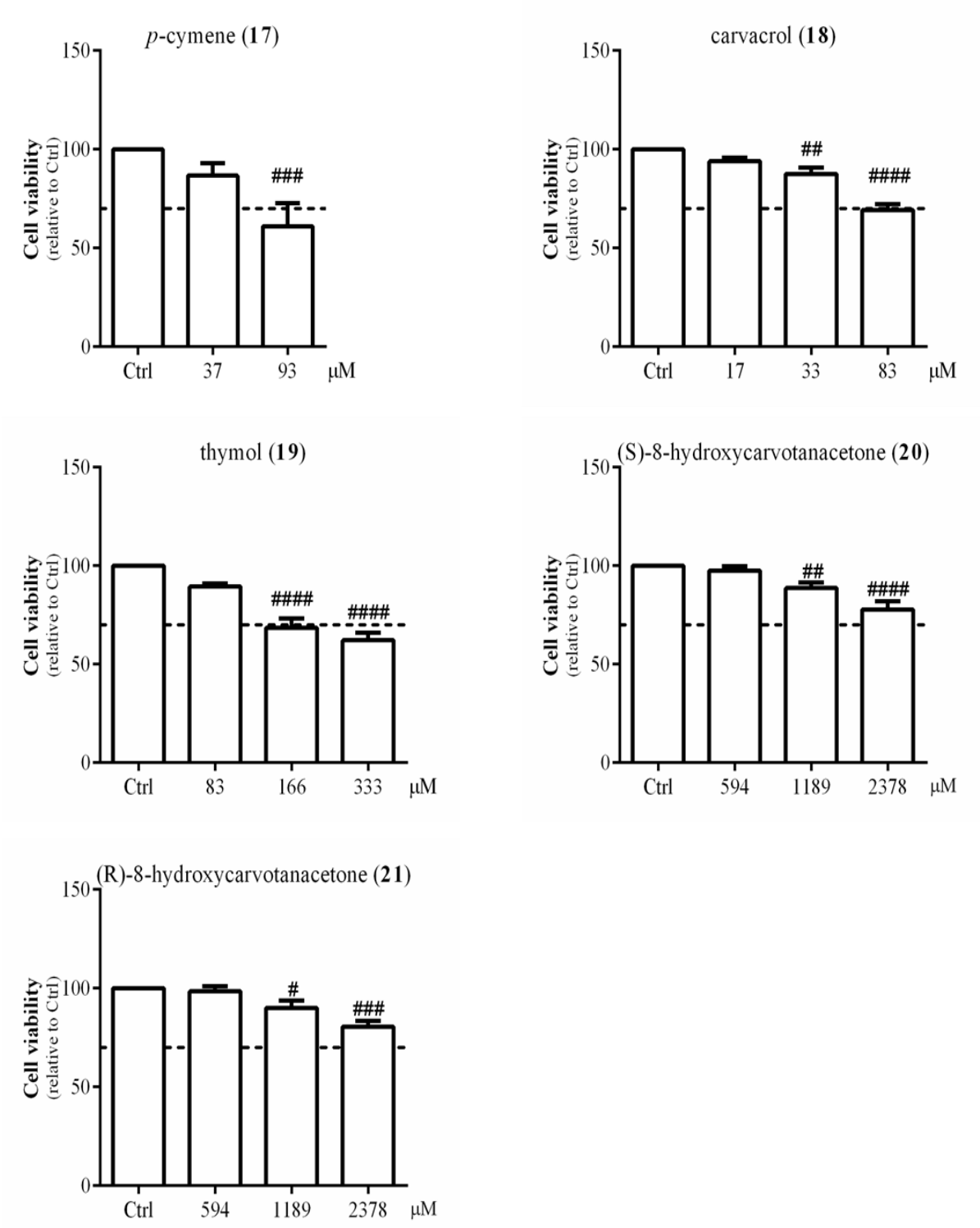

Figure S1. Evaluation of the cytotoxicity of the test compounds. Raw 264.7 cells were treated with the indicated concentrations of the each compound or with the vehicle (0.1% DMSO, control, Ctrl) for 18 h. Each column represents the mean ± SEM of, at least, three independent experiments. $^{\#}p \leq 0.05$, $^{\#\#}p \leq 0.01$, $^{\#\#\#}p \leq 0.001$ and $^{\#\#\#\#}p \leq 0.0001$ relative to Ctrl. The dotted line represents the threshold (70% of maximal viability) below which cytotoxicity is recognized, in agreement with standard ISO 10993-5.

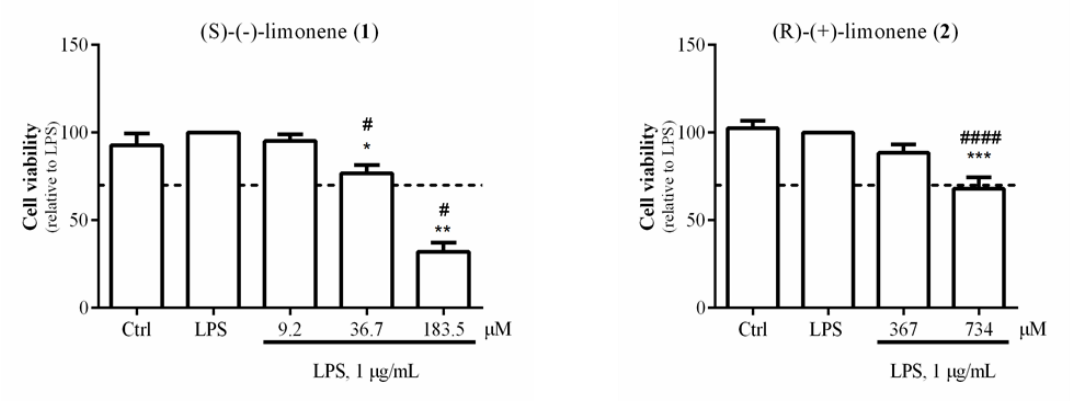
(S)-(-)-limonene (1)
Cell viability (relative to LPS)
150
100
50
0
#
*
#
**
Ctrl
LPS
9.2
36.7
183.5
μM
LPS, 1 μg/mL
(R)-(+)-limonene (2)
Cell viability (relative to LPS)
150
100
50
0
####
***
Ctrl
LPS
367
734
μM
LPS, 1 μg/mL

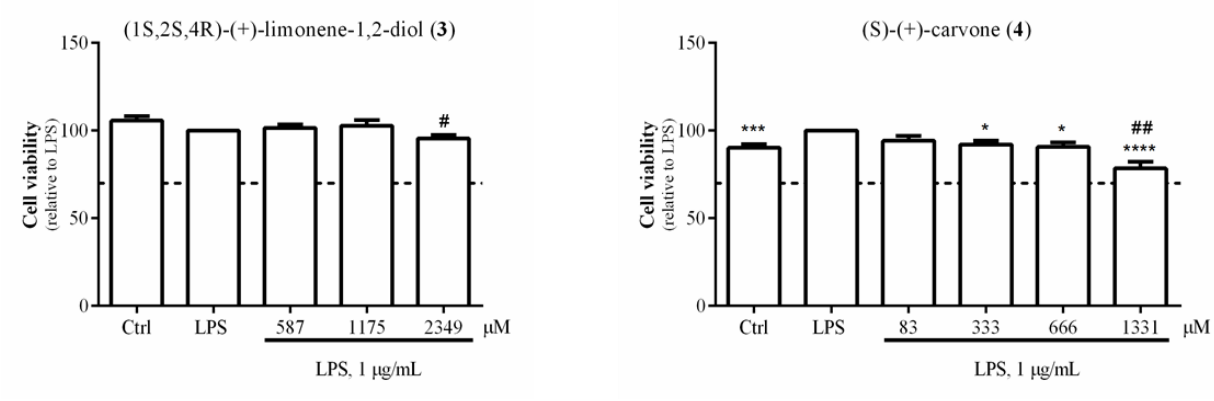
(1S,2S,4R)-(+)-limonene-1,2-diol (3)
Cell viability (relative to LPS)
150
100
50
0
#
Ctrl
LPS
587
1175
2349
μM
LPS, 1 μg/mL
(S)-(+)-carvone (4)
Cell viability (relative to LPS)
150
100
50
0
***
*
*
##
****
Ctrl
LPS
83
333
666
1331
μM
LPS, 1 μg/mL

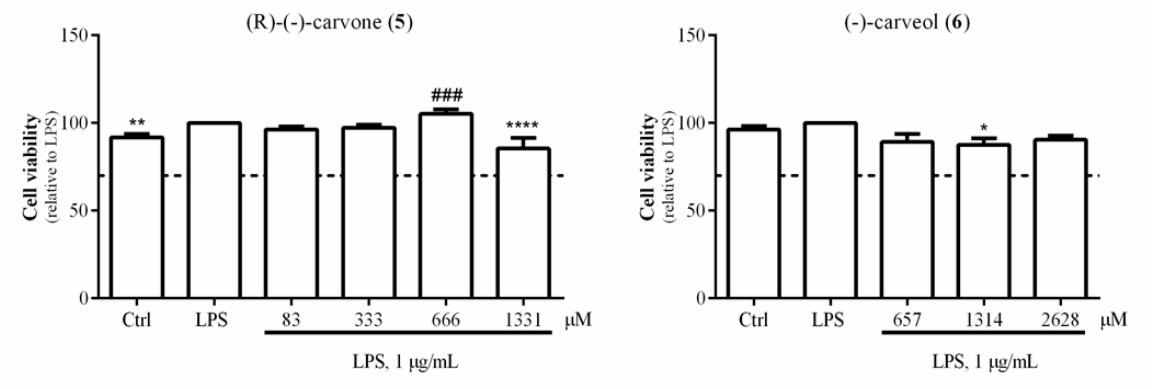
(R)-(-)-carvone (5)
Cell viability (relative to LPS)
150
100
50
0
**
###
****
Ctrl
LPS
83
333
666
1331
μM
LPS, 1 μg/mL
(-)-carveol (6)
Cell viability (relative to LPS)
150
100
50
0
*
Ctrl
LPS
657
1314
2628
μM
LPS, 1 μg/mL

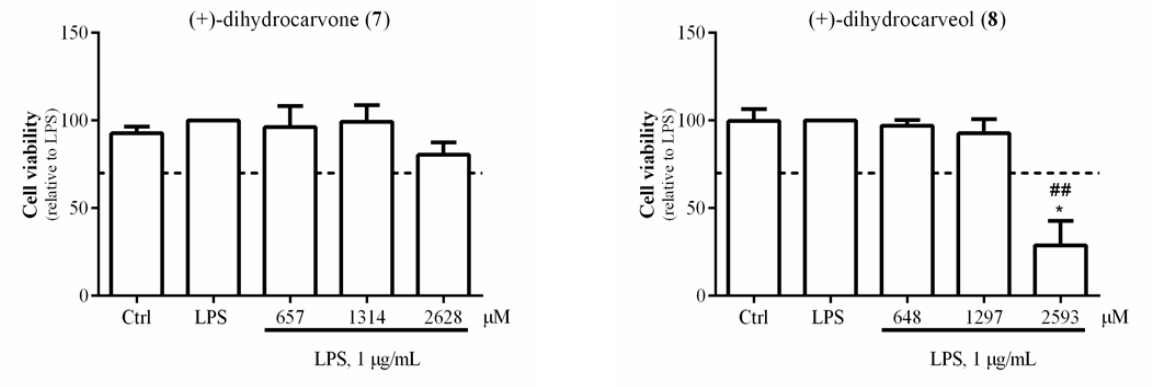
(+)-dihydrocarvone (7)
Cell viability (relative to LPS)
150
100
50
0
Ctrl
LPS
657
1314
2628
μM
LPS, 1 μg/mL
(+)-dihydrocarveol (8)
Cell viability (relative to LPS)
150
100
50
0
##
*
Ctrl
LPS
648
1297
2593
μM
LPS, 1 μg/mL

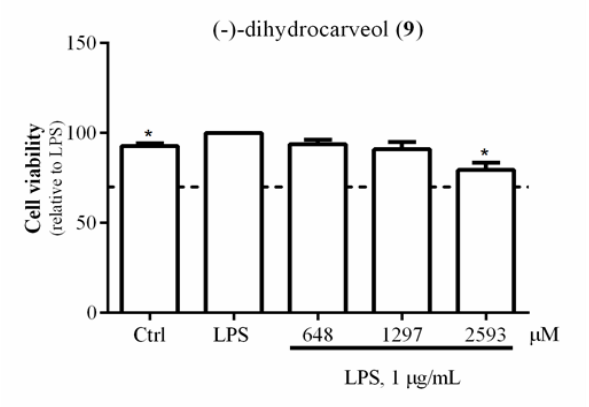
(-)-dihydrocarveol (9)
Cell viability (relative to LPS)
150
100
50
0
*
*
Ctrl
LPS
648
1297
2593
μM
LPS, 1 μg/mL

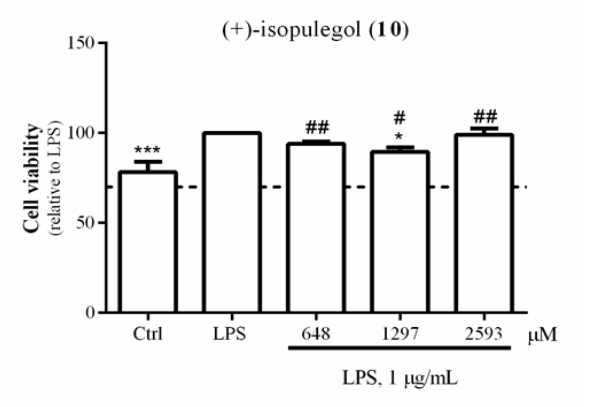
(+)-isopulegol (10)
Cell viability (relative to LPS)
150
100
50
0
***
##
#
*
##
Ctrl
LPS
648
1297
2593
μM
LPS, 1 μg/mL

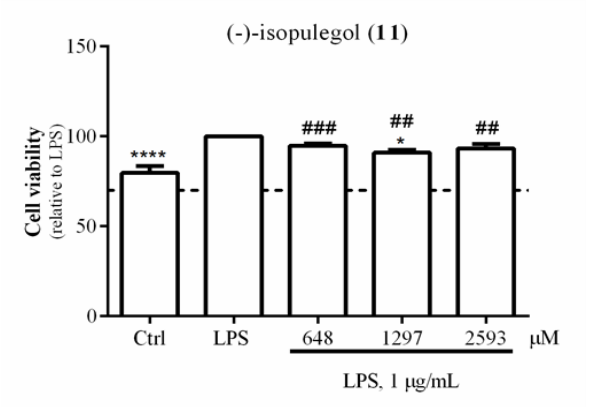
(-)-isopulegol (11)
Cell viability (relative to LPS)
150
100
50
0
****
###
##
*
##
Ctrl
LPS
648
1297
2593
μM
LPS, 1 μg/mL

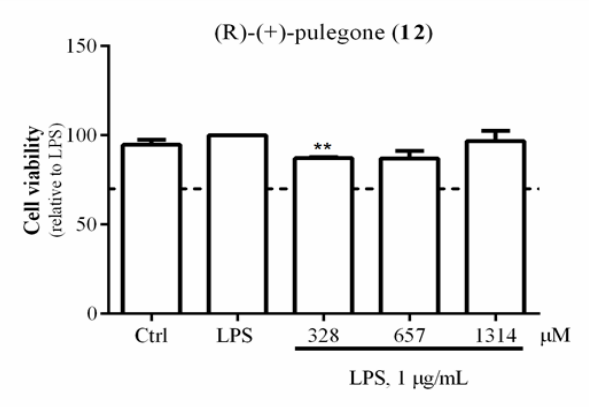
(R)-(+)-pulegone (12)
Cell viability (relative to LPS)
150
100
50
0
**
Ctrl
LPS
328
657
1314
μM
LPS, 1 μg/mL

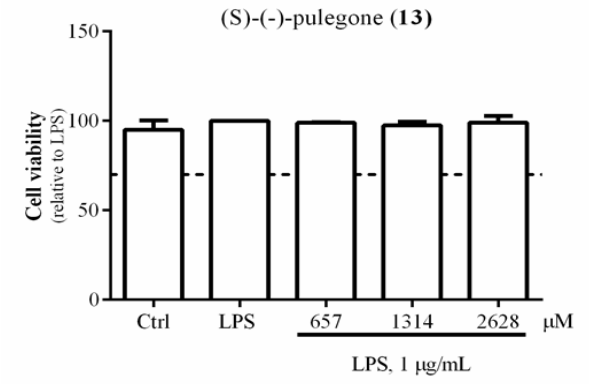
(S)-(-)-pulegone (13)
Cell viability (relative to LPS)
150
100
50
0
Ctrl
LPS
657
1314
2628
μM
LPS, 1 μg/mL

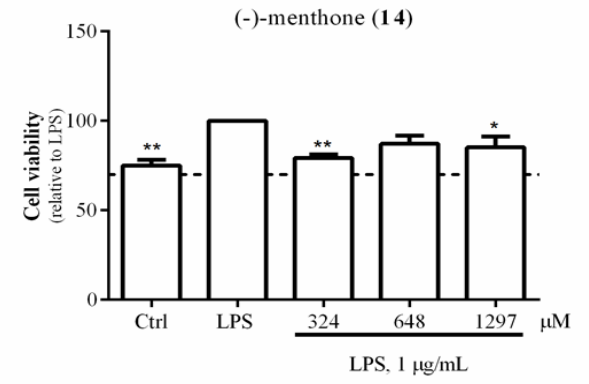
(-)-menthone (14)
Cell viability (relative to LPS)
150
100
50
0
**
**
*
Ctrl
LPS
324
648
1297
μM
LPS, 1 μg/mL

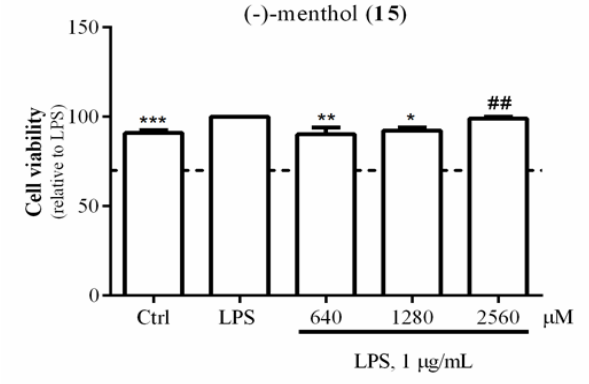
(-)-menthol (15)
Cell viability (relative to LPS)
150
100
50
0
***
**
*
##
Ctrl
LPS
640
1280
2560
μM
LPS, 1 μg/mL

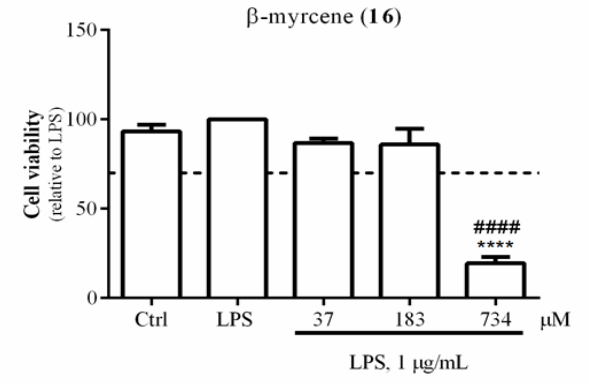
β-myrcene (16)
Cell viability (relative to LPS)
150
100
50
0
####
****
Ctrl
LPS
37
183
734
μM
LPS, 1 μg/mL

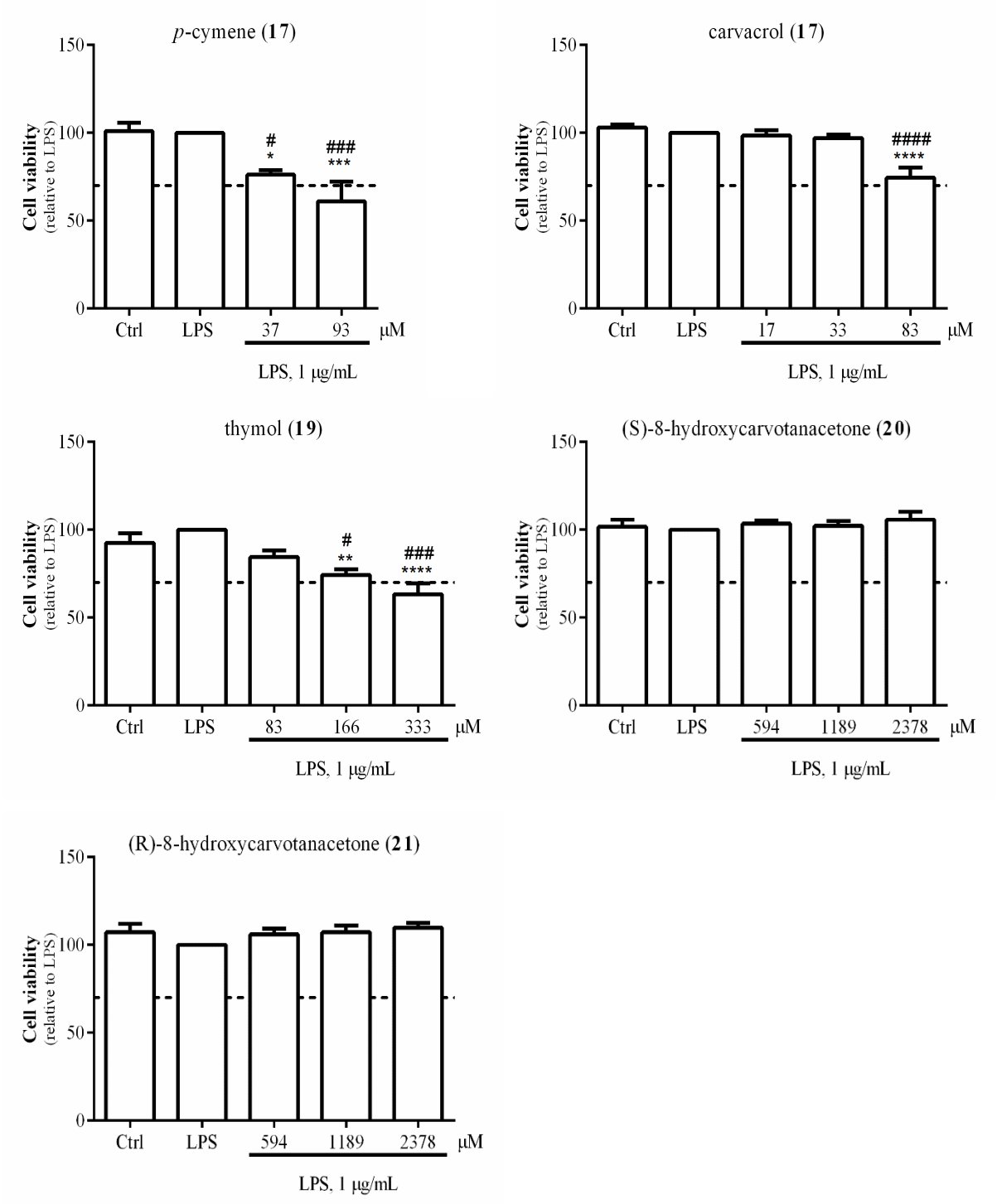

Figure S2. Evaluation of the cytotoxicity of the test compounds in the presence of bacterial lipopolysaccharide (LPS). Raw 264.7 cells were treated with LPS, 1 μg/mL, for 18 h, following pre-treatment for 1 h with the indicated concentrations of the test compounds or with vehicle (0.1% DMSO, Ctrl). Each column represents the mean ± SEM of, at least, three independent experiments. *$p \leq 0.05$, **$p \leq 0.01$, ***$p \leq 0.001$ and ****$p \leq 0.0001$ relative to LPS-treated cells. $^{\#}p \leq 0.05$, $^{\#\#}p \leq 0.01$, $^{\#\#\#}p \leq 0.001$ and $^{\#\#\#\#}p \leq 0.0001$ relative to Ctrl. The dotted line represents the threshold (70% of maximal viability) below which cytotoxicity is recognized, in agreement with standard ISO 10993-5.

Uncropped blots shown in **Figure 2b**

(S)-(+)-carvone (**4**)

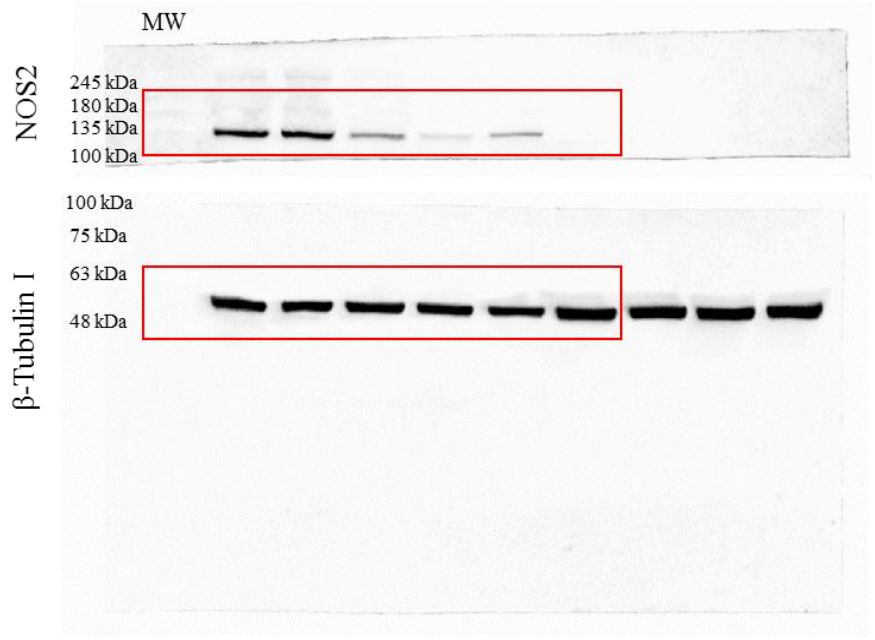

(R)-(-)-carvone (**5**)

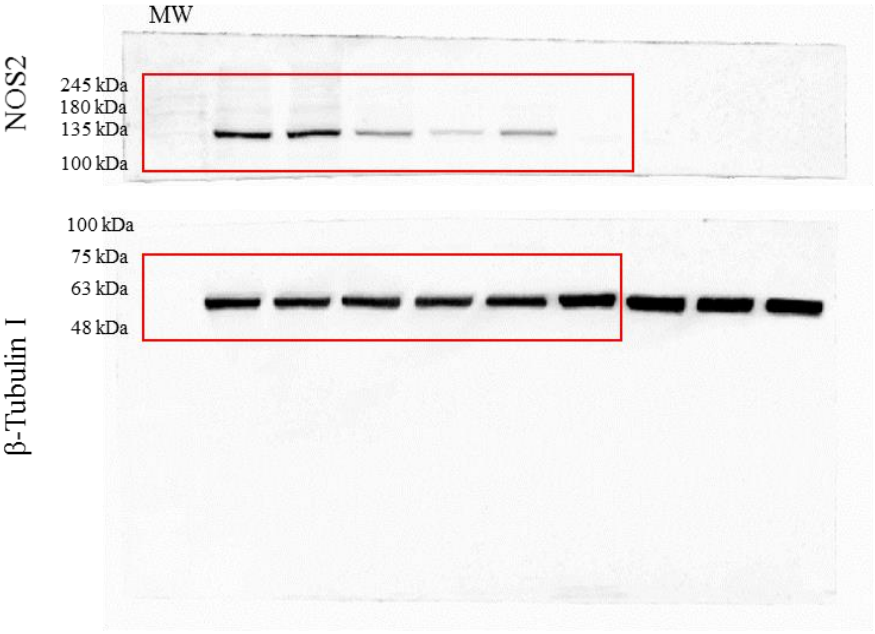

The membranes were cut at ≈ 100 kDa so that the upper piece was incubated with anti-NOS2 antibody and the lower one with the anti-β-Tubulin I antibody.

Uncropped blots shown in **Figure 3b**

(S)-(+)-carvone (**4**)

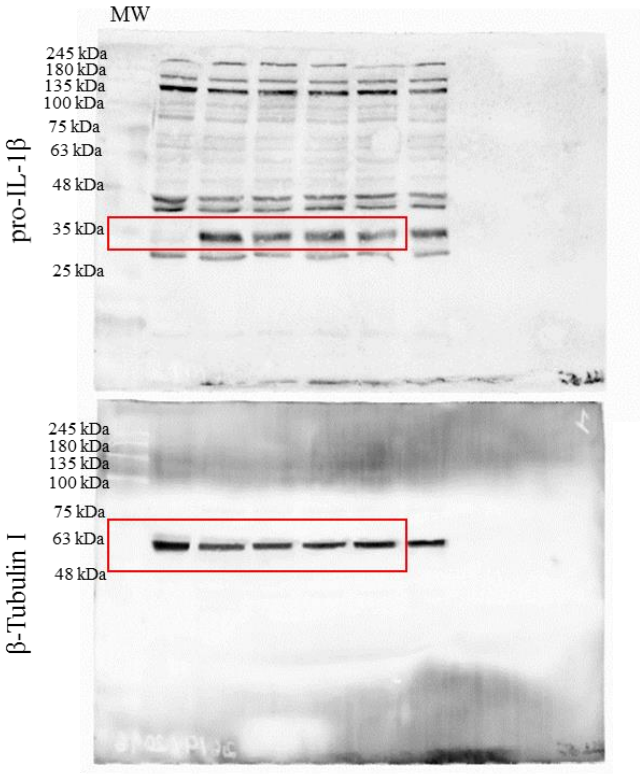

(R)-(-)-carvone (**5**)

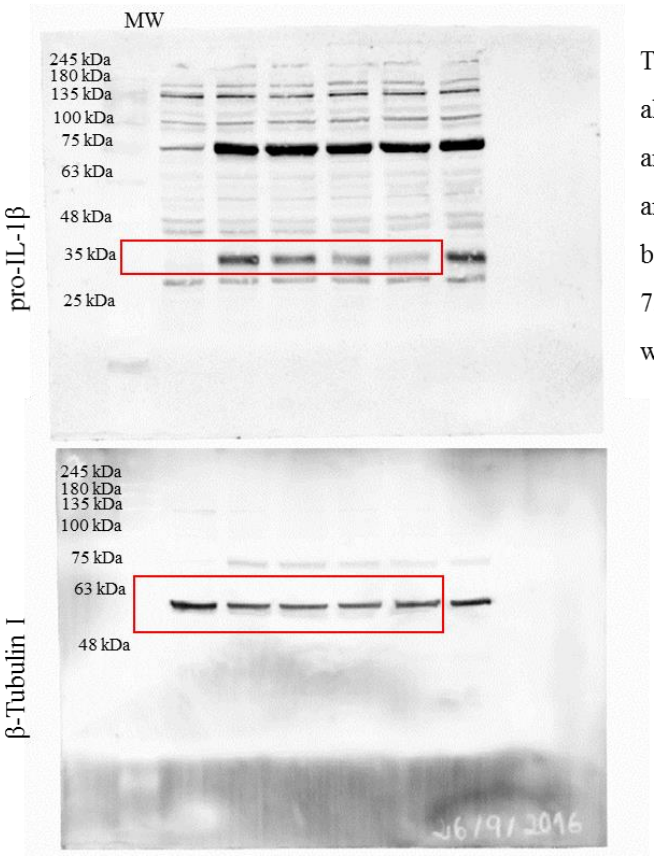

This membrane was also incubated with anti-COX2 antibody and the corresponding band appears near the 75 kDa molecular weight marker.

Uncropped blots shown in **Figure 4b**

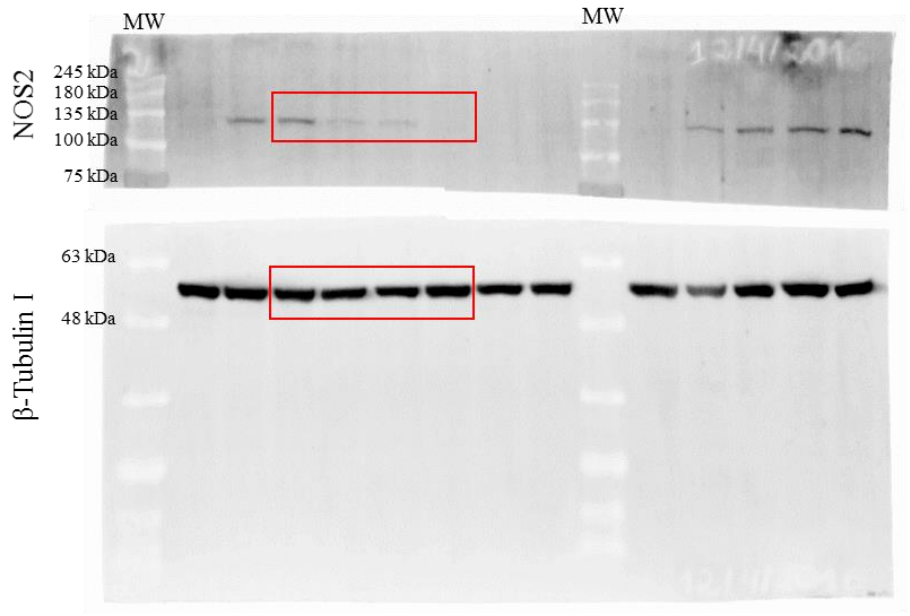

Uncropped blots shown in **Figure 4c**

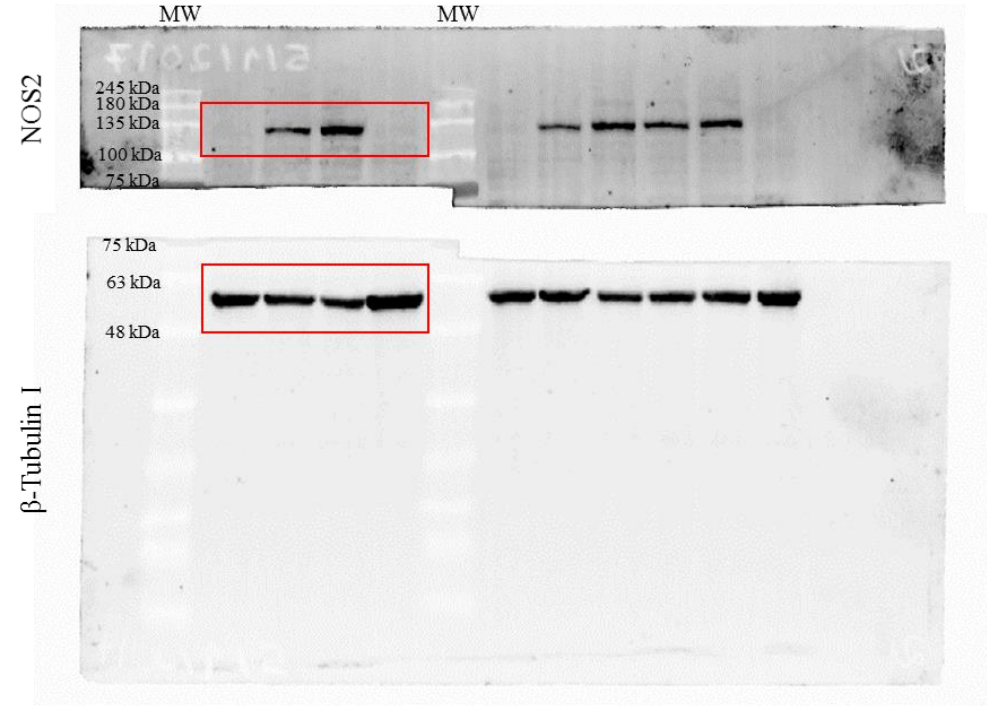

The membranes were cut at ≈ 75 kDa so that the upper piece was incubated with anti-NOS2 antibody and the lower one with the anti-β-Tubulin I antibody.

Uncropped blots shown in **Figures 5b and 5d**

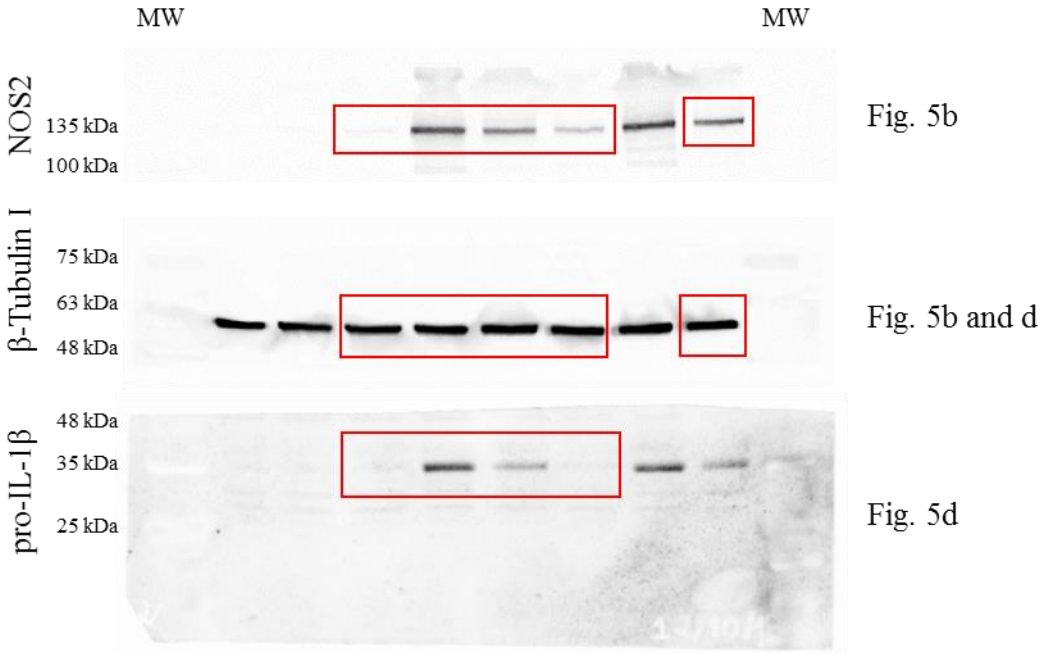

The membrane was cut between 100-75 kDa and 48 kDa so that the upper piece was incubated with anti-NOS2 antibody, the middle piece with anti-β-Tubulin I antibody and the lower one with the anti-IL-1β antibody.

Figure S3. Uncropped images of the blots shown in figures 2-5.

Table S1. Purity and isomer composition of the test compounds

Nº	Trivial name	IUPAC name of major isomer	Purity (%)*	Isomer composition	Catalog #, Vendor
1	(S)-(-)-limonene	(4S)-1-methyl-4-prop-1-en-2-ylclyclohexene	≥ 95%**	Purum	#62130, Sigma-Aldrich Co.
2	(R)-(+)-limonene	(4R)-1-methyl-4-prop-1-en-2-yl-cyclohexene	≥ 99%	Purum	#62118, Sigma-Aldrich Co.
3	(1S,2S,4R)-(+)-limonene-1,2-diol	(1S,2S,4R)-1-methyl-4-prop-1-en-2-ylcyclohexane-1,2-diol	≥ 97%	Purum	#669768, Sigma-Aldrich Co.
4	(S)-(+)-carvone	(5S)-2-methyl-4-prop-1-en-2-ylcyclohex-2-en-1-one	≥ 96%**	Purum	#435759, Sigma-Aldrich Co.
5	(R)-(-)-carvone	(5R)-2-methyl-4-prop-1-en-2-ylcyclohex-2-en-1-one	98%	Purum	#124931, Sigma-Aldrich Co.
6	(-)-carveol	(1R,5R)-2-methyl-5-prop-1-en-2-ylcyclohex-2-en-1-ol (1S,5R)-2-methyl-5-prop-1-en-2-ylcyclohex-2-en-1-ol	≥ 98%	Mixture of isomers	#61370, Sigma-Aldrich Co.
7	(+)-dihydrocarvone	(2R,5R)-2-methyl-5-prop-1-en-2-ylcyclohexan-1-one (2S,5R)-2-methyl-5-prop-1-en-2-ylcyclohexan-1-one	≥ 98%	Mixture of isomers	#09164, Sigma-Aldrich Co.
8	(+)-dihydrocarveol	(1S,2S,5S)- 2-methyl-5-prop-1-en-2-ylcyclohexan-1-ol	≥ 95%	Mixture of isomers – composition: n, ~ 75% iso, ~ 6% neo, ~ 3% neoiso, ~ 1.3%	#37277, Sigma-Aldrich Co.
9	(-)-dihydrocarveol	(1R,2R,5R)- 2-methyl-5-prop-1-en-2-ylcyclohexan-1-ol	≥ 95%	Mixture of isomers – composition: n, ~ 75% iso, ~ 6% neo, ~ 3% neoiso, ~ 1.3%	#37278, Sigma-Aldrich Co.

10	(+)-isopulegol	(1S,2R,5S)-5-methyl-2-prop-1-en-2-ylcyclohexan-1-ol	≥ 99%	Purum	#59765, Sigma-Aldrich Co.
11	(-)-isopulegol	(1R,2S,5R)-5-methyl-2-prop-1-en-2-ylcyclohexan-1-ol	≥ 99%	Purum	#59770, Sigma-Aldrich Co.
12	(R)-(+)-pulegone	(5R)-5-methyl-2-propan-2-ylidienecyclohexan-1-one	≥ 98.5%	Purum	#82569, Sigma-Aldrich Co.
13	(S)-(-)-pulegone	(5S)-5-methyl-2-propan-2-ylidienecyclohexan-1-one	98%	Purum	#328847, Sigma-Aldrich Co.
14	(-)-menthone	(2S,5R)-5-methyl-2-propan-2-ylcyclohexan-1-one	≥ 99%	Purum	#63677, Sigma-Aldrich Co.
15	(-)-menthol	(1R,2S,5R)-5-methyl-2-propan-2-ylcyclohexan-1-ol	≥ 99%	Purum	#63660, Sigma-Aldrich Co.
16	β-myrcene	7-methyl-3-methylideneocta-1,6-diene	≥ 90%	Purum	#64643, Sigma-Aldrich Co.
17	*p*-cymene	1-methyl-4-propan-2ylbenzene	≥ 99.5%	Purum	#30039, Sigma-Aldrich Co.
18	carvacrol	2-methyl-5-propan-2ylphenol	≥ 97%	Purum	#22051, Sigma-Aldrich Co.
19	thymol	5-methyl-2-propan-2ylphenol	98%	Purum	#30433, BDH

*Purity relative to sum of enantiomers determined by gas chromatography

The purities of (1**) (96.9%) and (**4**) (96.8%), which were in stock at our lab for over a year, were confirmed by GC-MS prior to starting the experiments and found to be within the limits defined by the manufacturer

Chapter 3: Elucidation of the mechanism underlying the anti-inflammatory properties of (S)-(+)-carvone identifies a novel class of Sirtuin-1 activators

Cátia Sousa, Bruno Miguel Neves, Fernando Judas, Alcino Jorge Leitão, Alexandrina Ferreira Mendes

Manuscript submitted for publication

Note: The results presented in this chapter are formatted according to the style of the journal where the paper was submitted, with minor modifications

Graphical abstract

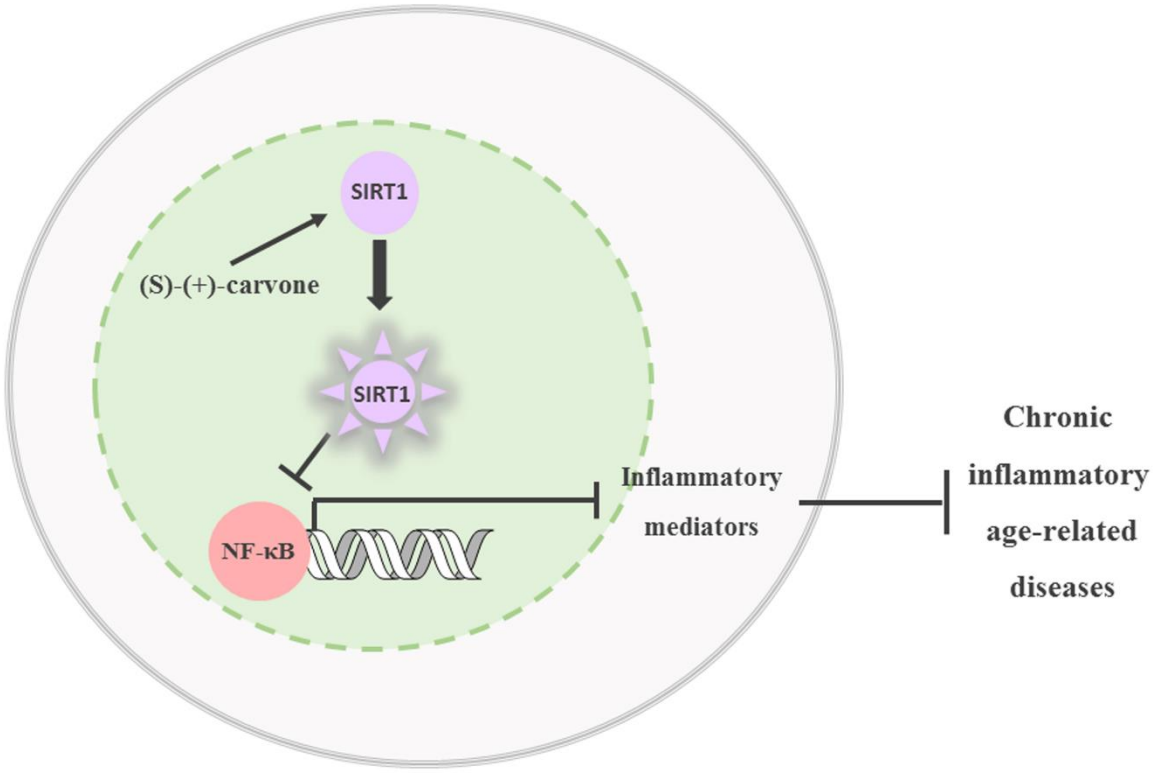

Highlights

- (S)-(+)-carvone decreases LPS-induced JNK1 phosphorylation
- (S)-(+)-carvone directly activates SIRT1 and NF-κB/p65 deacetylation at lysine 310
- (S)-(+)-carvone inhibits NF-κB-dependent gene expression
- (S)-(+)-carvone is a drug with potential to treat chronic age-related diseases

Abstract

The signaling pathways involved in age-related inflammation are increasingly recognized as relevant targets for the development of preventive and therapeutic strategies. Our previous study elucidated the structure-activity relationship of *p*-menthane derivatives as potential anti-inflammatory drugs and identified (S)-(+)-carvone as the most potent among the compounds tested. This study aims at identifying the molecular mechanism underlying the anti-inflammatory properties of (S)-(+)-carvone. The results obtained in the murine macrophage cell line, Raw264.7, stimulated with bacterial lipopolysaccharide (LPS) as a pro-inflammatory stimulus, show that (S)-(+)-carvone inhibited LPS-induced JNK1 phosphorylation, but not that of p38 and ERK1/2. Moreover, (S)-(+)-carvone also did not inhibit the phosphorylation and degradation of the NF-κB inhibitor, IκB-α. Accordingly, (S)-(+)-carvone did not affect LPS-induced phosphorylation of NF-κB/p65 on Ser536 and its nuclear translocation, but it significantly decreased LPS-induced IκB-α resynthesis, a NF-κB-dependent process, and NF-κB/p65 acetylation on lysine (Lys) 310. Deacetylation of that Lys residue is dependent on the activity of Sirtuin 1 (SIRT1). Using an *in vitro* fluorimetric assay (S)-(+)-carvone was found to directly activate SIRT1, while it did not affect SIRT1 protein levels in murine macrophages. The ability of (S)-(+)-carvone to activate SIRT1 was further confirmed by its capacity to deacetylate NF-κB/p65 on Lys310 in human chondrocytes treated with interleukin-1β, as a cell model of osteoarthritis. Taken together, these results show that (S)-(+)-carvone is a new SIRT1 activator with potential to counteract the chronic low grade inflammation characteristic of age-related diseases, like osteoarthritis. Human chondrocytes used for this study were isolated from distal femoral condyle cartilage collected from multi-organ donors at the Bone and Tissue Bank of the University and Hospital Center of Coimbra with approval by the Ethics Committee.

Keywords: Sirtuin-1 activating compound; aging; inflammation; NF-κB; SIRT1, osteoarthritis.

3.1 Introduction

Persistent low grade inflammation represents a pathological mechanism associated with age-related diseases, such as metabolic, cardiovascular, neurodegenerative and musculoskeletal diseases and cancer (Medzhitov 2010). A large range of stimuli, including inflammatory cytokines [e.g. Interleukin (IL)-1β, Tumor Necrosis Factor-α (TNF-α) and IL6], microbial products and cellular components released by dead or damaged cells (e.g. ATP and the alarmins, HMGB1 and members of the S100 family) (Malaquin, Martinez et al. 2016) activate multiple intracellular signalling cascades that bring about the inflammatory response. Of those signalling cascades, members of the Mitogen-Activated Protein Kinases (MAPKs) family and the transcription factor, Nuclear Factor kappa-light-chain-enhancer of activated B Cells (NF-κB), are especially relevant since their activation leads to the production of inflammatory mediators and effector enzymes that drive and perpetuate inflammation-associated tissue damage and functional impairment, thus promoting disease development and/or progression (Malaquin, Martinez et al. 2016, Chen, Deng et al. 2018).

Considering their role in chronic inflammation and the lack of efficient therapeutic strategies for chronic inflammation-associated diseases, the signalling pathways that lead to MAPKs and NF-κB activation are promising targets for drug development (Kaminska 2005, Gupta, Sundaram et al. 2010).

Our previous work screened various compounds of natural origin in standardised conditions to identify small molecules capable of interfering with those inflammatory pathways and to establish the structural features required for activity. (S)-(+)-carvone was identified as the lead compound of that serie, decreasing inducible nitric oxide (NO) synthase (NOS2) and IL-1β expression, both in a mouse macrophage cell line and in primary human chondrocytes in response to bacterial lipopolysaccharide (LPS) and IL-1β, respectively (Sousa, Leitão et al. 2020).

The purpose of this work was to elucidate the molecular mechanism(s) by which (S)-(+)-carvone interferes with the expression of pro-inflammatory mediators. Taking into account the crucial role of MAPKs and NF-κB activation on pro-inflammatory gene expression, we hypothesised that these signalling pathways may be targeted by this compound.

3.2 Material and methods

3.2.1 Cell culture and treatments

a) Macrophages

The mouse macrophage cell line, Raw 264.7 (ATCC No. TIB-71), was cultured in DMEM supplemented with 10% non-heat inactivated fetal bovine serum (FBS), 100 U/mL penicillin and 100 µg/mL streptomycin. Raw 264.7 cells were plated at a density of $3x10^5$ cells/mL and left to stabilize for up to 24 h.

b) Human chondrocytes

Human knee cartilage was collected within 24 h of death from the distal femoral condyles of multi-organ donors (48-77 years old, mean=66.7, n=6) at the Bone and Tissue Bank of the University and Hospital Centre of Coimbra (CHUC). Only waste tissue resulting from the preparation of bone tissue for cryopreservation was used. All procedures were approved by the Ethics Committee of CHUC (protocol approval number 8654/DC), which follows the Declaration of Helsinki and Oviedo Convention and the Portuguese legislation for organ donation.

Chondrocytes were isolated by enzymatic digestion from cartilage samples as previously described (Rosa, Judas et al. 2008). Briefly, cartilage shavings underwent sequential digestion with pronase (Roche, Indianapolis, IN, USA) and collagenase A (Roche, Indianapolis, IN, USA). To avoid chondrocyte dedifferentiation, non-proliferating monolayer cultures were setup by plating $1x10^6$ chondrocytes/mL in HAM: F12 medium containing 3% antibiotics and 5% FBS and allowed to recover for 24 h at 37ºC in a humidified atmosphere with 5% CO_2. Prior to any treatments, chondrocytes were serum-starved overnight and thereafter maintained in culture medium without FBS.

c) Cell treatments

For cell treatments, (S)-(+)-carvone (#435759, purity 96%, Sigma-Aldrich Co., St Louis, MO, USA), resveratrol (Res; Extrasynthese, Genay Cedex,France), Bay 11-7082 (Calbiochem, San Diego, CA, USA), MG-132 (Z-Leu-Leu-Leu-CHO, Boston Biochem, Cambridge, MA, USA) and SP600125 (Anthra[1,9-cd]pyrazol-6(2H)-one, Calbiochem, San Diego, CA, USA), were dissolved in dimethyl sulfoxide (DMSO; Sigma-Aldrich Co). LPS from Escherichia coli 026:B6 (Sigma-Aldrich Co.) were dissolved in phosphate buffered saline (PBS). Recombinant human interleukin-1β (IL-1β; Peprotech, Rocky Hill, NJ, USA) was dissolved in PBS containing 0.1% Bovine Serum Albumin (BSA). The concentrations

of each compound and the experimental treatment periods are indicated in figures and/or figure legends. DMSO was used as vehicle and added to control and LPS or IL-1β -treated cell cultures to match the same concentration as in cells treated with the chemicals indicated above. In any case, the final concentration of DMSO did not exceed 0.1% (v/v). The chemicals used or the vehicle were added to murine macrophage or human chondrocyte cultures 1 h before the pro-inflammatory stimulus, 1 μg/mL LPS or 10 ng/mL IL-1β, respectively, and maintained for the rest of the experimental period.

3.2.2 Preparation of cell extracts

For preparation of total cell extracts, cell cultures were washed with ice-cold PBS and lysed with ice-cold RIPA buffer [150 mM sodium chloride, 50 mM Tris (pH 7.5), 5 mM ethylene glycol-bis(2-aminoethylether)-N,N,N´,N´-tetraacetic acid (EGTA), 0.5% sodium deoxycholate, 0.1% sodium dodecyl sulfate (SDS), 1% Triton X-100] supplemented with protease (Complete, Mini, Roche Diagnostics, Mannheim, Germany] and phosphatase (PhosSTOP, Roche Diagnostics, Mannheim, Germany)] inhibitor cocktails for 30 min. The lysates were centrifuged at 14000 rpm for 10 min at 4ºC and the supernatants were stored at -20ºC until use.

For preparation of cytoplasmic and nuclear extracts, the Nuclear Extract Kit (Active Motif, La Hulpe, Belgium) was used, following the manufacturer's instructions.

Protein concentration in the extracts was determined with the bicinchoninic acid kit (Sigma-Aldrich Co.).

3.2.3 Western Blotting

Western Blot was performed as described previously (Sousa, Ribeiro et al. 2017). Briefly, total (25 μg for Raw 264.7 cell line and 20 μg for human chondrocytes), cytoplasmic (25 μg) or nuclear (30 μg for Raw 264.7 cell line and 90 μg for human chondrocytes) proteins were separated by SDS-PAGE under reducing conditions and electrotransferred onto PVDF membranes. These were probed overnight at 4 ºC or for 2 h at room temperature with the primary antibodies indicated in Table 1 and then with anti-rabbit or anti-mouse alkaline phosphatase-conjugated secondary antibodies (dilution 1:20000; GE Healthcare, Chalfont St. Giles, UK). Mouse monoclonal anti-β-Tubulin I and rabbit polyclonal anti-Lamin B1 were used as a loading controls of total and cytoplasmic extracts and of nuclear extracts,

respectively. Immune complexes were detected with Enhanced ChemiFluorescence reagent (GE Healthcare) in the imaging system Thyphoon™ FLA 9000 (GE Healthcare). Image analysis was performed with TotalLab TL120 software (Nonlinear Dynamics Ltd).

Table 1: List of primary antibodies used in Western Blot

Protein	Source	Clonality	Dilution	Supplier	Reference number
IκB-α	rabbit	polyclonal	1:1000	Cell Signaling Technology, Inc., Danvers, MA, USA	#9242
phospho-p44/42 MAPK (ERK1/2) (Thr202/Tyr204)	rabbit	polyclonal	1:1000	Cell Signaling Technology, Inc.	#9101
p44/42 MAPK (ERK1/2)	rabbit	polyclonal	1:1000	Cell Signaling Technology, Inc.	#9102
phospho-p38 MAPK (Thr180/Tyr182)	rabbit	polyclonal	1:1000	Cell Signaling Technology, Inc.	#9211
p38 MAPK	rabbit	polyclonal	1:1000	Cell Signaling Technology, Inc.	#9212
SAPK/JNK	rabbit	polyclonal	1:1000	Cell Signaling Technology, Inc.	#9252
acetyl-NF-κB p65 (Lys310)	rabbit	polyclonal	1:750	Cell Signaling Technology, Inc.	#3045
IL-1β (H-153)	rabbit	polyclonal	1:500	Santa Cruz Biotechnology, INC., Texas, USA	sc-7884
Sirtuin-1	rabbit	polyclonal	1:1000	Sigma-Aldrich Co.	07-131
Lamin B1	rabbit	polyclonal	1:1000	Abcam, Cambridge, UK	ab16048
phospho-SAPK/JNK (Thr183/Tyr185)	rabbit	monoclonal	1:1000	Cell Signaling Technology, Inc.	#4668
NF-κB p65 (D14E12) XP®	rabbit	monoclonal	1:1000	Cell Signaling Technology, Inc.	#8242

phospho-NF-κB p65 (Ser536)	rabbit	monoclonal	1:1000	Cell Signaling Technology, Inc.	#3033
phospho-IκB-α (Ser32/36)	mouse	monoclonal	1:1000	Cell Signaling Technology, Inc.	#9246
NOS2 (clone #2D2-B2)	mouse	monoclonal	1:1000	R&D Systems, Minneapolis, MN, USA	MAB9502
SOX9	mouse	monoclonal	1:240	Development Studies Hybridoma Bank, Department of Biology, University of Iowa, Iowa, IA, USA	PCRP-SOX9-1A2
β-Tubulin I	mouse	monoclonal	1:20000	Sigma-Aldrich Co.	T7816

3.2.4 Immunocytochemistry

Macrophages were seeded onto 1 µ-Slide 8 Well ibiTreat (Ibidi, Martinsried, Germany). After treatment, the cells were washed with ice-cold PBS pH=7.4 and, then, fixed in 4% paraformaldehyde at room temperature, for 15 minutes. After fixing, cells were washed three times with PBS pH=7,4 with 0.1 M glycine for 5 minutes each and blocked with 5% Goat Serum, 0.3% Triton in PBS, pH=7.4 for 1 h at room temperature. Then, the slides were incubated with a rabbit monoclonal anti-NF-κB p65 (D14E12) XP® antibody (dilution 1:400; #8242, Cell Signaling Technology, Inc.) in 1% BSA in PBS (pH=7.4) overnight at 4ºC. The cells were washed three times with PBS (pH=7.4) for 5 min each at room temperature and incubated for 1 h at room temperature with anti-rabbit IgG (H+L) CF™488A (dilution 1:400; Biothium, Inc., Fremont, CA, USA) and Alexa Fluor ™ 555 Phalloidin (dilution 1:1000; Molecular Probes, Invitrogen, Eugene, OR) to stain the cytoskeleton (especially F-actin) which enhances visualization of the cytoplasm (Wulf, Deboben et al. 1979). Following three washes with PBS (pH=7.4), the cells were counterstained with DAPI (0.2 ng/mL; Molecular Probes, Invitrogen, Eugene, OR) to allow nucleus visualization and after another washing step, the slides were mounted with Ibidi Mounting Medium (Ibidi, Martinsried, Germany). Specificity was evaluated in negative

controls set up by omitting the primary antibody. Fluorescence images were obtained in an Axio Observer ZI fluorescence microscope (Carl Zeiss, Germany).

3.2.5 Nitric oxide production

The production of nitric oxide (NO) was measured as the amount of nitrite accumulated in the culture supernatants under the conditions described in figure legends. Nitrite concentration was measured using the colorimetric method based on the Griess reaction (Green, Wagner et al. 1982).

3.2.6 SIRT1 activity assay

Interaction of (S)-(+)-carvone with human SIRT1 was evaluated using the SIRT1 Direct Florescent Screening Assay Kit (Cayman Chemical Company, Ann Arbor, MI, USA) following the manufacturer's instructions. Briefly, the assay uses a specific substrate, in this case, a peptide derived from the p53 sequence coupled to a fluorophore (Arg-His-Lys-Lys(e-acetyl)-AMC), which is incubated with human recombinant SIRT1 along with its co-substrate, NAD^+. Deacetylation sensitizes the substrate such that treatment with a developer reagent releases a fluorescent product. The activity of the enzyme is proportional to the fluorescence intensity. The ability of resveratrol to activate the enzyme was evaluated in parallel assays as a positive control. Results are presented as mean of fluorescence intensity (arbitrary units) ± SEM.

3.2.7 Statistical Analysis

Results are presented as mean ± SEM. Statistical analysis was performed using GraphPad Prism version 6.0 (GraphPad Software, San Diego, CA, USA). Statistical significance was evaluated with the t-test to compare each condition with its respective control and one-way ANOVA with the Dunnett post-test for comparison of all conditions to a control group, except in Fig. 6B and 8 where one-way ANOVA with the Tuckey post-test for multiple comparisons was used. Results were considered statistically significant at $p< 0.05$.

3.3 Results

3.3.1 (S)-(+)-carvone decreases JNK1 phosphorylation induced by LPS in macrophages

The effects of (S)-(+)- carvone on the three MAPK subfamilies, namely Extracellular signal-Regulated Kinase 1/2 (ERK1/2), p38 and Jun N-terminal Kinase (JNK), were evaluated by measuring their phosphorylated levels in response to macrophage stimulation with LPS.

The results obtained (Fig. 1) show that LPS induces the phosphorylation of all three MAPK family members when compared to vehicle-treated cells, as expected. (S)-(+)-carvone differentially affects LPS-induced activation of the three MAPKs, having no effect on ERK1/2 (Fig. 1A) and p38 phosphorylation (Fig. 1B), while significantly decreasing JNK1 phosphorylation to, approximately, 38% of the levels found in cells treated with LPS alone (Fig. 1C). Furthermore, a tendency for reduced JNK2 and 3 phosphorylation is also observed, but in no case did it reach statistical significance (Fig. 1C).

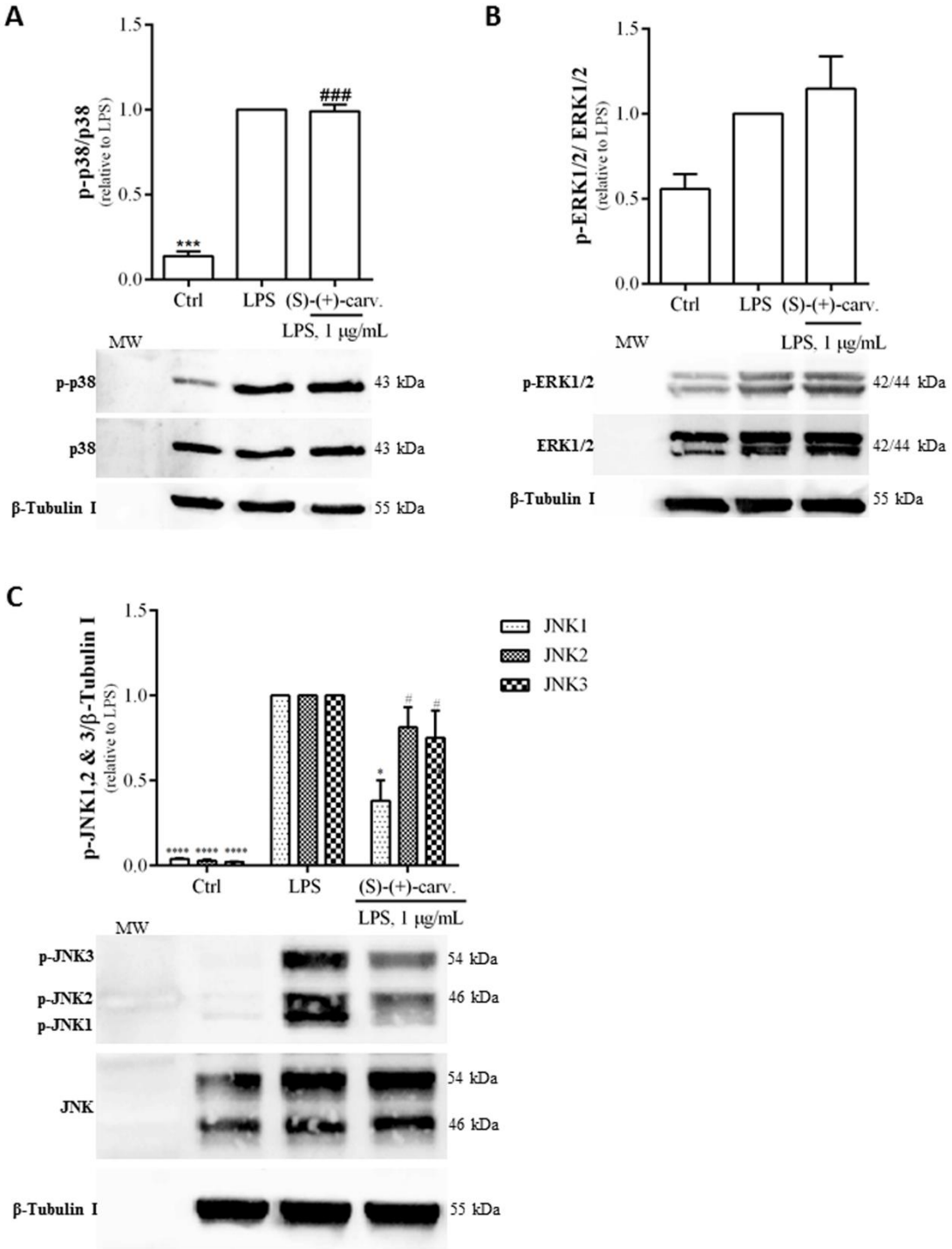

Figure 1. Effect of (S)-(+)-carvone on p38 (A), ERK1/2 (B) and JNK activation (C). Raw 264.7 macrophage cultures were pre-treated with 666 µM of (S)-(+)-carvone for 1 h and then with 1 µg/mL LPS for 5 min (**A** and **C)** or 1 h (**B**). Control cells (Ctrl) were treated with the vehicle (0.1% DMSO) in the absence of LPS for the same time periods. Each column represents the mean ± SEM of four (**A** and **C**) and three (**B**) independent experiments. Representative images are shown. *p<0.05, ***p<0.001 and ****p<0.0001 relative to LPS-treated cells. $^{\#}p$<0.05 and $^{\#\#\#}p$<0.001 relative to the Ctrl. MW: molecular weight marker.

To determine whether inhibition of JNK phosphorylation, especially of JNK1 which is the isoform most significantly affected by the test compound (Fig. 1C), can be involved in the anti-inflammatory effects observed in our previous study (Sousa, Leitão et al. 2020), we evaluated the ability of a non-cytotoxic concentration of SP600125, a known pan-JNK inhibitor, to decrease LPS-induced NOS2, NO and IL-1β production. SP600125 elicited a small decrease of LPS-induced NOS2 protein levels (Fig. 2A) and NO production (Fig. 2B) of approximately 30% and 20%, respectively, but was unable to affect IL-1β precursor protein levels (Fig. 2A). Taken together, these results suggest that JNKs contribute marginally for NOS2 expression and subsequent NO production in Raw 264.7 macrophages, but not for IL-1β expression under the experimental conditions used. Thus, these results suggest that inhibition of JNK1 cannot not play a major role in the ability of (S)-(+)-carvone to inhibit NOS2 expression and activity and is not all involved in the inhibition of IL-1β production that we observed previously (Sousa, Leitão et al. 2020).

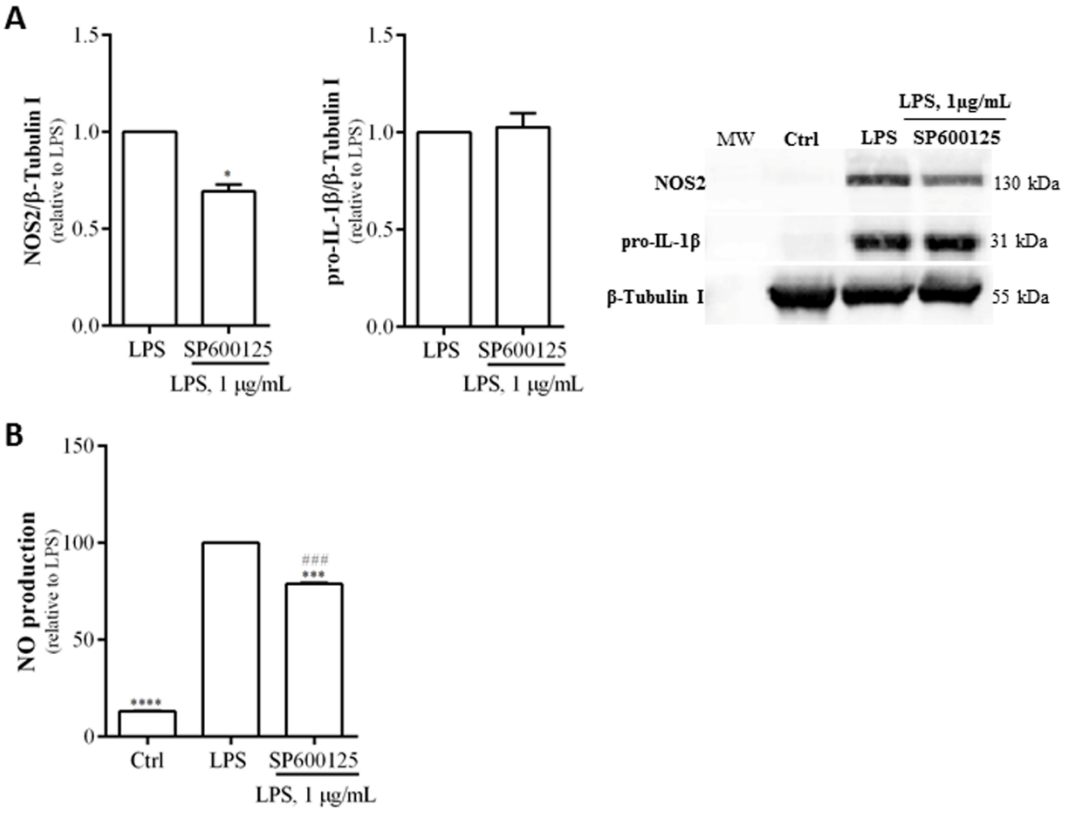

Figure 2. Effect of the selective JNK inhibitor, SP600125, on NOS2 expression (A), NO production (B), and pro-IL-1β expression (A). Raw 264.7 macrophage cultures were treated with 1 μg/mL LPS for 18 h, following pre-treatment with the vehicle (0.1% DMSO) or 20 μM SP600125 for 1 h. Control cells (Ctrl) were treated with the vehicle (0.1% DMSO) in the absence of LPS. Each column represents the mean ± SEM of three independent experiments. Representative images are shown. *p<0.05, ***p<0.001 and ****p<0.0001 relative to LPS-treated cells. $^{###}p$<0.001 relative to the Ctrl. MW: molecular weight marker.

3.3.2 (S)-(+)-carvone does not interfere with the canonical NF-κB activation pathway

NF-κB-inducing signals, like LPS upon binding to TLR4, trigger the activation of the IκB Kinase complex (IKK) which phosphorylates IκB-α, the natural inhibitor of NF-κB. Once phosphorylated, IκB-α is ubiquitinated and, subsequently, undergoes proteasomal degradation, releasing the NF-κB dimers, composed of p65 and p50 proteins, which constitutes the canonical NF-κB activation pathway. Upon release from IκB-α, the NF-κB dimers translocate to the nucleus and undergo several modifications that modulate their transcriptional activity on target genes (Roy, Srivastava et al. 2016). Since phosphorylation and degradation of IκB-α are essential for NF-κB activation, the ability of (S)-(+)-carvone to interfere with these steps was evaluated. Figure 3A and 3B show that LPS (1 μg/mL) induced IκB-α phosphorylation and degradation, respectively, but (S)-(+)-carvone was unable to block or even decrease those LPS-induced responses at concentration previously observed to be sufficient to decrease inflammatory gene expression (Sousa, Leitão et al. 2020). On the contrary, Bay 11-7082 (5 μM), a selective NF-κB inhibitor, decreased LPS-induced IκB-α phosphorylation and degradation (Fig. 3A and 3B), as expected, although the difference relative to cells treated with LPS alone did not reach statistical significance. Moreover, MG-132 (10 μM), a synthetic proteasome inhibitor peptide, increased the levels of phosphorylated IκB-α induced by LPS (Fig. 3A), showing that its proteasomal degradation was inhibited relative to LPS-treated cells (Fig. 3B). These results confirm that LPS effectively activated the canonical pathway, inducing IκB-α phosphorylation and degradation which were not affected by (S)-(+)-carvone (Fig. 3A and B).

Another target of IKK is NF-κB/p65 which is phosphorylated by this kinase on the Ser536 residue located in its transactivation domain (Sakurai, Chiba et al. 1999, Yang, Tang et al. 2003). Therefore, and to further confirm the results obtained for IκB-α, the ability of (S)-(+)-carvone to interfere with LPS-induced NF-κB/p65 phosphorylation at Ser536 was explored. The results in Fig. 3C show that the test compound was unable to decrease LPS-induced NF-κB/p65 phosphorylation on Ser536, further supporting that it does not interfere with the canonical NF-κB activation pathway.

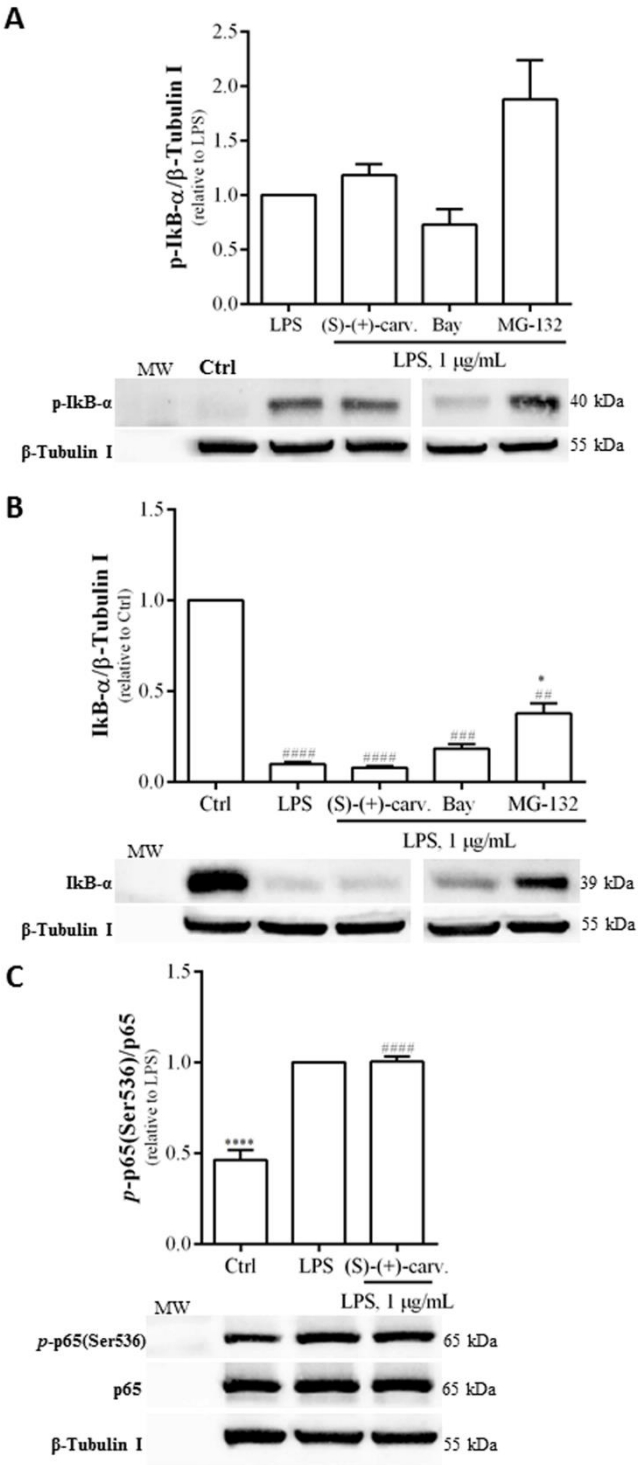

Figure 3. (S)-(+)-carvone does not interfere with the canonical NF-κB activation pathway, namely, phosphorylation (A) and degradation (B) of IκB-α and NF-κB/p65 phosphorylation at Ser536 (C) in Raw 264.7 macrophages. Macrophage cultures were treated with 1 μg/mL LPS for 5 min (**A**) or 15 min (**B** and **C**), following pre-treatment with the vehicle (0.1% DMSO, Ctrl), 666 μM (S)-(+)-carvone, the selective IKK inhibitor, 5 μM Bay 11-7082, or the proteasome inhibitor, 10 μM MG-132 for 1 h. Each column represents the

mean ± SEM of five (**A**) and four (**B** and **C**) independent experiments. Representative images are shown. *p<0.05 and ****p<0.0001 relative to LPS-treated cells. $^{\#}p$<0.05, $^{\#\#\#}p$<0.001 and $^{\#\#\#\#}p$<0.0001 relative to the Ctrl. MW: molecular weight marker.

3.3.3 NF-κB/p65 nuclear translocation is not affected by (S)-(+)-carvone

Since (S)-(+)-carvone was unable to prevent the dissociation of IκB-α from the NF-κB dimers, we hypothesized that this compound could be interfering with the nuclear translocation of this transcription factor. To explore this possibility, immunocytochemistry was performed to detect NF-κB/p65 traslocation to the nucleus. In vehicle-treated cells (Ctrl), NF-κB/p65 was clearly present in the cytoplasm, while upon treatment with LPS (1 µg/mL), immunoreactivity was exclusively located in the nucleus (Fig. 4). Pre-treatment with 10 µM MG-132 fully inhibited NF-κB/p65 nuclear translocation, as immunoreactivity is only visible in the cytoplasm. On the opposite, (S)-(+)-carvone was unable to prevent LPS-induced NF-κB/p65 nuclear translocation, as immunoreactivity is localized to the nucleus with no differences relative to cells treated with LPS alone (Fig. 4).

Confirming these results, western blot analysis shows that neither the LPS-induced decrease in the cytoplasmic levels of NF-κB/p65 (Fig. S1A), nor the increase in its nuclear levels (Fig. S1B) were affected by treatment with (S)-(+)-carvone. Thus, these results corroborate those found in the immunofluorescence assay, collectively showing that (S)-(+)-carvone does not interfere with LPS-induced NF-κB/p65 release from complexes with IκB-α and nuclear translocation.

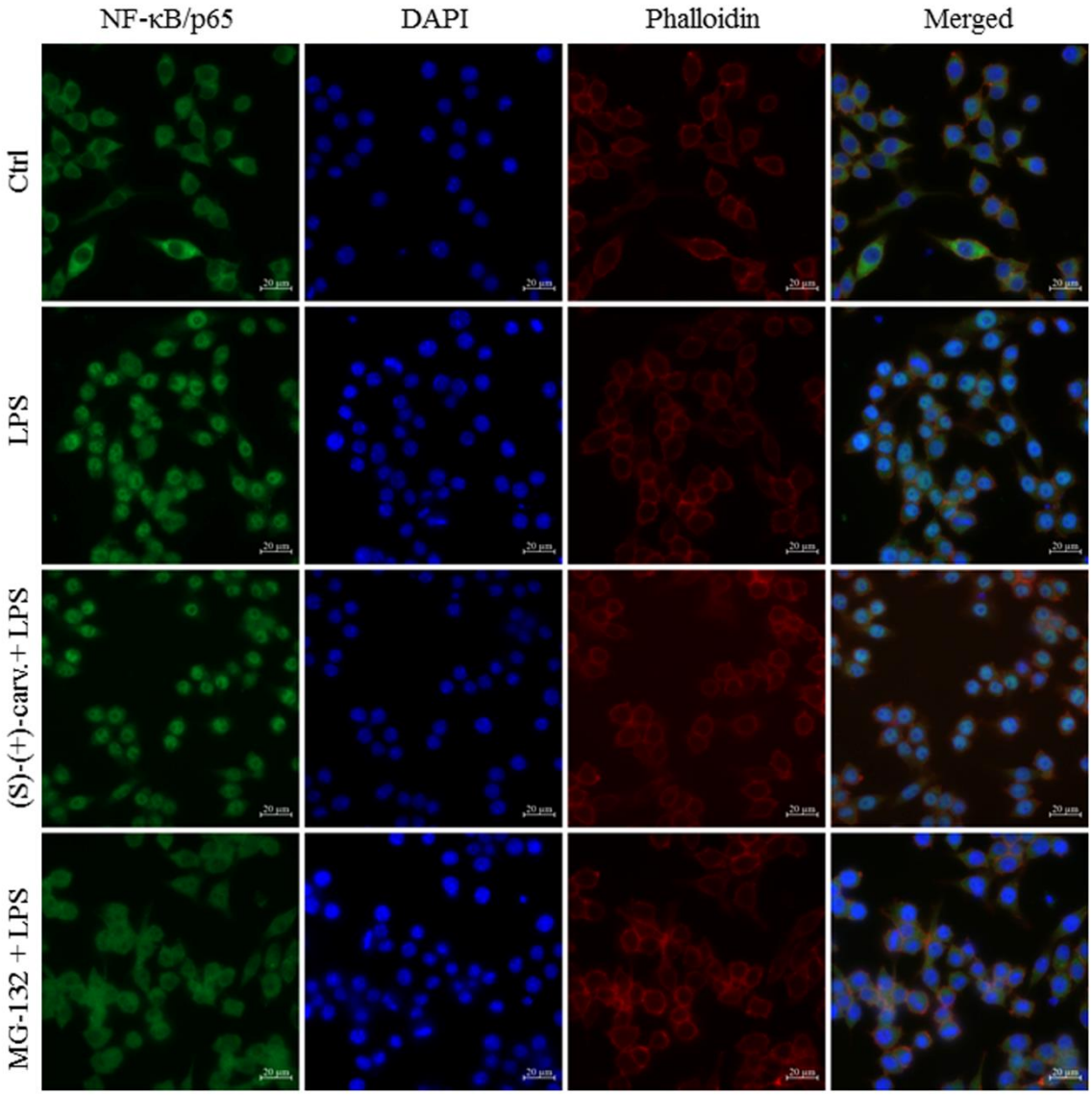

Figure 4. **(S)-(+)-carvone does not inhibit NF-κB nuclear translocation.** Raw 264.7 macrophages were treated with 1 µg/mL LPS for 20 min, following pre-treatment with the vehicle (0.1% DMSO), 666 µM (S)-(+)-carvone or 10 µM MG-132 for 1 h. Control cells (Ctrl) were treated with the vehicle in the absence of LPS. Immunofluorescence staining of NF-κB/p65 (green) and fluorescence staining of the cytoskeleton (red) and the nuclei (blue) were performed as described in the Materials and methods**.** Scale bar 20 µm. Representative images of each condition are shown.

3.3.4 NF-κB transcriptional activity is inhibited by (S)-(+)-carvone

Although (S)-(+)-carvone did not inhibit the canonical NF-κB activation pathway, our previous work demonstrated that this compound is capable of decreasing the expression of two NF-κB target genes and major inflammatory mediators, NOS2 and IL-1β (Sousa, Leitão et al. 2020). Thus and to further elucidate these findings, the protein product of another NF-κB target gene, the IκB-α gene (Cheng, Ryseck et al. 1998), was also evaluated. For this, we performed a time course of stimulation with LPS to determine the time points where IκB-α degradation ended and its resynthesis started. Figure S2 shows that IκB-α degradation was complete within 10 to 15 min after addition of LPS, whereas its resynthesis started at 20 min and reached its maximal level within 60 min. Thus, using this time point, we determined that (S)-(+)-carvone is effective in preventing LPS-induced IκB-α resynthesis (Fig. 5), supporting the hypothesis that the anti-inflammatory effects of this compound involve modulation of NF-κB activity.

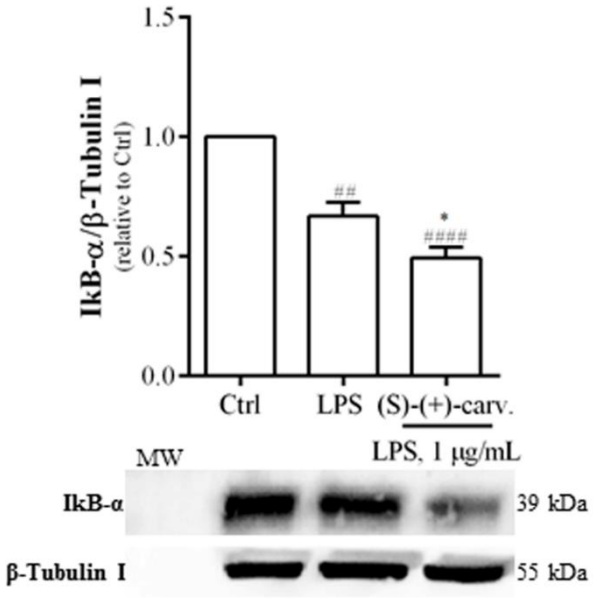

Figure 5. Effect of (S)-(+)-carvone on LPS-induced IκB-α resynthesis in Raw 264.7 macrophages. The cells were pre-treated with the vehicle (0.1% DMSO) or 666 µM (S)-(+)-carvone for 1 h, followed by stimulation with 1 µg/mL LPS for 1 h. Control cells (Ctrl) were treated with the vehicle in the absence of LPS. Each column represents the mean ± SEM of seven independent experiments. Representative images are shown. *p<0.05 relative to LPS-treated cells. $^{\#\#}p$<0.01 and $^{\#\#\#\#}p$<0.0001 relative to the Ctrl. MW: molecular weight marker.

3.3.5 (S)-(+)-carvone promotes NF-κB/p65 deacetylation at Lys310 and directly activates SIRT1 activity

Besides release from IκB-α and nuclear translocation, NF-κB full transcriptional activity requires several modifications of NF-κB/p65 which impact on DNA binding affinity, interaction with coactivators and corepressors and termination of the NF-κB response (Huang, Yang et al. 2010). Thus, we hypothesized that (S)-(+)-carvone may interfere with one or more of those modifications. Among those, NF-κB/p65 acetylation, particularly at Lys310, has been reported as essential for full NF-κB transcriptional activity (Huang, Yang et al. 2010). Thus, we evaluated the levels of NF-κB/p65 acetylated on Lys 310 induced by LPS. Figure 6A shows that pre-treatment with (S)-(+)-carvone decreased the levels of acetylated Lys310 on NF-κB/p65. (Fig. 6A). Furthermore, resveratrol (Res), a natural polyphenolic compound known to promote NF-κB/p65 deacetylation (Yeung, Hoberg et al. 2004) used as a positive pharmacological control, shows a tendency to reduce the levels of acetylated NF-κB/p65 present in the nucleus (Fig. 6A), although this effect was blunted because Res also inhibits the canonical NF-κB activation pathway, decreasing the nuclear levels of total NF-κB/p65 (Holmes-McNary and Baldwin 2000, Manna, Mukhopadhyay et al. 2000).

These results led us to hypothesize that (S)-(+)-carvone may directly activate Sirtuin 1 (SIRT1), a NAD^+-dependent class III histone/protein deacetylase. SIRT1interacts with NF-κB/p65 and specifically deacetylates its Lys310 residue, which inhibits NF-κB transcriptional activity (Yeung, Hoberg et al. 2004). To investigate this hypothesis, we used an *in vitro* fluorimetric assay based on the deacetylation of a p53-derived synthetic peptide by recombinant human SIRT1. Figure 6B shows that (S)-(+)-carvone activated SIRT1 in a concentration-dependent manner, reaching a maximum at a concentration of 266 μM (Fig. 6B). As expected, Res was also effective in increasing SIRT1 activity.

On the other hand, increased deacetylation of SIRT1 target proteins *in vivo* can also occur in response to stimuli that increase the expression of this enzyme, with or without affecting its activity. Thus and to further elucidate the mechanism underlying the ability of (S)-(+)-carvone to deacetylate NF-κB/p65, we evaluated the protein levels of SIRT1. Figure 6C shows that LPS did not significantly affect SIRT1 levels relative to untreated cells and (S)-(+)-carvone also had no influence on those levels.

Taken together, the results show that (S)-(+)-carvone promoted NF-κB/p65 deacetylation, likely by directly activating SIRT1 and this mechanism probably underlies the inhibitory effect of (S)-(+)-carvone on NF-κB-dependent gene transcription.

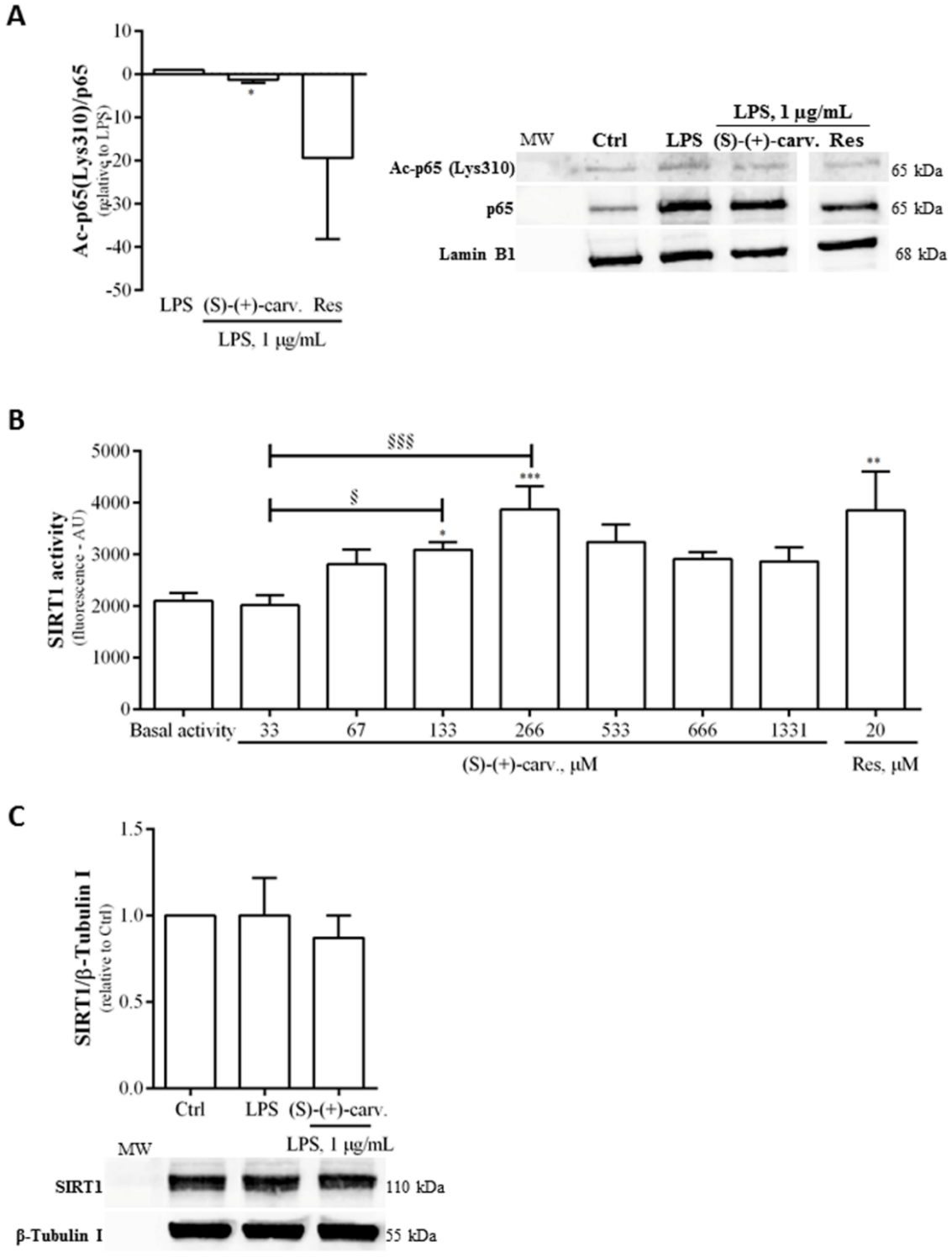

Figure 6. Effect of (S)-(+)-carvone on Lys310-acetylated NF-κB/p65 levels (A) and SIRT1 activity (B) and protein levels (C). (**A**) Raw 264.7 macrophages were pre-treated with vehicle (0.1% DMSO), 666 µM (S)-(+)-carvone or 5.5 µM Resveratrol (Res) for 1 h, before treatment with 1µg/mL LPS for 1 h. (**B**) Different concentrations of (S)-(+)-carvone were directly incubated with human recombinant SIRT1 and specific

substrate, as described under Materials and methods. Resveratrol (Res) was used as a pharmacological control of SIRT1 activation. (**C**) Raw 264.7 cells were treated with 1 µg/mL LPS, following pre-treatment with the vehicle (0.1% DMSO) or 666 µM (S)-(+)-carvone for 1 h. Control cells (Ctrl) were treated with the vehicle (0.1% DMSO) in the absence of LPS. Each column represents the mean ± SEM of four (**A**), six to fifteen (**B**) and three (**C**) independent experiments. On panel A, the intensities, in arbitrary units, of the bands corresponding to Ac-p65 (Lys310) and total NF-κB/p65 in the control were subtracted from the intensities of the corresponding bands in each condition to allow calculation of the ratio of Ac-p65 (Lys310) to total NF-κB/p65 and subsequent normalization to LPS. Representative images are shown. *p<0.05 relative to LPS-treated cells. For (B), *p<0.05, **p<0.01 and ***p<0.001 relative to SIRT1 basal activity; §p<0.05 and §§§p<0.001 between the conditions indicated. MW: molecular weight marker.

3.3.6 (S)-(+)-carvone also promotes NF-κB/p65 deacetylation at Lys310 in Il-1β-treated human chondrocytes

To confirm that the ability of (S)-(+)-carvone to activate SIRT1 and promote NF-κB/p65 deacetylation is a broad mechanism relevant in other cell types, we performed the same experiment in human chondrocytes treated with IL-1β. As expected, treatment with IL-1β (10 ng/mL) increased Lys310 acetylation which was decreased by pretreatment with either (S)-(+)-carvone or Res, used as a pharmacological control (Fig.7). However, neither the effect of (S)-(+)-carvone nor that of Res reached statistical significance, probably due to the large inter-individual variability of cartilage sample donors.

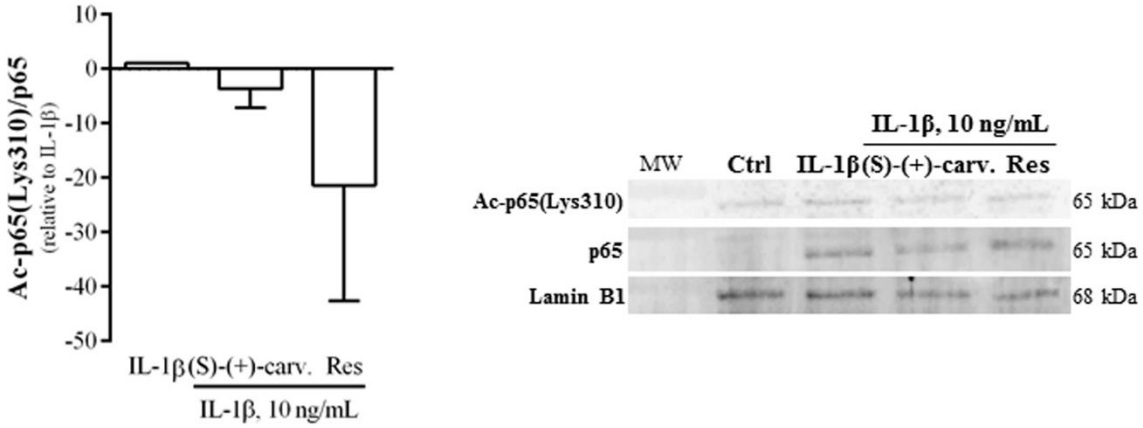

Figure 7. (S)-(+)-carvone decreases IL-1β-induced NF-κB/p65 acetylation at Lys310 in human chondrocytes. Human chondrocyte cultures were pre-treated with vehicle (0.1% DMSO), 666 µM (S)-(+)-carvone or 5.5 µM Resveratrol (Res) for 1h, and then stimulated for 45 min with 10 ng/mL IL-1β. Control cells (Ctrl) were treated with the vehicle (0.1% DMSO) in the absence of IL-1β. The intensities, in arbitrary units, of the bands corresponding to Ac-p65 (Lys310) and total NF-κB/p65 in the control were subtracted from the intensities of the corresponding bands in each condition to allow calculation of the ratio of Ac-p65 (Lys310) to total NF-κB/p65 and subsequent normalization to IL-1β. Each column represents the mean ± SEM of four independent experiments. Representative images are shown. MW: molecular weight marker.

3.3.7. (S)-(+)-carvone increases SOX9 levels in human chondrocytes

To further assess the relevance of (S)-(+)-carvone in regulating chondrocyte functions, besides inhibition of inflammatory responses, we evaluated its ability to modulate the protein levels of SRY-box transcription factor 9 (SOX9), a transcription factor essential for the expression of cartilage-specific genes, namely collagen 2 and aggrecan, whose activity is dependent on SIRT1(Dvir-Ginzberg, Gagarina et al. 2008, Bar Oz, Kumar et al. 2016). Figure 8 shows that treatment of human chondrocytes with (S)-(+)-carvone for 24 h increases SOX9 protein levels by approximately 2.5 fold. No significant differences were found between the two concentrations of (S)-(+)-carvone tested, suggesting that the maximal effect was achieved. This is in agreement with the results presented in Fig. 6B where the same concentrations also elicited maximal SIRT1 activation.

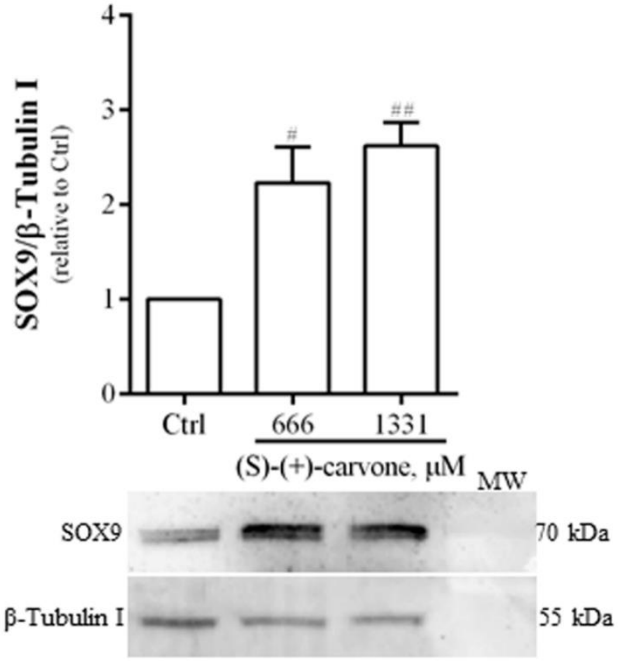

Figure 8. (S)-(+)-carvone increases SOX9 protein levels in human chondrocytes. The cells were treated with the indicated concentrations of the test compound or vehicle (0.1% DMSO) for 24 h. Each column represents the mean ± SEM of, at least, three independent experiments. A representative image is shown. $^{\#}p<0.05$ and $^{\#\#}p<0.01$ relative to the Ctrl MW: molecular weight marker.

3.4. Discussion

Inhibition of MAPK and/or NF-κB signaling pathways are mechanisms relevant to dampen chronic low-grade inflammation that are targeted by many compounds of natural origin (Azab, Nassar et al. 2016, Lin and Li 2018), from polyphenols, like Res (de Sá Coutinho, Pacheco et al. 2018), to monoterpenes, such as myrcene and limonene (Rufino, Ribeiro et al. 2015) and α-pinene (Rufino, Ribeiro et al. 2014). Thus, to elucidate the molecular mechanism of the anti-inflammatory effects of (S)-(+)-carvone that we observed in murine macrophages and human chondrocytes (Sousa et al., 2020), we started by evaluating its ability to inhibit those signaling pathways. Interestingly, the results demonstrate that only JNK1 is significantly inhibited by (S)-(+)-carvone, while it does not prevent LPS-induced activation of any of the other MAPK family members to a significant extent. Moreover, (S)-(+)-carvone also does not prevent any of the steps involved in the canonical NF-κB activation pathway, that is, IκB-α phosphorylation and degradation and NF-κB/p65 nuclear translocation and phosphorylation on Ser536 (Figs. 3 and 4).

Nonetheless, we further confirmed that this compound is effective in inhibiting the expression of IκB-α, another NF-κB target gene (Fig. 5).

Since several post-translational modifications of NF-κB/p65 play a critical role in modulating its DNA-binding affinity and transcriptional activity (Huang, Yang et al. 2010), we hypothesized that (S)-(+)-carvone may exert its anti-inflammatory effects by modulating such modifications. Among those, acetylation of Lys310 by the co-activator and histone/protein acetyltransferase, CBP/p300, is required for the full transcriptional activity of NF-κB, without interfering with DNA binding (Huang, Yang et al. 2010). Deacetylation of that Lys residue prevents and contributes to cease NF-κB transcriptional activity because it allows subsequent ubiquitination and degradation of promoter-associated NF-κB/p65 (Huang, Yang et al. 2010). As shown in Figure 6A, (S)-(+)-carvone significantly decreased LPS-induced Lys310-acetylated NF-κB/p65 levels in mouse macrophages, suggesting that this can be the mechanism underlying inhibition of NF-κB-dependent gene expression.

Decreased levels of acetylated NF-κB/p65 can occur due to inhibition of Histone AcetylTransferase (HAT) enzymes or activation of Histone DeAcetylases (HDAC). Among HDACs, SIRT1 has a major role in modulating NF-κB transcriptional activity by directly interacting with and deacetylating NF-κB/p65 on Lys310 (Yeung, Hoberg et al. 2004). Thus, we hypothesized that SIRT1 could be the target of (S)-(+)-carvone and found that it directly activates SIRT1 which correlates with decreased levels of acetylated NF-κB/p65 both in murine macrophages (Fig. 6) and human chondrocytes (Fig. 7), although in this case interindividual variability likely precluded the observation of statistically significant differences.

Finally and to further assess the relevance of SIRT1 activation by (S)-(+)-carvone in the context of a chronic disease like osteoarthritis, we evaluated its ability to modulate SOX9. SIRT1 is responsible for SOX9 deacetylation which is required for its nuclear translocation and enhancement of collagen 2 (Dvir-Ginzberg, Gagarina et al. 2008, Oppenheimer, Kumar et al. 2014) and aggrecan (Bar Oz, Kumar et al. 2016) expression. The results presented in Figure 8 show that treatment of human chondrocytes with (S)-(+)-carvone significantly increases the protein levels of SOX9. However, these results are in contrast with other studies that found no changes in SOX9 protein levels upon activation or inhibition of SIRT1 (Bar Oz et al., 2016). Nonetheless, a cleaved inactive form of SOX9 has been found to accumulate in OA and aged-chondrocytes, correlating with decreased expression and

activity of SIRT1 (Bar Oz et al., 2016). Moreover, known SIRT1 activators, like Res and fisetin, have been shown to increase basal SOX9 levels and to counteract the inhibitory effect induced by inflammatory stimuli (Buhrmann, Popper et al. 2017, Zheng, Feng et al. 2017). Clearly, more studies are required to fully assess the role of the acetylation status on the stability of SOX9 and the relevance of activating or inhibiting SIRT1 on that process (Zheng et al., 2017).

3.5. Conclusion

In summary, the results presented show that (S)-(+)-carvone directly activates SIRT1 which, in turn, leads to inhibition of NF-κB transcriptional activity, resulting in anti-inflammatory effects.

To our knowledge, this is the first study identifying a monoterpene compound as a direct activator of SIRT1. Although studies using (S)-(+)-carvone are scarce, previous studies using the racemic mixture containing both carvone enantiomers, (S)-(+)- and (R)-(-)-carvone, reported some pharmacological activities, including antioxidant (Sabir, Singh et al. 2015), anti-inflammatory (Sepúlveda-Arias, Veloza et al. 2013, Sousa, Leitão et al. 2020), anti-carcinogenic (Wattenberg, Sparnins et al. 1989), anti-hyperglycemic and anti-hyperlipidemic (Muruganathan and Srinivasan 2016, Alsanea and Liu 2017) properties. Interestingly, SIRT1 activation has been shown to have a role in all these processes (Haigis and Sinclair 2010, Gomes, Leal et al. 2019), suggesting that, at least in part, this can be the mechanism underlying the pharmacological activities previously reported for carvone.

Remarkably, NF-κB and SIRT1 are involved in an antagonistic crosstalk whereby SIRT1 inhibits NF-κB activity by deacetylating NF-κB/p65 and this transcription factor inhibits SIRT1 expression (Kauppinen, Suuronen et al. 2013). Decreased SIRT1 expression and increased NF-κB activity are found in many metabolic and age-related diseases, so that NF-κB inhibition is envisaged as a promising therapeutic strategy for those diseases, as well as to delay the consequences of aging (Gaspar, Álvaro et al. 2019, Gomes, Leal et al. 2019, Mahmoudi, Xu et al. 2019). Therefore, the ability of (S)-(+)-carvone to directly increase the activity of SIRT1 leading to NF-κB inhibition has a huge therapeutic potential. Further studies addressed at pharmacokinetic and further pharmacodynamic elucidation, namely in terms of selectivity, efficacy and safety, in cell and animal models of disease are required to

fully ascertain the therapeutic potential of (S)-(+)-carvone and support its role as the first in monoterpene class SIRT1 activator.

Funding Sources

This work was funded by the European Regional Development Fund (ERDF), through the Centro 2020 Regional Operational Program and through the COMPETE 2020 - Operational Program for Competitiveness and Internationalization and Portuguese national funds via FCT – Fundação para a Ciência e a Tecnologia, under projects POCI-01-0145-FEDER-028424 (CARTILFACTORY) and UID/NEU/04539/2019 and the PhD fellowship SFRH/79600/2011 to C. Sousa.

3.6 Supplementary material

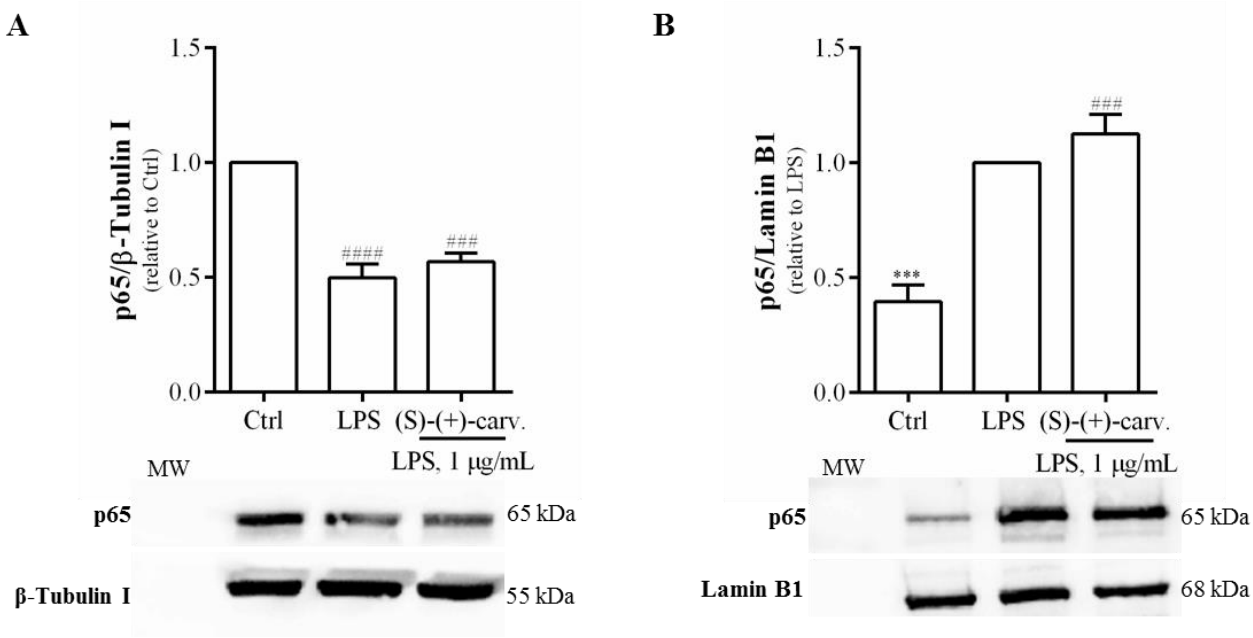

Figure S1.(S)-(+)-carvone does not inhibit NF-κB nuclear translocation in Raw 264.7 cells. Macrophages were treated with 1 µg/mL LPS for 1 h, following pre-treatment with the vehicle (0.1% DMSO) or 666 µM (S)-(+)-carvone for 1 h. Cytoplasmic (**A**) and nuclear (**B**) levels of RelA/p65 were evaluated by western blot. Control cells (Ctrl) were treated with the vehicle in the absence of LPS. Each column represents the mean ± SEM of three (**A**) and six (**B**) independent experiments. Representative images are shown. ***p<0.001 relative to LPS-treated cells. $^{###}p$<0.001 and $^{####}p$<0.0001 relative to the Ctrl. MW: molecular weight marker.

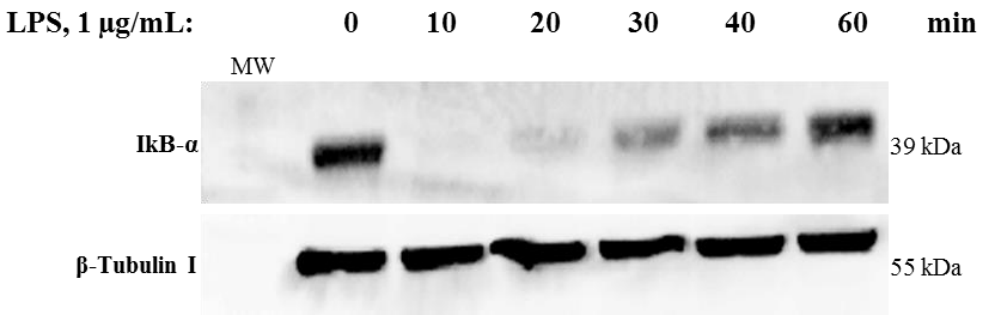

Figure S2. Effect of LPS on IκB-α degradation/resynthesis in Raw 264.7 cells. Cells were stimulated with 1 µg/mL LPS for the indicated time periods. MW: molecular weight marker.

Uncropped blots shown in **Figure 1A**

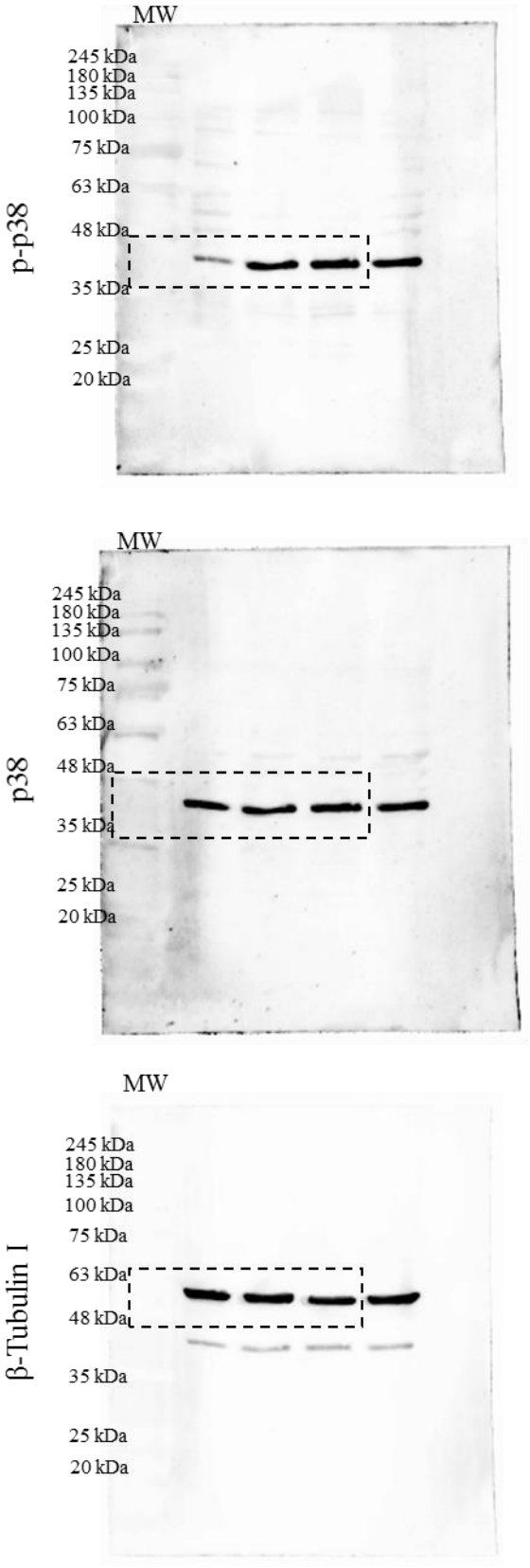

Uncropped blots shown in **Figure 1B**

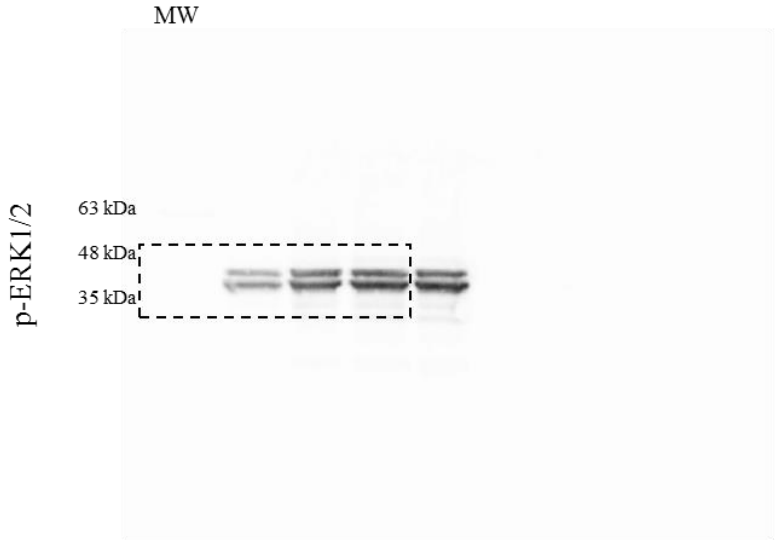

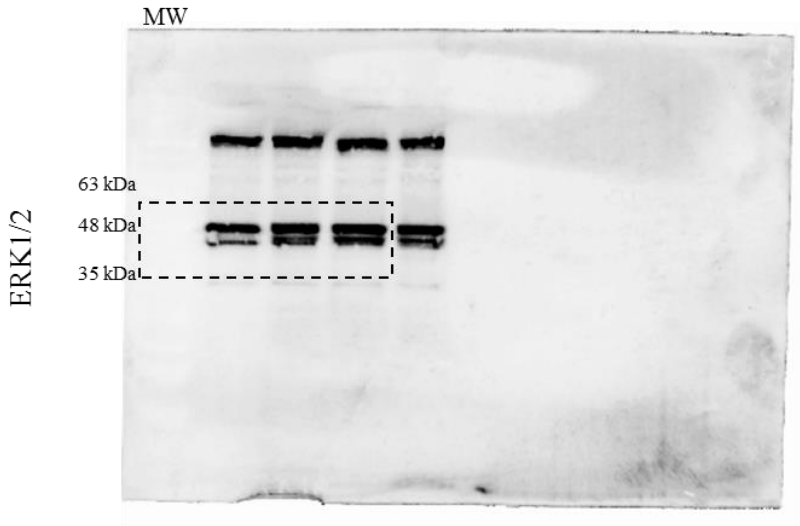

This membrane was also incubated with anti-SIRT1 antibody and the corresponding band appears near the 100 kDa molecular weight marker.

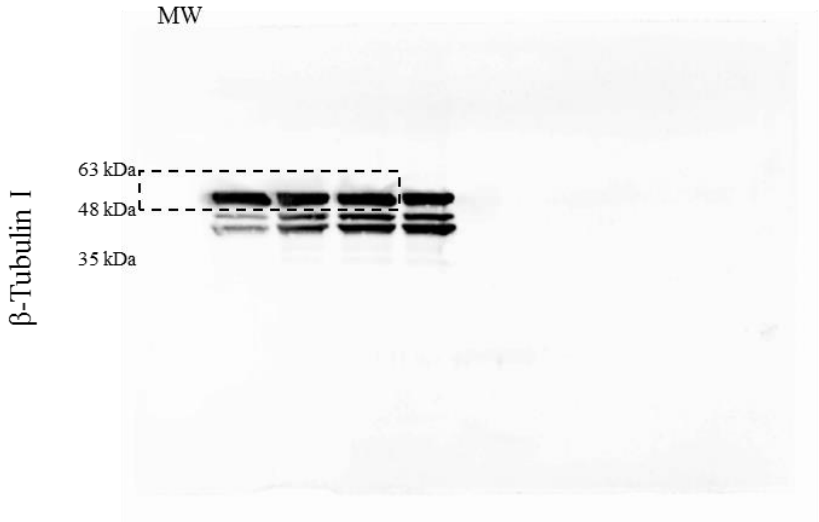

Uncropped blots shown in **Figure 1C**

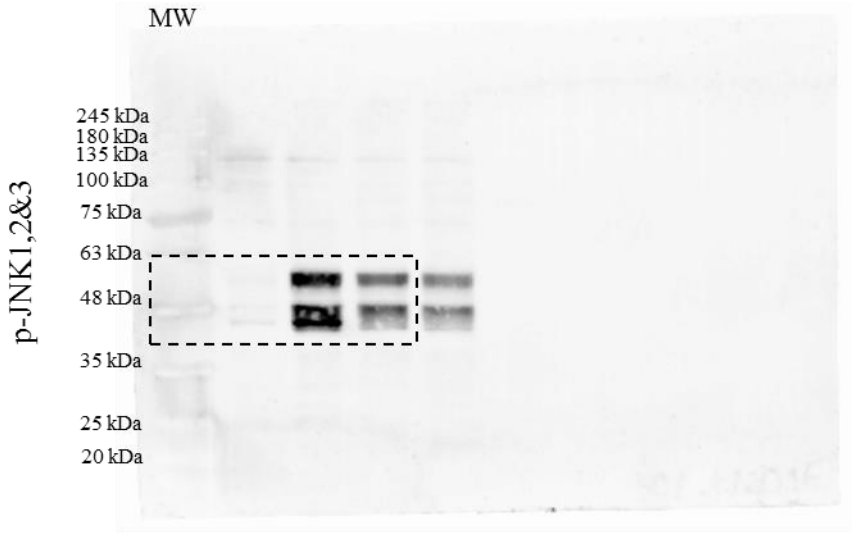

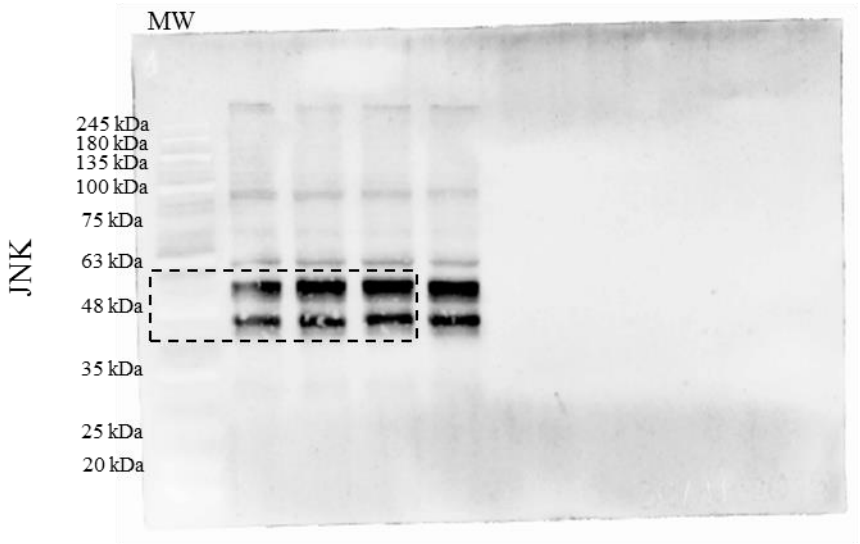

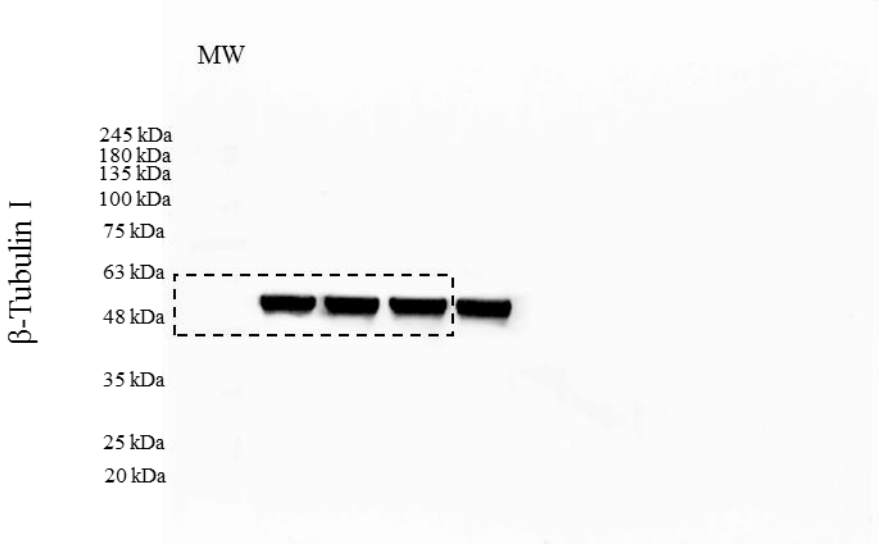

Uncropped blots shown in **Figure 2A**

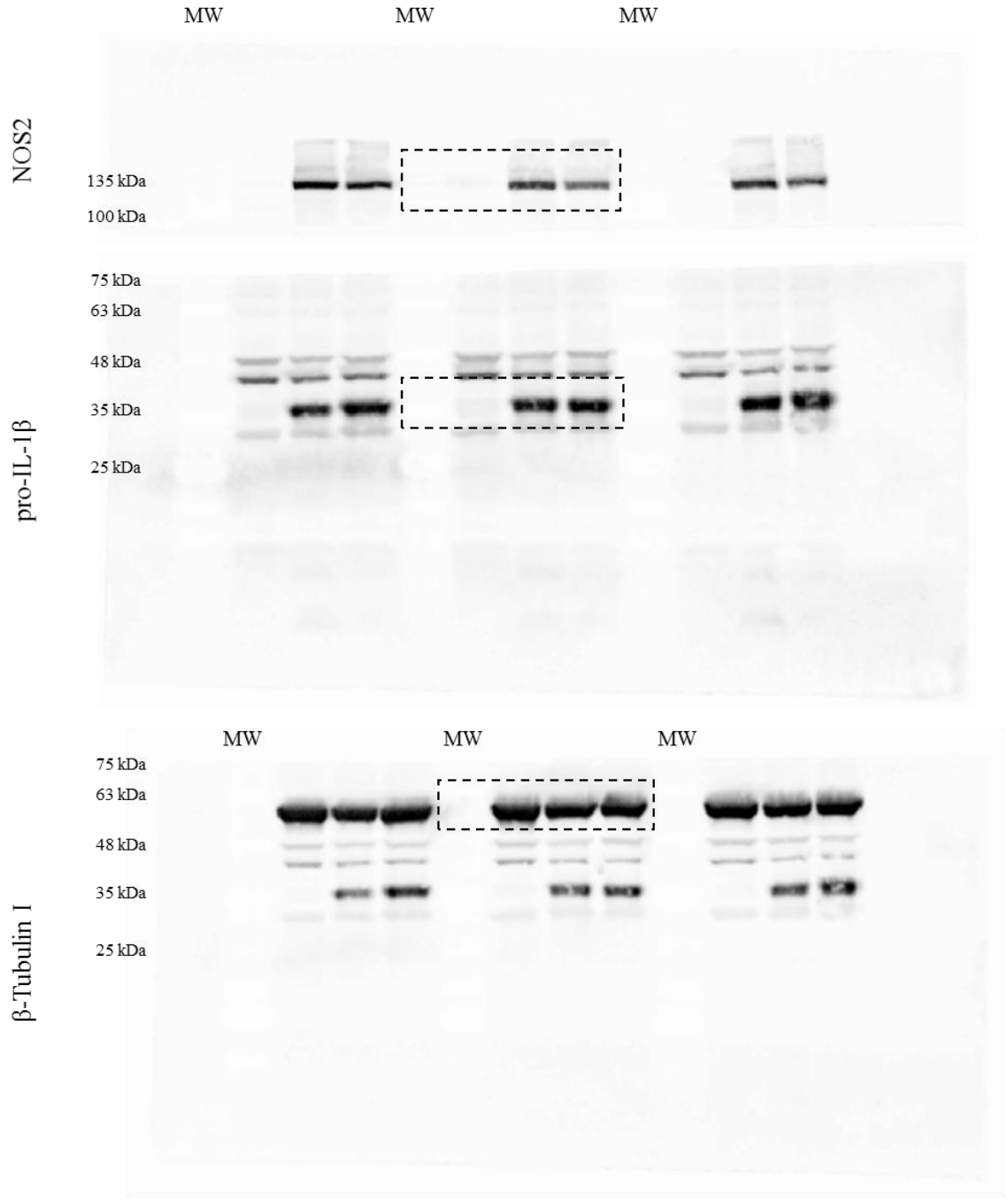

The membranes were cut at ≈ 75 kDa so that the upper piece was incubated with anti-NOS2 antibody and the lower one with the anti-pro-IL-1β antibody. Then, the lower piece was incubated with the β-Tubulin I antibody, without stripping.

Uncropped blots shown in **Figure 3A**

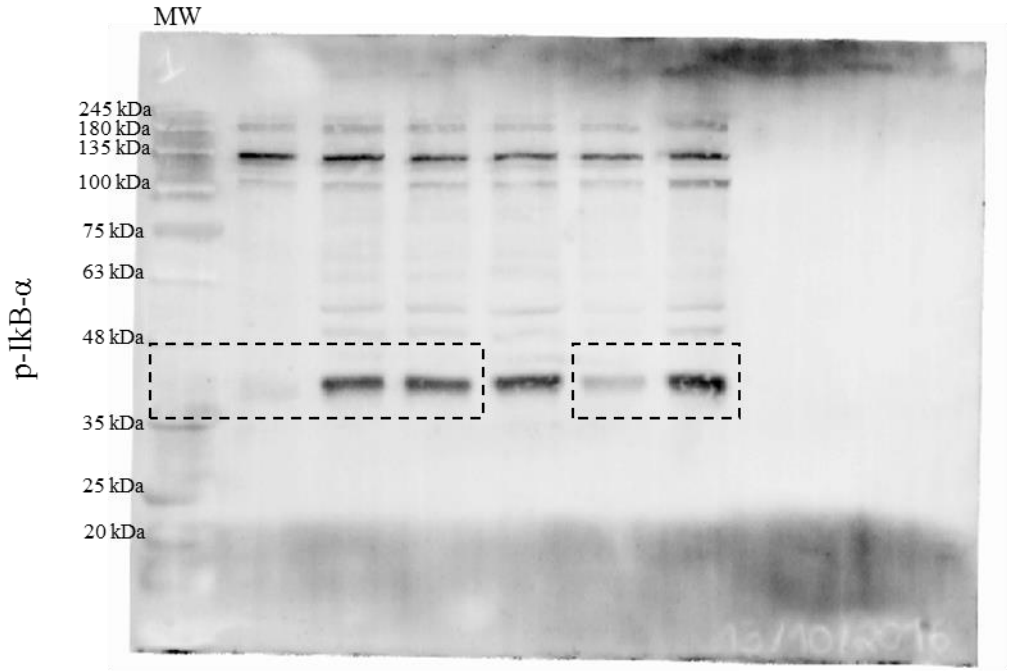

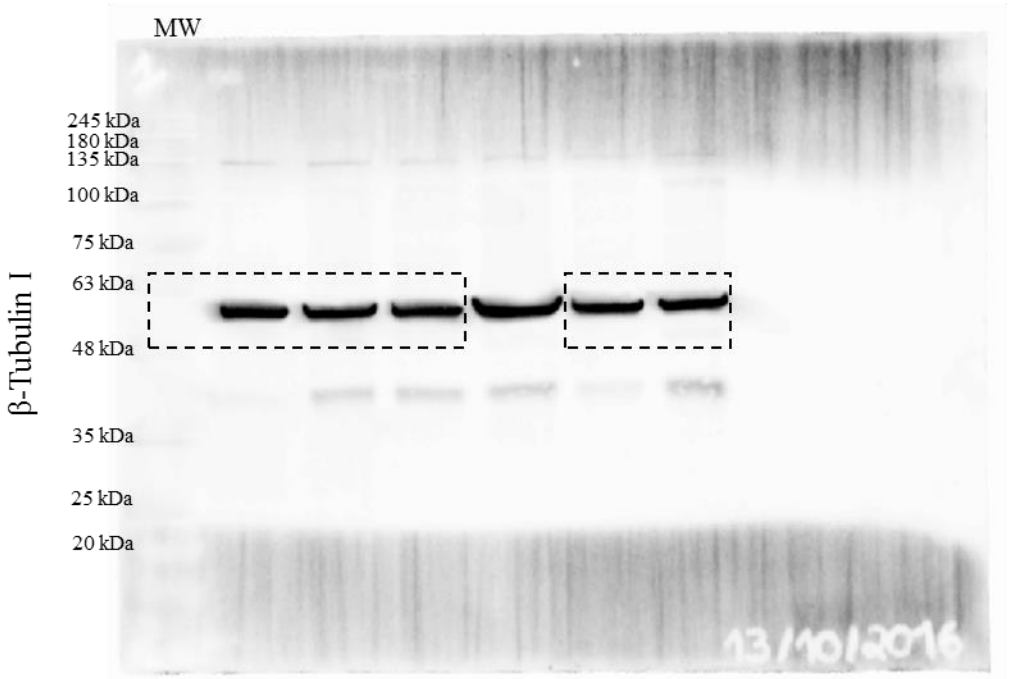

Uncropped blots shown in **Figure 3B**

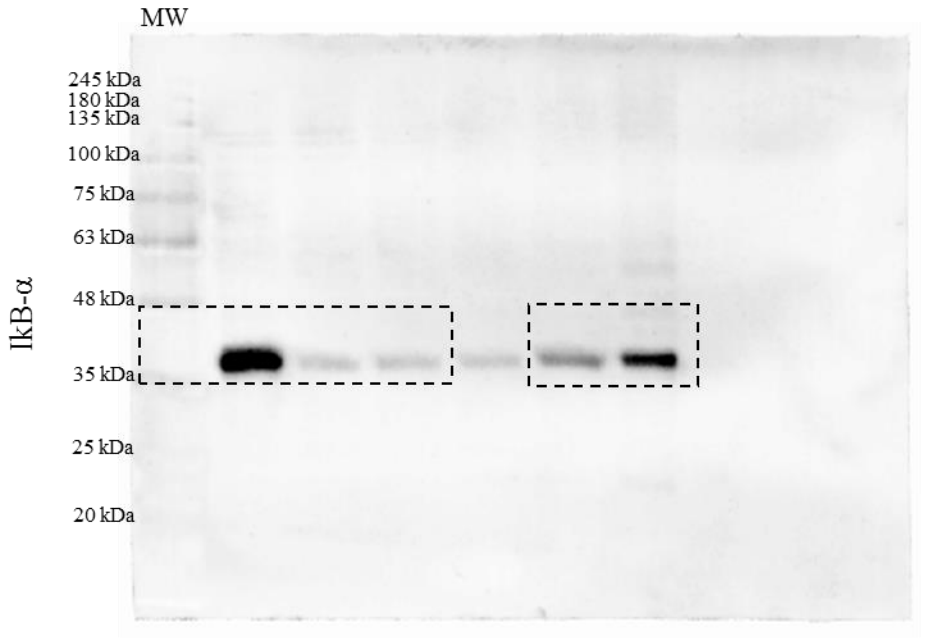

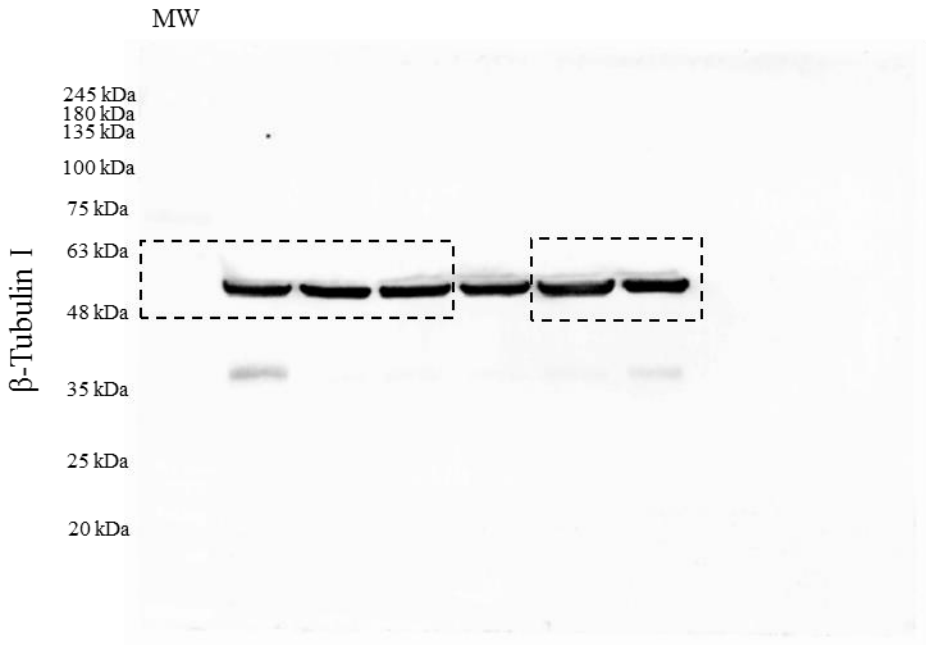

Uncropped blots shown in **Figure 3C**

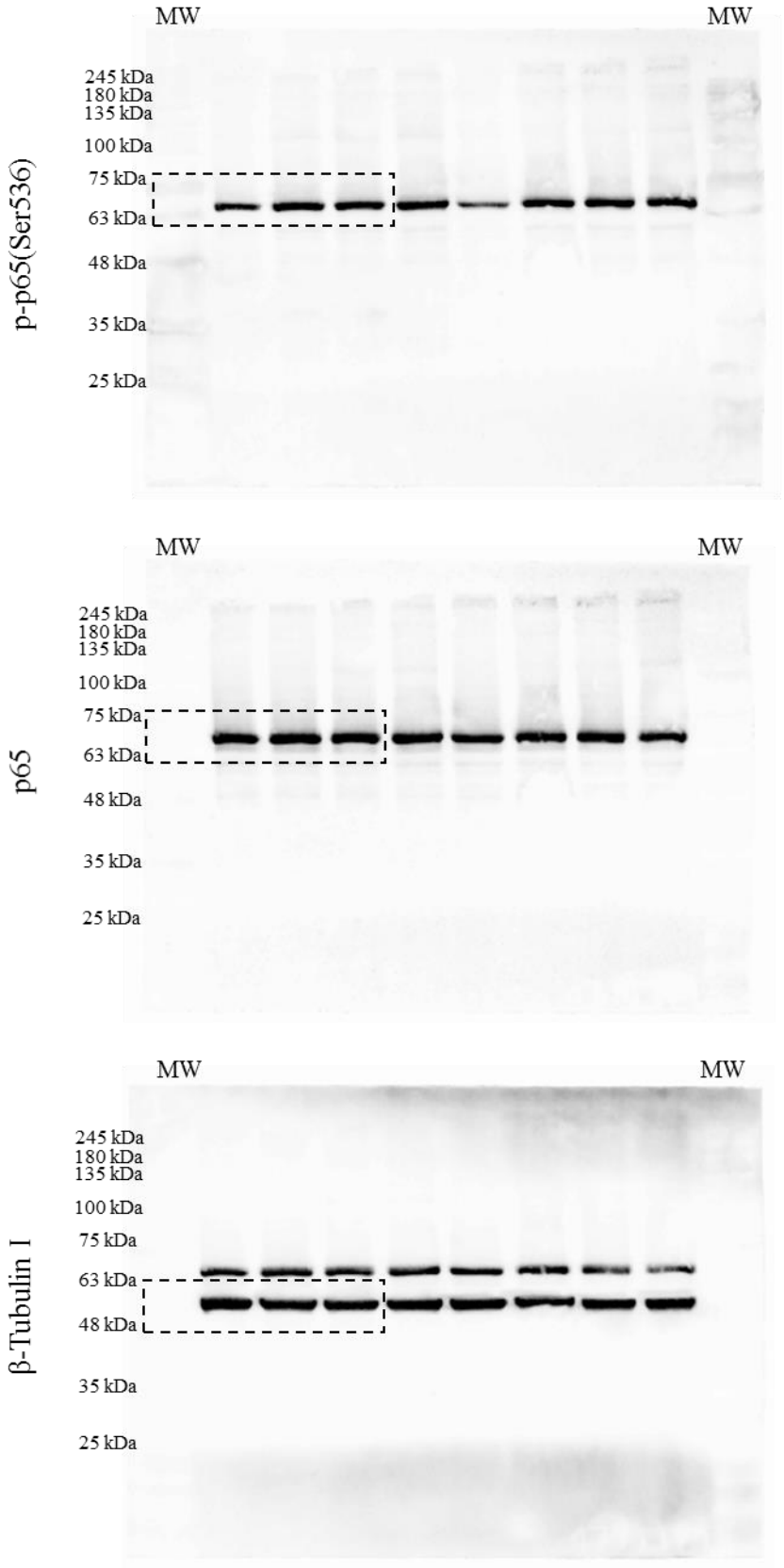

Uncropped blots shown in **Figure 5**

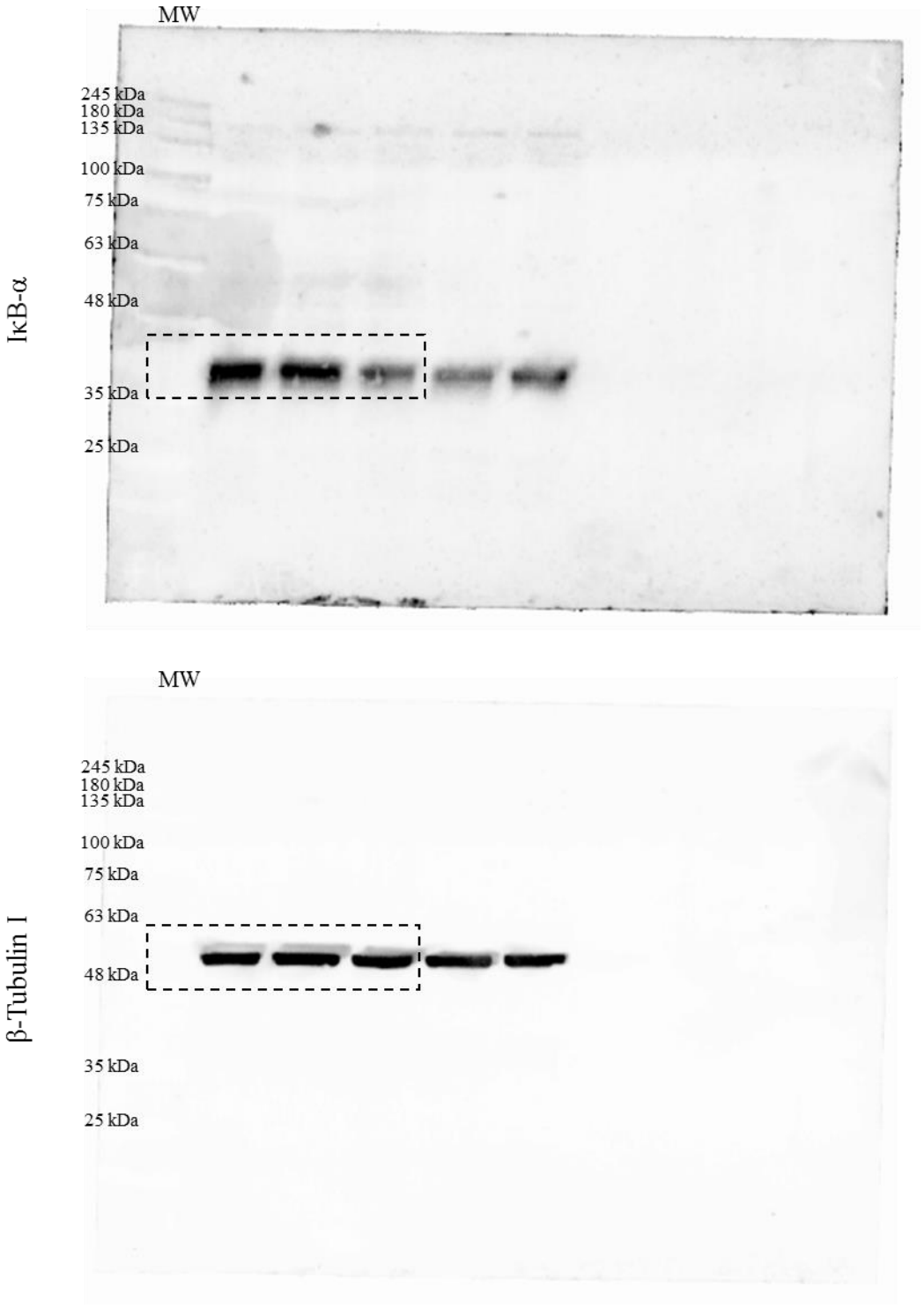

Uncropped blots shown in **Figure 6A**

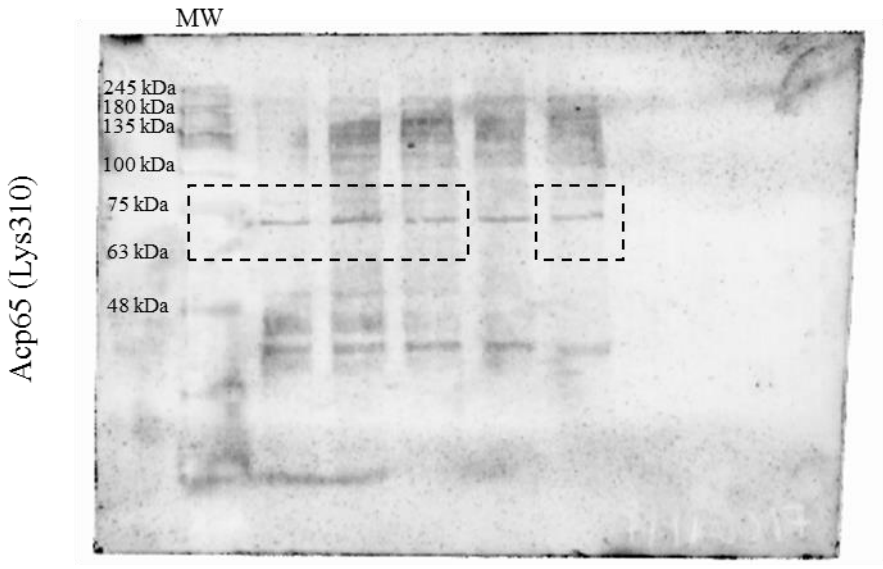

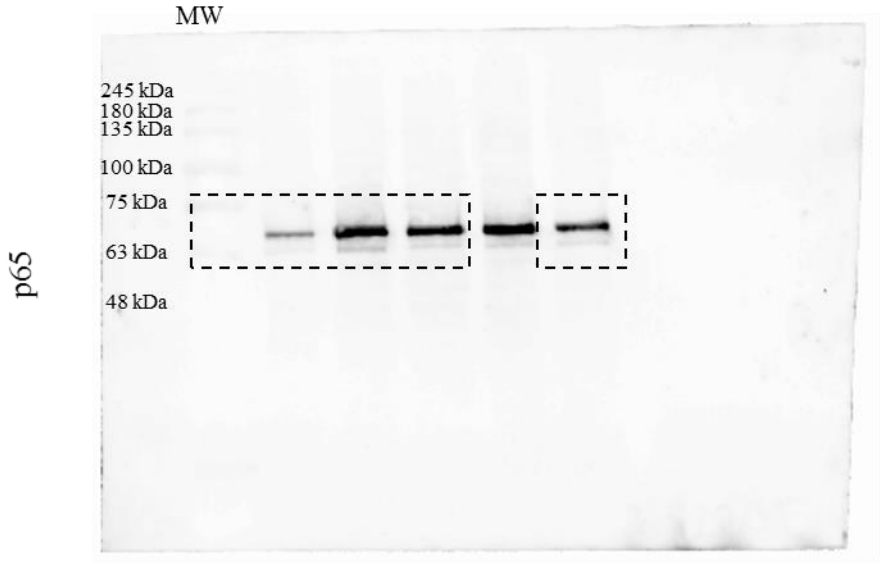

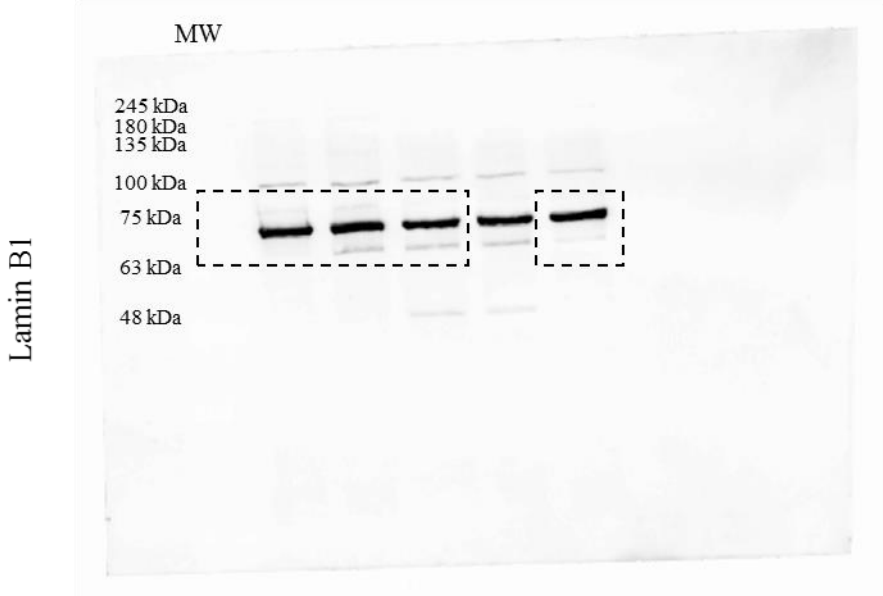

Uncropped blots shown in **Figure 6C**

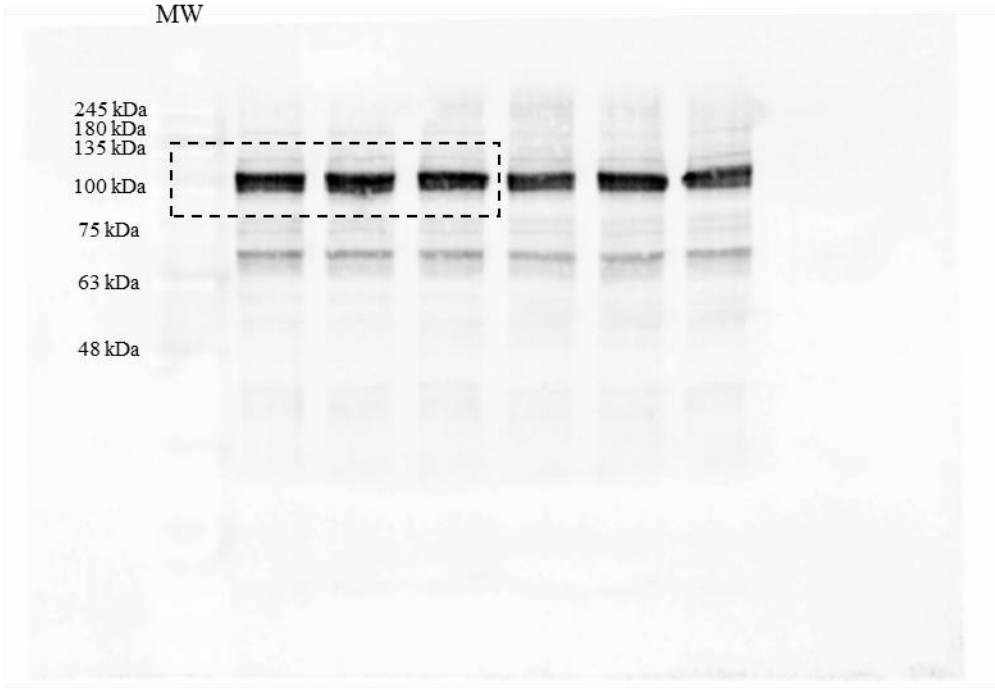

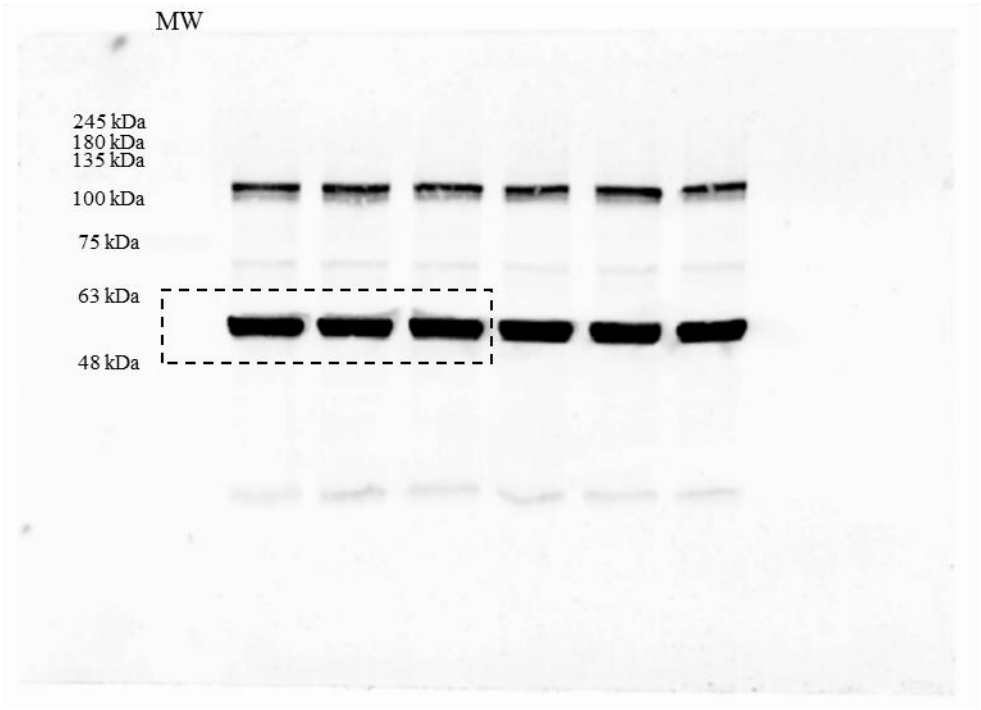

Uncropped blots shown in **Figure 7**

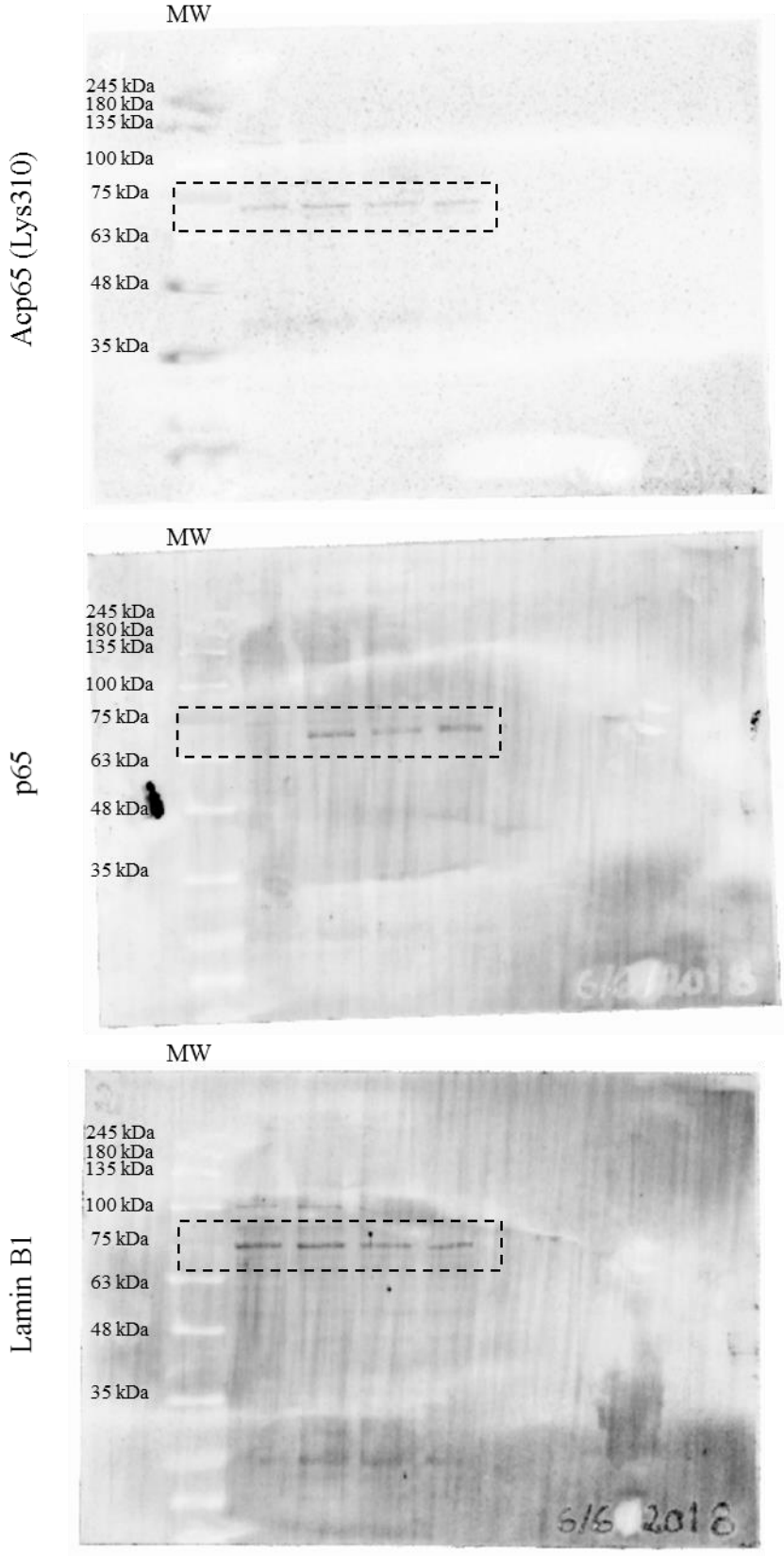

Uncropped blots shown in **Figure 8**

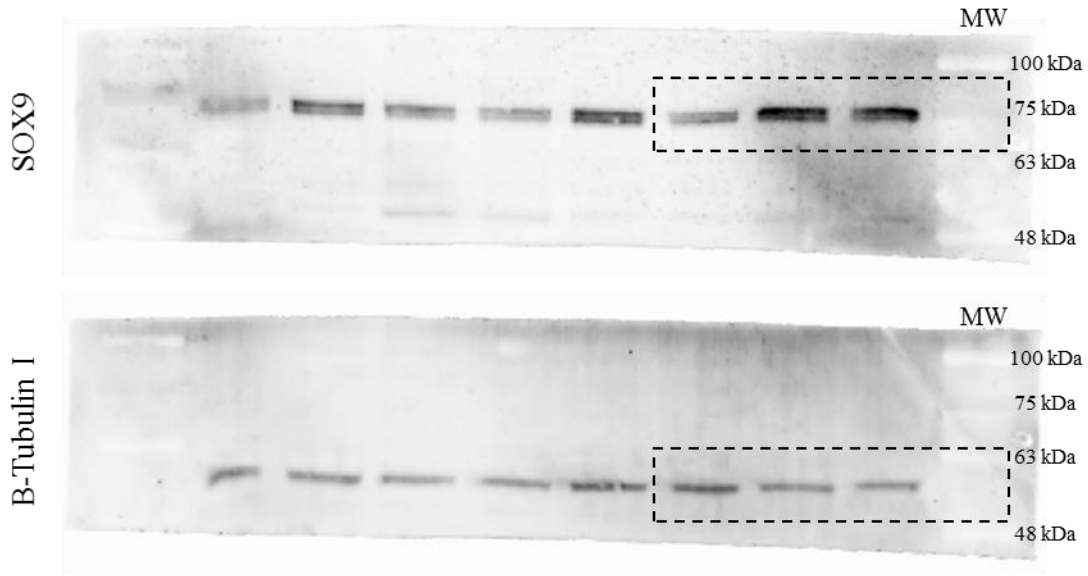

The membrane was cut between 135-100 kDa and 48 kDa. The upper and lower portions of the membrane were probed with different antibodies for unrelated proteins.

Figure S3. Uncropped images of the blots shown in figures 1-3 and 5-8. The portions of the membranes shown in each of those figures are surrounded by a dashed line box.

Chapter 4: JNK1 inhibition underlies the anti-inflammatory activity of (R)-(-)-carvone

Cátia Sousa, Bruno Miguel Neves, Fernando Judas, Alcino Jorge Leitão, Alexandrina Ferreira Mendes

Manuscript submitted for publication

Note: The results presented in this chapter are formatted according to the style of the journal where the paper was submitted, with minor modifications

Graphical Abstract

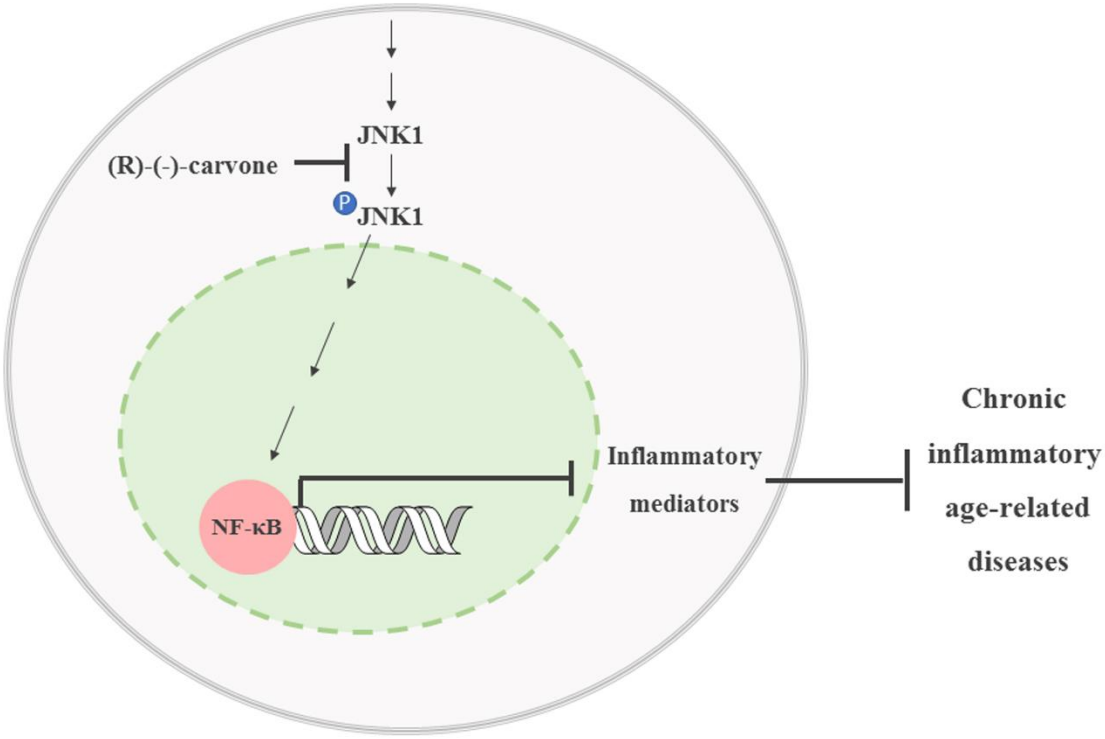

Highlights

- (R)-(-)-carvone decreases LPS-induced JNK1 phosphorylation
- (R)-(-)-carvone does not interfere with the canonical NF-κB activation pathway
- (R)-(-)-carvone inhibits NF-κB-dependent gene expression
- (R)-(-)-carvone does not affect SIRT1

Abstract

Our previous work identified two enantiomeric monoterpenes belonging to the limonene synthase pathway, (S)-(+)- and (R)-(-)-carvone, with promising anti-inflammatory activity. Despite being enantiomers, these two compounds showed differences in potency that suggest potentially distinct mechanisms of action. Thus, the purpose of this work was to explore the molecular mechanisms responsible for the anti-inflammatory activity of (R)-(-)-carvone, in particular its ability to inhibit the signaling pathways involving the Mitogen-Activated Protein Kinases (MAPKs) and the transcription factor, Nuclear Factor kappa-light-chain-enhancer of activated B Cells (NF-κB). (R)-(-)-carvone significantly decreased the phosphorylation levels of the MAPK, JNK1, induced by bacterial lipopolysaccharide (LPS) in the murine macrophage cell line, Raw264.7, while it did not interfere with the canonical NF-κB activation pathway, namely phosphorylation and degradation of its inhibitor, IκB-α, phosphorylation of its major component, p65, at serine 536 and nuclear translocation of its complexes. Nonetheless, (R)-(-)-carvone significantly inhibited IκB-α resynthesis induced by LPS, suggesting that it interferes with NF-κB transcriptional activity, even though it doesn't seem to affect its activation. Moreover, (R)-(-)-carvone also showed a tendency to decrease the levels of acetylated NF-κB/p65 in the nucleus, but the difference relative to cells treated with LPS alone did not reach statistical significance. Corroborating these results, (R)-(-)-carvone also did not affect the activity and protein levels of sirtuin-1, the major NF-κB/p65 deacetylating enzyme. Taken together, these results show that the anti-inflammatory activity of (R)-(-)-carvone probably involves inhibition of JNK1. Since JNK1 is involved in the regulation of NF-κB transcriptional activity by activating enzymes that contribute to its acetylation, inhibition of that enzyme by (R)-(-)-carvone is likely to negatively modulate NF-κB activity without interfering with its canonical activation pathway. Further studies are required to evaluate the ability of (R)-(-)-carvone to modulate other mechanisms required for full NF-κB transcriptional activity. This study highlights the diversity of molecular mechanisms that can be involved in the anti-inflammatory activity of natural compounds, particularly of monoterpenes, and identifies (R)-(-)-carvone as the prototype of a new class of anti-inflammatory compounds capable of modulating JNK1 and NF-κB activity without interfering with its canonical activation pathway.

Keywords: (R)-(-)-carvone; inflammation; aging; NF-κB; MAPKs

4.1 Introduction

Natural products are an enriched source of compounds with a variety of pharmacological activities. Anti-inflammatory activity is among the most studied and reported for natural products and their components (Azab, Nassar et al. 2016). Monoterpenes are a well-known class of natural compounds with anti-inflammatory activity (de Cassia da Silveira e Sa, Andrade et al. 2013). The anti-inflammatory properties of most of these compounds result from the inhibition of one or both of two critical signalling pathways that orchestrate the inflammatory response and include members of the Mitogen-Activated Protein Kinase (MAPK) family and the transcription factor, Nuclear Factor kappa-light-chain-enhancer of activated B Cells (NF-κB) (Rufino, Ribeiro et al. 2014, Rufino, Ribeiro et al. 2015, Chen, Deng et al. 2018). Nonetheless, significant differences have been reported, with distinct compounds presenting different abilities to inhibit each one of those signalling pathways, even in the same cell type (Rufino, Ribeiro et al. 2014, Rufino, Ferreira et al. 2015).

In our previous work, we performed a standardized screening of the anti-inflammatory activity of selected monoterpene compounds that identified nine compounds with anti-inflammatory activity and allowed the recognition of structure-activity relationships. Among the active compounds, (S)-(+)-carvone and (R)-(-)-carvone were the most potent, inhibiting the expression of pro-inflammatory mediators [e.g. inducible nitric oxide synthase (NOS2) and interleukin-1β (IL-1β)] induced by lipopolysaccharides (LPS) in murine macrophages (Sousa, Leitão et al. 2020). Nonetheless, the two enantiomers showed distinct potencies which prompted us to further investigate their molecular mechanism of action. Thus, the purpose of this study is to explore the molecular mechanism involved in the anti-inflammatory activity of (R)-(-)-carvone. Considering the importance of the MAPKs and NF-κB in orchestrating the inflammatory response by inducing inflammatory gene and protein expression, we evaluated the ability of (R)-(-)-carvone to modulate these signaling pathways.

4.2 Material and methods

4.2.1 Cell culture and treatments

The mouse macrophage cell line, Raw 264.7 (ATCC No. TIB-71), was cultured in DMEM supplemented with 10% non-heat inactivated fetal bovine serum, 100 U/mL penicillin and 100 µg/mL streptomycin. Raw 264.7 cells were plated at a density of $3x10^5$ cells/mL and left to stabilize for up to 24 h.

For cell treatments, (R)-(-)-carvone (#124931, purity 98%, Sigma-Aldrich Co., St Louis, MO, USA), resveratrol (Res; Extrasynthese, Genay Cedex,France), Bay 11-7082 (Calbiochem, San Diego, CA, USA) and MG-132 (Z-Leu-Leu-Leu-CHO, Boston Biochem, Cambridge, MA, USA) were dissolved in dimethyl sulfoxide (DMSO; Sigma-Aldrich Co). LPS from Escherichia coli 026:B6 (Sigma-Aldrich Co.) were dissolved in phosphate buffered saline (PBS). DMSO was used as vehicle and added to control and LPS-treated cell cultures, so that its final concentration did not exceed 0.1% (v/v). The chemicals used or the vehicle were added to macrophage cell cultures 1 h before the pro-inflammatory stimulus, 1 µg/mL LPS, and maintained for the rest of the experimental period. The concentrations of each chemical and the experimental treatment periods are indicated in figures and/or figure legends.

4.2.2 Preparation of cell extracts

Preparation of total cell extracts was performed as described previously (Sousa, Leitão et al. 2020).

Nuclear Extract Kit (Active Motif, La Hulpe, Belgium) was used for the preparation of cytoplasmic and nuclear extracts, following the manufacturer's instructions.

Protein concentration in the extracts was determined with the bicinchoninic acid kit (Sigma-Aldrich Co.).

4.2.3 Western Blotting

Western Blot was performed as described previously (Sousa, Ribeiro et al. 2017). Briefly, total (25 µg), cytoplasmic (25 µg) or nuclear (30 µg) proteins were separated by SDS-PAGE under reducing conditions and electrotransferred onto PVDF membranes which were probed overnight at 4ºC or for 2 h at room temperature with the primary antibodies listed in Table 1 and then with anti-rabbit or anti-mouse alkaline phosphatase-conjugated secondary

antibodies (dilution 1:20000; GE Healthcare, Chalfont St. Giles, UK). Mouse monoclonal anti-β-Tubulin I and rabbit polyclonal anti-Lamin B1 were used as a loading controls of total and cytoplasmic extracts and of nuclear extracts, respectively. Immune complexes were detected with Enhanced ChemiFluorescence reagent (GE Healthcare) in the imaging system Thyphoon^{TM} FLA 9000 (GE Healthcare). Image analysis was performed with TotalLab TL120 software (Nonlinear Dynamics Ltd).

Table 1: List of primary antibodies used in Western Blot

Protein	Source	Clonality	Dilution	Supplier	Reference number
IκB-α	rabbit	polyclonal	1:1000	Cell Signaling Technology, Inc., Danvers, MA, USA	#9242
phospho-p44/42 MAPK (ERK1/2) (Thr202/Tyr204)	rabbit	polyclonal	1:1000	Cell Signaling Technology, Inc.	#9101
p44/42 MAPK (ERK1/2)	rabbit	polyclonal	1:1000	Cell Signaling Technology, Inc.	#9102
phospho-p38 MAPK (Thr180/Tyr182)	rabbit	polyclonal	1:1000	Cell Signaling Technology, Inc.	#9211
p38 MAPK	rabbit	polyclonal	1:1000	Cell Signaling Technology, Inc.	#9212
SAPK/JNK	rabbit	polyclonal	1:1000	Cell Signaling Technology, Inc.	#9252
acetyl-NF-κB p65 (Lys310)	rabbit	polyclonal	1:750	Cell Signaling Technology, Inc.	#3045
Sirtuin-1	rabbit	polyclonal	1:1000	Sigma-Aldrich Co.	07-131
Lamin B1	rabbit	polyclonal	1:1000	Abcam, Cambridge, UK	ab16048
phospho-SAPK/JNK (Thr183/Tyr185)	rabbit	monoclonal	1:1000	Cell Signaling Technology, Inc.	#4668

NF-κB p65 (D14E12) XP®	rabbit	monoclonal	1:1000	Cell Signaling Technology, Inc.	#8242
phospho-NF-κB p65 (Ser536)	rabbit	monoclonal	1:1000	Cell Signaling Technology, Inc.	#3033
phospho-IκB-α (Ser32/36)	mouse	monoclonal	1:1000	Cell Signaling Technology, Inc.	#9246
β-Tubulin I	mouse	monoclonal	1:20000	Sigma-Aldrich Co.	T7816

4.2.4 Immunocytochemistry

To evaluate NF-κB/p65 nuclear translocation, immunocytochemistry was performed. Macrophages seeded onto 1 µ-Slide 8 Well ibiTreat (Ibidi, Martinsried, Germany) and treated as indicated in figure legends. At the end of the treatment period, cells were washed with ice-cold PBS pH=7.4 and, then, fixed in 4% paraformaldehyde at room temperature, for 15 min. After fixing, cells were washed three times with PBS pH=7,4 with 0.1 M glycine for 5 min each and blocked with 5% Goat Serum, 0.3% Triton in PBS, pH=7.4 for 1 h at room temperature. Then, the slides were incubated with a rabbit monoclonal anti-NF-κB p65 (D14E12) XP® antibody (dilution 1:400; #8242S, Cell Signaling Technology, Inc.) in 1% Bovine Serum Albumin (BSA) in PBS (pH=7.4) overnight at 4ºC and then incubated with anti-rabbit IgG (H+L) CF™488A (dilution 1:400; Biothium, Inc., Fremont, CA, USA) and Alexa Fluor ™ 555 Phalloidin (dilution 1:1000; Molecular Probes, Invitrogen, Eugene, OR) to stain the cytoskeleton (especially F-actin) and enhance visualization of the cytoplasm (Wulf, Deboben et al. 1979). The cells were counterstained with DAPI (0.2 ng/mL; Molecular Probes, Invitrogen, Eugene, OR) to stain the nuclei. Specificity was confirmed in negative controls set up by omitting the primary antibody. Fluorescence images were obtained in an Axio Observer ZI fluorescence microscope (Carl Zeiss, Germany).

4.2.5 SIRT1 activity assay

Interaction of (R)-(-)-carvone with human SIRT1 enzyme was evaluated using the SIRT1 Direct Florescent Screening Assay Kit (Cayman Chemical Company, Ann Arbor, MI, USA) following the manufacturer's instructions. Results are presented as mean of fluorescence intensity (arbitrary units) ± SEM.

4.2.6 Statistical Analysis

Results are presented as means ± SEM. Statistical analysis was performed using GraphPad Prism version 6.0 (GraphPad Software, San Diego, CA, USA). Statistical analysis was performed by using the t-test to compare each condition with its respective control and one-way ANOVA with the Dunnett post-test for comparison of all conditions to a control group, except in Fig.5B where one-way ANOVA with the Tuckey post-test for multiple comparisons was used. Results were considered statistically significant at $p< 0.05$.

4.3 Results

4.3.1 (R)-(-)-carvone inhibits LPS-induced phosphorylation of JNK1, but not of p38 and ERK1/2

Upon binding to its receptor, the Toll-Like Receptor 4 (TLR4), LPS triggers the activation of all MAPK family members, namely Extracellular signal-Regulated Kinase (ERK)1/2, p38 and c-Jun N terminal Kinase (JNK), by inducing their phosphorylation on specific serine/threonine residues (Arthur and Ley 2013). Treatment with LPS for 5 min was sufficient to significantly increase p38 and JNK phosphorylation in comparison to control cells, while ERK1/2 phosphorylation was maximal after 1 h (data not shown). Using these time points, pre-treatment with (R)-(-)-carvone did not significantly affect LPS-induced p38 (Fig.1A) and ERK1/2 (Fig.1B) phosphorylation. On the opposite, (R)-(-)-carvone significantly decreased LPS-induced phosphorylation of JNK1 (Fig.1C), while the other two isoforms, JNK2 and 3, were not significantly affected (Fig.1C). Taken together, these results suggest that only inhibition of JNK1 by (R)-(-)-carvone can contribute to its anti-inflammatory activity.

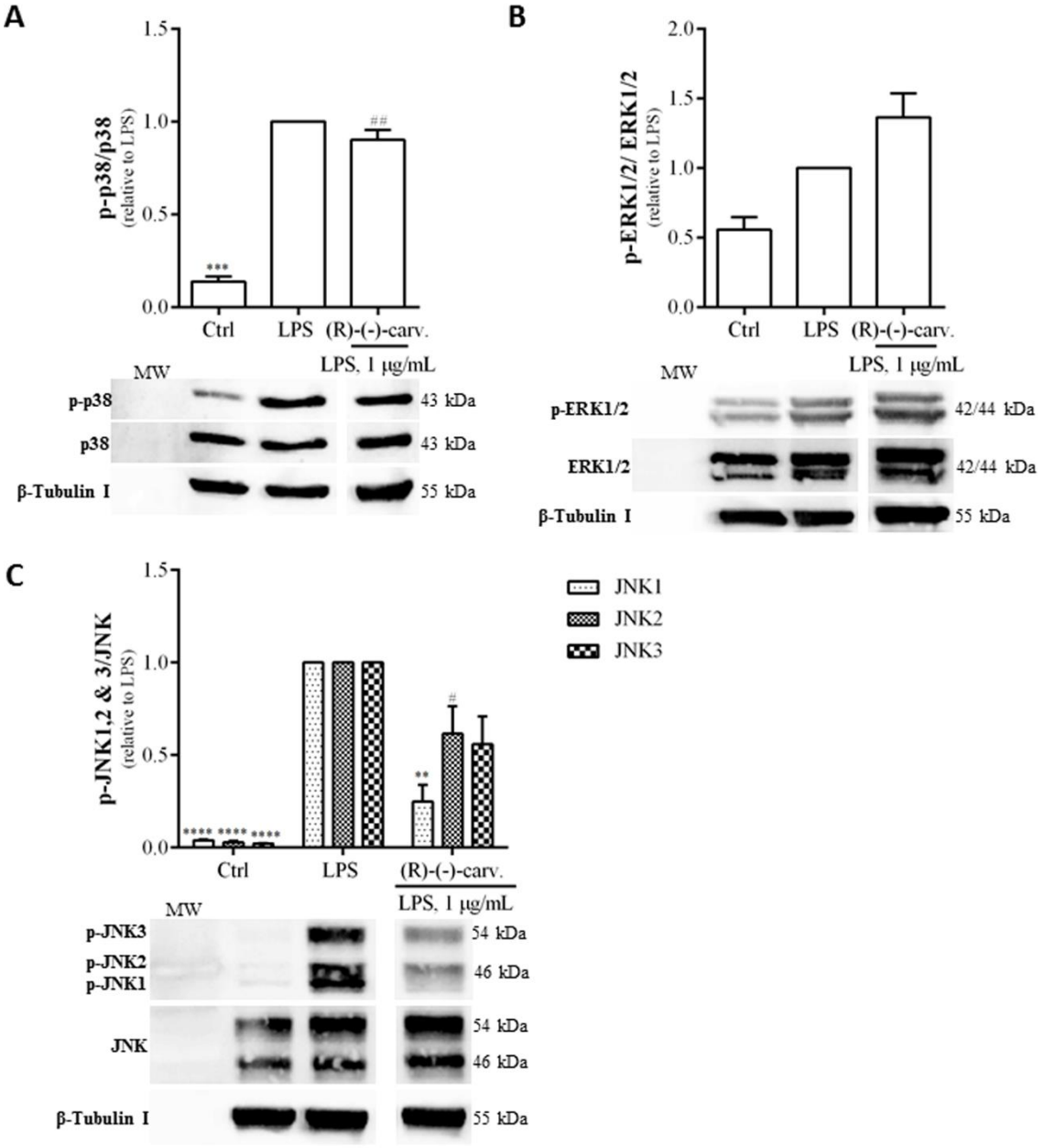

Figure 1. Effect of (R)-(-)-carvone on p38 (A), ERK1/2 (B) and JNK (C) phosphorylation induced by LPS in Raw 264.7 cells. Macrophage cultures were pre-treated with 666 µM of (R)-(-)-carvone or with the vehicle (0.1% DMSO) for 1 h and then with 1 µg/mL LPS for 5 min (**A** and **C)** or 1 h (**B**). Control cells (Ctrl) were treated with the vehicle (0.1% DMSO) in the absence of LPS. Each column represents the mean ± SEM of four (**A** and **C**) or three (**B**) independent experiments. Representative images are shown. **p<0.001, ***p<0.001 and ****p<0.0001 relative to LPS-treated cells. $^{\#}p$<0.05 and $^{\#\#}p$<0.01 relative to the Ctrl. MW: molecular weight marker.

4.3.2 (R)-(-)-carvone does not interfere with the NF-κB canonical pathway activation and nuclear translocation

In the NF-κB canonical pathway, recognition of a stimulatory ligand (e.g. LPS) by its receptor (e.g. TLR4) triggers a signaling cascade targeting IκB kinase complex (IKK), in particular its catalytic subunit, IKKβ (Mulero, Huxford et al. 2019). Once activated, IKKβ phosphorylates IκBα, the natural inhibitor of NF-κB, at serine (Ser) 32 and 36, which triggers its ubiquitination and subsequent proteasomal degradation (Mulero, Huxford et al. 2019). Thus, NF-κB dimers, typically composed of p65 and p50 proteins, are freed and translocate to the nucleus (Mulero, Huxford et al. 2019). Since phosphorylation and degradation of IκBα are key steps in the canonical signaling pathway for NF-κB activation, the effect of (R)-(-)-carvone on these processes was evaluated. As expected, LPS induced IκBa phosphorylation (Fig. 2A) and, consequently, its degradation (Fig. 2B) in comparison to control cells. However, (R)-(-)-carvone did not interfere with any of these steps (Fig. 2A and B). Bay 11-7082, a selective IKK inhibitor, and MG-132, a synthetic proteasome inhibitor peptide, were used as pharmacological controls. Despite not being statistically significant, Bay 11-7082 showed a tendency to decrease LPS-induced IκBα phosphorylation (Fig. 2A) and degradation (Fig. 2B) while MG-132 increased the levels of phosphorylated and total IκBa protein (Fig. 2B), consistent with the inhibition of its proteasomal degradation (Fig. 2A). Thus, LPS effectively activated the canonical NF-κB activation pathway which was not affected by pre-treatment with (R)-(-)-carvone.

Besides release from complexes with IκB-α, NF-κB activation requires the NF-κB/p65 subunit to undergo various post-translation modifications (PTM) for full transcriptional activity (Mitchell and Carmody 2018). Phosphorylation of NF-κB/p65 on the Ser536 residue by IKKβ is one of those PTM and is considered a marker of the canonical NF-κB activation pathway (Sakurai, Chiba et al. 1999, Yang, Tang et al. 2003, Huang, Yang et al. 2010). Thus, the ability of (R)-(-)-carvone to affect NF-κB/p65 phosphorylation at Ser536 was evaluated. Figure 2C shows that LPS significantly induced NF-κB/p65 phosphorylation at Ser536, relative to control cells, but the test compound had no effect (Fig.2C).

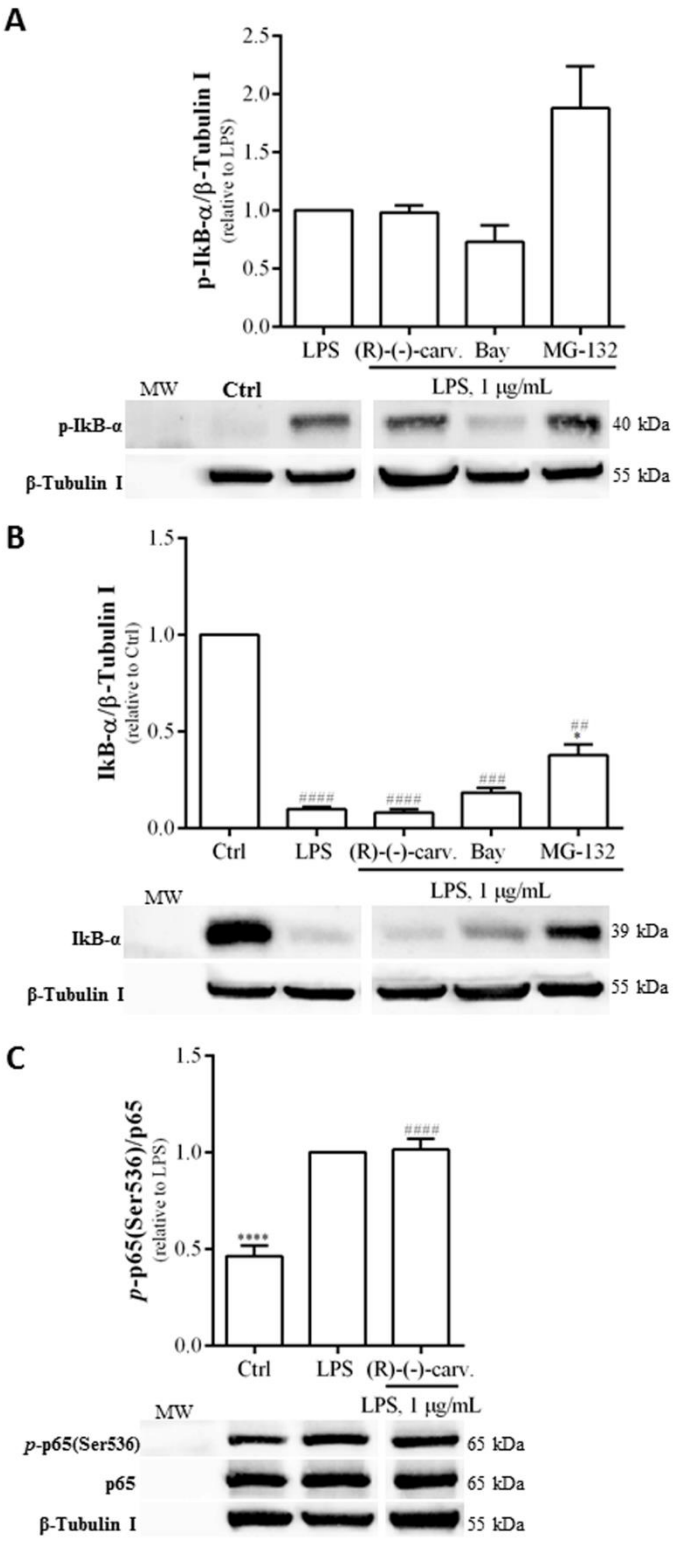

Figure 2. (R)-(-)-carvone does not affect the NF-κB activation pathway, namely, phosphorylation (A) and degradation (B) of IκB-α and NF-κB/p65 phosphorylation at Ser536 (C). Macrophage cultures were pre-treated with the vehicle (0.1% DMSO, Ctrl), 666 μM (R)-(-)-carvone, the selective IKK inhibitor, Bay 11-

7082 (5 μM), or the proteasome inhibitor, MG-132 (10 μM) for 1 h, following treatment with 1 μg/mL LPS for 5 min (**A**) or 15 min (**B** and **C**). Each column represents the mean ± SEM of five (**A**) or four (**B** and **C**) independent experiments. Representative images are shown. **p*<0.05 and *****p*<0.0001 relative to LPS-treated cells. $^{\#\#}p$<0.01, $^{\#\#\#}p$<0.001 and $^{\#\#\#\#}p$<0.0001 relative to the Ctrl. MW: molecular weight marker.

Since (R)-(-)-carvone was found to not interfere with activation of the canonical NF-κB signalling pathway, we hypothesized that it could interfere with the nuclear translocation of the NF-κB dimers. To detect NF-κB translocation to the nucleus, an immunocytochemistry assay for NF-κB/p65 was performed. Figure 3 shows that NF-κB/p65 is clearly present in the cytoplasm in vehicle-treated control cells, while after treatment with LPS for 20 min, immunoreactivity is exclusively located in the nucleus (Fig. 3). Pre-treatment with (R)-(-)-carvone is unable to interfere with LPS-induced NF-κB/p65 nuclear translocation as immunoreactivity is still localized to the nucleus (Fig. 3). Pre-treatment with MG-132, however, completely abrogated NF-κB/p65 nuclear translocation, as immunoreactivity is only visible in the cytoplasm.

Further confirming these results, western blot analyses show that LPS decreased the cytoplasmic (Fig. S1A) and increased the nuclear (Fig. S1B) levels of NF-κB/p65.

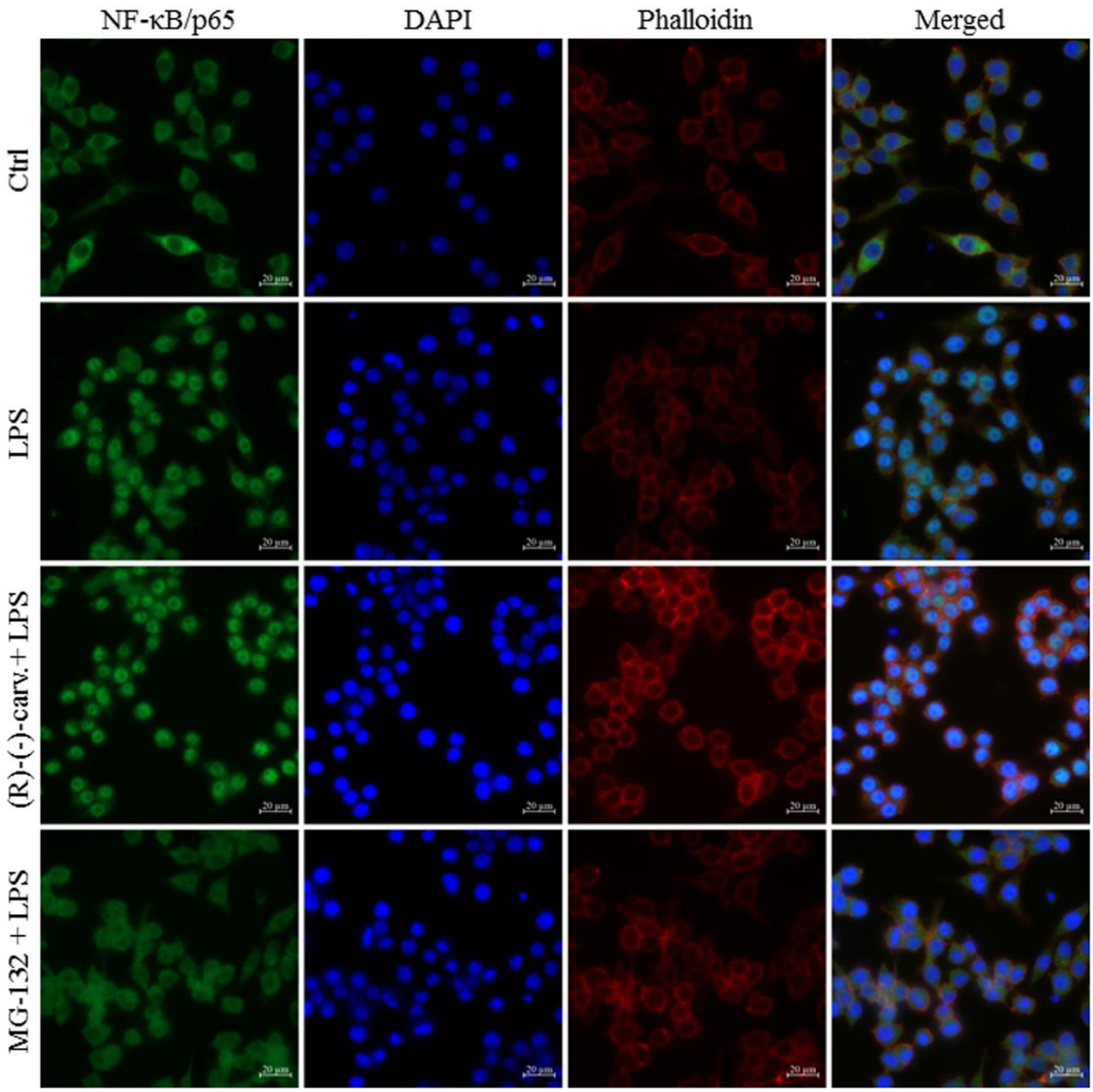

Figure 3. NF-κB/p65 nuclear translocation is not inhibited by (R)-(-)-carvone. Macrophages were pre-treated with the vehicle (0.1% DMSO), 666 µM (R)-(-)-carvone or 10 µM MG-132 for 1 h and, then, treated with 1 µg/mL LPS for 20 min. Control cells (Ctrl) were treated with the vehicle (0.1% DMSO) in the absence of LPS. Immunofluorescence staining of NF-κB/p65 (green) and fluorescence staining of the cytoskeleton (red) and the nuclei (blue) were performed as described in Materials and methods**.** Scale bar: 20 µm. Representative images of each condition are shown.

4.3.3 (R)-(-)-carvone inhibits IκB-α resynthesis

Our previous results demonstrated that (R)-(-)-carvone decreased the expression of two NF-κB target genes, NOS2 and IL-1β (Sousa, Leitão et al. 2020). However, the results above showed that this compound did not interfere with the canonical NF-κB activation pathway, nor with its nuclear translocation. Thus, to further confirm that (R)-(-)-carvone does inhibit the transcriptional activity of NF-κB, the expression of another NF-κB-dependent gene, IκB-α, (Cheng, Ryseck et al. 1998) was evaluated. For this, we first performed time course experiments to determine the time point after addition of the inflammatory stimulus, at which IκB-α protein levels start to increase after having been degraded. IκBα resynthesis began to be detectable 20 min after addition of LPS to macrophage cultures, reaching the maximum at 60 min (data not shown). Thus, the effect of (R)-(-)-carvone on IκB-α expression was assessed 60 min after addition of LPS. Figure 4 shows that pre-treatment of macrophage cultures with (R)-(-)-carvone significantly reduced the increase in protein levels of IκBα induced by LPS. This result further confirms that (R)-(-)-carvone interferes with NF-κB transcriptional activity.

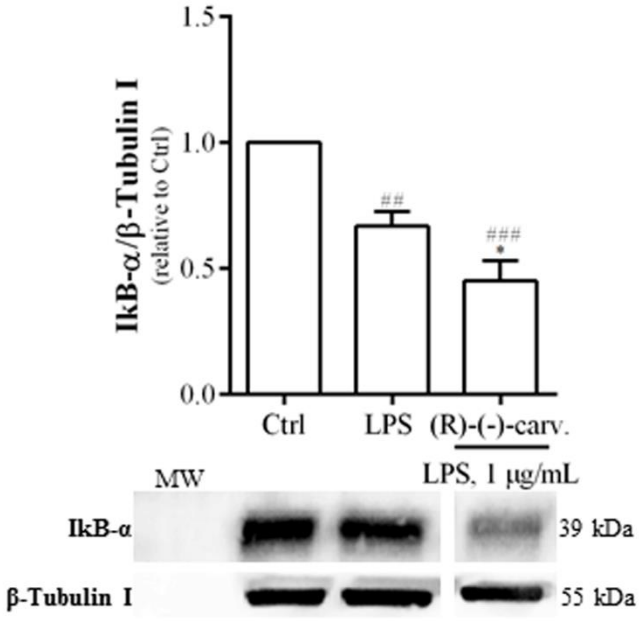

Figure 4. LPS-induced IκB-α resynthesis is inhibited by (R)-(-)-carvone. Cell cultures were pre-treated with the vehicle (0.1% DMSO) or 666 µM (R)-(-)-carvone for 1 h, followed by stimulation with 1 µg/mL LPS for 1 h. Control cells (Ctrl) were treated with the vehicle (0.1% DMSO) in the absence of LPS. Each column represents the mean ± SEM of seven independent experiments. Representative images are shown. $*p<0.05$ relative to LPS-treated cells. $^{\#\#}p<0.01$ and $^{\#\#\#}p<0.001$ relative to the Ctrl. MW: molecular weight marker.

4.3.4 (R)-(-)-carvone decreases LPS-induced acetylation of NF-κB/p65 at Lys310 independently of SIRT1 activity and expression

The results presented above show that despite not interfering with the canonical NF-κB activation pathway and its nuclear translocation, (R)-(-)-carvone negatively affects its transcriptional activity. Thus, we hypothesized that the underlying mechanism may involve inhibition of activating PTM of the NF-κB/p65 subunit. Among these PTM, acetylation of lysine (Lys) 310 on NF-κB/p65 is especially relevant, being required for full transcriptional activity of NF-κB, without affecting its DNA binding and IκBα assembly (Chen, Mu et al. 2002). Therefore, we hypothesized that (R)-(-)-carvone may interfere with NF-κB/p65 acetylation at Lys310. Figure 5A shows that treatment with LPS increased the levels of NF-κB/p65 acetylated at Lys310, which tended to decrease by pre-treatment with either (R)-(-)-carvone or Res used as a positive pharmacological control of NF-κB/p65 deacetylation (Yeung, Hoberg et al. 2004). Nonetheless, the differences are not statistically significant with either compound, perhaps because the increase in acetylated NF-κB/p65 levels induced by LPS is small.

Changes in the levels of acetylated NF-κB/p65 can be caused by either activation of acetylating enzymes, namely p300, by inducing stimuli like LPS or by activation of deacetylase enzymes. Among these, Sirtuin 1 (SIRT1), a NAD^+-dependent class III Histone DeAcetylase (HDAC), has been shown to physically interact with NF-κB/p65, specifically deacetylating its Lys310 residue, and, consequently, inhibiting the transcriptional activity of NF-κB (Yeung, Hoberg et al. 2004). Thus, we next evaluated the ability of (R)-(-)-carvone to modulate SIRT1 activity and expression. Figure 5B shows that (R)-(-)-carvone was unable to modify the activity of SIRT1 towards a specific acetylated substrate, while Res, used as a positive pharmacological control (Howitz, Bitterman et al. 2003), significantly increased fluorescence intensity relative to the basal enzyme activity (Fig.5B). Furthermore, (R)-(-)-carvone also did not affect SIRT1 protein levels when compared to cells treated with LPS alone (Fig.5C). Altogether, these results point out that induction of SIRT1expression and/or activity is unlike to be the mechanism responsible for the inhibitory effect of (R)-(-)-carvone on the transcriptional activity of NF-κB induced by LPS.

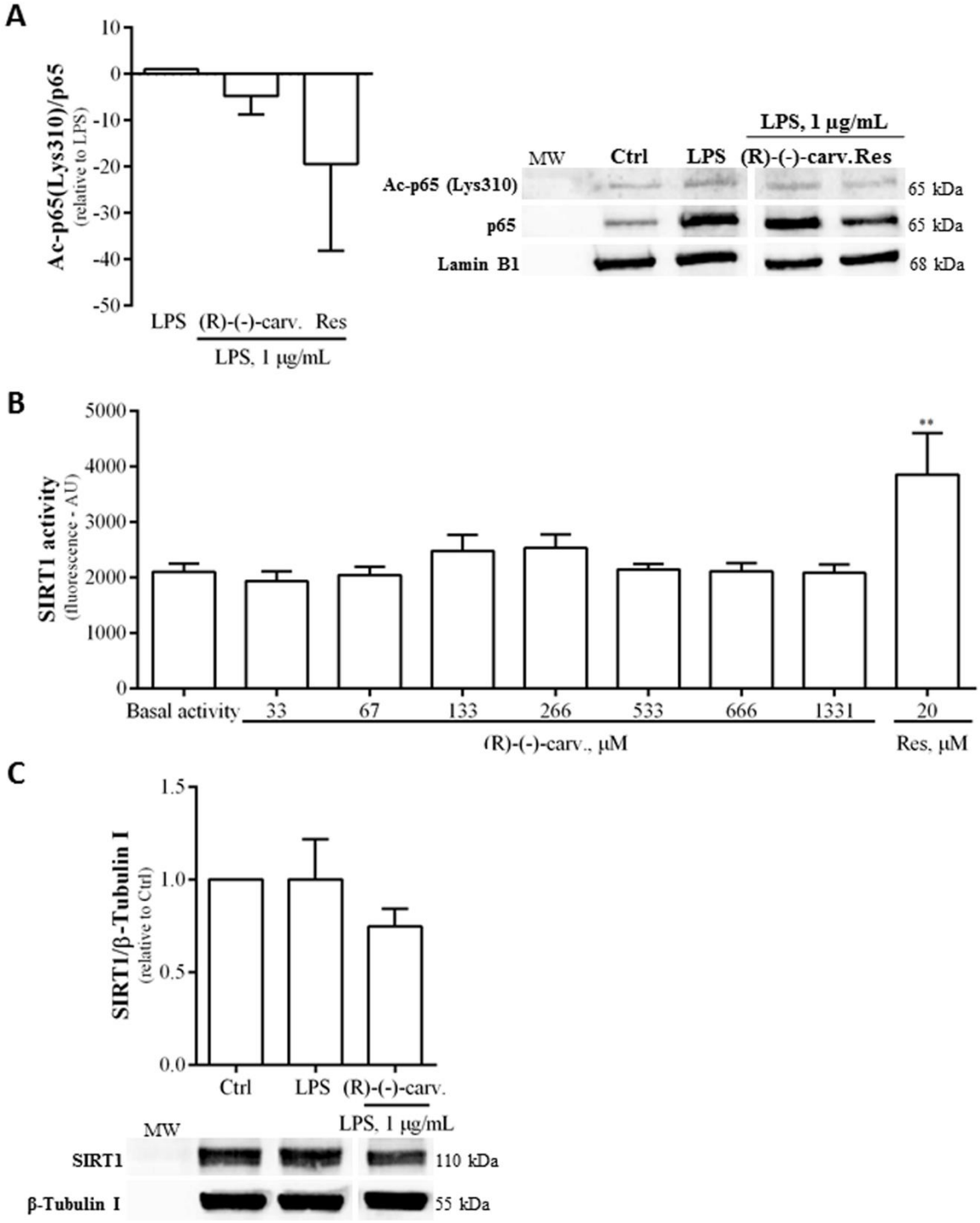

Figure 5. Effect of (R)-(-)-carvone on acetylated Lys310 NF-κB/p65 (Ac-p65) levels (A) and SIRT1 activity (B) and protein levels (C). In **A** and **C,** macrophages were pre-treated with vehicle (0.1% DMSO), 666 µM (R)-(-)-carvone or 5.5 µM Resveratrol (Res) for 1 h, following treatment with 1µg/mL LPS for 1 h. Control cells (Ctrl) were treated with the vehicle (0.1% DMSO) in the absence of LPS. (**B**) Different concentrations of (R)-(-)-carvone were directly incubated with human recombinant SIRT1 and a specific substrate, as described under Materials and methods. Res was used as a pharmacological control of SIRT1

activation. Each column represents the mean ± SEM of four (**A**), six to fifteen (**B**) and three (**C**) independent experiments. On panel A, the intensities, in arbitrary units, of the bands corresponding to Ac-p65 and total NF-κB/p65 in the control were subtracted from the intensities of the corresponding bands in each condition to allow calculation of the ratio of Ac-p65 to total NF-κB/p65 and subsequent normalization to LPS. Representative images are shown. ***p*<0.01 relative to SIRT1 basal activity. MW: molecular weight marker.

4.4 Discussion

The results presented demonstrate that (R)-(-)-carvone inhibits LPS-induced JNK1 phosphorylation, but does not affect other MAPK family members (Fig. 1), nor does it interfere with the canonical NF-κB activation pathway (Figs. 2 and 3), even though it effectively decreases its transcriptional activity [Fig. 4 and (Sousa, Leitão et al. 2020)].

JNK plays an important role in the inflammatory response, especially by phosphorylating c-Jun, which reduces its ubiquitination and subsequent degradation and increases its transcriptional activity, particularly as a component of the transcription factor, Activating Protein-1 (AP-1) (Hambleton, Weinstein et al. 1996, Meng and Xia 2011) which is associated to the induction of inflammatory genes, like *Nos2* (Spitsin, Koprowski et al. 1996, Martin and Wesche 2002). Moreover, c-Jun phosphorylation induced by IL-1 has been shown to be required for NF-κB/p65 recruitment to the *ccl2* gene which codes for C-C Motif Chemokine Ligand 2 (CCL2) or Monocyte Chemoattractant Protein-1 (MCP-1), a potent chemokine and inflammatory mediator (Wolter, Doerrie et al. 2008). Interestingly, this study also showed that JNK1/2-induced phosphorylation of c-Jun facilitates Histone DeAcetylase 3 (HDAC3) dissociation from that gene, while enhancing the recruitment of the acetylase, CBP/p300, and NF-κB, thus promoting *ccl2* transcription. CBP/p300 is a co-activator and histone/protein acetyltransferase essential for full NF-κB transcriptional activity by acetylating NF-κB/p65 on Lys310, without interfering with its DNA binding (Huang, Yang et al. 2010). Even though cell, stimulus and gene specificities can be involved, the ability of (R)-(-)-carvone to inhibit LPS-induced JNK1 activation is in line with that mechanism, whereby inhibition of c-Jun phosphorylation would impair NF-κB/p65 recruitment to target genes and acetylation by CBP/p300, thus inhibiting NF-κB-dependent gene expression. This mechanism may also explain the small effect of this compound on NF-κB/p65 acetylation on Lys310 (Fig. 5), since it affects HDAC3, but may not interfere with SIRT1 which has been reported to be essential to deacetylate NF-κB/p65 in response to many different stimuli in various cell types (Kauppinen, Suuronen et al. 2013), but whose expression and activity

are not affected by (R)-(-)-carvone (Fig. 5). Thus, inhibition of c-Jun phosphorylation may decrease NF-κB/p65 recruitment to target genes without significantly affecting its acetylation status. Further studies are required to confirm these mechanisms and that phosphorylated c-Jun plays the same role in modulating the expression of other NF-κB-dependent genes, like IκB-α (Fig. 4), NOS2 and IL-1β (Sousa, Leitão et al. 2020), in response to a different yet also pro-inflammatory stimulus, such as LPS.

4.5 Conclusion

To sum up, these results demonstrate that inhibition of JNK activation, in particular isoform 1, by (R)-(-)-carvone is likely the mechanism through which it decreases NF-κB transcriptional activity in LPS-treated macrophages. This is in agreement with a recent study that reported the ability of (R)-(-)-carvone to inhibit NF-κB transcriprional activity induced by TNF-α in human embryonic kidney cell line (Marques, Figueira et al. 2019).

Considering the role of the JNK and NF-κB pathways in chronic age-related inflammation, (R)-(-)-carvone shows potential to slow down age-related diseases and their consequences.

Funding Sources

This work was funded by the European Regional Development Fund (ERDF), through the Centro 2020 Regional Operational Program and through the COMPETE 2020 - Operational Program for Competitiveness and Internationalization and Portuguese national funds via FCT – Fundação para a Ciência e a Tecnologia, under projects POCI-01-0145-FEDER-028424 (CARTILFACTORY) and UID/NEU/04539/2019 and the PhD fellowship SFRH/79600/2011 to C. Sousa.

4.6 Supplementary material

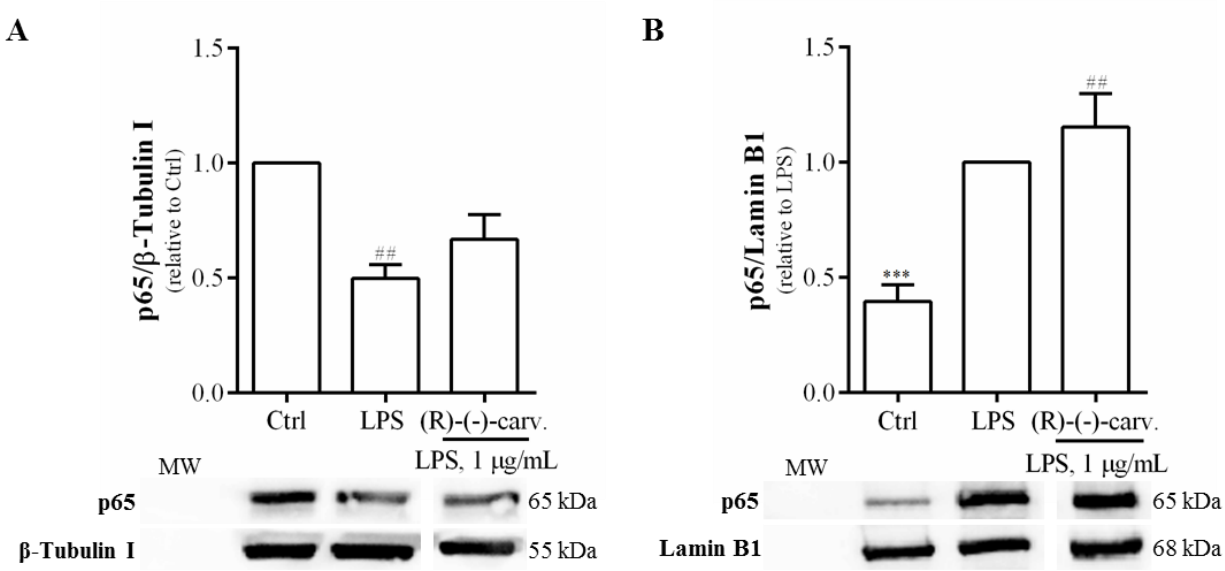

Figure S1. (R)-(-)-carvone does not inhibit NF-κB/p65 nuclear translocation in Raw 264.7 cells. Macrophages were pre-treated with the vehicle (0.1% DMSO) or 666 μM (R)-(-)-carvone for 1 h, following treatment with 1 μg/mL LPS for 1 h. Control cells (Ctrl) were treated with the vehicle in the absence of LPS. Cytoplasmic (**A**) and nuclear (**B**) levels of RelA/p65 were evaluated by western blot. Each column represents the mean ± SEM of four (**A**) or six (**B**) independent experiments. Representative images are shown. ***p<0.001 relative to LPS-treated cells. $^{\#\#}p$<0.01 relative to the Ctrl. MW: molecular weight marker

Uncropped blots shown in **Figure 1A**

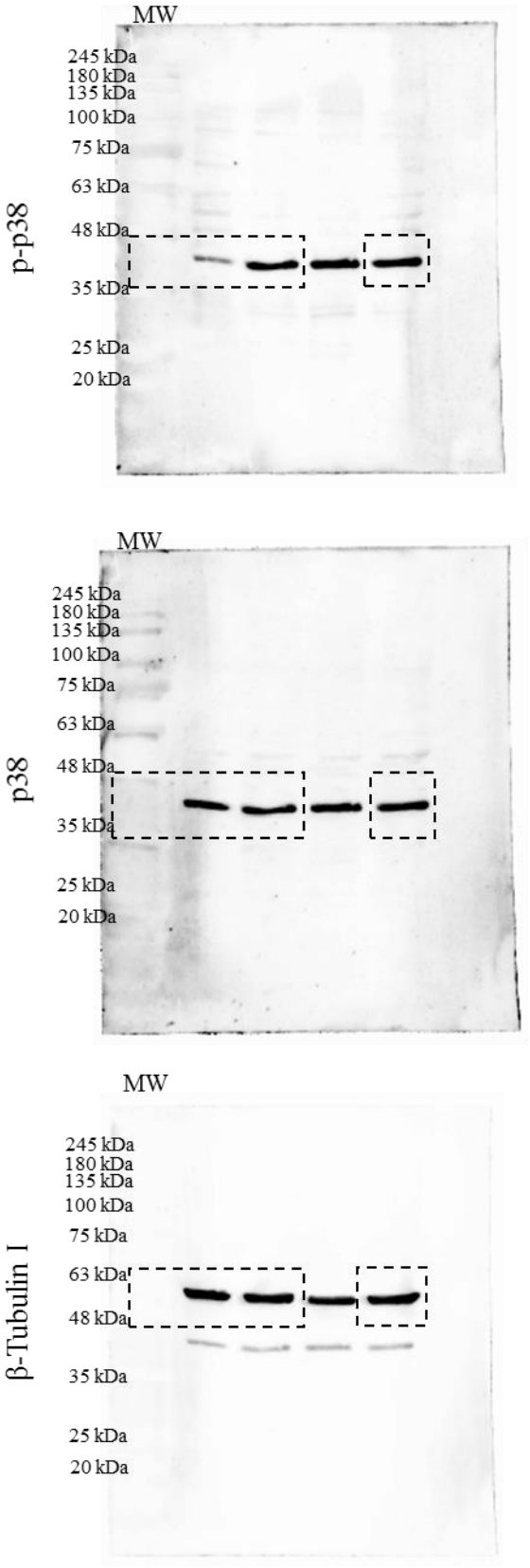

Uncropped blots shown in **Figure 1B**

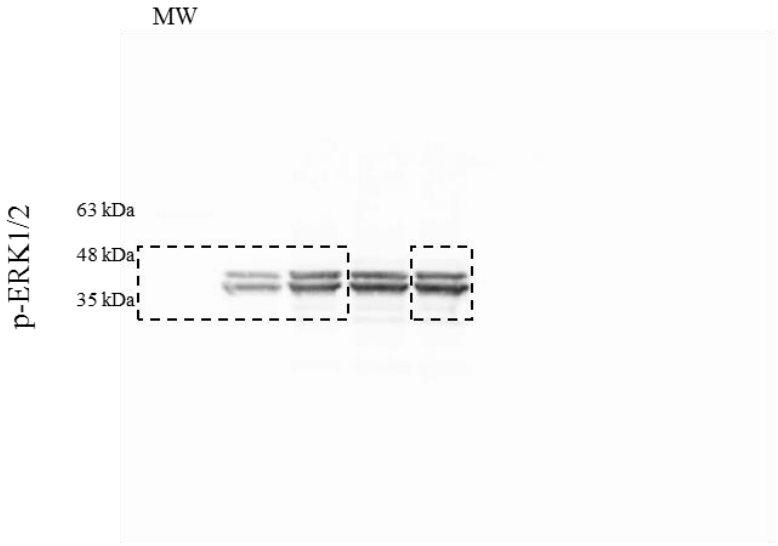

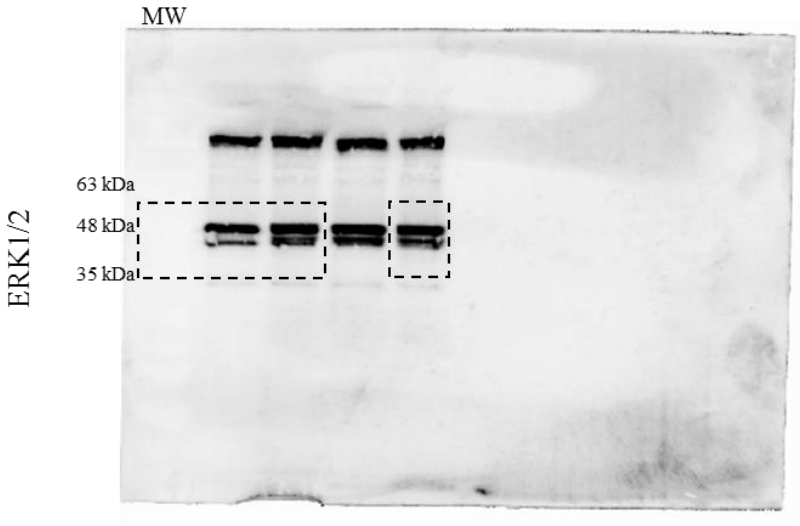

This membrane was also incubated with anti-SIRT1 antibody and the corresponding band appears near the 100 kDa molecular weight marker.

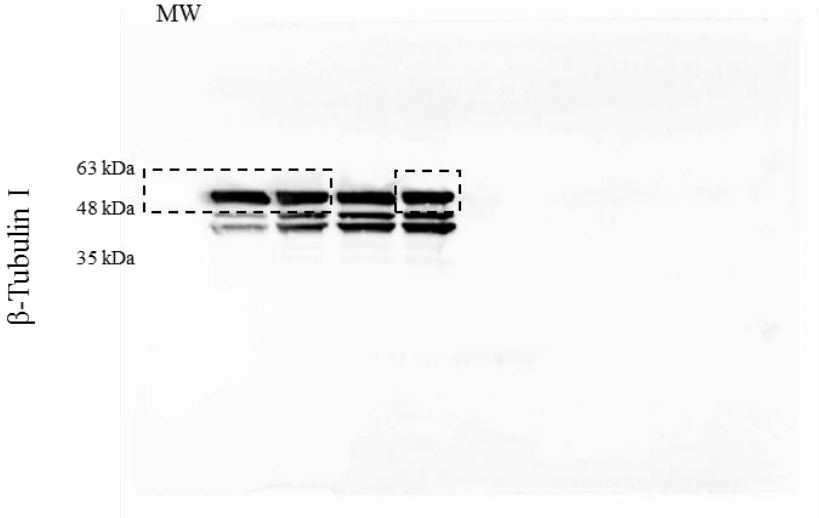

Uncropped blots shown in **Figure 1C**

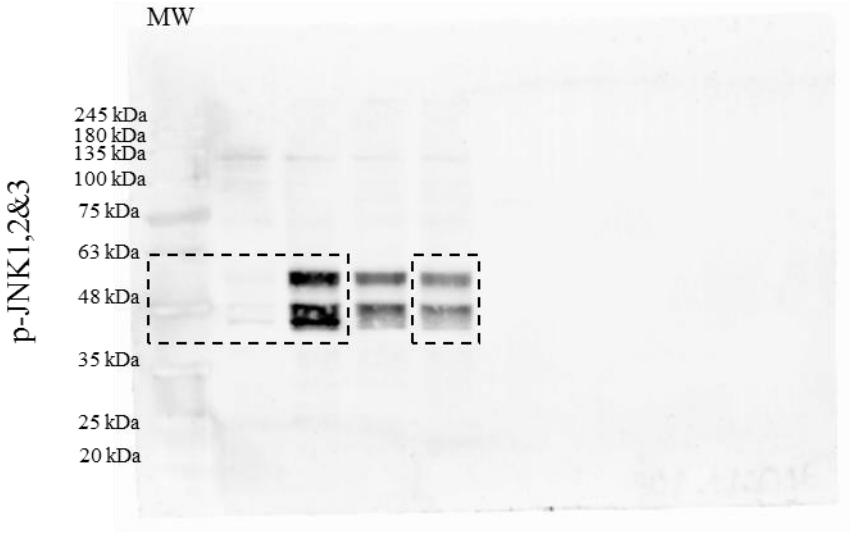

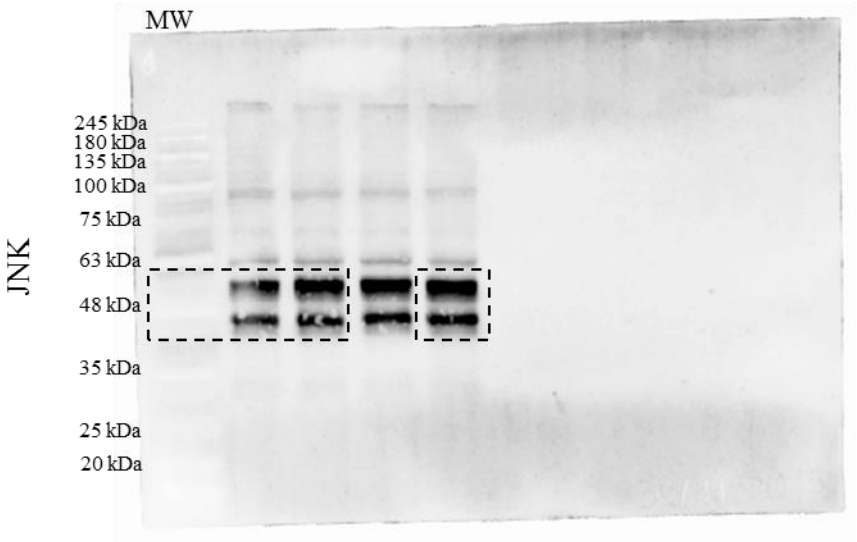

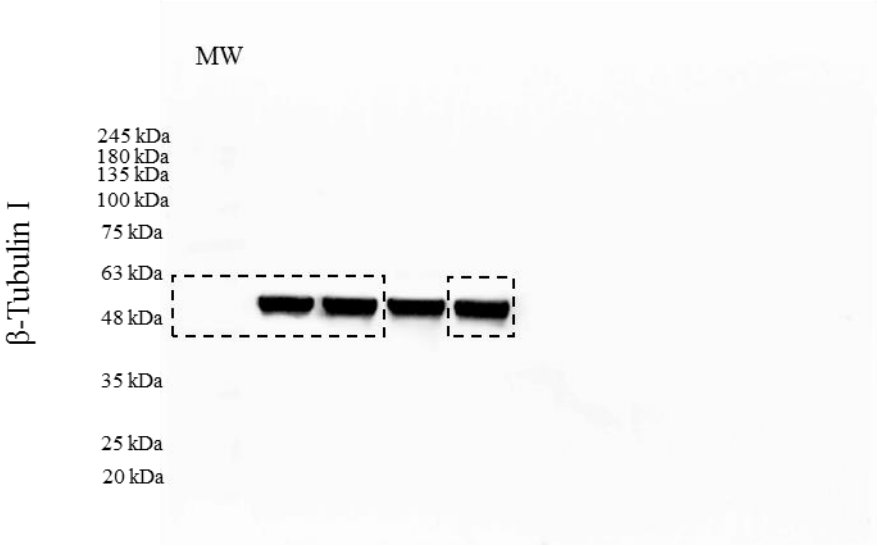

Uncropped blots shown in **Figure 2A**

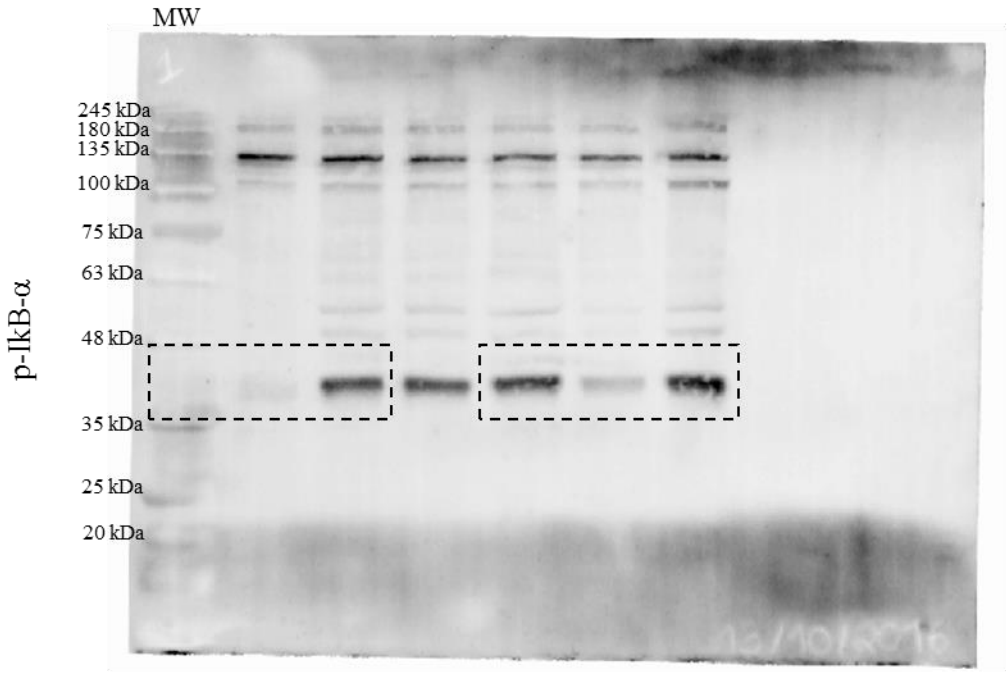

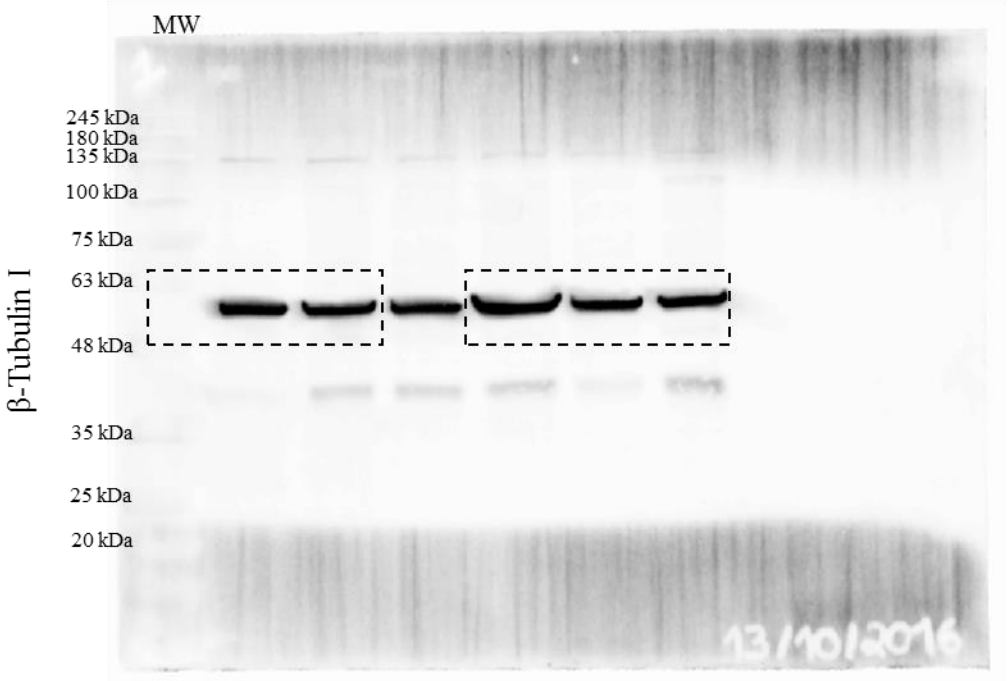

Uncropped blots shown in **Figure 2B**

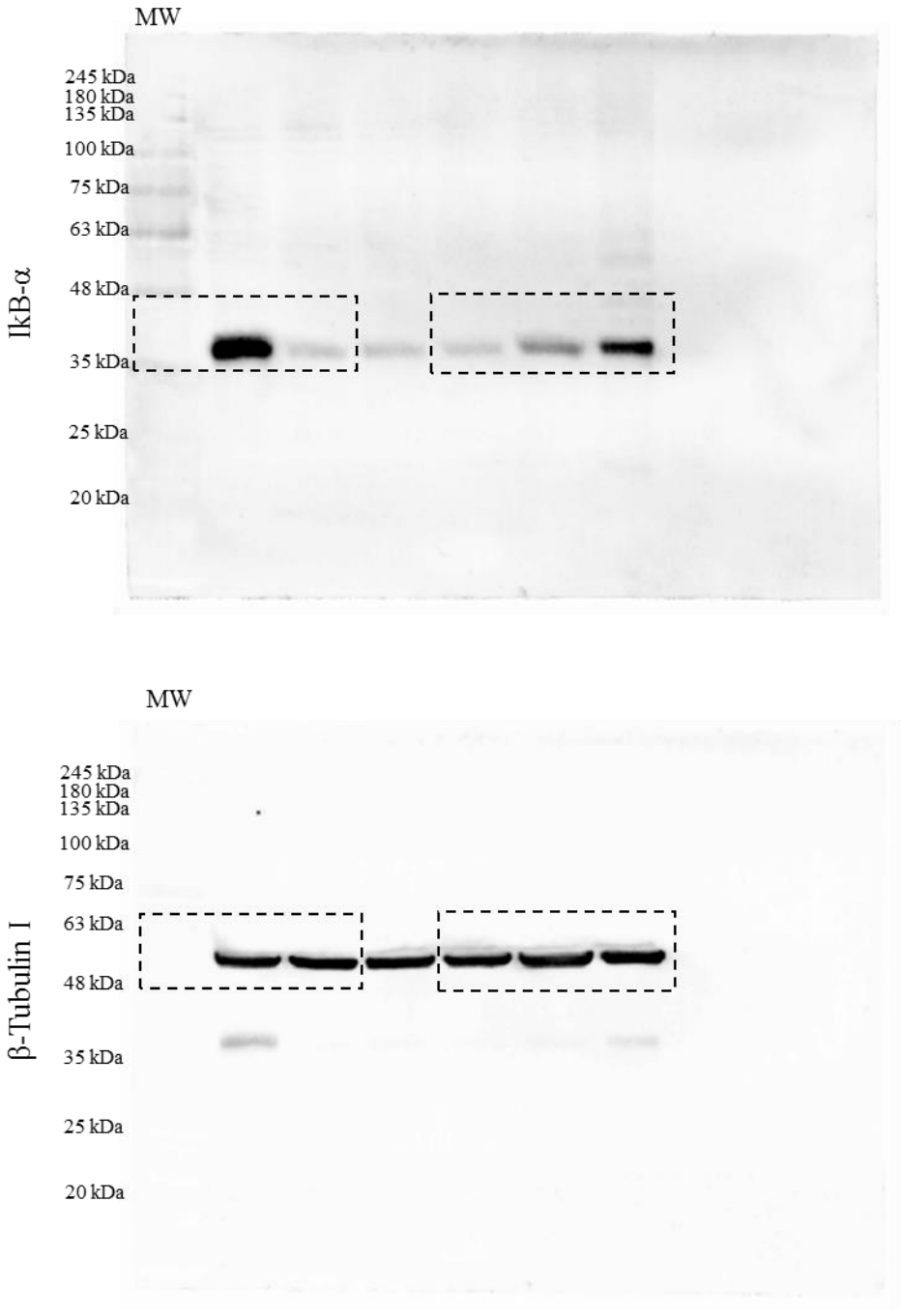

Uncropped blots shown in **Figure 2C**

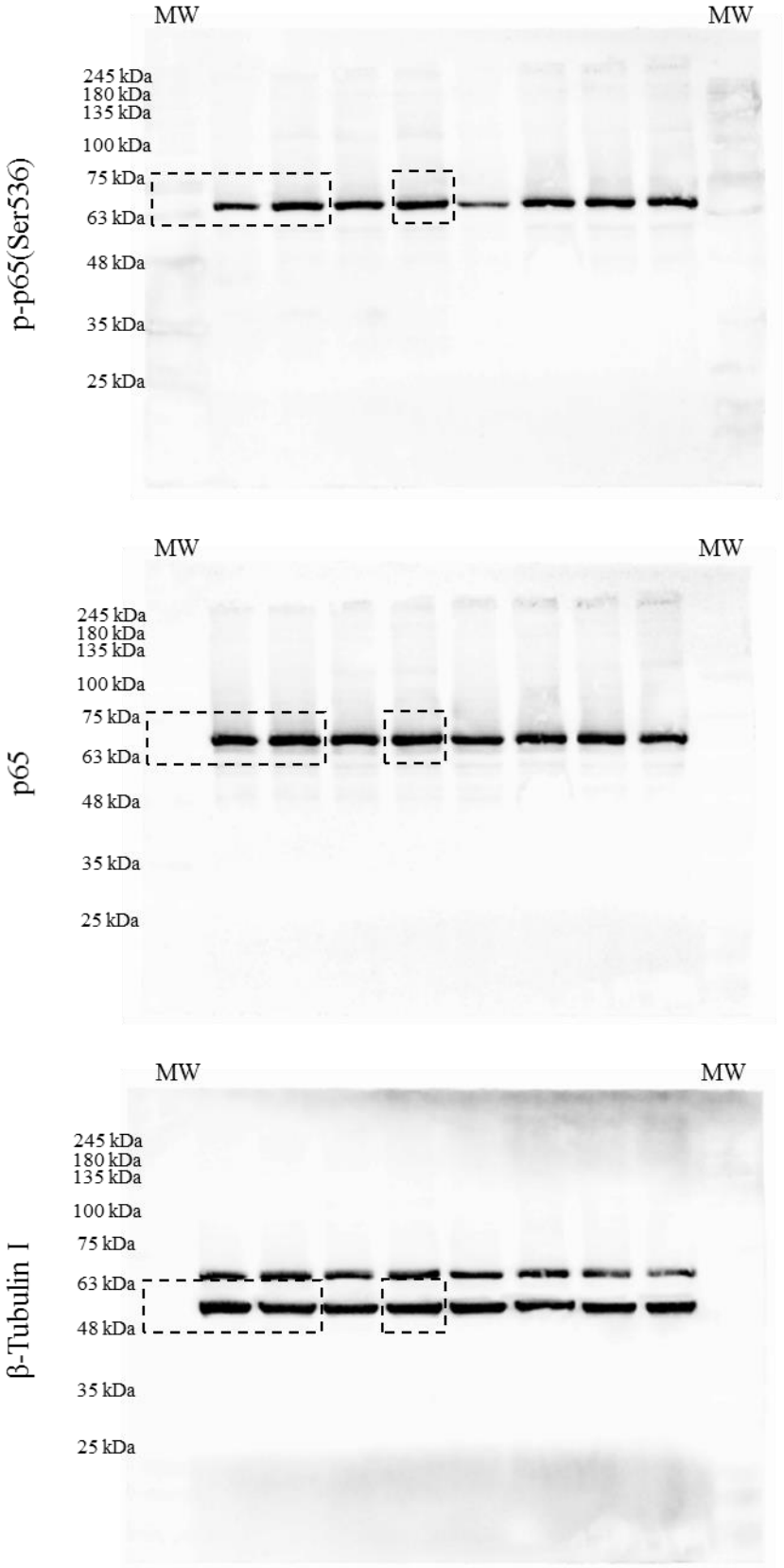

Uncropped blots shown in **Figure 4**

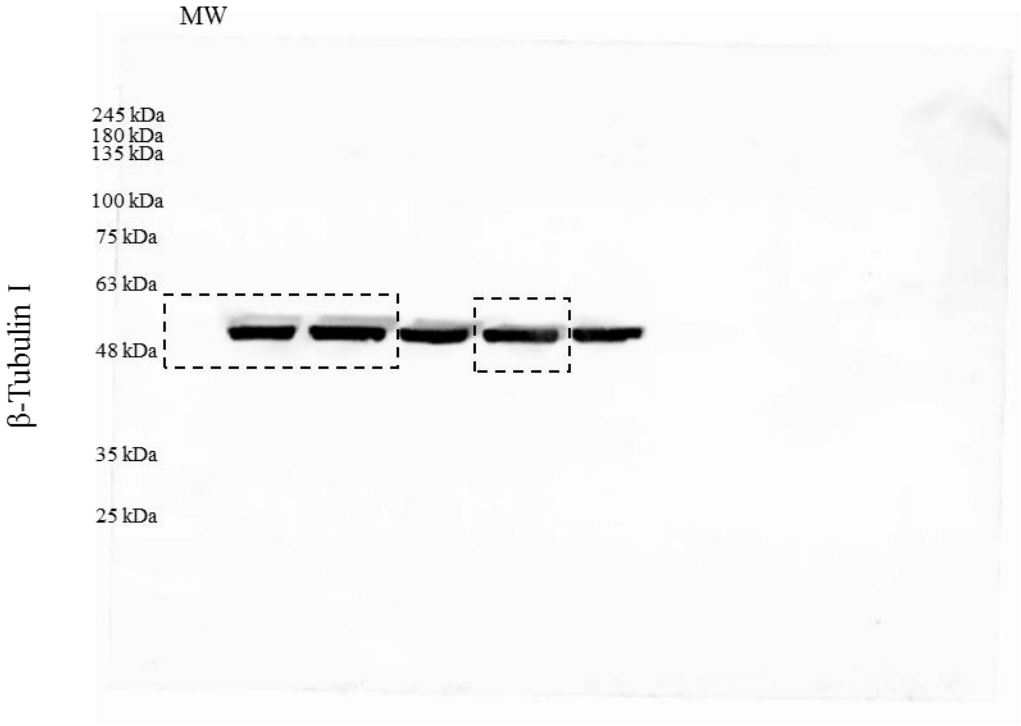

Uncropped blots shown in **Figure 5A**

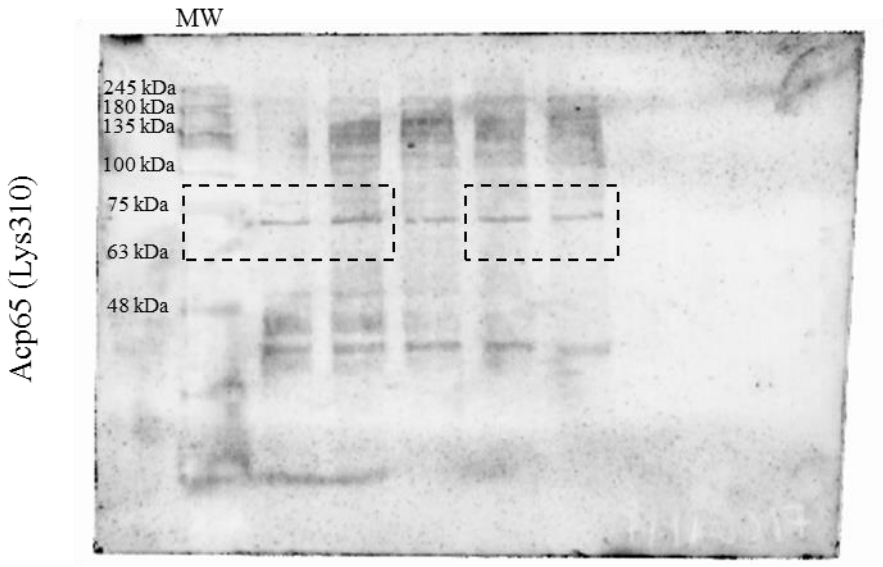

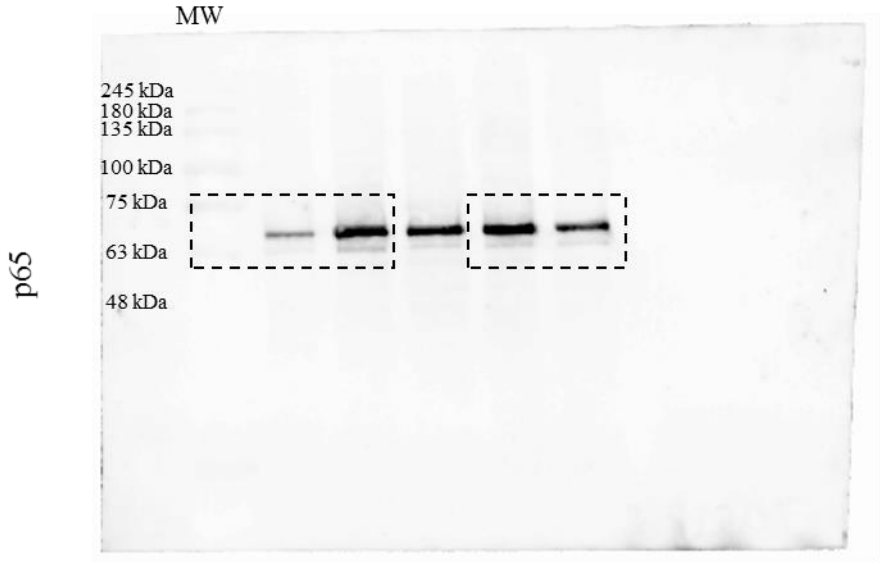

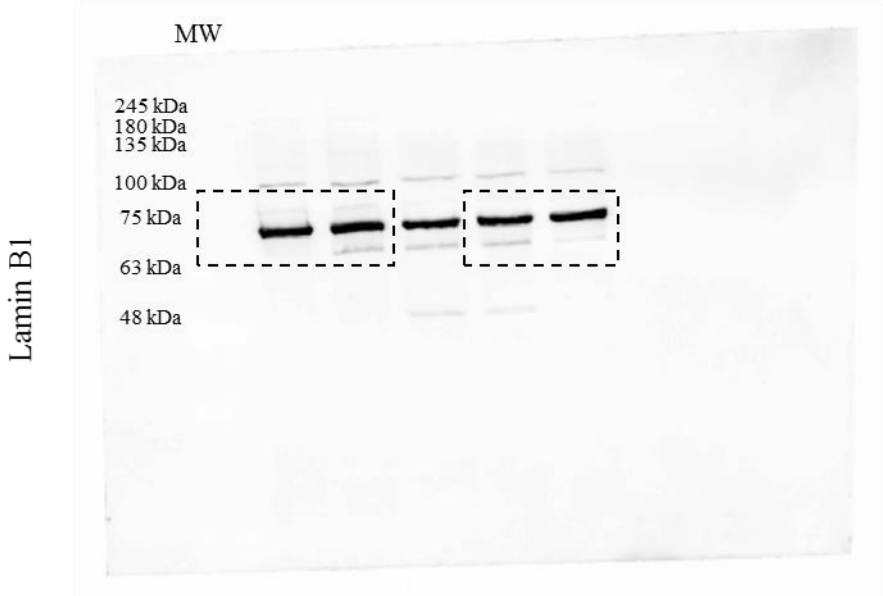

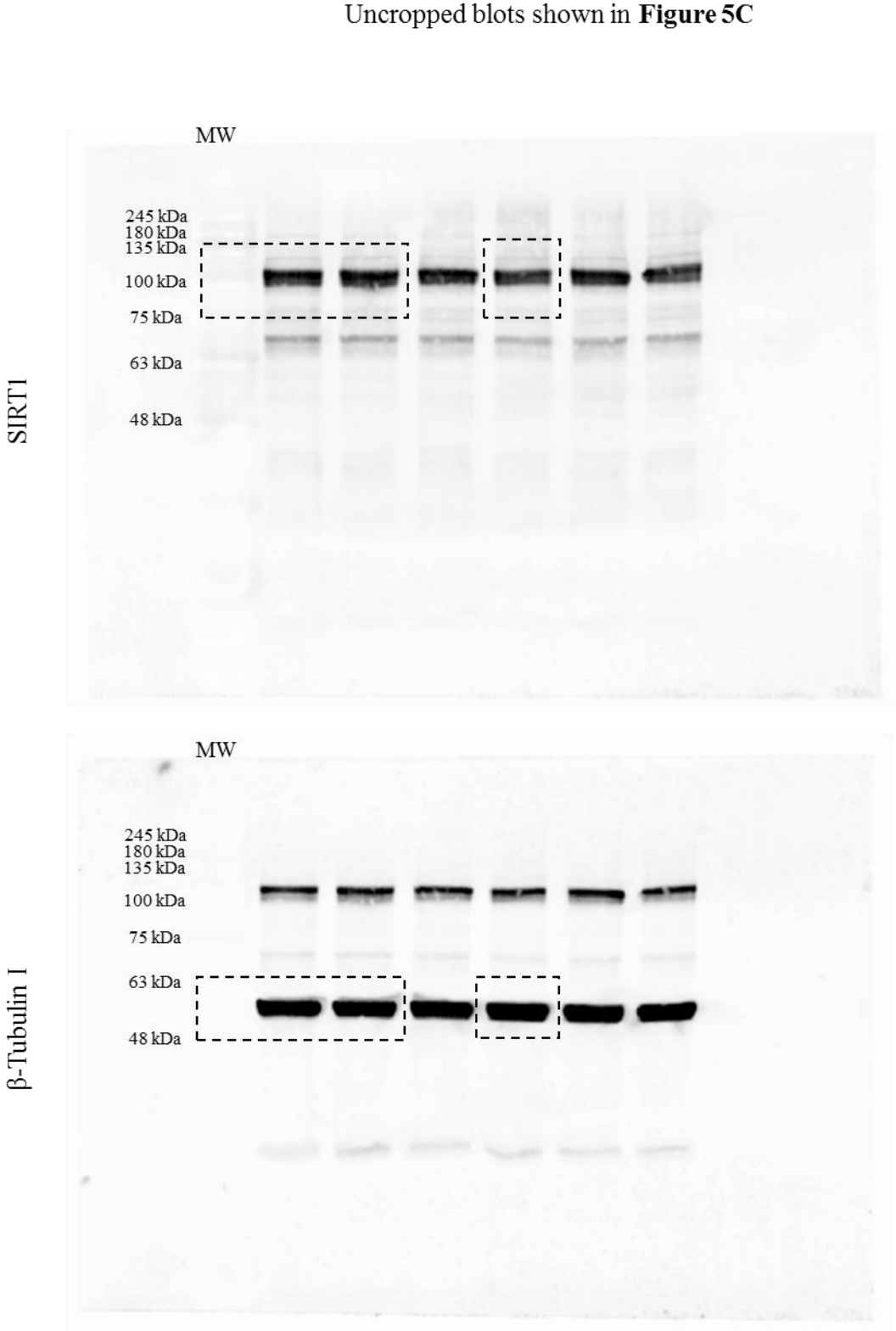

Figure S2. Uncropped images of the blots shown in figures 1-2 and 4-5. The portions of the membranes shown in each of those figures are surrounded by a dashed line box.

Chapter 5: Discussion and Conclusion

The role of inflammation in chronic age-related diseases prompted us to look for new molecules capable of interfering with pro-inflammatory signaling pathways and establishing the SAR to guide the drug discovery process. The results presented in chapter 2 identified nine compounds with potential anti-inflammatory activity, based on their ability to inhibit LPS-induced NO production in murine macrophages. Moreover, calculation of IC_{50} values allowed the comparison of those active compounds and the identification of the structural features most relevant for efficacy and potency. In summary, the results show that:

- Nine compounds, (S)-(+)-carvone (**4**), (R)-(-)-carvone (**5**), (-)-carveol (**6**), (+)-dihydrocarvone (**7**), (+)-dihydrocarveol (**8**), (-)-dihydrocarveol (**9**), (S)-(-)-pulegone (**13**), (S)-8-hidroxycarvotanacetone (**20**) and (R)-8-hidroxycarvotanacetone (**21**), are capable of significantly inhibiting NO production by more than 30%, at concentrations that do not affect cell viability.
- Calculation of IC_{50} values was possible for eight of those compounds and was used to rank their order of potency: (S)-(+)-carvone (**4**) > (R)-(-)-carvone (**5**) >> (+)-dihydrocarveol (**8**) > (S)-8-hidroxycarvotanacetone (**20**) > (R)-8-hidroxycarvotanacetone (**21**) > (+)-dihydrocarvone (**7**) > (-)-carveol (**6**) > (-)-dihydrocarveol (**9**).
- The conjugation of an α,β double bond at C1 with a carbonyl group at C6 is the major determinant of potency, while the presence of an isopropenyl group at C4 and the S configuration of the chiral center at C4 are decreasingly important.

Figure 1 summarizes the chemical features found relevant for the anti-inflammatory activity.

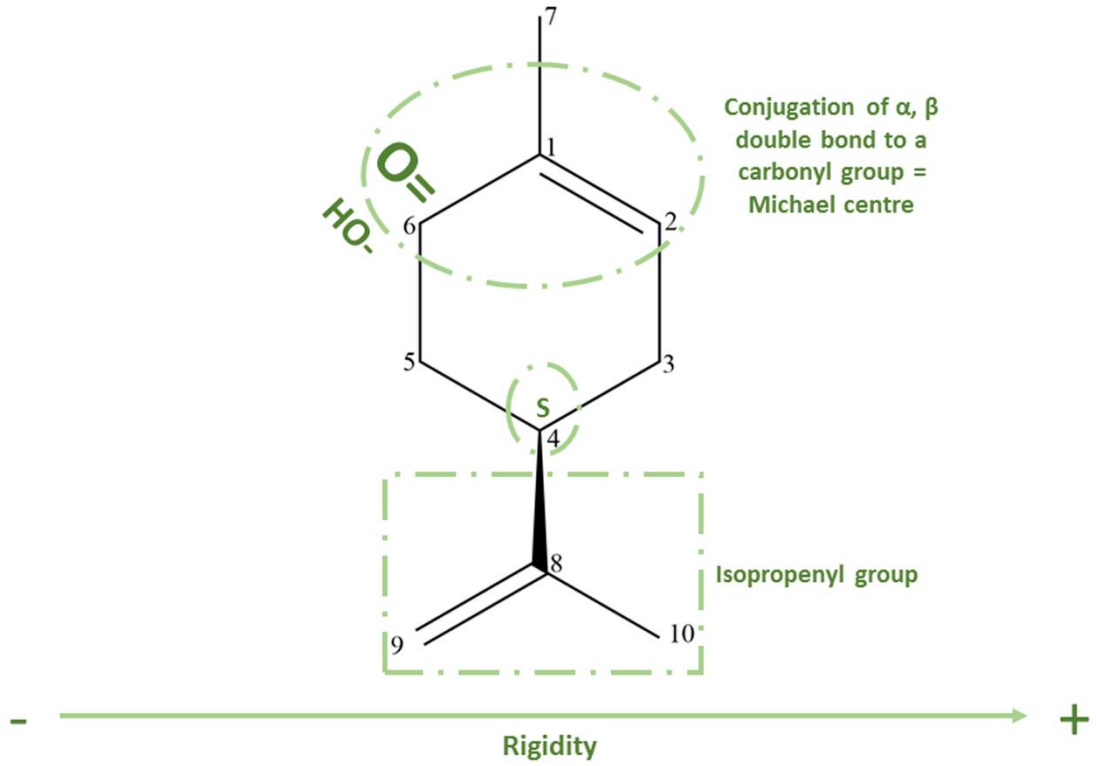

Figure 1. Chemical features relevant for anti-inflammatory activity and potency. The presence of an oxygenated group (hydroxyl or carbonyl group) at C6 is essential for activity. When the oxygenated group at C6 is a carbonyl, potency is maximal due to its conjugation to the α,β double bond at C1, which provides a Michael centre. The presence of an isopropenyl group at C4 favours the anti-inflammatory activity or, at least, the absence of hydrogen binding sites and bulky groups at that position. The S configuration at C4 is also important for potency. Neither too flexible nor too rigid structures are suitable for activity.

Findings about chemical features are very useful to predict the anti-inflammatory activity of distinct mint species and their chemotypes once the composition in limonene-derived monoterpenes is known. Furthermore, the identification of these features represents a critical insight into the chemistry of this class of compounds and, thus, a significant contribution to the drug discovery process by guiding the synthesis of new compounds with improved pharmacological and physicochemical characteristics. In particular, the SAR established identifies the isopropenyl group at C4 as a potential site for chemical modification that does not affect efficacy, even though potency may be decreased. Nonetheless, modifications at that site may be useful to modify the physicochemical characteristics of these compounds, for instance, in order to increase molecular weight and, thus, decrease volatility which may be important, for instance, to increase shelf life. On the other hand, it is conceptually possible

to modify that centre in such a way that volatility can be decreased without affecting or even increasing potency, relative to the parent compounds, namely (S)-(+)- and (R)-(-)-carvone.

The anti-inflammatory properties of these two compounds were further confirmed by their ability to inhibit the expression of two major inflammatory mediators, NOS2 (chapter 2, Fig. 2) and IL-1β (chapter 2, Fig. 3), in LPS-treated murine macrophages. Furthermore, (S)-(+)-carvone was also found to inhibit the expression of those mediators in IL-1β-treated human chondrocytes (chapter 2, Fig. 4), which are widely used as a cell model of osteoarthritis. Thus, the results obtained point out that (S)-(+)-carvone effectively inhibits the responses induced by distinct inflammatory and catabolic stimuli in different cell types.

Taking the potential of (S)-(+)-carvone to interfere with the expression of pro-inflammatory mediators in mouse macrophages and human chondrocytes, the mechanisms behind these effects were then investigated, in particular those involving the MAPK and NF-κB signalling pathways. (S)-(+)-carvone significantly inhibited LPS-induced JNK activation (chapter 3, Fig. 1C), in particular JNK1 phosphorylation, in macrophages, but had no effect on the activation of the other two MAPK family members, p38 and ERK1/2 (chapter 3, Fig. 1A and B). Inhibition of JNK activation may not be sufficient to explain its anti-inflammatory effects, since SP600125, a selective JNK inhibitor, decreased NOS2 expression and NO production, but did not affect the expression of IL-1β (chapter 3, Fig. 2). Moreover, (S)-(+)-carvone did not interfere with the initial steps of NF-κB activation, namely phosphorylation and degradation of IκB-α, phosphorylation of RelA/p65 at Ser536 (chapter 3, Fig. 3) and NF-κB nuclear translocation (chapter 3, Fig. 4). Nevertheless, LPS-induced IκB-α resynthesis was inhibited by (S)-(+)-carvone (chapter 3, Fig. 5). Since PTM confer another layer of regulation of NF-κB, we hypothesised that (S)-(+)-carvone could be interfering with a specific modification, in particular acetylation at Lys310 of RelA/p65 which is necessary for full NF-κB transcriptional activity (Huang, Yang et al. 2010). (S)-(+)-carvone did decrease LPS-induced acetylation of RelA/p65 at Lys310 in macrophages (chapter 3, Fig. 6A). The involvement of SIRT1 in deacetylation of RelA/p65 at Lys310 and consequent inhibition of NF-κB transcriptional activity has been described (Yeung, Hoberg et al. 2004, Kauppinen, Suuronen et al. 2013). Thus, we hypothesised that (S)-(+)-carvone could target SIRT1 activity and/or expression. *In chemico* assays demonstrated that (S)-(+)-carvone directly activates SIRT1 (chapter 3, Fig. 6B), while studies in mouse macrophages showed its ability to decrease the levels of acetylated RelA/p65without interfering with

SIRT1 expression (chapter 3, Fig. 6C). These results were essentially confirmed in human chondrocytes (chapter 3, Fig. 7), although the decrease in the levels of acetylated RelA/p65 at Lys310 induced by IL-1β did not reach statistical significance, most likely due to the substantial variability observed among cells from distinct cartilage donors. Further studies using a larger number of cartilage samples would be required to compensate for that variability. On the other hand, further studies, namely silencing SIRT1 expression and/or using known SIRT1 inhibitors, such as sirtinol or EX-527 (Wang, He et al. 2019) would be useful to confirm the direct activation of SIRT1 as the mechanism underlying the anti-inflammatory effects of (S)-(+)-carvone.

Figure 2 summarizes the mechanisms responsible for the anti-inflammatory effects of (S)-(+)-carvone in mouse macrophages and human chondrocytes.

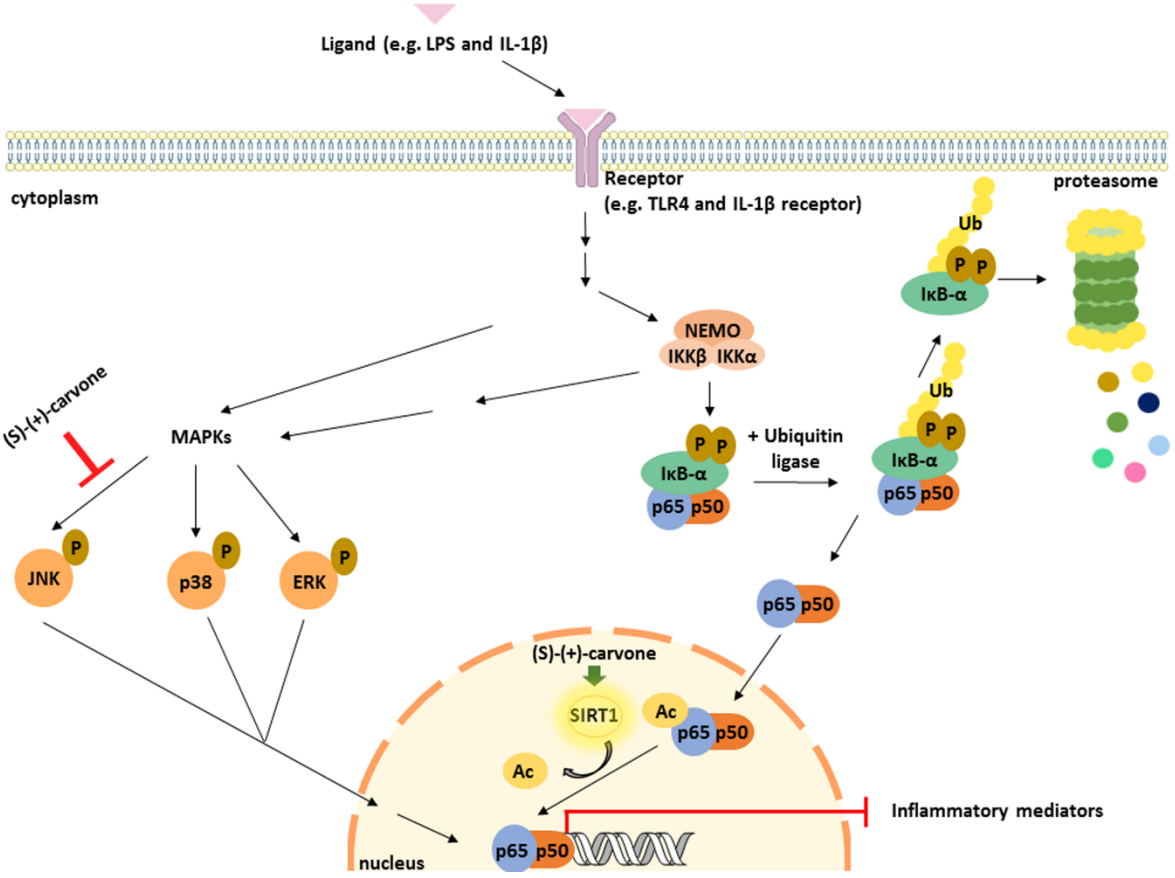

Figure 2. Molecular mechanisms responsible for the anti-inflammatory effects of (S)-(+)-carvone. (S)-(+)-carvone inhibits JNK activation, in particular JNK1, while activating SIRT1 which directly deacetylates RelA/p65, decreasing the transcriptional activity of the master regulator of inflammatory gene expression, NF-κB. Ac, acetyl;p65, RelA/p65; P, phosphate; Ub, ubiquitin.

To our knowledge, (S)-(+)-carvone is the first monoterpene reported as a direct activator of SIRT1. Other compounds of natural origin have also been reported as SIRT1 activators, such as Res, curcumin, fisetin and berberine (Iside, Scafuro et al. 2020), but these are compounds with a polyphenolic structure which is quite different from that of (S)-(+)-carvone. The availability of different compounds with diverse chemical structures, capable of activating SIRT1 provides the variety required for innovative drug design and development. In this particular case, the identification of a monoterpene structure like (S)-(+)-carvone as a SIRT1 activator may be especially important by providing a completely new scaffold whose chemical modification may provide new compounds that overcome the bioavailability and solubility issues presented by the polyphenolic SIRT1 activators that currently represent a significant obstacle for their therapeutic use (Iside, Scafuro et al. 2020).

SIRT1 has been emerging as a promising therapeutic target for metabolic and age-related diseases (Haigis and Sinclair 2010, Gomes, Leal et al. 2019). Particularly, its antagonistic crosstalk with NF-κB seems quite relevant for those diseases (Kauppinen, Suuronen et al. 2013). As mentioned in Chapter 1, NF-κB has been shown to play a central role in the development of metabolic and age-related diseases (Salminen and Kaarniranta 2009, Baker, Hayden et al. 2011). Thus, mechanisms that interfere with the NF-κB signalling pathway, such as SIRT1 activation, are quite relevant and promising targets for the development of innovative strategies to prevent and treat those diseases. Moreover, SIRT1 expression has been reported as being downregulated in age-related diseases and increasing its expression and/or activity represents an effective strategy to slow down aging effects (Grabowska, Sikora et al. 2017). Accordingly, various clinical trials to assess the efficacy of SIRT1 activators, like fisetin and Res, in various diseases are currently underway (Gaspar, Sousa et al. 2020). One of those diseases is OA (Dvir-Ginzberg, Mobasheri et al. 2016). For this reason, we confirmed the results regarding the acetylation of RelA/p65 at Lys310 in primary human chondrocyte cultures treated with IL-1β, as a cell model of OA. Moreover, (S)-(+)-carvone also increased the protein levels of another target of SIRT1, the transcription factor SOX9 (chapter 3, Fig. 8). SIRT1 deacetylates SOX9 which is required for its nuclear translocation and enhancement of collagen 2 (Dvir-Ginzberg, Gagarina et al. 2008, Oppenheimer, Kumar et al. 2014) and aggrecan (Bar Oz, Kumar et al. 2016) expression, the major components of the cartilage ECM that are downregulated in OA (Charlier, Deroyer et al. 2019). Despite contradictory studies, Res and fisetin, known SIRT1 activators, have been

shown to increase SOX9 protein levels or to reverse the decrease induced by an inflammatory stimulus, respectively (Buhrmann, Popper et al. 2017, Zheng, Feng et al. 2017). Clearly, further studies are needed to clarify the role of SIRT1 in SOX9 protein levels and transcriptional activity and its significance in cartilage homeostasis in health and disease.

Given the relevance of macrophages and chondrocytes, which were used in this work, and the inflammatory stimuli used to OA pathophysiology (Goldring and Berenbaum 2015, Liu-Bryan and Terkeltaub 2015), further studies in animal models of the disease are warranted to further demonstrate the efficacy of (S)-(+)-carvone in halting join destruction in OA and to evaluate safety and pharmacokinetic issues, including identification of the best route of administration, namely by comparing the oral and intra-articular routes. In parallel, evaluation of the selectivity of (S)-(+)-carvone to SIRT1 is an essential requirement due to the great homology with other SIRTs (Wang, He et al. 2019). Moreover, potential off target effects also need to be addressed since (S)-(+)-carvone is quite lipophilic which is a feature that facilitates interaction with multiple protein targets and thus is associated with pharmacological promiscuity (Sturm, Desaphy et al. 2012, Gilberg, Jasial et al. 2016). Furthermore, (S)-(+)-carvone is a volatile low water solubility organic compound (Kesselmeier and Staudt 1999), which may represent limitations for its pharmaceutical formulation, production and storage. Nonetheless, these limitations can be overcome by encapsulation of (S)-(+)-carvone, for example. in cyclodextrin particles (Guimarães, Oliveira et al. 2015) or by lead optimization for which the SAR identified is an important tool.

On the other hand, volatility of (S)-(+)-carvone may be an advantage for some applications, namely for nose-to-brain administration, providing a minimally invasive way of targeting neurological diseases, such as Alzheimer's and Parkinson's diseases (Gänger and Schindowski 2018) for which no curative therapies yet exist and pharmacological activation of SIRT1 represents a promising therapeutic strategy (Fujita and Yamashita 2018). This prompted us to evaluate the potential of (S)-(+)-carvone in a Parkinson's disease model that uses mesencephalic mouse neuron cultures treated with LPS. This is a well-established *in vitro* model of Parkinson's disease that elicits its major cellular alterations and pathological hallmarks, namely the accumulation, misfolding, and aggregation of α-Synuclein and its progressive deposition in large intracellular aggregates (Tufekci, Genc et

al. 2011). The smaller aggregates, namely soluble oligomers, are the most toxic species of α-Synuclein (Ingelsson 2016) and thus, inhibition of their formation is a major target to prevent disease development and progression (Tufekci, Genc et al. 2011). Preliminary results show that (S)-(+)-carvone completely abolished the formation and accumulation of α-synuclein oligomers induced by LPS, thus suggesting that it can have protective effects against Parkinson's disease development and progression (data not shown).

Even though SIRT1 activation and, to a less extent, JNK1 inhibition were identified as major mechanisms behind the anti-inflammatory effects of (S)-(+)-carvone , the question remained whether its enantiomer, (R)-(-)-carvone, acts by the same mechanisms. Following the same experimental approach used for (S)-(+)-carvone, we found that (R)-(-)-carvone also significantly inhibited JNK1 (chapter 4, Fig. 1C), but not p38 and ERK1/2 (chapter 4, Fig. 1A and B) phosphorylation induced by LPS in murine macrophages. Similarly, (R)-(-)-carvone also did not interfere with the canonical NF-κB activation pathway, namely phosphorylation and degradation of IκB-α, phosphorylation of RelA/p65 subunit at Ser536 (chapter 4, Fig. 2) and its nuclear translocation (chapter 4, Fig. 3), but significantly inhibited IκB-α resynthesis induced by LPS (chapter 4, Fig. 4), suggesting that it interferes with NF-κB transcriptional activity. Unlike its enantiomer, however, (R)-(-)-carvone did not significantly decrease the levels of acetylated RelA/p65 in the nucleus in response to treatment of murine macrophages with LPS (chapter 4, Fig. 5A). Importantly, (R)-(-)-carvone also did not affect the activity and protein levels of SIRT1 (chapter 4, Fig. 5B and C). Thus, contrary to its enantiomer, (R)-(-)-carvone does not seem to block NF-κB transcriptional activity through modulation of SIRT1 expression and/or activity, suggesting that enantiomerism may play a relevant role in SIRT1 activation.

Nonetheless, the mechanism underlying the anti-inflammatory effect of (R)-(+)-carvone also involves inhibition of the NF-κB transcriptional activity, without affecting its canonical activation pathway. Interestingly, (R)-(-)-carvone significantly decreased LPS-induced JNK1 phosphorylation which has been shown to enhance the recruitment and association of the acetylase, CBP/p300, with NF-κB, thus promoting its acetylation and activation of transcription. While this mechanisms can explain, at least in part, the anti-inflammatory effects of (R)-(-)-carvone, further studies are required to confirm its relevance in the cell model of inflammation used in our study. Furthermore, this mechanism may explain the

differences in potency observed in inhibition of NO production by both carvone enantiomers.

Figure 3 summarizes the mechanisms involved in the anti-inflammatory effects of (R)-(-)-carvone.

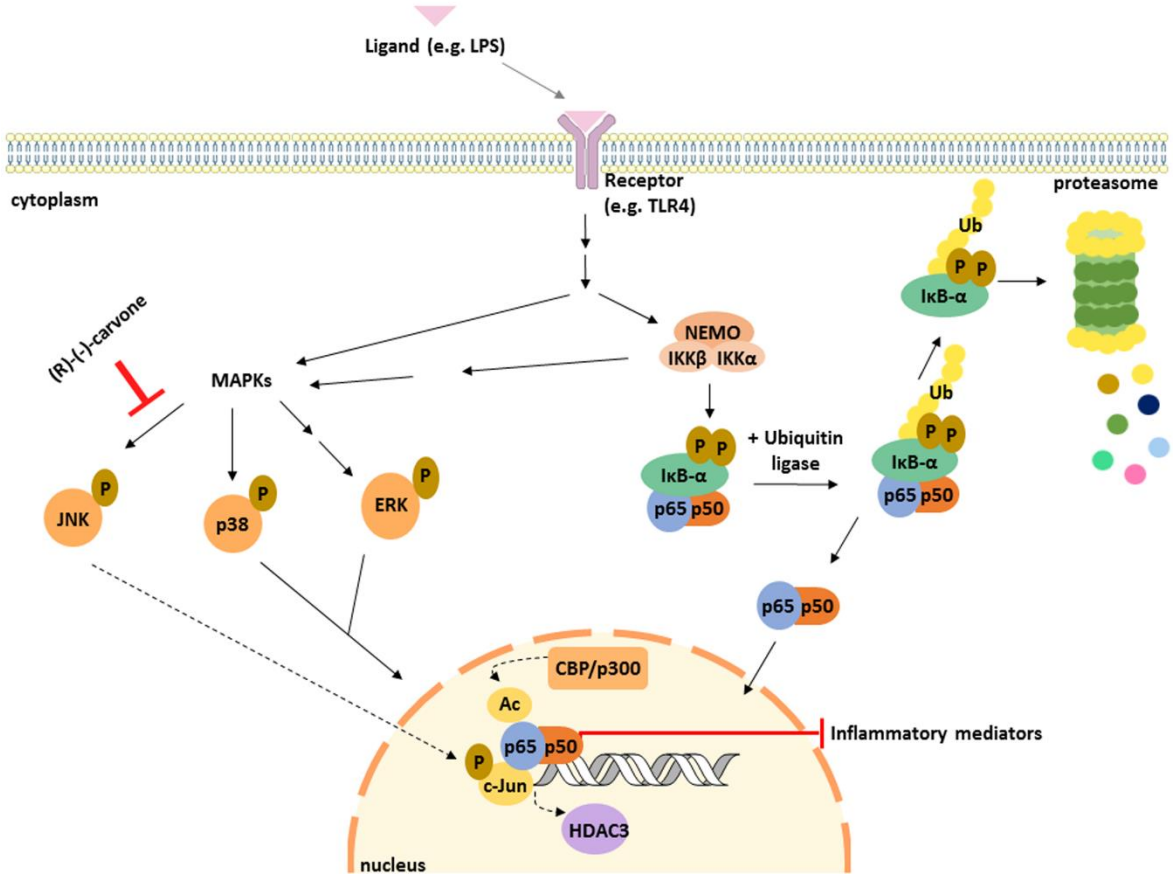

Figure 3. Molecular mechanism involved in the anti-inflammatory effects of (R)-(-)-carvone. JNK, in particular JNK1, inhibition is likely to interfere with p65 acetylation at Lys310 and thus, impair the transcriptional activity of NF-κB. Ac, acetyl; p65, RelA/p65 P, phosphate; Ub, ubiquitin.

To conclude, this work identified the relevant chemical features for anti-inflammatory activity of monoterpenes belonging to the limonene synthase pathway which are abundant in mint species. Among those, (S)-(+)-carvone and (R)-(-)-carvone are the most potent, although they differ partially, at least, regarding the underlying mechanism. While (S)-(+)-carvone is a direct activator of SIRT1, its enantiomer does neither affect the expression nor the activity of this enzyme. Nonetheless, both carvone enantiomers are capable of inhibiting JNK1 which impairs c-Jun phosphorylation and, thus, may interfere with the transcriptional activity of NF-κB by hindering RelA/p65 acetylation by CBP/p300. Moreover, inhibition of

c-Jun phosphorylation also interferes with the activation of other transcription factors, namely AP-1, that is required to enhance the transcription of many inflammation-related genes, like NOS2 (Spitsin, Koprowski et al. 1996, Martin and Wesche 2002) and the matrix metalloproteases, MMP-1 and MMP-13 (Catterall, Carrère et al. 2001, Mengshol, Vincenti et al. 2001, Tardif, Reboul et al. 2001, Sun, Wenger et al. 2002). Thus, the carvone enantiomers have the potential to tackle distinct mechanisms relevant in promoting and maintaining the chronic low-grade inflammatory responses that drive many age-related diseases. Further studies, *in vitro* and *in vivo*, are required to fully ascertain their therapeutic potential. Combining those results with the ones presented here will be essential to inform drug design in order to obtain the compounds with the pharmacological and pharmacokinetic profiles required for the development of new drugs successful in halting the chronic low-grade inflammation that drives age-related functional decline and associated diseases.

References

Abe, S., N. Maruyama, K. Hayama, H. Ishibashi, S. Inoue, H. Oshima and H. Yamaguchi (2003). "Suppression of tumor necrosis factor-alpha-induced neutrophil adherence responses by essential oils." Mediators Inflamm **12**(6): 323-328.

Akira, S., S. Uematsu and O. Takeuchi (2006). "Pathogen recognition and innate immunity." Cell **124**(4): 783-801.

Alsanea, S. and D. Liu (2017). "BITC and S-Carvone Restrain High-Fat Diet-Induced Obesity and Ameliorate Hepatic Steatosis and Insulin Resistance." Pharm Res **34**(11): 2241-2249.

Amarante-Mendes, G. P., S. Adjemian, L. M. Branco, L. C. Zanetti, R. Weinlich and K. R. Bortoluci (2018). "Pattern Recognition Receptors and the Host Cell Death Molecular Machinery." Front Immunol **9**: 2379.

Amir-Zilberstein, L., E. Ainbinder, L. Toube, Y. Yamaguchi, H. Handa and R. Dikstein (2007). "Differential regulation of NF-kappaB by elongation factors is determined by core promoter type." Mol Cell Biol **27**(14): 5246-5259.

Angel, P., M. Imagawa, R. Chiu, B. Stein, R. J. Imbra, H. J. Rahmsdorf, C. Jonat, P. Herrlich and M. Karin (1987). "Phorbol ester-inducible genes contain a common cis element recognized by a TPA-modulated trans-acting factor." Cell **49**(6): 729-739.

Antonelli, M. and I. Kushner (2017). "It's time to redefine inflammation." FASEB J **31**(5): 1787-1791.

Antonelli, M. and I. Kushner (2017). "It's time to redefine inflammation." FASEB J.

Arthur, J. S. and S. C. Ley (2013). "Mitogen-activated protein kinases in innate immunity." Nat Rev Immunol **13**(9): 679-692.

Ashburner, B. P., S. D. Westerheide and A. S. Baldwin, Jr. (2001). "The p65 (RelA) subunit of NF-kappaB interacts with the histone deacetylase (HDAC) corepressors HDAC1 and HDAC2 to negatively regulate gene expression." Mol Cell Biol **21**(20): 7065-7077.

Asiimwe, N., S. G. Yeo, M. S. Kim, J. Jung and N. Y. Jeong (2016). "Nitric Oxide: Exploring the Contextual Link with Alzheimer's Disease." Oxid Med Cell Longev **2016**: 7205747.

Atsaves, V., V. Leventaki, G. Z. Rassidakis and F. X. Claret (2019). "AP-1 Transcription Factors as Regulators of Immune Responses in Cancer." Cancers (Basel) **11**(7).

Azab, A., A. Nassar and A. N. Azab (2016). "Anti-Inflammatory Activity of Natural Products." Molecules **21**(10).

Baker, R. G., M. S. Hayden and S. Ghosh (2011). "NF-kappaB, inflammation, and metabolic disease." Cell Metab **13**(1): 11-22.

Bar Oz, M., A. Kumar, J. Elayyan, E. Reich, M. Binyamin, L. Kandel, M. Liebergall, J. Steinmeyer, V. Lefebvre and M. Dvir-Ginzberg (2016). "Acetylation reduces SOX9 nuclear entry and ACAN gene transactivation in human chondrocytes." Aging Cell **15**(3): 499-508.

Barth, K., D. G. Remick and C. A. Genco (2013). "Disruption of immune regulation by microbial pathogens and resulting chronic inflammation." J Cell Physiol **228**(7): 1413-1422.

Basak, S., V. F. Shih and A. Hoffmann (2008). "Generation and activation of multiple dimeric transcription factors within the NF-kappaB signaling system." Mol Cell Biol **28**(10): 3139-3150.

Basil, M. C. and B. D. Levy (2016). "Specialized pro-resolving mediators: endogenous regulators of infection and inflammation." Nat Rev Immunol **16**(1): 51-67.

Beinke, S., M. J. Robinson, M. Hugunin and S. C. Ley (2004). "Lipopolysaccharide activation of the TPL-2/MEK/extracellular signal-regulated kinase mitogen-activated protein kinase cascade is regulated by IkappaB kinase-induced proteolysis of NF-kappaB1 p105." Mol Cell Biol **24**(21): 9658-9667.

Bernell, S. and S. W. Howard (2016). "Use Your Words Carefully: What Is a Chronic Disease?" Front Public Health **4**: 159.

Biswas, S. K. (2016). "Does the Interdependence between Oxidative Stress and Inflammation Explain the Antioxidant Paradox?" Oxid Med Cell Longev **2016**: 5698931.

Blanco, F. J., R. L. Ochs, H. Schwarz and M. Lotz (1995). "Chondrocyte apoptosis induced by nitric oxide." Am J Pathol **146**(1): 75-85.

Buerki, C., K. M. Rothgiesser, T. Valovka, H. R. Owen, H. Rehrauer, M. Fey, W. S. Lane and M. O. Hottiger (2008). "Functional relevance of novel p300-mediated lysine 314 and 315 acetylation of RelA/p65." Nucleic Acids Res **36**(5): 1665-1680.

Buhrmann, C., B. Popper, B. B. Aggarwal and M. Shakibaei (2017). "Resveratrol downregulates inflammatory pathway activated by lymphotoxin α (TNF-β) in articular chondrocytes: Comparison with TNF-α." PLoS One **12**(11): e0186993.

Buss, H., A. Dorrie, M. L. Schmitz, R. Frank, M. Livingstone, K. Resch and M. Kracht (2004). "Phosphorylation of serine 468 by GSK-3beta negatively regulates basal p65 NF-kappaB activity." J Biol Chem **279**(48): 49571-49574.

Cadwell, K. (2016). "Crosstalk between autophagy and inflammatory signalling pathways: balancing defence and homeostasis." Nat Rev Immunol **16**(11): 661-675.

Calcinotto, A., J. Kohli, E. Zagato, L. Pellegrini, M. Demaria and A. Alimonti (2019). "Cellular Senescence: Aging, Cancer, and Injury." Physiol Rev **99**(2): 1047-1078.

Campa, V. M., J. M. Iglesias, M. T. Carcedo, R. Rodriguez, J. Riera, S. Ramos and P. S. Lazo (2005). "Polyinosinic acid induces TNF and NO production as well as NF-kappaB and AP-1 transcriptional activation in the monocytemacrophage cell line RAW 264.7." Inflamm Res **54**(8): 328-337.

Cao, Y., Y. Sun, H. Chang, X. Sun and S. Yang (2019). "The E3 ubiquitin ligase RNF182 inhibits TLR-triggered cytokine production through promoting p65 ubiquitination and degradation." FEBS Lett **593**(22): 3210-3219.

Caramés, B., A. Hasegawa, N. Taniguchi, S. Miyaki, F. J. Blanco and M. Lotz (2012). "Autophagy activation by rapamycin reduces severity of experimental osteoarthritis." Ann Rheum Dis **71**(4): 575-581.

Carames, B., N. Taniguchi, S. Otsuki, F. J. Blanco and M. Lotz (2010). "Autophagy is a protective mechanism in normal cartilage, and its aging-related loss is linked with cell death and osteoarthritis." Arthritis Rheum **62**(3): 791-801.

Castro-Caldas, M., A. F. Mendes, A. P. Carvalho, C. B. Duarte and M. C. Lopes (2003). "Dexamethasone prevents interleukin-1beta-induced nuclear factor-kappaB activation by upregulating IkappaB-alpha synthesis, in lymphoblastic cells." Mediators Inflamm **12**(1): 37-46.

Catterall, J. B., S. Carrère, P. J. Koshy, B. A. Degnan, W. D. Shingleton, C. E. Brinckerhoff, J. Rutter, T. E. Cawston and A. D. Rowan (2001). "Synergistic induction of matrix metalloproteinase 1 by interleukin-1alpha and oncostatin M in human chondrocytes involves signal transducer and activator of transcription and activator protein 1 transcription factors via a novel mechanism." Arthritis Rheum **44**(10): 2296-2310.

Charlier, E., C. Deroyer, F. Ciregia, O. Malaise, S. Neuville, Z. Plener, M. Malaise and D. de Seny (2019). "Chondrocyte dedifferentiation and osteoarthritis (OA)." Biochem Pharmacol **165**: 49-65.

Chaudhari, N., P. Talwar, A. Parimisetty, C. Lefebvre d'Hellencourt and P. Ravanan (2014). "A Molecular Web: Endoplasmic Reticulum Stress, Inflammation, and Oxidative Stress." Front Cell Neurosci **8**: 213.

Chen, B., J. Li and H. Zhu (2016). "AMP-activated protein kinase attenuates oxLDL uptake in macrophages through PP2A/NF-kappaB/LOX-1 pathway." Vascul Pharmacol **85**: 1-10.

Chen, H., D. Wu, X. Ding and W. Ying (2015). "SIRT2 is required for lipopolysaccharide-induced activation of BV2 microglia." Neuroreport **26**(2): 88-93.

Chen, J., J. J. Xie, K. S. Shi, Y. T. Gu, C. C. Wu, J. Xuan, Y. Ren, L. Chen, Y. S. Wu, X. L. Zhang, J. Xiao, D. Z. Wang and X. Y. Wang (2018). "Glucagon-like peptide-1 receptor regulates endoplasmic reticulum stress-induced apoptosis and the associated inflammatory response in chondrocytes and the progression of osteoarthritis in rat." Cell Death Dis **9**(2): 212.

Chen, J., Y. Zhou, S. Mueller-Steiner, L. F. Chen, H. Kwon, S. Yi, L. Mucke and L. Gan (2005). "SIRT1 protects against microglia-dependent amyloid-beta toxicity through inhibiting NF-kappaB signaling." J Biol Chem **280**(48): 40364-40374.

Chen, L., H. Deng, H. Cui, J. Fang, Z. Zuo, J. Deng, Y. Li, X. Wang and L. Zhao (2018). "Inflammatory responses and inflammation-associated diseases in organs." Oncotarget **9**(6): 7204-7218.

Chen, L., W. Fischle, E. Verdin and W. C. Greene (2001). "Duration of nuclear NF-kappaB action regulated by reversible acetylation." Science **293**(5535): 1653-1657.

Chen, L. F., Y. Mu and W. C. Greene (2002). "Acetylation of RelA at discrete sites regulates distinct nuclear functions of NF-kappaB." EMBO J **21**(23): 6539-6548.

Chen, L. F., S. A. Williams, Y. Mu, H. Nakano, J. M. Duerr, L. Buckbinder and W. C. Greene (2005). "NF-kappaB RelA phosphorylation regulates RelA acetylation." Mol Cell Biol **25**(18): 7966-7975.

Chen, X.-H., Y.-P. Zhao, M. Xue, C.-B. Ji, C.-L. Gao, J.-G. Zhu, D.-N. Qin, C.-Z. Kou, X.-H. Qin, M.-L. Tong and X.-R. Guo (2010). "TNF-α induces mitochondrial dysfunction in 3T3-L1 adipocytes." Mol Cell Endocrinol **328**(1): 63-69.

Cheng, J. D., R. P. Ryseck, R. M. Attar, D. Dambach and R. Bravo (1998). "Functional redundancy of the nuclear factor kappa B inhibitors I kappa B alpha and I kappa B beta." J Exp Med **188**(6): 1055-1062.

Cherry, A. D. and C. A. Piantadosi (2015). "Regulation of mitochondrial biogenesis and its intersection with inflammatory responses." Antioxid Redox Signal **22**(12): 965-976.

Chew, J., S. Biswas, S. Shreeram, M. Humaidi, E. T. Wong, M. K. Dhillion, H. Teo, A. Hazra, C. C. Fang, E. Lopez-Collazo, D. V. Bulavin and V. Tergaonkar (2009). "WIP1 phosphatase is a negative regulator of NF-kappaB signalling." Nat Cell Biol **11**(5): 659-666.

Choi, M. C., J. Jo, J. Park, H. K. Kang and Y. Park (2019). "NF-kappaB Signaling Pathways in Osteoarthritic Cartilage Destruction." Cells **8**(7).

Choi, Y. Y., M. H. Kim, H. Lee, S. Y. Jo and W. M. Yang (2018). "(R)-(+)-pulegone suppresses allergic and inflammation responses on 2,4-dinitrochlorobenzene-induced atopic dermatitis in mice model." J Dermatol Sci **91**(3): 292-300.

Chovatiya, R. and R. Medzhitov (2014). "Stress, inflammation, and defense of homeostasis." Mol Cell **54**(2): 281-288.

Christian, F., E. L. Smith and R. J. Carmody (2016). "The Regulation of NF-kappaB Subunits by Phosphorylation." Cells **5**(1).

Chung, H. Y., E. K. Lee, Y. J. Choi, J. M. Kim, D. H. Kim, Y. Zou, C. H. Kim, J. Lee, H. S. Kim, N. D. Kim, J. H. Jung and B. P. Yu (2011). "Molecular inflammation as an underlying mechanism of the aging process and age-related diseases." J Dent Res **90**(7): 830-840.

Cildir, G., K. C. Low and V. Tergaonkar (2016). "Noncanonical NF-kappaB Signaling in Health and Disease." Trends Mol Med **22**(5): 414-429.

Cillero-Pastor, B., M. A. Martin, J. Arenas, M. J. Lopez-Armada and F. J. Blanco (2011). "Effect of nitric oxide on mitochondrial activity of human synovial cells." BMC Musculoskelet Disord **12**: 42.

Colleran, A., P. E. Collins, C. O'Carroll, A. Ahmed, X. Mao, B. McManus, P. A. Kiely, E. Burstein and R. J. Carmody (2013). "Deubiquitination of NF-kappaB by Ubiquitin-Specific Protease-7 promotes transcription." Proc Natl Acad Sci U S A **110**(2): 618-623.

Collins, P. E., I. Mitxitorena and R. J. Carmody (2016). "The Ubiquitination of NF-kappaB Subunits in the Control of Transcription." Cells **5**(2).

Cominacini, L., A. F. Pasini, U. Garbin, A. Davoli, M. L. Tosetti, M. Campagnola, A. Rigoni, A. M. Pastorino, V. Lo Cascio and T. Sawamura (2000). "Oxidized low density lipoprotein (ox-LDL) binding to ox-LDL receptor-1 in endothelial cells induces the activation of NF-kappaB through an increased production of intracellular reactive oxygen species." J Biol Chem **275**(17): 12633-12638.

Cross, M., E. Smith, D. Hoy, S. Nolte, I. Ackerman, M. Fransen, L. Bridgett, S. Williams, F. Guillemin, C. L. Hill, L. L. Laslett, G. Jones, F. Cicuttini, R. Osborne, T. Vos, R. Buchbinder, A. Woolf and L. March (2014). "The global burden of hip and knee osteoarthritis: estimates from the global burden of disease 2010 study." Ann Rheum Dis **73**(7): 1323-1330.

de Cassia da Silveira e Sa, R., L. N. Andrade and D. P. de Sousa (2013). "A review on anti-inflammatory activity of monoterpenes." Molecules **18**(1): 1227-1254.

de Sá Coutinho, D., M. T. Pacheco, R. L. Frozza and A. Bernardi (2018). "Anti-Inflammatory Effects of Resveratrol: Mechanistic Insights." Int J Mol Sci **19**(6).

Deeks, S. G., S. R. Lewin and D. V. Havlir (2013). "The end of AIDS: HIV infection as a chronic disease." Lancet **382**(9903): 1525-1533.

Dinarello, C. A. (2010). "Anti-inflammatory Agents: Present and Future." Cell **140**(6): 935-950.

Dvir-Ginzberg, M., V. Gagarina, E. J. Lee and D. J. Hall (2008). "Regulation of cartilage-specific gene expression in human chondrocytes by SirT1 and nicotinamide phosphoribosyltransferase." J Biol Chem **283**(52): 36300-36310.

Dvir-Ginzberg, M., A. Mobasheri and A. Kumar (2016). "The Role of Sirtuins in Cartilage Homeostasis and Osteoarthritis." Curr Rheumatol Rep **18**(7): 43.

Ea, C. K. and D. Baltimore (2009). "Regulation of NF-kappaB activity through lysine monomethylation of p65." Proc Natl Acad Sci U S A **106**(45): 18972-18977.

Eitner, A., G. O. Hofmann and H. G. Schaible (2017). "Mechanisms of Osteoarthritic Pain. Studies in Humans and Experimental Models." Front Mol Neurosci **10**: 349.

Fatiha Brahmi, M. K., Chibane Mohamed and Duez Pierre (2017). Chemical Composition and Biological Activities of Mentha Species. Aromatic and Medicinal Plants - Back to Nature. H. A. El-Shemy, IntechOpen**:** 47-80.

Feehan, K. T. and D. W. Gilroy (2019). "Is Resolution the End of Inflammation?" Trends Mol Med **25**(3): 198-214.

Fialkow, L., Y. Wang and G. P. Downey (2007). "Reactive oxygen and nitrogen species as signaling molecules regulating neutrophil function." Free Radic Biol Med **42**(2): 153-164.

Fiordelisi, A., G. Iaccarino, C. Morisco, E. Coscioni and D. Sorriento (2019). "NFkappaB is a Key Player in the Crosstalk between Inflammation and Cardiovascular Diseases." Int J Mol Sci **20**(7).

Forstermann, U. and H. Kleinert (1995). "Nitric oxide synthase: expression and expressional control of the three isoforms." Naunyn Schmiedebergs Arch Pharmacol **352**(4): 351-364.

Fotakis, G. and J. A. Timbrell (2006). "In vitro cytotoxicity assays: comparison of LDH, neutral red, MTT and protein assay in hepatoma cell lines following exposure to cadmium chloride." Toxicol Lett **160**(2): 171-177.

Franceschi, C., P. Garagnani, P. Parini, C. Giuliani and A. Santoro (2018). "Inflammaging: a new immune-metabolic viewpoint for age-related diseases." Nat Rev Endocrinol **14**(10): 576-590.

Freund, A., A. V. Orjalo, P. Y. Desprez and J. Campisi (2010). "Inflammatory networks during cellular senescence: causes and consequences." Trends Mol Med **16**(5): 238-246.

Fujita, Y. and T. Yamashita (2018). "Sirtuins in Neuroendocrine Regulation and Neurological Diseases." Front Neurosci **12**: 778.

Fulop, T., J. M. Witkowski, F. Olivieri and A. Larbi (2018). "The integration of inflammaging in age-related diseases." Semin Immunol.

Galluzzi, L., E. H. Baehrecke, A. Ballabio, P. Boya, J. M. Bravo-San Pedro, F. Cecconi, A. M. Choi, C. T. Chu, P. Codogno, M. I. Colombo, A. M. Cuervo, J. Debnath, V. Deretic, I. Dikic, E. L. Eskelinen, G. M. Fimia, S. Fulda, D. A. Gewirtz, D. R. Green, M. Hansen, J. W. Harper, M. Jaattela, T. Johansen, G. Juhasz, A. C. Kimmelman, C. Kraft, N. T. Ktistakis, S. Kumar, B. Levine, C. Lopez-Otin, F. Madeo, S. Martens, J. Martinez, A. Melendez, N. Mizushima, C. Munz, L. O. Murphy, J. M. Penninger, M. Piacentini, F. Reggiori, D. C. Rubinsztein, K. M. Ryan, L. Santambrogio, L. Scorrano, A. K. Simon, H. U. Simon, A. Simonsen, N. Tavernarakis, S. A. Tooze, T. Yoshimori, J. Yuan, Z. Yue, Q. Zhong and G. Kroemer (2017). "Molecular definitions of autophagy and related processes." Embo J **36**(13): 1811-1836.

Galluzzi, L., I. Vitale, S. A. Aaronson, J. M. Abrams, D. Adam, P. Agostinis, E. S. Alnemri, L. Altucci, I. Amelio, D. W. Andrews, M. Annicchiarico-Petruzzelli, A. V. Antonov, E. Arama, E. H. Baehrecke, N. A. Barlev, N. G. Bazan, F. Bernassola, M. J. M. Bertrand, K. Bianchi, M. V. Blagosklonny, K. Blomgren, C. Borner, P. Boya, C. Brenner, M. Campanella, E. Candi, D. Carmona-Gutierrez, F. Cecconi, F. K. Chan, N. S. Chandel, E. H. Cheng, J. E. Chipuk, J. A. Cidlowski, A. Ciechanover, G. M. Cohen, M. Conrad, J. R. Cubillos-Ruiz, P. E. Czabotar, V. D'Angiolella, T. M. Dawson, V. L. Dawson, V. De

Laurenzi, R. De Maria, K. M. Debatin, R. J. DeBerardinis, M. Deshmukh, N. Di Daniele, F. Di Virgilio, V. M. Dixit, S. J. Dixon, C. S. Duckett, B. D. Dynlacht, W. S. El-Deiry, J. W. Elrod, G. M. Fimia, S. Fulda, A. J. Garcia-Saez, A. D. Garg, C. Garrido, E. Gavathiotis, P. Golstein, E. Gottlieb, D. R. Green, L. A. Greene, H. Gronemeyer, A. Gross, G. Hajnoczky, J. M. Hardwick, I. S. Harris, M. O. Hengartner, C. Hetz, H. Ichijo, M. Jaattela, B. Joseph, P. J. Jost, P. P. Juin, W. J. Kaiser, M. Karin, T. Kaufmann, O. Kepp, A. Kimchi, R. N. Kitsis, D. J. Klionsky, R. A. Knight, S. Kumar, S. W. Lee, J. J. Lemasters, B. Levine, A. Linkermann, S. A. Lipton, R. A. Lockshin, C. Lopez-Otin, S. W. Lowe, T. Luedde, E. Lugli, M. MacFarlane, F. Madeo, M. Malewicz, W. Malorni, G. Manic, J. C. Marine, S. J. Martin, J. C. Martinou, J. P. Medema, P. Mehlen, P. Meier, S. Melino, E. A. Miao, J. D. Molkentin, U. M. Moll, C. Munoz-Pinedo, S. Nagata, G. Nunez, A. Oberst, M. Oren, M. Overholtzer, M. Pagano, T. Panaretakis, M. Pasparakis, J. M. Penninger, D. M. Pereira, S. Pervaiz, M. E. Peter, M. Piacentini, P. Pinton, J. H. M. Prehn, H. Puthalakath, G. A. Rabinovich, M. Rehm, R. Rizzuto, C. M. P. Rodrigues, D. C. Rubinsztein, T. Rudel, K. M. Ryan, E. Sayan, L. Scorrano, F. Shao, Y. Shi, J. Silke, H. U. Simon, A. Sistigu, B. R. Stockwell, A. Strasser, G. Szabadkai, S. W. G. Tait, D. Tang, N. Tavernarakis, A. Thorburn, Y. Tsujimoto, B. Turk, T. Vanden Berghe, P. Vandenabeele, M. G. Vander Heiden, A. Villunger, H. W. Virgin, K. H. Vousden, D. Vucic, E. F. Wagner, H. Walczak, D. Wallach, Y. Wang, J. A. Wells, W. Wood, J. Yuan, Z. Zakeri, B. Zhivotovsky, L. Zitvogel, G. Melino and G. Kroemer (2018). "Molecular mechanisms of cell death: recommendations of the Nomenclature Committee on Cell Death 2018." Cell Death Differ **25**(3): 486-541.

Gänger, S. and K. Schindowski (2018). "Tailoring Formulations for Intranasal Nose-to-Brain Delivery: A Review on Architecture, Physico-Chemical Characteristics and Mucociliary Clearance of the Nasal Olfactory Mucosa." Pharmaceutics **10**(3).

Gaspar, L. S., A. R. Álvaro, S. Carmo-Silva, A. F. Mendes, A. Relógio and C. Cavadas (2019). "The importance of determining circadian parameters in pharmacological studies." Br J Pharmacol **176**(16): 2827-2847.

Gaspar, L. S., C. Sousa, A. R. Álvaro, C. Cavadas and A. F. Mendes (2020). "Common risk factors and therapeutic targets in obstructive sleep apnea and osteoarthritis: an unexpectable link?" Pharmacological Res: 105369.

Gejjalagere Honnappa, C. and U. Mazhuvancherry Kesavan (2016). "A concise review on advances in development of small molecule anti-inflammatory therapeutics emphasising AMPK: An emerging target." Int J Immunopathol Pharmacol **29**(4): 562-571.

Geng, H., T. Wittwer, O. Dittrich-Breiholz, M. Kracht and M. L. Schmitz (2009). "Phosphorylation of NF-kappaB p65 at Ser468 controls its COMMD1-dependent ubiquitination and target gene-specific proteasomal elimination." EMBO Rep **10**(4): 381-386.

Ghasemi-Pirbaluti, M., E. Motaghi and H. Bozorgi (2017). "The effect of menthol on acute experimental colitis in rats." Eur J Pharmacol **805**: 101-107.

Ghosh, N., A. Ali, R. Ghosh, S. Das, S. C. Mandal and M. Pal (2016). "Chronic Inflammatory Diseases: Progress and Prospect with Herbal Medicine." Curr Pharm Des **22**(2): 247-264.

Gilberg, E., S. Jasial, D. Stumpfe, D. Dimova and J. Bajorath (2016). "Highly Promiscuous Small Molecules from Biological Screening Assays Include Many Pan-Assay Interference Compounds but Also Candidates for Polypharmacology." J Med Chem **59**(22): 10285-10290.

Goldring, M. B. and F. Berenbaum (2015). "Emerging targets in osteoarthritis therapy." Curr Opin Pharmacol **22**: 51-63.

Gomes, P., H. Leal, A. F. Mendes, F. Reis and C. Cavadas (2019). "Dichotomous Sirtuins: Implications for Drug Discovery in Neurodegenerative and Cardiometabolic Diseases." Trends Pharmacol Sci **40**(12): 1021-1039.

Gong, T., L. Liu, W. Jiang and R. Zhou (2020). "DAMP-sensing receptors in sterile inflammation and inflammatory diseases." Nat Rev Immunol **20**(2): 95-112.

Grabowska, W., E. Sikora and A. Bielak-Zmijewska (2017). "Sirtuins, a promising target in slowing down the ageing process." Biogerontology **18**(4): 447-476.

Green, L. C., D. A. Wagner, J. Glogowski, P. L. Skipper, J. S. Wishnok and S. R. Tannenbaum (1982). "Analysis of nitrate, nitrite, and [15N]nitrate in biological fluids." Anal Biochem **126**(1): 131-138.

Grootjans, J., A. Kaser, R. J. Kaufman and R. S. Blumberg (2016). "The unfolded protein response in immunity and inflammation." Nat Rev Immunol **16**(8): 469-484.

Gu, R., B. Lei, C. Jiang and G. Xu (2017). "Glucocorticoid-Induced Leucine Zipper Suppresses ICAM-1 and MCP-1 Expression by Dephosphorylation of NF-kappaB p65 in Retinal Endothelial Cells." Invest Ophthalmol Vis Sci **58**(1): 631-641.

Guimarães, A. G., M. A. Oliveira, S. Alves Rdos, P. Menezes Pdos, M. R. Serafini, A. A. Araújo, D. P. Bezerra and L. J. Quintans Júnior (2015). "Encapsulation of carvacrol, a monoterpene present in the essential oil of oregano, with β-cyclodextrin, improves the pharmacological response on cancer pain experimental protocols." Chem Biol Interact **227**: 69-76.

Gupta, S. C., C. Sundaram, S. Reuter and B. B. Aggarwal (2010). "Inhibiting NF-kappaB activation by small molecules as a therapeutic strategy." Biochim Biophys Acta **1799**(10-12): 775-787.

Gyorfi, A. H., A. E. Matei and J. H. W. Distler (2018). "Targeting TGF-beta signaling for the treatment of fibrosis." Matrix Biol **68-69**: 8-27.

Hahn, W. S., J. Kuzmicic, J. S. Burrill, M. A. Donoghue, R. Foncea, M. D. Jensen, S. Lavandero, E. A. Arriaga and D. A. Bernlohr (2014). "Proinflammatory cytokines differentially regulate adipocyte mitochondrial metabolism, oxidative stress, and dynamics." Am J Physiol Endocrinol Metab **306**(9): E1033-E1045.

Haigis, M. C. and D. A. Sinclair (2010). "Mammalian sirtuins: biological insights and disease relevance." Annu Rev Pathol **5**: 253-295.

Hambleton, J., S. L. Weinstein, L. Lem and A. L. DeFranco (1996). "Activation of c-Jun N-terminal kinase in bacterial lipopolysaccharide-stimulated macrophages." Proc Natl Acad Sci U S A **93**(7): 2774-2778.

Hannemann, N., J. Jordan, S. Paul, S. Reid, H. W. Baenkler, S. Sonnewald, T. Bauerle, J. Vera, G. Schett and A. Bozec (2017). "The AP-1 Transcription Factor c-Jun Promotes Arthritis by Regulating Cyclooxygenase-2 and Arginase-1 Expression in Macrophages." J Immunol **198**(9): 3605-3614.

Harris, D. P., S. Bandyopadhyay, T. J. Maxwell, B. Willard and P. E. DiCorleto (2014). "Tumor necrosis factor (TNF)-alpha induction of CXCL10 in endothelial cells requires protein arginine methyltransferase 5 (PRMT5)-mediated nuclear factor (NF)-kappaB p65 methylation." J Biol Chem **289**(22): 15328-15339.

Harris, D. P., U. M. Chandrasekharan, S. Bandyopadhyay, B. Willard and P. E. DiCorleto (2016). "PRMT5-Mediated Methylation of NF-kappaB p65 at Arg174 Is Required for

Endothelial CXCL11 Gene Induction in Response to TNF-alpha and IFN-gamma Costimulation." PLoS One **11**(2): e0148905.

Harris, J., M. Hartman, C. Roche, S. G. Zeng, A. O'Shea, F. A. Sharp, E. M. Lambe, E. M. Creagh, D. T. Golenbock, J. Tschopp, H. Kornfeld, K. A. Fitzgerald and E. C. Lavelle (2011). "Autophagy controls IL-1beta secretion by targeting pro-IL-1beta for degradation." J Biol Chem **286**(11): 9587-9597.

Harris, S. G., R. S. Smith and R. P. Phipps (2002). "15-deoxy-Delta 12,14-PGJ2 induces IL-8 production in human T cells by a mitogen-activated protein kinase pathway." J Immunol **168**(3): 1372-1379.

Hasnain, S. Z., R. Lourie, I. Das, A. C. Chen and M. A. McGuckin (2012). "The interplay between endoplasmic reticulum stress and inflammation." Immunol Cell Biol **90**(3): 260-270.

Hayden, M. S. and S. Ghosh (2004). "Signaling to NF-kappaB." Genes Dev **18**(18): 2195-2224.

Hayden, M. S. and S. Ghosh (2008). "Shared principles in NF-kappaB signaling." Cell **132**(3): 344-362.

Hayflick, L. (2007). "Biological aging is no longer an unsolved problem." Ann N Y Acad Sci **1100**: 1-13.

Headland, S. E. and L. V. Norling (2015). "The resolution of inflammation: Principles and challenges." Semin Immunol **27**(3): 149-160.

Herlaar, E. and Z. Brown (1999). "p38 MAPK signalling cascades in inflammatory disease." Mol Med Today **5**(10): 439-447.

Hernandez-Segura, A., J. Nehme and M. Demaria (2018). "Hallmarks of Cellular Senescence." Trends Cell Biol **28**(6): 436-453.

Hinz, M. and C. Scheidereit (2014). "The IkappaB kinase complex in NF-kappaB regulation and beyond." EMBO Rep **15**(1): 46-61.

Hochrainer, K., G. Racchumi, S. Zhang, C. Iadecola and J. Anrather (2012). "Monoubiquitination of nuclear RelA negatively regulates NF-kappaB activity independent of proteasomal degradation." Cell Mol Life Sci **69**(12): 2057-2073.

Holmes-McNary, M. and A. S. Baldwin, Jr. (2000). "Chemopreventive properties of trans-resveratrol are associated with inhibition of activation of the IkappaB kinase." Cancer Res **60**(13): 3477-3483.

Hotamisligil, G. S. (2006). "Inflammation and metabolic disorders." Nature **444**: 860.

Hou, Y., F. Moreau and K. Chadee (2012). "PPARgamma is an E3 ligase that induces the degradation of NFkappaB/p65." Nat Commun **3**: 1300.

Hou, Y., Z. Zhang, Q. Xu, H. Wang, Y. Xu and K. Chen (2014). "Inhibitor of growth 4 induces NFkappaB/p65 ubiquitin-dependent degradation." Oncogene **33**(15): 1997-2003.

Howitz, K. T., K. J. Bitterman, H. Y. Cohen, D. W. Lamming, S. Lavu, J. G. Wood, R. E. Zipkin, P. Chung, A. Kisielewski, L. L. Zhang, B. Scherer and D. A. Sinclair (2003). "Small molecule activators of sirtuins extend Saccharomyces cerevisiae lifespan." Nature **425**(6954): 191-196.

Huang, B., X. D. Yang, A. Lamb and L. F. Chen (2010). "Posttranslational modifications of NF-kappaB: another layer of regulation for NF-kappaB signaling pathway." Cell Signal **22**(9): 1282-1290.

Huang, B., X. D. Yang, M. M. Zhou, K. Ozato and L. F. Chen (2009). "Brd4 coactivates transcriptional activation of NF-kappaB via specific binding to acetylated RelA." Mol Cell Biol **29**(5): 1375-1387.

Hughes, J. P., S. Rees, S. B. Kalindjian and K. L. Philpott (2011). "Principles of early drug discovery." Br J Pharmacol **162**(6): 1239-1249.

Huynh, Q. K., H. Boddupalli, S. A. Rouw, C. M. Koboldt, T. Hall, C. Sommers, S. D. Hauser, J. L. Pierce, R. G. Combs, B. A. Reitz, J. A. Diaz-Collier, R. A. Weinberg, B. L. Hood, B. F. Kilpatrick and C. S. Tripp (2000). "Characterization of the recombinant IKK1/IKK2 heterodimer. Mechanisms regulating kinase activity." J Biol Chem **275**(34): 25883-25891.

Hwang, J. W., H. Yao, S. Caito, I. K. Sundar and I. Rahman (2013). "Redox regulation of SIRT1 in inflammation and cellular senescence." Free Radic Biol Med **61**: 95-110.

Ingelsson, M. (2016). "Alpha-Synuclein Oligomers-Neurotoxic Molecules in Parkinson's Disease and Other Lewy Body Disorders." Front Neurosci **10**: 408.

Iside, C., M. Scafuro, A. Nebbioso and L. Altucci (2020). "SIRT1 Activation by Natural Phytochemicals: An Overview." Front Pharmacol **11**: 1225.

Jeon, O. H., N. David, J. Campisi and J. H. Elisseeff (2018). "Senescent cells and osteoarthritis: a painful connection." J Clin Invest **128**(4): 1229-1237.

Jeon, O. H., C. Kim, R. M. Laberge, M. Demaria, S. Rathod, A. P. Vasserot, J. W. Chung, D. H. Kim, Y. Poon, N. David, D. J. Baker, J. M. van Deursen, J. Campisi and J. H. Elisseeff

(2017). "Local clearance of senescent cells attenuates the development of post-traumatic osteoarthritis and creates a pro-regenerative environment." Nat Med **23**(6): 775-781.

Jeon, O. H., D. R. Wilson, C. C. Clement, S. Rathod, C. Cherry, B. Powell, Z. Lee, A. M. Khalil, J. J. Green, J. Campisi, L. Santambrogio, K. W. Witwer and J. H. Elisseeff (2019). "Senescence cell-associated extracellular vesicles serve as osteoarthritis disease and therapeutic markers." JCI Insight **4**(7).

Jin, J., Z. Lu, X. Wang, Y. Liu, T. Han, Y. Wang, T. Wang, M. Gan, C. Xie, J. Wang and B. Yu (2020). "E3 ubiquitin ligase TRIM7 negatively regulates NF-kappa B signaling pathway by degrading p65 in lung cancer." Cell Signal **69**: 109543.

Johnson, C. I., D. J. Argyle and D. N. Clements (2016). "In vitro models for the study of osteoarthritis." Vet J **209**: 40-49.

Jones, D. P. (2006). "Redefining oxidative stress." Antioxid Redox Signal **8**(9-10): 1865-1879.

Kacheva, S., S. Lenzen and E. Gurgul-Convey (2011). "Differential effects of proinflammatory cytokines on cell death and ER stress in insulin-secreting INS1E cells and the involvement of nitric oxide." Cytokine **55**(2): 195-201.

Kaminska, B. (2005). "MAPK signalling pathways as molecular targets for anti-inflammatory therapy--from molecular mechanisms to therapeutic benefits." Biochim Biophys Acta **1754**(1-2): 253-262.

Karin, M. (1995). "The regulation of AP-1 activity by mitogen-activated protein kinases." J Biol Chem **270**(28): 16483-16486.

Karin, M. (1999). "How NF-kappaB is activated: the role of the IkappaB kinase (IKK) complex." Oncogene **18**(49): 6867-6874.

Karousou, R., M. Balta, E. Hanlidou and S. Kokkini (2007). ""Mints", smells and traditional uses in Thessaloniki (Greece) and other Mediterranean countries." J Ethnopharmacol **109**(2): 248-257.

Kauppinen, A., T. Suuronen, J. Ojala, K. Kaarniranta and A. Salminen (2013). "Antagonistic crosstalk between NF-kappaB and SIRT1 in the regulation of inflammation and metabolic disorders." Cell Signal **25**(10): 1939-1948.

Kennedy, B. K., S. L. Berger, A. Brunet, J. Campisi, A. M. Cuervo, E. S. Epel, C. Franceschi, G. J. Lithgow, R. I. Morimoto, J. E. Pessin, T. A. Rando, A. Richardson, E. E.

Schadt, T. Wyss-Coray and F. Sierra (2014). "Geroscience: linking aging to chronic disease." Cell **159**(4): 709-713.

Kesselmeier, J. and M. Staudt (1999). "Biogenic Volatile Organic Compounds (VOC): An Overview on Emission, Physiology and Ecology." J Atmos Chem **33**(1): 23-88.

Kiernan, R., V. Bres, R. W. Ng, M. P. Coudart, S. El Messaoudi, C. Sardet, D. Y. Jin, S. Emiliani and M. Benkirane (2003). "Post-activation turn-off of NF-kappa B-dependent transcription is regulated by acetylation of p65." J Biol Chem **278**(4): 2758-2766.

Kikuchi, T., T. Matsuguchi, N. Tsuboi, A. Mitani, S. Tanaka, M. Matsuoka, G. Yamamoto, T. Hishikawa, T. Noguchi and Y. Yoshikai (2001). "Gene expression of osteoclast differentiation factor is induced by lipopolysaccharide in mouse osteoblasts via Toll-like receptors." J Immunol **166**(5): 3574-3579.

Killeen, M. J., M. Linder, P. Pontoniere and R. Crea (2014). "NF-kappabeta signaling and chronic inflammatory diseases: exploring the potential of natural products to drive new therapeutic opportunities." Drug Discov Today **19**(4): 373-378.

Kim, E. K. and E. J. Choi (2015). "Compromised MAPK signaling in human diseases: an update." Arch Toxicol **89**(6): 867-882.

Kim, K. N., Y. J. Ko, H. M. Yang, Y. M. Ham, S. W. Roh, Y. J. Jeon, G. Ahn, M. C. Kang, W. J. Yoon, D. Kim and T. Oda (2013). "Anti-inflammatory effect of essential oil and its constituents from fingered citron (Citrus medica L. var. sarcodactylis) through blocking JNK, ERK and NF-kappaB signaling pathways in LPS-activated RAW 264.7 cells." Food Chem Toxicol **57**: 126-131.

Klaips, C. L., G. G. Jayaraj and F. U. Hartl (2018). "Pathways of cellular proteostasis in aging and disease." J Cell Biol **217**(1): 51.

Kolaczkowska, E. and P. Kubes (2013). "Neutrophil recruitment and function in health and inflammation." Nat Rev Immunol **13**(3): 159-175.

Kotas, M. E. and R. Medzhitov (2015). "Homeostasis, inflammation, and disease susceptibility." Cell **160**(5): 816-827.

Kryczka, J. and J. Boncela (2017). "Proteases Revisited: Roles and Therapeutic Implications in Fibrosis." Mediators Inflamm **2017**: 2570154.

Kulkarni, O. P., J. Lichtnekert, H. J. Anders and S. R. Mulay (2016). "The Immune System in Tissue Environments Regaining Homeostasis after Injury: Is "Inflammation" Always Inflammation?" Mediators Inflamm **2016**: 2856213.

Kumar, A., Y. Takada, A. M. Boriek and B. B. Aggarwal (2004). "Nuclear factor-kappaB: its role in health and disease." J Mol Med (Berl) **82**(7): 434-448.

Kumar, R. P. and A. Abraham (2017). "Inhibition of LPS induced pro-inflammatory responses in RAW 264.7 macrophage cells by PVP-coated naringenin nanoparticle via down regulation of NF-kappaB/P38MAPK mediated stress signaling." Pharmacol Rep **69**(5): 908-915.

Labbadia, J. and R. I. Morimoto (2015). "The biology of proteostasis in aging and disease." Annu Rev Biochem **84**: 435-464.

Lapaquette, P., J. Guzzo, L. Bretillon and M. A. Bringer (2015). "Cellular and Molecular Connections between Autophagy and Inflammation." Mediators Inflamm **2015**: 398483.

Lee, A. S., Y. J. Jung, D. Kim, T. Nguyen-Thanh, K. P. Kang, S. Lee, S. K. Park and W. Kim (2014). "SIRT2 ameliorates lipopolysaccharide-induced inflammation in macrophages." Biochem Biophys Res Commun **450**(4): 1363-1369.

Lee, J. I. and G. J. Burckart (1998). "Nuclear factor kappa B: important transcription factor and therapeutic target." J Clin Pharmacol **38**(11): 981-993.

Leidal, A. M., B. Levine and J. Debnath (2018). "Autophagy and the cell biology of age-related disease." Nat Cell Biol **20**(12): 1338-1348.

Levy, D., A. J. Kuo, Y. Chang, U. Schaefer, C. Kitson, P. Cheung, A. Espejo, B. M. Zee, C. L. Liu, S. Tangsombatvisit, R. I. Tennen, A. Y. Kuo, S. Tanjing, R. Cheung, K. F. Chua, P. J. Utz, X. Shi, R. K. Prinjha, K. Lee, B. A. Garcia, M. T. Bedford, A. Tarakhovsky, X. Cheng and O. Gozani (2011). "Lysine methylation of the NF-kappaB subunit RelA by SETD6 couples activity of the histone methyltransferase GLP at chromatin to tonic repression of NF-kappaB signaling." Nat Immunol **12**(1): 29-36.

Li, J., T. Lan, C. Zhang, C. Zeng, J. Hou, Z. Yang, M. Zhang, J. Liu and B. Liu (2015). "Reciprocal activation between IL-6/STAT3 and NOX4/Akt signalings promotes proliferation and survival of non-small cell lung cancer cells." Oncotarget **6**(2): 1031-1048.

Li, S., L. Wang, M. A. Berman, Y. Zhang and M. E. Dorf (2006). "RNAi screen in mouse astrocytes identifies phosphatases that regulate NF-kappaB signaling." Mol Cell **24**(4): 497-509.

Li, Z., C. Hua, X. Pan, X. Fu and W. Wu (2016). "Carvacrol Exerts Neuroprotective Effects Via Suppression of the Inflammatory Response in Middle Cerebral Artery Occlusion Rats." Inflammation **39**(4): 1566-1572.

Lin, G. D. and R. W. Li (2018). Chapter 10 - Natural Products Targeting Inflammation Processes and Multiple Mediators. Natural Products and Drug Discovery. S. C. Mandal, V. Mandal and T. Konishi, Elsevier**:** 277-308.

Lin, J., B. Sun, C. Jiang, H. Hong and Y. Zheng (2013). "Sirt2 suppresses inflammatory responses in collagen-induced arthritis." Biochem Biophys Res Commun **441**(4): 897-903.

Liu-Bryan, R. and R. Terkeltaub (2015). "Emerging regulators of the inflammatory process in osteoarthritis." Nat Rev Rheumatol **11**(1): 35-44.

Liu, W., X. Ouyang, J. Yang, J. Liu, Q. Li, Y. Gu, M. Fukata, T. Lin, J. C. He, M. Abreu, J. C. Unkeless, L. Mayer and H. Xiong (2009). "AP-1 activated by toll-like receptors regulates expression of IL-23 p19." J Biol Chem **284**(36): 24006-24016.

Liu, Y., P. W. Smith and D. R. Jones (2006). "Breast cancer metastasis suppressor 1 functions as a corepressor by enhancing histone deacetylase 1-mediated deacetylation of RelA/p65 and promoting apoptosis." Mol Cell Biol **26**(23): 8683-8696.

Lopez-Armada, M. J., B. Carames, M. Lires-Dean, B. Cillero-Pastor, C. Ruiz-Romero, F. Galdo and F. J. Blanco (2006). "Cytokines, tumor necrosis factor-alpha and interleukin-1beta, differentially regulate apoptosis in osteoarthritis cultured human chondrocytes." Osteoarthritis Cartilage **14**(7): 660-669.

Lopez-Armada, M. J., B. Carames, M. A. Martin, B. Cillero-Pastor, M. Lires-Dean, I. Fuentes-Boquete, J. Arenas and F. J. Blanco (2006). "Mitochondrial activity is modulated by TNFalpha and IL-1beta in normal human chondrocyte cells." Osteoarthritis Cartilage **14**(10): 1011-1022.

Lopez-Armada, M. J., R. R. Riveiro-Naveira, C. Vaamonde-Garcia and M. N. Valcarcel-Ares (2013). "Mitochondrial dysfunction and the inflammatory response." Mitochondrion **13**(2): 106-118.

Lopez-Otin, C., M. A. Blasco, L. Partridge, M. Serrano and G. Kroemer (2013). "The hallmarks of aging." Cell **153**(6): 1194-1217.

Lu, T., M. W. Jackson, B. Wang, M. Yang, M. R. Chance, M. Miyagi, A. V. Gudkov and G. R. Stark (2010). "Regulation of NF-kappaB by NSD1/FBXL11-dependent reversible lysine methylation of p65." Proc Natl Acad Sci U S A **107**(1): 46-51.

Lu, T. and G. R. Stark (2015). "NF-kappaB: Regulation by Methylation." Cancer Res **75**(18): 3692-3695.

Mahboubi, M. (2017). "Mentha spicata as natural analgesia for treatment of pain in osteoarthritis patients." Complement Ther Clin Pract **26**: 1-4.

Mahmoudi, S., L. Xu and A. Brunet (2019). "Turning back time with emerging rejuvenation strategies." Nat Cell Biol **21**(1): 32-43.

Maine, G. N., X. Mao, C. M. Komarck and E. Burstein (2007). "COMMD1 promotes the ubiquitination of NF-kappaB subunits through a cullin-containing ubiquitin ligase." Embo j **26**(2): 436-447.

Malaquin, N., A. Martinez and F. Rodier (2016). "Keeping the senescence secretome under control: Molecular reins on the senescence-associated secretory phenotype." Exp Gerontol **82**: 39-49.

Maneiro, E., M. J. Lopez-Armada, M. C. de Andres, B. Carames, M. A. Martin, A. Bonilla, P. Del Hoyo, F. Galdo, J. Arenas and F. J. Blanco (2005). "Effect of nitric oxide on mitochondrial respiratory activity of human articular chondrocytes." Ann Rheum Dis **64**(3): 388-395.

Manna, S. K., A. Mukhopadhyay and B. B. Aggarwal (2000). "Resveratrol suppresses TNF-induced activation of nuclear transcription factors NF-kappa B, activator protein-1, and apoptosis: potential role of reactive oxygen intermediates and lipid peroxidation." J Immunol **164**(12): 6509-6519.

Mao, X., N. Gluck, D. Li, G. N. Maine, H. Li, I. W. Zaidi, A. Repaka, M. W. Mayo and E. Burstein (2009). "GCN5 is a required cofactor for a ubiquitin ligase that targets NF-kappaB/RelA." Genes Dev **23**(7): 849-861.

Mariathasan, S., D. S. Weiss, K. Newton, J. McBride, K. O'Rourke, M. Roose-Girma, W. P. Lee, Y. Weinrauch, D. M. Monack and V. M. Dixit (2006). "Cryopyrin activates the inflammasome in response to toxins and ATP." Nature **440**(7081): 228-232.

Marques, F. M., M. M. Figueira, E. F. P. Schmitt, T. P. Kondratyuk, D. C. Endringer, R. Scherer and M. Fronza (2019). "In vitro anti-inflammatory activity of terpenes via suppression of superoxide and nitric oxide generation and the NF-kappaB signalling pathway." Inflammopharmacology **27**(2): 281-289.

Martel-Pelletier, J., A. J. Barr, F. M. Cicuttini, P. G. Conaghan, C. Cooper, M. B. Goldring, S. R. Goldring, G. Jones, A. J. Teichtahl and J. P. Pelletier (2016). "Osteoarthritis." Nat Rev Dis Primers **2**: 16072.

Martin, J. A., T. D. Brown, A. D. Heiner and J. A. Buckwalter (2004). "Chondrocyte senescence, joint loading and osteoarthritis." Clin Orthop Relat Res(427 Suppl): S96-103.

Martin, M. U. and H. Wesche (2002). "Summary and comparison of the signaling mechanisms of the Toll/interleukin-1 receptor family." Biochim Biophys Acta **1592**(3): 265-280.

Martin, S. J. (2016). "Cell death and inflammation: the case for IL-1 family cytokines as the canonical DAMPs of the immune system." Febs j **283**(14): 2599-2615.

Martins, A. S., I. Alves, L. Helguero, M. R. Domingues and B. M. Neves (2016). "The Unfolded Protein Response in Homeostasis and Modulation of Mammalian Immune Cells." Int Rev Immunol **35**(6): 457-476.

Mattioli, I., H. Geng, A. Sebald, M. Hodel, C. Bucher, M. Kracht and M. L. Schmitz (2006). "Inducible phosphorylation of NF-kappa B p65 at serine 468 by T cell costimulation is mediated by IKK epsilon." J Biol Chem **281**(10): 6175-6183.

Mauro, C., S. C. Leow, E. Anso, S. Rocha, A. K. Thotakura, L. Tornatore, M. Moretti, E. De Smaele, A. A. Beg, V. Tergaonkar, N. S. Chandel and G. Franzoso (2011). "NF-kappaB controls energy homeostasis and metabolic adaptation by upregulating mitochondrial respiration." Nat Cell Biol **13**(10): 1272-1279.

McIntyre, R. L., E. G. Daniels, M. Molenaars, R. H. Houtkooper and G. E. Janssens (2019). "From molecular promise to preclinical results: HDAC inhibitors in the race for healthy aging drugs." EMBO Mol Med **11**(9): e9854.

Medzhitov, R. (2008). "Origin and physiological roles of inflammation." Nature **454**(7203): 428-435.

Medzhitov, R. (2010). "Inflammation 2010: new adventures of an old flame." Cell **140**(6): 771-776.

Mendes, A. F., M. M. Caramona, A. P. Carvalho and M. C. Lopes (2003). "Differential roles of hydrogen peroxide and superoxide in mediating IL-1-induced NF-kappa B activation and iNOS expression in bovine articular chondrocytes." J Cell Biochem **88**(4): 783-793.

Mendes, K. L., D. F. Lelis and S. H. S. Santos (2017). "Nuclear sirtuins and inflammatory signaling pathways." Cytokine Growth Factor Rev **38**: 98-105.

Mendes Sdos, S., A. Candi, M. Vansteenbrugge, M. R. Pignon, H. Bult, K. Z. Boudjeltia, C. Munaut and M. Raes (2009). "Microarray analyses of the effects of NF-kappaB or PI3K

pathway inhibitors on the LPS-induced gene expression profile in RAW264.7 cells: synergistic effects of rapamycin on LPS-induced MMP9-overexpression." Cell Signal **21**(7): 1109-1122.

Meng, Q. and Y. Xia (2011). "c-Jun, at the crossroad of the signaling network." Protein Cell **2**(11): 889-898.

Mengshol, J. A., M. P. Vincenti and C. E. Brinckerhoff (2001). "IL-1 induces collagenase-3 (MMP-13) promoter activity in stably transfected chondrocytic cells: requirement for Runx-2 and activation by p38 MAPK and JNK pathways." Nucleic Acids Res **29**(21): 4361-4372.

Miguel, M. G. (2010). "Antioxidant and anti-inflammatory activities of essential oils: a short review." Molecules **15**(12): 9252-9287.

Mimica-Dukic, N. and B. Bozin (2008). "Mentha L. species (Lamiaceae) as promising sources of bioactive secondary metabolites." Curr Pharm Des **14**(29): 3141-3150.

Mitchell, J. P. and R. J. Carmody (2018). "NF-kappaB and the Transcriptional Control of Inflammation." Int Rev Cell Mol Biol **335**: 41-84.

Mitchell, S., J. Vargas and A. Hoffmann (2016). "Signaling via the NFkappaB system." Wiley Interdiscip Rev Syst Biol Med **8**(3): 227-241.

Motori, E., J. Puyal, N. Toni, A. Ghanem, C. Angeloni, M. Malaguti, G. Cantelli-Forti, B. Berninger, K.-K. Conzelmann, M. Götz, Konstanze F. Winklhofer, S. Hrelia and M. Bergami (2013). "Inflammation-Induced Alteration of Astrocyte Mitochondrial Dynamics Requires Autophagy for Mitochondrial Network Maintenance." Cell Metabolism **18**(6): 844-859.

Mraz, M. and M. Haluzik (2014). "The role of adipose tissue immune cells in obesity and low-grade inflammation." J Endocrinol **222**(3): R113-127.

Mulero, M. C., T. Huxford and G. Ghosh (2019). "NF-kappaB, IkappaB, and IKK: Integral Components of Immune System Signaling." Adv Exp Med Biol **1172**: 207-226.

Muruganathan, U. and S. Srinivasan (2016). "Beneficial effect of carvone, a dietary monoterpene ameliorates hyperglycemia by regulating the key enzymes activities of carbohydrate metabolism in streptozotocin-induced diabetic rats." Biomed Pharmacother **84**: 1558-1567.

Nagoor Meeran, M. F., G. S. Jagadeesh and P. Selvaraj (2015). "Thymol attenuates inflammation in isoproterenol induced myocardial infarcted rats by inhibiting the release of

lysosomal enzymes and downregulating the expressions of proinflammatory cytokines." Eur J Pharmacol **754**: 153-161.

Nagy, G., J. M. Clark, E. I. Buzas, C. L. Gorman and A. P. Cope (2007). "Nitric oxide, chronic inflammation and autoimmunity." Immunol Lett **111**(1): 1-5.

Nakahira, K., J. A. Haspel, V. A. Rathinam, S. J. Lee, T. Dolinay, H. C. Lam, J. A. Englert, M. Rabinovitch, M. Cernadas, H. P. Kim, K. A. Fitzgerald, S. W. Ryter and A. M. Choi (2011). "Autophagy proteins regulate innate immune responses by inhibiting the release of mitochondrial DNA mediated by the NALP3 inflammasome." Nat Immunol **12**(3): 222-230.

Nathan, C. and A. Ding (2010). "Nonresolving inflammation." Cell **140**(6): 871-882.

Netea-Maier, R. T., T. S. Plantinga, F. L. van de Veerdonk, J. W. Smit and M. G. Netea (2016). "Modulation of inflammation by autophagy: Consequences for human disease." Autophagy **12**(2): 245-260.

Netea, M. G., F. Balkwill, M. Chonchol, F. Cominelli, M. Y. Donath, E. J. Giamarellos-Bourboulis, D. Golenbock, M. S. Gresnigt, M. T. Heneka, H. M. Hoffman, R. Hotchkiss, L. A. B. Joosten, D. L. Kastner, M. Korte, E. Latz, P. Libby, T. Mandrup-Poulsen, A. Mantovani, K. H. G. Mills, K. L. Nowak, L. A. O'Neill, P. Pickkers, T. van der Poll, P. M. Ridker, J. Schalkwijk, D. A. Schwartz, B. Siegmund, C. J. Steer, H. Tilg, J. W. M. van der Meer, F. L. van de Veerdonk and C. A. Dinarello (2017). "A guiding map for inflammation." Nat Immunol **18**(8): 826-831.

Nita, M., A. Grzybowski, F. J. Ascaso and V. Huerva (2014). "Age-related macular degeneration in the aspect of chronic low-grade inflammation (pathophysiological parainflammation)." Mediators Inflamm **2014**: 930671.

O'Brien, J., I. Wilson, T. Orton and F. Pognan (2000). "Investigation of the Alamar Blue (resazurin) fluorescent dye for the assessment of mammalian cell cytotoxicity." Eur J Biochem **267**(17): 5421-5426.

O'Dea, E. and A. Hoffmann (2009). "NF-κB signaling." Wiley Interdiscip Rev Syst Biol Med **1**(1): 107-115.

Oppenheimer, H., A. Kumar, H. Meir, I. Schwartz, A. Zini, A. Haze, L. Kandel, Y. Mattan, M. Liebergall and M. Dvir-Ginzberg (2014). "Set7/9 impacts COL2A1 expression through binding and repression of SirT1 histone deacetylation." J Bone Miner Res **29**(2): 348-360.

Osorio, F. G., C. Soria-Valles, O. Santiago-Fernandez, J. M. Freije and C. Lopez-Otin (2016). "NF-kappaB signaling as a driver of ageing." Int Rev Cell Mol Biol **326**: 133-174.

Pahl, H. L. (1999). "Activators and target genes of Rel/NF-kappaB transcription factors." Oncogene **18**(49): 6853-6866.

Pais, T. F., E. M. Szego, O. Marques, L. Miller-Fleming, P. Antas, P. Guerreiro, R. M. de Oliveira, B. Kasapoglu and T. F. Outeiro (2013). "The NAD-dependent deacetylase sirtuin 2 is a suppressor of microglial activation and brain inflammation." Embo J **32**(19): 2603-2616.

Pandey, S., T. Kawai and S. Akira (2014). "Microbial sensing by Toll-like receptors and intracellular nucleic acid sensors." Cold Spring Harb Perspect Biol **7**(1): a016246.

Park, J. M., S. H. Jo, M. Y. Kim, T. H. Kim and Y. H. Ahn (2015). "Role of transcription factor acetylation in the regulation of metabolic homeostasis." Protein Cell **6**(11): 804-813.

Patel, M. N., R. G. Carroll, S. Galvan-Pena, E. L. Mills, R. Olden, M. Triantafilou, A. I. Wolf, C. E. Bryant, K. Triantafilou and S. L. Masters (2017). "Inflammasome Priming in Sterile Inflammatory Disease." Trends Mol Med **23**(2): 165-180.

Perkins, N. D. (2007). "Integrating cell-signalling pathways with NF-kappaB and IKK function." Nat Rev Mol Cell Biol **8**(1): 49-62.

Perkins, N. D. and T. D. Gilmore (2006). "Good cop, bad cop: the different faces of NF-kappaB." Cell Death Differ **13**(5): 759-772.

Pfaffl, M. W. (2001). "A new mathematical model for relative quantification in real-time RT-PCR." Nucleic Acids Res **29**(9): e45.

Pierce, J. W., R. Schoenleber, G. Jesmok, J. Best, S. A. Moore, T. Collins and M. E. Gerritsen (1997). "Novel inhibitors of cytokine-induced IkappaBalpha phosphorylation and endothelial cell adhesion molecule expression show anti-inflammatory effects in vivo." J Biol Chem **272**(34): 21096-21103.

Poltorak, A., X. He, I. Smirnova, M. Y. Liu, C. Van Huffel, X. Du, D. Birdwell, E. Alejos, M. Silva, C. Galanos, M. Freudenberg, P. Ricciardi-Castagnoli, B. Layton and B. Beutler (1998). "Defective LPS signaling in C3H/HeJ and C57BL/10ScCr mice: mutations in Tlr4 gene." Science **282**(5396): 2085-2088.

Poulain-Godefroy, O., O. Le Bacquer, P. Plancq, C. Lecoeur, F. Pattou, G. Fruhbeck and P. Froguel (2010). "Inflammatory role of Toll-like receptors in human and murine adipose tissue." Mediators Inflamm **2010**: 823486.

Prabst, K., H. Engelhardt, S. Ringgeler and H. Hubner (2017). "Basic Colorimetric Proliferation Assays: MTT, WST, and Resazurin." Methods Mol Biol **1601**: 1-17.

Price, J. S., J. G. Waters, C. Darrah, C. Pennington, D. R. Edwards, S. T. Donell and I. M. Clark (2002). "The role of chondrocyte senescence in osteoarthritis." Aging Cell **1**(1): 57-65.

Qian, M., X. Fang and X. Wang (2017). "Autophagy and inflammation." Clin Transl Med **6**(1): 24.

Rampersad, S. N. (2012). "Multiple applications of Alamar Blue as an indicator of metabolic function and cellular health in cell viability bioassays." Sensors (Basel) **12**(9): 12347-12360.

Rea, I. M., D. S. Gibson, V. McGilligan, S. E. McNerlan, H. D. Alexander and O. A. Ross (2018). "Age and Age-Related Diseases: Role of Inflammation Triggers and Cytokines." Front Immunol **9**: 586.

Reber, L., L. Vermeulen, G. Haegeman and N. Frossard (2009). "Ser276 phosphorylation of NF-kB p65 by MSK1 controls SCF expression in inflammation." PLoS One **4**(2): e4393.

Recio, M. C., I. Andujar and J. L. Rios (2012). "Anti-inflammatory agents from plants: progress and potential." Curr Med Chem **19**(14): 2088-2103.

Remst, D. F., E. N. Blaney Davidson and P. M. van der Kraan (2015). "Unravelling osteoarthritis-related synovial fibrosis: a step closer to solving joint stiffness." Rheumatology (Oxford) **54**(11): 1954-1963.

Robinson, W. H., C. M. Lepus, Q. Wang, H. Raghu, R. Mao, T. M. Lindstrom and J. Sokolove (2016). "Low-grade inflammation as a key mediator of the pathogenesis of osteoarthritis." Nat Rev Rheumatol **12**(10): 580-592.

Rock, K. L., E. Latz, F. Ontiveros and H. Kono (2010). "The sterile inflammatory response." Annu Rev Immunol **28**: 321-342.

Roget, K., A. Ben-Addi, A. Mambole-Dema, T. Gantke, H. T. Yang, J. Janzen, N. Morrice, D. Abbott and S. C. Ley (2012). "IkappaB kinase 2 regulates TPL-2 activation of extracellular signal-regulated kinases 1 and 2 by direct phosphorylation of TPL-2 serine 400." Mol Cell Biol **32**(22): 4684-4690.

Rosa, S. C., J. Goncalves, F. Judas, A. Mobasheri, C. Lopes and A. F. Mendes (2009). "Impaired glucose transporter-1 degradation and increased glucose transport and oxidative

stress in response to high glucose in chondrocytes from osteoarthritic versus normal human cartilage." Arthritis Res Ther **11**(3): R80.

Rosa, S. C., F. Judas, M. C. Lopes and A. F. Mendes (2008). "Nitric oxide synthase isoforms and NF-kappaB activity in normal and osteoarthritic human chondrocytes: regulation by inducible nitric oxide." Nitric Oxide **19**(3): 276-283.

Rothgiesser, K. M., S. Erener, S. Waibel, B. Luscher and M. O. Hottiger (2010). "SIRT2 regulates NF-kappaB dependent gene expression through deacetylation of p65 Lys310." J Cell Sci **123**(Pt 24): 4251-4258.

Rothgiesser, K. M., M. Fey and M. O. Hottiger (2010). "Acetylation of p65 at lysine 314 is important for late NF-kappaB-dependent gene expression." BMC Genomics **11**: 22.

Roy, A., M. Srivastava, U. Saqib, D. Liu, S. M. Faisal, S. Sugathan, S. Bishnoi and M. S. Baig (2016). "Potential therapeutic targets for inflammation in toll-like receptor 4 (TLR4)-mediated signaling pathways." Int Immunopharmacol **40**: 79-89.

Rufino, A. T., I. Ferreira, F. Judas, L. Salgueiro, M. C. Lopes, C. Cavaleiro and A. F. Mendes (2015). "Differential effects of the essential oils of Lavandula luisieri and Eryngium duriaei subsp. juresianum in cell models of two chronic inflammatory diseases." Pharm Biol **53**(8): 1220-1230.

Rufino, A. T., M. Ribeiro, F. Judas, L. Salgueiro, M. C. Lopes, C. Cavaleiro and A. F. Mendes (2014). "Anti-inflammatory and chondroprotective activity of (+)-alpha-pinene: structural and enantiomeric selectivity." J Nat Prod **77**(2): 264-269.

Rufino, A. T., M. Ribeiro, C. Sousa, F. Judas, L. Salgueiro, C. Cavaleiro and A. F. Mendes (2015). "Evaluation of the anti-inflammatory, anti-catabolic and pro-anabolic effects of E-caryophyllene, myrcene and limonene in a cell model of osteoarthritis." Eur J Pharmacol **750**: 141-150.

Ryo, A., F. Suizu, Y. Yoshida, K. Perrem, Y. C. Liou, G. Wulf, R. Rottapel, S. Yamaoka and K. P. Lu (2003). "Regulation of NF-kappaB signaling by Pin1-dependent prolyl isomerization and ubiquitin-mediated proteolysis of p65/RelA." Mol Cell **12**(6): 1413-1426.

Sabio, G. and R. J. Davis (2014). "TNF and MAP kinase signalling pathways." Semin Immunol **26**(3): 237-245.

Sabir, S. M., D. Singh and J. B. T. Rocha (2015). "In Vitro Antioxidant Activity of S-Carvone Isolated from Zanthoxylum alatum." Pharm Chem J **49**(3): 187-191.

Saccani, S., I. Marazzi, A. A. Beg and G. Natoli (2004). "Degradation of promoter-bound p65/RelA is essential for the prompt termination of the nuclear factor kappaB response." J Exp Med **200**(1): 107-113.

Sakurai, H. (2012). "Targeting of TAK1 in inflammatory disorders and cancer." Trends Pharmacol Sci **33**(10): 522-530.

Sakurai, H., H. Chiba, H. Miyoshi, T. Sugita and W. Toriumi (1999). "IkappaB kinases phosphorylate NF-kappaB p65 subunit on serine 536 in the transactivation domain." J Biol Chem **274**(43): 30353-30356.

Salminen, A. and K. Kaarniranta (2009). "NF-kappaB signaling in the aging process." J Clin Immunol **29**(4): 397-405.

Samavati, L., I. Lee, I. Mathes, F. Lottspeich and M. Hüttemann (2008). "Tumor Necrosis Factor α Inhibits Oxidative Phosphorylation through Tyrosine Phosphorylation at Subunit I of Cytochrome c Oxidase." J Biol Chem **283**(30): 21134-21144.

Sato, S., H. Sanjo, K. Takeda, J. Ninomiya-Tsuji, M. Yamamoto, T. Kawai, K. Matsumoto, O. Takeuchi and S. Akira (2005). "Essential function for the kinase TAK1 in innate and adaptive immune responses." Nat Immunol **6**(11): 1087-1095.

Schaefer, L. (2014). "Complexity of danger: the diverse nature of damage-associated molecular patterns." J Biol Chem **289**(51): 35237-35245.

Scheibel, M., B. Klein, H. Merkle, M. Schulz, R. Fritsch, F. R. Greten, M. C. Arkan, G. Schneider and R. M. Schmid (2010). "IkappaBbeta is an essential co-activator for LPS-induced IL-1beta transcription in vivo." J Exp Med **207**(12): 2621-2630.

Schmitz, M. L. and P. A. Baeuerle (1995). "Multi-step activation of NF-kappa B/Rel transcription factors." Immunobiology **193**(2-4): 116-127.

Schoonbroodt, S., V. Ferreira, M. Best-Belpomme, J. R. Boelaert, S. Legrand-Poels, M. Korner and J. Piette (2000). "Crucial role of the amino-terminal tyrosine residue 42 and the carboxyl-terminal PEST domain of I kappa B alpha in NF-kappa B activation by an oxidative stress." J Immunol **164**(8): 4292-4300.

Schreiner, B., J. Voss, J. Wischhusen, Y. Dombrowski, A. Steinle, H. Lochmuller, M. Dalakas, A. Melms and H. Wiendl (2006). "Expression of toll-like receptors by human muscle cells in vitro and in vivo: TLR3 is highly expressed in inflammatory and HIV myopathies, mediates IL-8 release and up-regulation of NKG2D-ligands." Faseb j **20**(1): 118-120.

Schuliga, M. (2015). "NF-kappaB Signaling in Chronic Inflammatory Airway Disease." Biomolecules **5**(3): 1266-1283.

Schwabe, R. F. and H. Sakurai (2005). "IKKbeta phosphorylates p65 at S468 in transactivaton domain 2." Faseb j **19**(12): 1758-1760.

Seals, D. R., J. N. Justice and T. J. LaRocca (2016). "Physiological geroscience: targeting function to increase healthspan and achieve optimal longevity." J Physiol **594**(8): 2001-2024.

Sen, R. and D. Baltimore (1986). "Inducibility of kappa immunoglobulin enhancer-binding protein Nf-kappa B by a posttranslational mechanism." Cell **47**(6): 921-928.

Sen, R. and D. Baltimore (1986). "Multiple nuclear factors interact with the immunoglobulin enhancer sequences." Cell **46**(5): 705-716.

Sepúlveda-Arias, J. C., L. A. Veloza, L. M. Escobar, L. M. Orozco and I. A. Lopera (2013). "Anti-inflammatory effects of the main constituents and epoxides derived from essential oils obtained from Tagetes lucida, Cymbopogon citratus, Lipia alba and Eucalyptus citriodora." The Journal of Essential Oil Research **25**(3): 186-193.

Serhan, C. N. (2017). "Treating inflammation and infection in the 21st century: new hints from decoding resolution mediators and mechanisms." FASEB J **31**(4): 1273-1288.

Serrano, R. L., L. Y. Chen, M. K. Lotz, R. Liu-Bryan and R. Terkeltaub (2018). "Impaired Proteasomal Function in Human Osteoarthritic Chondrocytes Can Contribute to Decreased Levels of SOX9 and Aggrecan." Arthritis Rheumatol **70**(7): 1030-1041.

Shaulian, E. and M. Karin (2002). "AP-1 as a regulator of cell life and death." Nat Cell Biol **4**(5): E131-136.

Shen, Z., J. M. Ajmo, C. Q. Rogers, X. Liang, L. Le, M. M. Murr, Y. Peng and M. You (2009). "Role of SIRT1 in regulation of LPS- or two ethanol metabolites-induced TNF-alpha production in cultured macrophage cell lines." Am J Physiol Gastrointest Liver Physiol **296**(5): G1047-1053.

Shi, C. S., K. Shenderov, N. N. Huang, J. Kabat, M. Abu-Asab, K. A. Fitzgerald, A. Sher and J. H. Kehrl (2012). "Activation of autophagy by inflammatory signals limits IL-1beta production by targeting ubiquitinated inflammasomes for destruction." Nat Immunol **13**(3): 255-263.

Shimada, K., Timothy R. Crother, J. Karlin, J. Dagvadorj, N. Chiba, S. Chen, V. K. Ramanujan, Andrea J. Wolf, L. Vergnes, David M. Ojcius, A. Rentsendorj, M. Vargas, C.

Guerrero, Y. Wang, Katherine A. Fitzgerald, David M. Underhill, T. Town and M. Arditi (2012). "Oxidized Mitochondrial DNA Activates the NLRP3 Inflammasome during Apoptosis." Immunity **36**(3): 401-414.

Shin, C., Y. Ito, S. Ichikawa, M. Tokunaga, K. Sakata-Sogawa and T. Tanaka (2017). "MKRN2 is a novel ubiquitin E3 ligase for the p65 subunit of NF-kappaB and negatively regulates inflammatory responses." Sci Rep **7**: 46097.

Sierra, F. (2016). "The Emergence of Geroscience as an Interdisciplinary Approach to the Enhancement of Health Span and Life Span." Cold Spring Harb Perspect Med **6**(4): a025163.

Sillat, T., G. Barreto, P. Clarijs, A. Soininen, M. Ainola, J. Pajarinen, M. Korhonen, Y. T. Konttinen, R. Sakalyte, M. Hukkanen, P. Ylinen and D. C. E. Nordström (2013). "Toll-like receptors in human chondrocytes and osteoarthritic cartilage." Acta Orthop **84**(6): 585-592.

Singh, P. and A. K. Pandey (2018). "Prospective of Essential Oils of the Genus Mentha as Biopesticides: A Review." Front Plant Sci **9**(1295).

Sivandzade, F., S. Prasad, A. Bhalerao and L. Cucullo (2019). "NRF2 and NF-B interplay in cerebrovascular and neurodegenerative disorders: Molecular mechanisms and possible therapeutic approaches." Redox Biol **21**: 101059.

Snyder, C. M., E. H. Shroff, J. Liu and N. S. Chandel (2009). "Nitric oxide induces cell death by regulating anti-apoptotic BCL-2 family members." PLoS One **4**(9): e7059.

So, J. S. (2018). "Roles of Endoplasmic Reticulum Stress in Immune Responses." Mol Cells **41**(8): 705-716.

Soto-Gamez, A. and M. Demaria (2017). "Therapeutic interventions for aging: the case of cellular senescence." Drug Discov Today **22**(5): 786-795.

Sousa, C., A. J. Leitão, B. M. Neves, F. Judas, C. Cavaleiro and A. F. Mendes (2020). "Standardised comparison of limonene-derived monoterpenes identifies structural determinants of anti-inflammatory activity." Sci Rep **10**(1): 7199.

Sousa, C., M. Ribeiro, A. T. Rufino, A. J. Leitao and A. F. Mendes (2017). "Assessment of cell line competence for studies of pharmacological GPR30 modulation." J Recept Signal Transduct Res **37**(2): 181-188.

Spitsin, S. V., H. Koprowski and F. H. Michaels (1996). "Characterization and functional analysis of the human inducible nitric oxide synthase gene promoter." Mol Med **2**(2): 226-235.

Standardization, I. O. f. (2009). Biological evaluation of medical devices. Part 5: Tests for in vitro cytotoxicity. Switzerland, IHS. **ISO 10993-5:2009(E):** 1-34.

Stuart, L. M., N. Paquette and L. Boyer (2013). "Effector-triggered versus pattern-triggered immunity: how animals sense pathogens." Nat Rev Immunol **13**(3): 199-206.

Sturm, N., J. Desaphy, R. J. Quinn, D. Rognan and E. Kellenberger (2012). "Structural insights into the molecular basis of the ligand promiscuity." J Chem Inf Model **52**(9): 2410-2421.

Sun, S. C. (2011). "Non-canonical NF-kappaB signaling pathway." Cell Res **21**(1): 71-85.

Sun, S. C. (2017). "The non-canonical NF-κB pathway in immunity and inflammation." Nat Rev Immunol **17**(9): 545-558.

Sun, Y., L. Wenger, C. E. Brinckerhoff, R. R. Misra and H. S. Cheung (2002). "Basic calcium phosphate crystals induce matrix metalloproteinase-1 through the Ras/mitogen-activated protein kinase/c-Fos/AP-1/metalloproteinase 1 pathway. Involvement of transcription factor binding sites AP-1 and PEA-3." J Biol Chem **277**(2): 1544-1552.

Suryavanshi, S. V. and Y. A. Kulkarni (2017). "NF-kappabeta: A Potential Target in the Management of Vascular Complications of Diabetes." Front Pharmacol **8**: 798.

Suthahar, N., W. C. Meijers, H. H. W. Sillje and R. A. de Boer (2017). "From Inflammation to Fibrosis-Molecular and Cellular Mechanisms of Myocardial Tissue Remodelling and Perspectives on Differential Treatment Opportunities." Curr Heart Fail Rep **14**(4): 235-250.

Suzuki, K., T. Hayashi, O. Taguchi and E. Gabazza (2008). Coagulation, Inflammation, and Tissue Remodeling. Recent Advances in Thrombosis and Hemostasis 2008. K. Tanaka, E. W. Davie, Y. Ikeda et al. Tokyo, Springer Japan**:** 203-210.

Takano, S., K. Uchida, G. Inoue, M. Miyagi, J. Aikawa, D. Iwase, K. Iwabuchi, T. Matsumoto, M. Satoh, M. Mukai, A. Minatani and M. Takaso (2017). "Nerve growth factor regulation and production by macrophages in osteoarthritic synovium." Clin Exp Immunol **190**(2): 235-243.

Talalay, P., M. J. De Long and H. J. Prochaska (1988). "Identification of a common chemical signal regulating the induction of enzymes that protect against chemical carcinogenesis." Proc Natl Acad Sci U S A **85**(21): 8261-8265.

Tanaka, T., M. J. Grusby and T. Kaisho (2007). "PDLIM2-mediated termination of transcription factor NF-kappaB activation by intranuclear sequestration and degradation of the p65 subunit." Nat Immunol **8**(6): 584-591.

Tardif, G., P. Reboul, M. Dupuis, C. Geng, N. Duval, J. P. Pelletier and J. Martel-Pelletier (2001). "Transforming growth factor-beta induced collagenase-3 production in human osteoarthritic chondrocytes is triggered by Smad proteins: cooperation between activator protein-1 and PEA-3 binding sites." J Rheumatol **28**(7): 1631-1639.

Thibaudeau, T. A. and D. M. Smith (2019). "A Practical Review of Proteasome Pharmacology." Pharmacol Rev **71**(2): 170-197.

Thomas, D. D. and D. A. Wink (2017). "NOS2 as an Emergent Player in Progression of Cancer." Antioxid Redox Signal **26**(17): 963-965.

Tilstra, J. S., C. L. Clauson, L. J. Niedernhofer and P. D. Robbins (2011). "NF-κB in Aging and Disease." Aging Dis **2**(6): 449-465.

Trop-Steinberg, S. and Y. Azar (2017). "AP-1 Expression and its Clinical Relevance in Immune Disorders and Cancer." Am J Med Sci **353**(5): 474-483.

Tsuchiya, Y., K. Osaki, M. Kanamoto, Y. Nakao, E. Takahashi, T. Higuchi and H. Kamata (2017). "Distinct B subunits of PP2A regulate the NF-kappaB signalling pathway through dephosphorylation of IKKbeta, IkappaBalpha and RelA." FEBS Lett **591**(24): 4083-4094.

Tsui, R., J. D. Kearns, C. Lynch, D. Vu, K. A. Ngo, S. Basak, G. Ghosh and A. Hoffmann (2015). "IκBβ enhances the generation of the low-affinity NFκB/RelA homodimer." Nat Commun **6**: 7068.

Tufekci, K. U., S. Genc and K. Genc (2011). "The endotoxin-induced neuroinflammation model of Parkinson's disease." Parkinsons Dis **2011**: 487450.

Ueha, S., F. H. Shand and K. Matsushima (2012). "Cellular and molecular mechanisms of chronic inflammation-associated organ fibrosis." Front Immunol **3**: 71.

van Horssen, J., P. van Schaik and M. Witte (2017). "Inflammation and mitochondrial dysfunction: A vicious circle in neurodegenerative disorders?" Neurosci Lett.

Vermeulen, L., G. De Wilde, P. Van Damme, W. Vanden Berghe and G. Haegeman (2003). "Transcriptional activation of the NF-kappaB p65 subunit by mitogen- and stress-activated protein kinase-1 (MSK1)." EMBO J **22**(6): 1313-1324.

Voeltz, G. K., M. M. Rolls and T. A. Rapoport (2002). "Structural organization of the endoplasmic reticulum." EMBO reports **3**(10): 944-950.

Wang, B., Y. Zhang, W. Cao, X. Wei, J. Chen and W. Ying (2016). "SIRT2 Plays Significant Roles in Lipopolysaccharides-Induced Neuroinflammation and Brain Injury in Mice." Neurochem Res **41**(9): 2490-2500.

Wang, C., L. Deng, M. Hong, G. R. Akkaraju, J. Inoue and Z. J. Chen (2001). "TAK1 is a ubiquitin-dependent kinase of MKK and IKK." Nature **412**(6844): 346-351.

Wang, Y., J. He, M. Liao, M. Hu, W. Li, H. Ouyang, X. Wang, T. Ye, Y. Zhang and L. Ouyang (2019). "An overview of Sirtuins as potential therapeutic target: Structure, function and modulators." Eur J Med Chem **161**: 48-77.

Wang, Y., L. Hu, X. Tong and X. Ye (2014). "Casein kinase 1gamma1 inhibits the RIG-I/TLR signaling pathway through phosphorylating p65 and promoting its degradation." J Immunol **192**(4): 1855-1861.

Wang, Y., J. Yang, T. Hong, X. Chen and L. Cui (2019). "SIRT2: Controversy and multiple roles in disease and physiology." Ageing Res Rev **55**: 100961.

Wattenberg, L. W., V. L. Sparnins and G. Barany (1989). "Inhibition of N-nitrosodiethylamine carcinogenesis in mice by naturally occurring organosulfur compounds and monoterpenes." Cancer Res **49**(10): 2689-2692.

Wei, H., L. Prabhu, A. Hartley, M. Martin, E. Sun, G. Jiang, Y. Liu and T. Lu (2018). Methylation of NF-κB and its Role in Gene Regulation. Gene Expression and Regulation in Mammalian Cells - Transcription From General Aspects. F. Uchiumi, IntechOpen.

Wei, H., B. Wang, M. Miyagi, Y. She, B. Gopalan, D. B. Huang, G. Ghosh, G. R. Stark and T. Lu (2013). "PRMT5 dimethylates R30 of the p65 subunit to activate NF-kappaB." Proc Natl Acad Sci U S A **110**(33): 13516-13521.

Weissmann, G. (2010). "It's complicated: inflammation from Metchnikoff to Meryl Streep." FASEB J **24**(11): 4129-4132.

WHO. (2018). "Noncommunicable diseases." Retrieved 24/10/2018, from http://www.who.int/news-room/fact-sheets/detail/noncommunicable-diseases.

Wolter, S., A. Doerrie, A. Weber, H. Schneider, E. Hoffmann, J. von der Ohe, L. Bakiri, E. F. Wagner, K. Resch and M. Kracht (2008). "c-Jun controls histone modifications, NF-kappaB recruitment, and RNA polymerase II function to activate the ccl2 gene." Mol Cell Biol **28**(13): 4407-4423.

Wong, E. T. and V. Tergaonkar (2009). "Roles of NF-kappaB in health and disease: mechanisms and therapeutic potential." Clin Sci (Lond) **116**(6): 451-465.

Wu, Y., J. Lu, S. Antony, A. Juhasz, H. Liu, G. Jiang, J. L. Meitzler, M. Hollingshead, D. C. Haines, D. Butcher, K. Roy and J. H. Doroshow (2013). "Activation of TLR4 is required for the synergistic induction of dual oxidase 2 and dual oxidase A2 by IFN-gamma and lipopolysaccharide in human pancreatic cancer cell lines." J Immunol **190**(4): 1859-1872.

Wulf, E., A. Deboben, F. A. Bautz, H. Faulstich and T. Wieland (1979). "Fluorescent phallotoxin, a tool for the visualization of cellular actin." Proc Natl Acad Sci U S A **76**(9): 4498-4502.

Wynn, T. A. (2007). "Common and unique mechanisms regulate fibrosis in various fibroproliferative diseases." J Clin Invest **117**(3): 524-529.

Xia, L., S. Tan, Y. Zhou, J. Lin, H. Wang, L. Oyang, Y. Tian, L. Liu, M. Su, H. Wang, D. Cao and Q. Liao (2018). "Role of the NFκB-signaling pathway in cancer." Onco Targets Ther **11**: 2063-2073.

Xu, Y., C. Jagannath, X. D. Liu, A. Sharafkhaneh, K. E. Kolodziejska and N. T. Eissa (2007). "Toll-like receptor 4 is a sensor for autophagy associated with innate immunity." Immunity **27**(1): 135-144.

Xue, J., H. Li, X. Deng, Z. Ma, Q. Fu and S. Ma (2015). "L-Menthone confers antidepressant-like effects in an unpredictable chronic mild stress mouse model via NLRP3 inflammasome-mediated inflammatory cytokines and central neurotransmitters." Pharmacol Biochem Behav **134**: 42-48.

Yang, C. J., Y. P. Liu, H. Y. Dai, Y. L. Shiue, C. J. Tsai, M. S. Huang and Y. T. Yeh (2015). "Nuclear HDAC6 inhibits invasion by suppressing NF-kappaB/MMP2 and is inversely correlated with metastasis of non-small cell lung cancer." Oncotarget **6**(30): 30263-30276.

Yang, D., Z. Han and J. J. Oppenheim (2017). "Alarmins and immunity." Immunol Rev **280**(1): 41-56.

Yang, F., E. Tang, K. Guan and C. Y. Wang (2003). "IKK beta plays an essential role in the phosphorylation of RelA/p65 on serine 536 induced by lipopolysaccharide." J Immunol **170**(11): 5630-5635.

Yang, J., G. H. Fan, B. E. Wadzinski, H. Sakurai and A. Richmond (2001). "Protein phosphatase 2A interacts with and directly dephosphorylates RelA." J Biol Chem **276**(51): 47828-47833.

Yang, X. D., B. Huang, M. Li, A. Lamb, N. L. Kelleher and L. F. Chen (2009). "Negative regulation of NF-kappaB action by Set9-mediated lysine methylation of the RelA subunit." Embo j **28**(8): 1055-1066.

Yang, X. D., E. Tajkhorshid and L. F. Chen (2010). "Functional interplay between acetylation and methylation of the RelA subunit of NF-kappaB." Mol Cell Biol **30**(9): 2170-2180.

Yang, Y., G. Jiang, P. Zhang and J. Fan (2015). "Programmed cell death and its role in inflammation." Mil Med Res **2**: 12.

Yao, Q. S. and G. C. Chiou (1993). "Inhibition of crystallins-induced inflammation in rabbit eyes with five phytogenic compounds." Zhongguo Yao Li Xue Bao **14**(1): 13-17.

Ye, J., Z. Qing, J. Ma and Z. Wang (2017). "Effect of proteasome inhibitor on NF-κB and MMP-9 expression in synovial tissues of osteoarthritis rats. ." Int J Clin Exp Med **10**(1): 402-409.

Yeung, F., J. E. Hoberg, C. S. Ramsey, M. D. Keller, D. R. Jones, R. A. Frye and M. W. Mayo (2004). "Modulation of NF-kappaB-dependent transcription and cell survival by the SIRT1 deacetylase." EMBO J **23**(12): 2369-2380.

Yoon, W. J., N. H. Lee and C. G. Hyun (2010). "Limonene suppresses lipopolysaccharide-induced production of nitric oxide, prostaglandin E2, and pro-inflammatory cytokines in RAW 264.7 macrophages." J Oleo Sci **59**(8): 415-421.

Yu, Q., K. Zeng, X. Ma, F. Song, Y. Jiang, P. Tu and X. Wang (2016). "Resokaempferol-mediated anti-inflammatory effects on activated macrophages via the inhibition of JAK2/STAT3, NF-kappaB and JNK/p38 MAPK signaling pathways." Int Immunopharmacol **38**: 104-114.

Zell, R., P. Geck, K. Werdan and P. Boekstegers (1997). "Tnf-α and IL-1α inhibit both pyruvate dehydrogenase activity and mitochondrial function in cardiomyocytes: Evidence

for primary impairment of mitochondrial function." Molecular and Cellular Biochemistry **177**(1): 61-67.

Zhang, G., Y. Xia, F. Wan, K. Ma, X. Guo, L. Kou, S. Yin, C. Han, L. Liu, J. Huang, N. Xiong and T. Wang (2018). "New Perspectives on Roles of Alpha-Synuclein in Parkinson's Disease." Front Aging Neurosci **10**: 370.

Zhang, L., M. J. Yousefzadeh, Y. Suh, L. J. Niedernhofer and P. D. Robbins (2019). "Signal Transduction, Ageing and Disease." Subcell Biochem **91**: 227-247.

Zhang, Q., M. J. Lenardo and D. Baltimore (2017). "30 Years of NF-kappaB: A Blossoming of Relevance to Human Pathobiology." Cell **168**(1-2): 37-57.

Zheng, G. Q., P. M. Kenney and L. K. Lam (1992). "Anethofuran, carvone, and limonene: potential cancer chemopreventive agents from dill weed oil and caraway oil." Planta Med **58**(4): 338-341.

Zheng, W., Z. Feng, S. You, H. Zhang, Z. Tao, Q. Wang, H. Chen and Y. Wu (2017). "Fisetin inhibits IL-1β-induced inflammatory response in human osteoarthritis chondrocytes through activating SIRT1 and attenuates the progression of osteoarthritis in mice." Int Immunopharmacol **45**: 135-147.

Zhong, H., H. SuYang, H. Erdjument-Bromage, P. Tempst and S. Ghosh (1997). "The transcriptional activity of NF-kappaB is regulated by the IkappaB-associated PKAc subunit through a cyclic AMP-independent mechanism." Cell **89**(3): 413-424.

Zhong, H., R. E. Voll and S. Ghosh (1998). "Phosphorylation of NF-kappa B p65 by PKA stimulates transcriptional activity by promoting a novel bivalent interaction with the coactivator CBP/p300." Mol Cell **1**(5): 661-671.

Zhou, R., A. S. Yazdi, P. Menu and J. Tschopp (2011). "A role for mitochondria in NLRP3 inflammasome activation." Nature **469**(7329): 221-225.

Ziesche, E., D. Kettner-Buhrow, A. Weber, T. Wittwer, L. Jurida, J. Soelch, H. Muller, D. Newel, P. Kronich, H. Schneider, O. Dittrich-Breiholz, S. Bhaskara, S. W. Hiebert, M. O. Hottiger, H. Li, E. Burstein, M. L. Schmitz and M. Kracht (2013). "The coactivator role of histone deacetylase 3 in IL-1-signaling involves deacetylation of p65 NF-kappaB." Nucleic Acids Res **41**(1): 90-109.

Zlotnik, A. and O. Yoshie (2012). "The chemokine superfamily revisited." Immunity **36**(5): 705-716.